Cell-Autonomous Gene Function and Non-Cell-Autonomous Effects in Radial Projection Neuron Migration

by

Andi Harley Hansen

June, 2021

A thesis presented to the

Graduate School

of the

Institute of Science and Technology Austria, Klosterneuburg, Austria

in partial fulfillment of the requirements

for the degree of

Doctor of Philosophy

Committee in charge:
Dr. Martin Loose, Chair
Dr. Johannes Nimpf
Dr. Michael Sixt
Dr. Simon Hippenmeyer

The thesis of Andi Harley Hansen, titled *Cell-Autonomous Gene Function and Non-Cell-Autonomous Effects in Radial Projection Neuron Migration*, is approved by:

Supervisor: Simon Hippenmeyer, IST Austria, Klosterneuburg, Austria

Signature: _____

Committee Member: Michael Sixt, IST Austria, Klosterneuburg, Austria

Signature: _____

Committee Member: Johannes Nimpf, Max F. Perutz Laboratories, Vienna, Austria

Signature: _____

Exam Chair: Martin Loose, IST Austria, Klosterneuburg, Austria

Signature: _____

signed page is on file

IST Austria Thesis, ISSN: 2663-337X

I hereby declare that this thesis is my own work and that it does not contain other people's work without this being so stated; this thesis does not contain my previous work without this being stated, and the bibliography contains all the literature that I used in writing the dissertation.

I declare that this is a true copy of my thesis, including any final revisions, as approved by my thesis committee, and that this thesis has not been submitted for a higher degree to any other university or institution.

I certify that any republication of materials presented in this thesis has been approved by the relevant publishers and co-authors.

Signature: _____

Andi Harley Hansen

June, 2021

signed page is on file

Abstract

The brain is one of the largest and most complex organs and it is composed of billions of neurons that communicate together enabling e.g. consciousness. The cerebral cortex is the largest site of neural integration in the central nervous system. Concerted radial migration of newly born cortical projection neurons, from their birthplace to their final position, is a key step in the assembly of the cerebral cortex. The cellular and molecular mechanisms regulating radial neuronal migration *in vivo* are however still unclear. Recent evidence suggests that distinct signaling cues act cell-autonomously but differentially at certain steps during the overall migration process. Moreover, functional analysis of genetic mosaics (mutant neurons present in wild-type/heterozygote environment) using the MADM (Mosaic Analysis with Double Markers) analyses in comparison to global knockout also indicate a significant degree of non-cell-autonomous and/or community effects in the control of cortical neuron migration. The interactions of cell-intrinsic (cell-autonomous) and cell-extrinsic (non-cell-autonomous) components are largely unknown. In part of this thesis work we established a MADM-based experimental strategy for the quantitative analysis of cell-autonomous gene function versus non-cell-autonomous and/or community effects. The direct comparison of mutant neurons from the genetic mosaic (cell-autonomous) to mutant neurons in the conditional and/or global knockout (cell-autonomous + non-cell-autonomous) allows to quantitatively analyze non-cell-autonomous effects. Such analysis enable the high-resolution analysis of projection neuron migration dynamics in distinct environments with concomitant isolation of genomic and proteomic profiles. Using these experimental paradigms and in combination with computational modeling we show and characterize the nature of non-cell-autonomous effects to coordinate radial neuron migration. Furthermore, this thesis discusses recent developments in neurodevelopment with focus on neuronal polarization and non-cell-autonomous mechanisms in neuronal migration.

Dedication

The work presented here was carried out in the Hippenmeyer laboratory which is part of the Life Science Department at IST Austria.

First, I want to thank Dr. Simon Hippenmeyer for his support and guidance during my PhD. The first day I met Simon, I immediately knew that I wanted to join his research group to start my PhD project. Over the years we have had many scientific and non-scientific highlights which positively influenced my time in Simon's research group. I especially want to highlight some of the many research conferences which we attended, which not only helped me mature scientifically and expand my network, but also developed the student-supervisor relationship further. Furthermore, his scientific vision provided me with a project that was worth working on.

I want to thank the Austrian Academy of Sciences (ÖAW) for granting me a three year DOC-fellowship to support my PhD research.

I would also like to thank the members of my thesis committee, Dr. Michael Sixt and Dr. Johannes Nimpf, and defense chair Dr. Martin Loose for their time and support.

I also want to say a big thank you to all the Hippenmeyer lab members, both present and past, and IST Facility staff. I want to thank Carmen Streicher for helping introducing me to the lab when I started and for always being available for help, especially with the mouse work. A special thanks goes out to Florian Pauler, he is a great team-mate and I really value our great discussions. I have learned a lot from him.

I also want to thank Michael Riedl for helping me during my PhD project and for some very interesting conversations.

I want to thank Martin Breuss, Mattias Lauwers, Thomas Gstrein, Andreas Pöhlmann, John Stowers and David Keays, without them I would not have considered doing a PhD.

I want to thank my family, especially my mom and dad, who always supported and encouraged me no matter what. I want to thank all my friends for support and being there for me in both joyful and difficult times.

Last but not least, I want to thank Ximena Contreras for support and patience while being a great colleague and friend. Thank you for always being there for me.

About the Author

Andi H. Hansen completed a BSc in Biomedical Engineering at the UAS Technikum Wien and a MSc in in Behavior-, Neuro- and Cognitive biology at the University of Vienna before joining IST Austria Phd program in September 2015. His main research interests include cellular and molecular mechanisms of brain development and disease with particular interest in non-cell-autonomous mechanisms underlying brain development. After a detour in various jobs, spanning from ski instructor to servicing firefighting equipment in a shipyard, he worked on research projects in the Keays group at the IMP Vienna before starting his PhD studies in the Hippenmeyer laboratory at IST Austria. During his PhD work in the Hippenmeyer laboratory he contributed to a range of research projects and presented his research progress at several international conferences including the Gordon Research Conference on Neural Development and the SfN Neuroscience Meeting. To support his PhD work, he was awarded the DOC fellowship of the Austrian Academy of Sciences in 2017.

List of Publications

Appearing in the thesis

1. **Hansen AH**, Duellberg C, Mieck C, Loose M, Hippenmeyer S. *Cell Polarity in Cerebral Cortex Development-Cellular Architecture Shaped by Biochemical Networks*. Front Cell Neurosci. 2017 Jun 28;11:176. doi: 10.3389/fncel.2017.00176

2. **Andi H. Hansen** & Simon Hippenmeyer. *Non-cell-autonomous mechanisms in radial projection neuron migration in the developing cerebral cortex.* Frontiers in Cell and Developmental Biology. 2020;8(9). doi:10.3389/fcell.2020.574382

3. **Andi H. Hansen**, Florian M. Pauler, Michael Riedl, Carmen Streicher, Susanne Laukoter, Justine Renno, Lill Andersen, Thomas Ruelicke, Björn Hof & Simon Hippenmeyer. *Cell-Autonomous and Non-Autonomous Mechanisms Controlling Projection Neuron Migration*. (In preparation)

Other contributions during PhD research

4. Ximena Contreras, Nicole Amberg, Amarbayasgalan Davaatseren, **Andi H. Hansen**, Johanna Sonntag, Lill Kristin Andersen, Tina Bernthaler, Carmen Streicher, Anna Heger, Randy L. Johnson, Lindsay Schwarz, Liqun Luo, Thomas Ruelicke & Simon Hippenmeyer. *A genome-wide library of MADM mice for single-cell genetic mosaic analysis.* Cell Reports. 2021. doi: 10.1016/j.celrep.2021.109274

5. Susanne Laukoter, Florian M. Pauler, Robert Beattie, Nicole Amberg, **Andi H. Hansen**, Carmen Streicher, Thomas Penz, Christoph Bock & Simon Hippenmeyer. *Cell-type specificity of genomic imprinting in cerebral cortex.* Neuron. 107(9):1-20. doi:10.1016/j.neuron.2020.06.031

6. Tingting Zhang, Tengyuan Liu, Natalia Mora, Justine Guegan, Mathilde Bertran, Ximena Contreras, **Andi H. Hansen**, Carmen Streicher, Marica Anderle, Natasha Danda, Luca Tiberi, Simon Hippenmeyer and Bassem A. Hassan. *Generation of excitatory and inhibitory neurons from common progenitors via Notch signaling in the cerebellum*. Cell Reports. doi: 10.1016/j.celrep.2021.109208

7. Robert Beattie, Carmen Steicher, Nicole Amberg, Giselle Cheung, Ximena Contreras, **Andi H. Hansen** and Simon Hippenmeyer. *Lineage Tracing and Clonal Analysis in Developing Cerebral Cortex Using Mosaic Analysis with Double Markers (MADM)*. Journal of Visual Experiments (JoVE). 2020;(159). doi:10.3791/61147

Table of Contents

List of Figures

List of Tables

List of Symbols/Abbreviations

MADM	Mosaic Analysis with Double Markers
Cdk5r1	Cyclin Dependent Kinase 5 Regulatory Subunit 1
Cdk5	Cyclin Dependent Kinase 5
Dab1	Disabled-1
Cre	Carbapanem-resistant Enterobacteriaceae
KO	Knockout
cKO	Conditional Knockout
WM	White Matter
VZ	Ventricular Zone
SVZ	Subventricular Zone
PP	Pre Plate
IZ	Intermediate Zone
SP	Subplate
CP	Cortical Plate
MZ	Marginal Zone
GTP	Guanosine triphosphate
GDP	Guanosine dihosphate
GDI	Guanosine nucleotide dissociation inhibitor
GEF	Guanine nucleotide exchange factors
µm	micrometer
tdT	Tandem dimer tomato
GFP	Green fluorescent protein
RT	Room temperature
RNA	Ribonucleic acid
oRG	Outer radial glia
rpm	Revolutions per minute
PBS	Phosphate buffered saline

P	Postnatal
E	Embryonic
GO	Gene ontology
FACS	Fluorescence associated cell sorting
MCD	Malformation of cortical development
FMCD	Focal malformation of cortical development
RNA-Seq	Ribonucleic acid-Sequencing
p	p(probability)-value
padj	Adjusted p-value

1 Chapter 1 - Introduction

1.1 Thesis Outline

The thesis consists of 5 chapters each featuring the topic of radial neuronal migration, a central aspect of cerebral cortex development. The first chapter gives a general introduction to the main topic of radial neuronal migration, setting the stage for the following chapters where each chapter cover specific aspects of cellular and molecular mechanisms of neuronal migration. The second chapter is focused on cell polarity in a neuronal context, considering intrinsic and extrinsic regulation of the polarization of neurons. Neurons are highly polarized cells, meaning, they have a cell body (soma) which in one end has dendrites and the other end an axon, which can have a relatively huge distance spatially, between them. The chapter is in form of a published review article, which discusses recent literature on neuronal polarity. The review was written in collaboration with my supervisor Simon Hippenmeyer, Martin Loose and two postdocs from the Loose Group at IST Austria.

The third chapter covers the scarcely studied subject matter of non-cell-autonomous mechanisms in radial neuronal migration. In this chapter the current state of what is known about non-cell-autonomous mechanisms is discussed and more importantly present and discuss approaches how to study this phenomenon further, as our current knowledge is very limited. The chapter consists of a published review manuscript which was written together with my supervisor.

The fourth chapter contains original research elaborating on the previous topic of non-cell-autonomous mechanisms in neuronal migration. In this chapter, an assembled research manuscript is presented, containing my main PhD research which provides substantial insights into the nature of non-cell-autonomous effects and their relevance in radial neuronal migration. The chapter presents data which, for the first time, shows that non-cell-autonomous effects might mainly be exerted through cell-adhesion and might be a common or even universal feature of disorganized cerebral cortex layering in disease condition. This study was carried out with support from Hippenmeyer lab members, especially Florian M. Pauler and Carmen Streicher, Michael Riedl from the Hof/Sixt Group and staff from Bio imaging (BIF), Pre-clinical (PCF) and Mass Spectrometry (LSF) IST Austria core facilities.

The fifth chapter concludes the thesis with general conclusion concerning previous chapters and the sixth chapter puts a future perspective of the exciting field of neuronal migration and brain development in general.

1.2 Development of the cerebral neocortex

The morphological and functional development of the central nervous system relies on neurogenesis, neuronal migration and circuit formation. To orchestrate a complex organ like the brain in any organism a complex sequence of cellular and molecular events is involved. The phenomenon of neuronal migration is essential to bring cells into their correct position and is vital for normal cerebral cortex development. If the migratory process is disturbed at any point of development it can lead to severe brain malformations which mostly result in devastating disease phenotypes (Juric-Sekhar and Hevner, 2019).

1.2.1 How do neurons move?

Neuronal migration is a tightly controlled process which involves newborn neurons migrating from their origin in germinal layers of the neuroepithelia to their final destination where they form a structural layering allowing for proper functioning neuronal circuits (Ayala et al., 2007; Marín et al., 2010). Neurons are highly dependent on their cytoskeleton in combination with receptors and cell adhesion which involves a wide range of molecules, both cell intrinsically and extrinsically, for the migratory process to succeed (Heng et al., 2010; Nguyen and Hippenmeyer, 2014). In general, neurons follow either a radial or tangential migratory path depending on their origin. Projection neurons and interneurons comprises the two main classes of cortical neurons (Ayala et al., 2007; Marín et al., 2010). Cortical interneurons originate from the ventral ganglionic eminences and migrate tangentially whereas cortical projection neurons are generated in the dorsal ventricular zone and migrate radially. Projection neurons and interneurons comprise the two main classes of cortical neurons. GABAergic interneurons mainly display inhibitory properties and form local connections whereas glutamatergic projection neurons display excitatory properties and can extend axons to distant areas within and outside of the cortex (Marín et al., 2010; Valiente and Marín, 2010). Radial and tangential migration is defined by the perpendicular or parallel movement with respect the to the neuroepithelial surface, respectively. While neurons are migrating along a directed path they display a polarized cell morphology with an anterior leading

process in the moving direction and a trailing process posterior to the cell body (Cooper, 2013). The structures of the leading and trailing processes consist of lamellipodia and filopodia which exhibit wide and thin plasma membrane protrusions, respectively. Lamellipodia are comprised of a sheet-like branched network of actin filaments, whereas filopodia are cross-linked long bundles of unidirectional and parallel actin filaments protruding from the lamellipodia acting as probes to navigate and steer the migrating cell (Cooper, 2013; Marín et al., 2010). The migration process relies on the dynamic regulation, polymerization and crosslinking of actin and actin-associated proteins. In addition, cytoskeletal proteins consisting of microtubules, actin and actomyosin play important roles during nucleokinesis (translocation of the nucleus) and locomotion (movement of the cell somata) (Cooper, 2013). Translocation of the neuronal somata, also called somal translocation, is the main mode of neuronal migration during the early stages of embryonic development (Hatanaka et al., 2004; Nadarajah, 2003). Neuronal locomotion consists of sequential phases where the neurons extend the leading process, perform nucleokinesis and then retract the trailing process, which is continuously repeated during this migration mode. During locomotion, the centrosome (aka the microtubule organizing center) positions itself in the leading process in front of the nucleus (Cooper, 2013; Marín et al., 2010). Microtubules then extend toward the leading edge and employ force to propel the leading edge further and while connecting the centrosome to the nucleus by forming a cage-like structure around it that then pulls it forward into the new position (Cooper, 2013).

1.2.2 Radial neuronal migration builds up a layered neocortex

The adult mammalian neocortex is structured into six distinct layers (I-VI), each displaying different cellular composition (Lodato and Arlotta, 2015; McConnell, 1995). The layered brain structure is composed by projection neurons arising from radial glial cells (RGCs) in the ventricular zone (VZ) intermediate progenitor cells (IPCs), and outer radial glial cells (oRGs, aka basal radial glia, bRGs) which divide in the subventricular zone (SVZ) (Ayala et al., 2007; Borrell and Götz, 2014; Hansen et al., 2010; Wang et al., 2011). In order to populate the correct cortical layer during embryogenesis, projection neurons exhibit radial migration from the VZ/SVZ to the cortical plate. Around embryonic day 11 (E11), postmitotic neurons migrate mainly by pulling up the soma in the upright direction with a process firmly attached to the

pial surface, a migration mode termed somal translocation (Nadarajah et al., 2001). This first cohort of neurons form the preplate (PP) structure which only exists transiently (Figure 1) (Allendoerfer and Shatz, 1994; Nadarajah et al., 2001).

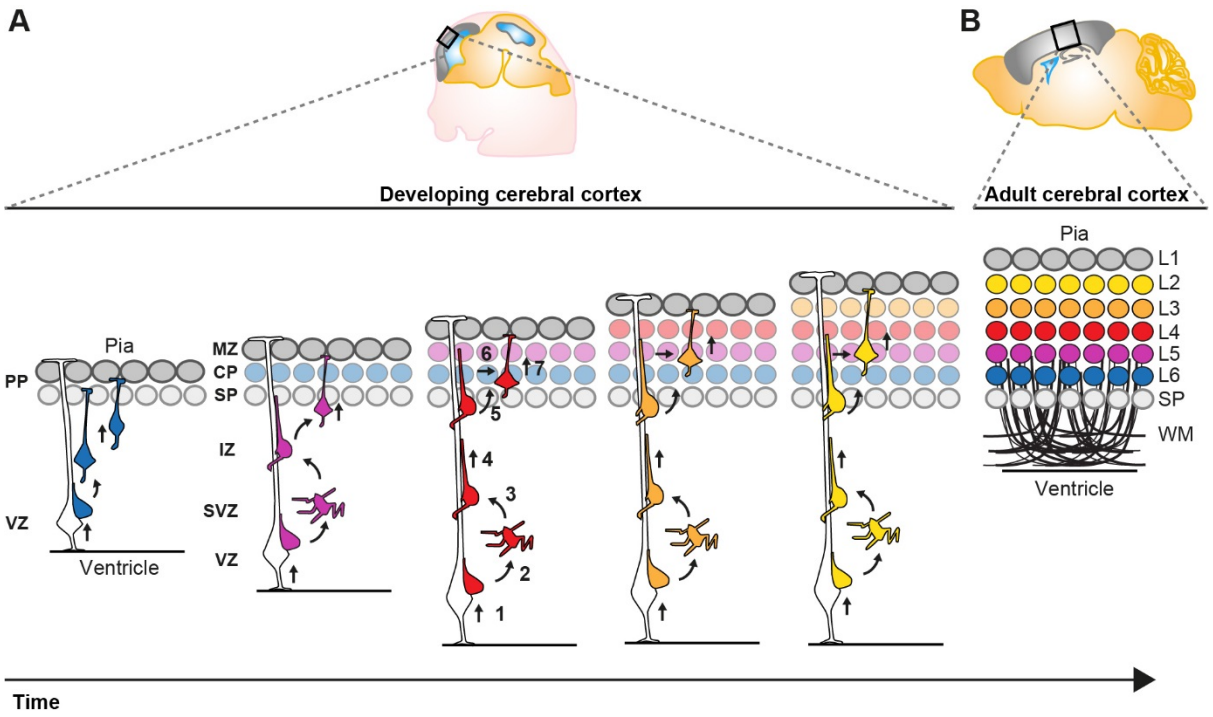

Figure 1 Radial Neuronal Migration

Migrating cortical projection neurons go through several steps and phases during their journey from their birthplace in the ventricular/subventricular zone (VZ/SVZ) to their final position in the cortical plate (CP). (A) Around embryonic day 11 (E11), postmitotic neurons migrate mainly by pulling up the soma in the upright direction with a process firmly attached to the pial surface, a migration mode termed somal translocation. This first cohort of neurons form the preplate (PP) structure which only exists transiently. At around E12/E13, consecutive waves of neurons migrate toward the pial surface and establish the CP by splitting the PP into the two distinct structures: the deeper located subplate (SP) and the superficial positioned marginal zone (MZ) (Layer I) mainly consisting of Cajal-Retzius cells. The early migrating neurons establish the first layer of projection neurons (layer VI) in the CP which later expands in the vertical direction in an inside-out fashion. (1) Nascent neurons delaminate from the ventricular surface in the VZ and take on a bipolar morphology towards the sub-ventricular zone (SVZ) where they switch to a multipolar shape (2). After remaining in a multipolar state for up to 24hours neurons undergo multi-to-bipolar transition (3) and start locomotion along the radial glial fiber through the intermediate zone (IZ) (4). Once reaching the SP, neurons enter the CP (5) and migrate towards the marginal zone (MZ) where they detach from the radial glial fiber (6). Finally, neurons settle in their appropriate position in the CP by terminal somal translocation (7). (C) Adult cerebral cortex consisting of 6 layers and white matter containing projected axons of the neurons.

At around E12/E13, consecutive waves of neurons migrate toward the pial surface and establish the CP by splitting the PP into the two distinct structures: the deeper located subplate (SP) consisting of primordial cells (Price et al., 1997) and the superficial positioned marginal zone (MZ) (Layer I) mainly consisting of Cajal-Retzius cells (Figure 1) (Ayala et al., 2007). The early migrating neurons establish the first layer of projection neurons (layer VI) in the CP which later expands in the vertical direction in an inside-out fashion. In other words, earlier generated neurons settle in the deeper layers (layer VI-V) whereas later generated neurons migrate through the deep positioned neurons creating more superficial layers (IV-II) with the white matter containing projected axons (Figure 1) (Angevine and Sidman, 1961; McConnell, 1995; Valiente and Marín, 2010).

Histological and live-imaging studies have shed light on the radial migration process and described distinct sequential steps of projection neuron migration (Nadarajah, 2003; Noctor et al., 2004; Tabata and Nakajima, 2003). First, neurons delaminate from the VZ and move towards the SVZ where they acquire a multipolar shape, characterized by multiple processes pointing in different directions. In the SVZ, multipolar neurons move tangentially, towards the pia or towards the VZ (Noctor et al., 2004; Tabata and Nakajima, 2003). Multipolar neurons can remain up to 24hours in the multipolar state in the SVZ. Next, multipolar neurons switch to a bipolar state with a ventricle oriented process extending to become the axon. The pial oriented leading process is established by reorienting the Golgi and the centrosome towards the pial surface (Hatanaka et al., 2004; Yanagida et al., 2012). Upon multi-to-bipolar transition, neurons attach to the radial glial fiber and move through the intermediate zone along RGCs in a migration mode termed locomotion, while trailing the axon behind and rapidly extending and retracting their leading neurite before reaching the SP (Hatanaka et al., 2004; Noctor et al., 2004). Neurons then cross the SP and enter the CP still migrating along the RGCs until they reach the marginal zone (MZ). Just beneath the MZ neurons stop migrating in the locomotion mode and detach from the radial glia fiber to perform terminal somal translocation and settle in their target position where they eventually assemble into microcircuits (Hatanaka et al., 2016; Nadarajah et al., 2001; Noctor et al., 2004; Rakic, 1972). All sequential steps of projection neuron migration are critical and disruption of any stage can lead to severe cortical malformations (Gleeson and Walsh, 2000; Guerrini and Parrini, 2010). Therefore each step of projection neuron migration must be tightly regulated.

Many genes have been identified as causative factors for cortical malformations (Heng et al., 2010; Valiente and Marín, 2010) and several of the key molecules involved in neuronal migration e.g. *Lis1*, *Dcx*, and *Reelin* have thus far mainly been investigated by molecular genetics (Kawauchi, 2015). Recently, approaches involving *in-vivo* electroporation and time-lapse imaging of brain slice cultures have shed light on crucial roles for the dynamic regulation of the cytoskeleton, extracellular cues and cell adhesion during neuronal migration (Franco et al., 2011; Jossin and Cooper, 2011; Noctor et al., 2004; Schaar and McConnell, 2005; Sekine et al., 2012). An emerging picture is arising on the distinct molecular programs regulating neuronal migration through the different compartments VZ/SVZ, IZ and CP (Greig et al., 2013; Hippenmeyer, 2014; Kwan et al., 2012). The precise regulatory mechanisms which coordinate each and every specific step of radial migration are still largely unknown. It is intuitive to speculate that also specific transcriptional programs could control neuronal migration (Ayoub et al., 2011; Miyoshi and Fishell, 2012), but the detailed function of such transcriptional programs and whether there are differences in gene expression in each compartment during migration is not well understood. Moreover, the regulation of neuronal migration is taking place at both a cell intrinsic and extrinsic level as the cell need to navigate and interact with the surrounding tissue environment which will be discussed in more detail in chapters 2 and 3.

1.2.3 Neuronal migration disorders

The migratory process of neurons is tightly regulated and as soon as this process is impaired neurons cannot position themselves properly and mostly results in malformations of the brain. Disorders caused by abnormal neuronal positioning due to aberrant neuronal migration display a wide range of more or less severe disease phenotypes (Guerrini and Parrini, 2010; Leventer et al., 2008; Moffat et al., 2015). Neuronal migration disorders are classified into specific disorder types, however clinicians mostly identify several types within the same individual and can occur as mixed phenotypes or part of a disease syndrome (Guerrini and Parrini, 2010). The specific subtypes of disorders are mainly classified based on visible morphologic anomalies of the cortex and mostly identified through magnetic resonance imaging (MRI) (Leventer et al., 2008). The more commonly known diseases such as epilepsy, autism spectrum disorders, schizophrenia and dyslexia have also been associated with

abnormal neuronal migration (Galaburda, 2005; Muraki and Tanigaki, 2015; Pan et al., 2019), whereas neuronal migration associated with dyslexia is still debated (Guidi et al., 2018). While non-genetic factors including exposure to alcohol or drugs (Gressens et al., 1992; Mattson and Riley, 1998; Stanwood, 2001; Thompson et al., 2009), hypoxia (Golan et al., 2009), heavy metals (Kakita et al., 2001), or *in utero* viral infection (Oliveira Melo et al., 2016) during pregnancy can predispose to or cause malformations of cortical development and neuropsychiatric disorders the majority of neuronal migration disorders have a genetic basis (Buchsbaum and Cappello, 2019; Guerrini and Parrini, 2010; Juric-Sekhar and Hevner, 2019).

A well characterized type of neuronal migration disorder is lissencephaly which is designated by the absence of folds, gyri and sulci, therefore displaying a smooth brain surface (Figure 2B&D) (Borrell and Reillo, 2012; Leventer et al., 2008). Classical lissencephaly is frequently associated with mutations in genes encoding components of cytoskeletal structures (Moffat et al., 2015). So far, several genes have been identified causing lissencephaly, including *LIS1* (Lissencephaly 1), *DCX* (doublecortin) usually only occurring in males, *TUBA1A*, *Reelin* and *CDK5* (Dobyns, 1993; Di Donato et al., 2018; Gleeson et al., 1998; Hong et al., 2000; Keays et al., 2007; Magen et al., 2015; Reiner et al., 1993). In addition, cobblestone lissencephaly (Type 2 lissencephaly), is a type of lissencephaly involving another range of genes, and is presented by regional agyria and no defined neuronal layers present in the cortex (Juric-Sekhar and Hevner, 2019).

Subcortical band heterotopias are functionally related to lissencephaly, however, they display a different morphological phenotype highlighted by a thick band of misplaced neurons just below the cortex (Figure 2E) (D'Agostino et al., 2002; Moffat et al., 2015). The misplaced neurons assemble a structure which appear similar to an additional reduced sized cortex, thus this disease phenotype is also referred to as "doublecortex".

Focal cortical dysplasia represents a cortical neuronal migration malformation which only affects a subpopulation of the neurons in a focal location in the cortex (Figure 2F) (Leventer et al., 2008; Siedlecka et al., 2016). The etiology of this disorder is still unclear and it has been assumed that genetic risk factors and/or somatic mutations contribute to the disease phenotype (Juric-Sekhar and Hevner, 2019; Siedlecka et al., 2016).

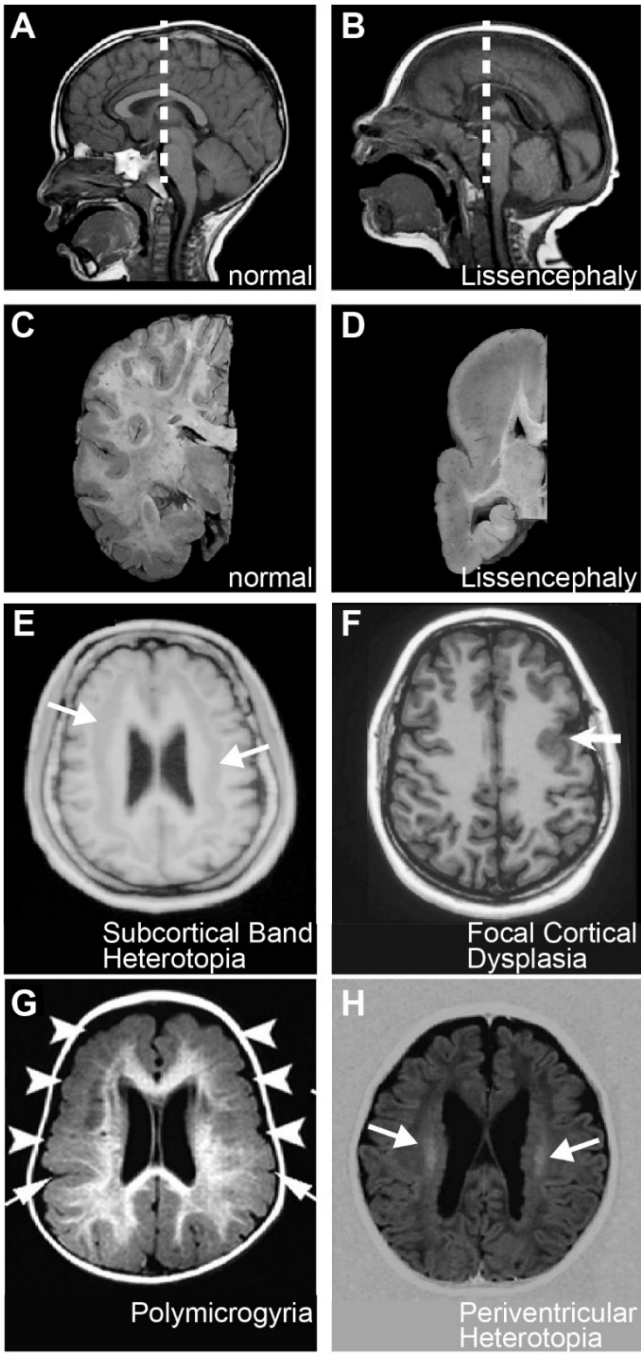

Figure 2 Neuronal Migration Disorders

(A-D) Saggital MRIs and histological sections depicting an unaffected normal control brain (A&C) and a patient suffering from lissencephaly (B&D; *LIS1* mutation). White stabled line in A&B indicate cutting plane for C&D. (E-F) Horizontal MRIs showing patients suffering from subcortical band heterotopia (E; *DCX* mutation), focal cortical dysplasia (F; mutation not known), polymicrogyria (G; GPR56 mutation) and periventricular heterotopia (H; *ARFGEF2* mutation). Arrows in E, F and H indicate abnormal disease structures. Arrowheads in G indicate regions of polymicrogyria. Panels were adapted from (Borrell and Reillo, 2012) (A-D; normal and lissencephalic), (Feng and Walsh, 2001)(E; subcortical band heterotopia) (Leventer et al., 2008) (F; focal cortical dysplasia), (Piao, 2004) (G; polymicrogyria) and (Sheen et al., 2004) (H; periventricular heterotopia).

Polymicrogyria (too many and too small gyri), like the name indicates is attributed to an increased number of aberrantly small sulci and gyri (folds) (Figure 2G) (Barkovich et al., 1999; Juric-Sekhar and Hevner, 2019). A wide spectrum of clinical phenotypes have been associated with this disease and therefore the clear definitions of polymicrogyria remain unsettled (Juric-Sekhar and Hevner, 2019). Polymicrogyria is also often associated with schizencephaly, which consist of clefts in the cerebral hemisphere (Verrotti et al., 2010). A few genes so far have been reported to cause polymicrogyria, including the tubulin genes *TUBA1A*, *TUBB2B* and *TUBB3* (Jaglin et al., 2009; Judkins et al., 2011; Poirier et al., 2010) and *ADGRG1*, (Formerly known as *GPR56)* (Piao, 2004). However, the underlying cellular and molecular mechanisms of this disease remain poorly understood (Juric-Sekhar and Hevner, 2019; Moffat et al., 2015)

In periventricular heterotopia, some neurons fail to migrate properly and form clusters of neurons near the ventricles (Figure 2H). In most cases, the disease is caused by mutations in the gene *FLNA* (*FILAMIN A*) and in other cases also be caused by mutations in the *ARFGEF2 (ADP ribosylation factor guanine nucleotide exchange factor 2)* gene (Fox et al., 1998; Sheen et al., 2004).

Although presenting devastating disease phenotypes, neurodevelopmental disorders permit research to further study and understand the brain through its pathogenesis. The pathogenesis of the brain facilitates a “window” which allows for the insight into this very complex cellular structure. Thus, to treat and overcome neuronal migration disorders it is necessary to comprehend the underlying cellular and molecular mechanisms responsible for the pathogenesis.

2 Cell Polarity in Cerebral Cortex Development - Cellular Architecture Shaped by Biochemical Networks

The content of this chapter was published as a review article in the Journal Frontiers in Cellular Neuroscience

Andi H. Hansen†[1], Christian Duellberg†[1], Christine Mieck†[1], Martin Loose[1*] and Simon Hippenmeyer[1*]

[1] Institute of Science and Technology Austria, Am Campus 1, 3400 Klosterneuburg, Austria

†These authors have contributed equally to this work.

*Corresponding authors

2.1 Author Contributions

AHH, CD, CM, ML and SH contributed equally to the writing of the initial draft. All authors revised the manuscript.

2.2 Summary

The human cerebral cortex is the seat of our cognitive abilities and composed of an extraordinary number of neurons, organized in six distinct layers. The establishment of specific morphological and physiological features in individual neurons needs to be regulated with high precision. Impairments in the sequential developmental programs instructing corticogenesis lead to alterations in the cortical cytoarchitecture which is thought to represent the major underlying cause for several neurological disorders including neurodevelopmental and psychiatric diseases. In this review article we discuss the role of cell polarity at sequential stages during cortex development. We first provide an overview of morphological cell polarity features in cortical neural stem cells and newly-born postmitotic neurons. We then synthesize a conceptual molecular and biochemical framework how cell polarity is established at the cellular level through a break in symmetry in nascent cortical projection neurons. Lastly we provide a perspective how the molecular mechanisms applying to single cells could be probed and integrated in an *in vivo* and tissue-wide context.

2.3 Establishment of Cellular Polarity in Sequential Stages of Cortical Development

2.3.1 Neural Stem Cell Polarity

The mammalian cerebral cortex emerges from the neuroectoderm. At the end of neurulation and neural tube closure, occurring from embryonic day (E) 7 to E9 in mice, the early neuroepithelium is composed of neuroepithelial stem cells (NESCs) from which all subsequent neural progenitor cells and their neuron lineages derive (Figure 3). NESCs are highly polarized and their nuclei exhibit interkinetic nuclear migration whereby they translocate from the ventricular (apical) side to the more basal side in concert with the cell cycle (Lee and Norden, 2013). NESC polarity correlates with the asymmetric distribution of cell fate determinants which are thought to control the fine balance between symmetric and asymmetric progenitor divisions (Shitamukai and Matsuzaki, 2012). Such balance is critical for the generation of the correct number of radial glia progenitor cells (RGPCs), which are not only lineally related to NESCs but exhibit even more polarized cellular morphology with an extended basal process (Taverna et al., 2014). In the initial stages of neurogenesis, NESCs arrange the mitotic spindle in parallel (division plane perpendicular) to the ventricular zone (VZ) and divide mostly symmetrically, thereby expanding the progenitor pool (Postiglione and Hippenmeyer, 2014; Taverna et al., 2014). The disruption of the mitotic spindle, anchored to the lateral walls of NESCs, results in the precocious generation of neurons and apoptosis (Yingling et al., 2008). Thus the correct cellular polarization of the earliest neural progenitor cells in the developing cerebral cortex is absolutely essential for the correct lineage progression and eventual neuron production. While it has been well established that components of the planar cell polarity signaling pathway play critical roles in establishing and maintaining progenitor polarity (Homem et al., 2015; Knoblich, 2008), the signaling cues and molecular mechanisms that instruct polarization and the break of symmetry in NESCs are not well understood in vivo.

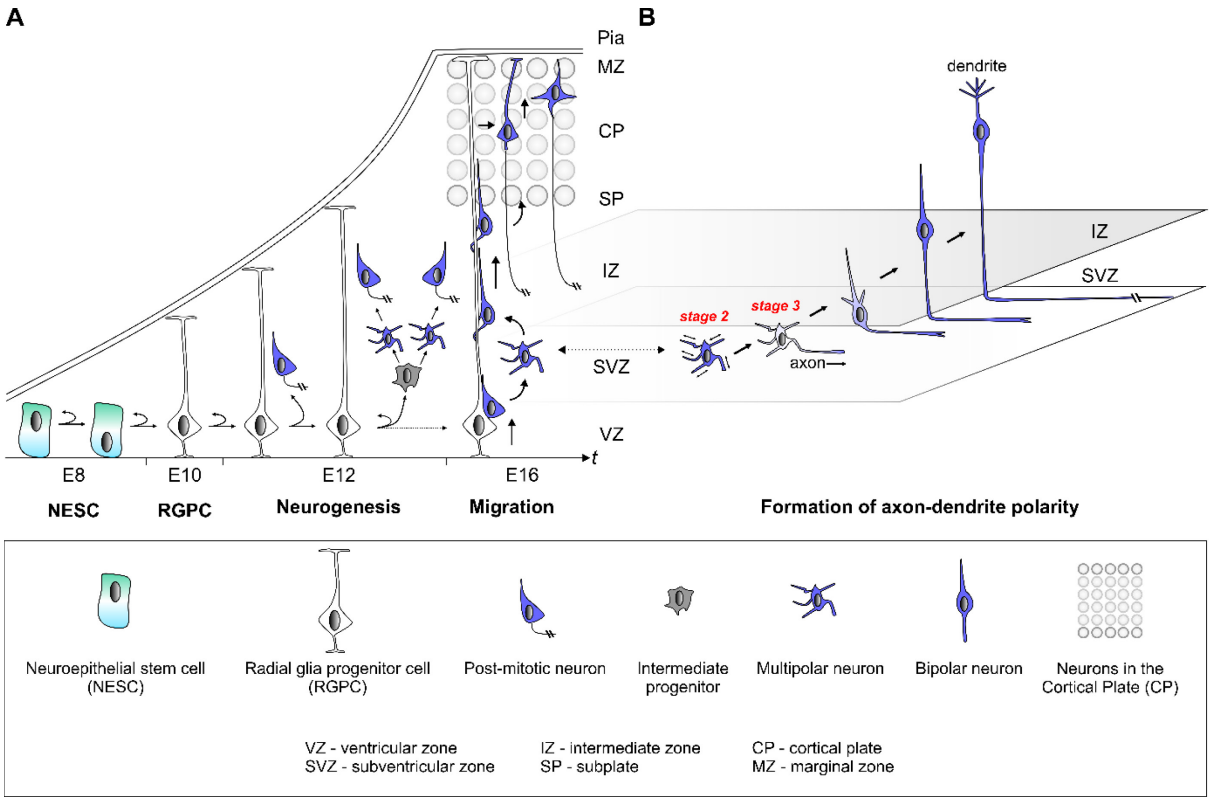

Figure 3 Establishment of cell polarity in cerebral cortex development.

(A) The early neuroepithelium is composed of highly polarized neuroepithelial stem cells (NESCs, apical-basal polarity is indicated). NESCs give rise to radial glia progenitor stem cells (RGPCs) which exhibit even more polarized cellular morphology with an extended basal process. During neurogenesis symmetric radial glia progenitor (RGP) divisions may generate two RGPs but asymmetric divisions produce a renewing RGP and a neuron or an intermediate progenitor (IP). IPs further divide symmetrically in the subventricular zone (SVZ) to produce neurons. The basal processes of RGPs serve as a scaffold for nascent post-mitotic neurons, which migrate in a step-wise fashion coupled with changes in cell polarity, from the ventricular zone (VZ)/SVZ through the intermediate zone (IZ) in order to reach the cortical plate (CP). After nascent cortical projection neurons have delaminated from the neuroepithelium at the ventricular surface they move radially away to the SVZ exhibiting bipolar (BP) morphology. Within the SVZ/IZ, neurons "sojourn" for about 24 h or longer and most adopt a multipolar (MP) morphology, extending and retracting processes in all directions. At one point fundamental cellular polarization events take place that predetermine the future axon of the neuron before the neuron again adopts a bipolar morphology and starts locomoting along the radial glial fiber through the IZ. Once reaching the subplate (SP), neurons enter the CP and migrate towards the marginal zone (MZ) where they detach from the radial glial fiber. Finally, neurons settle in their appropriate position in the CP and the leading process will eventually become the dendrite. **(B)** This panel depicts the migrating neuron from panel **(A)** in higher detail with the leading and trailing processes which eventually become the dendrite and axon, respectively.

Radial glia progenitors (RGPs) have been demonstrated to be the major neural progenitors in the developing cortex responsible for producing the vast majority of cortical excitatory neurons (Anthony et al., 2004; Borrell and Götz, 2014; Franco and Müller, 2013; Lui et al., 2011; Malatesta et al., 2000a; Noctor et al., 2001; Taverna et al., 2014). The RGP division patterns and dynamics determine the number of neurons in the mature cortex. RGP cell division during mitosis occurs at the surface of the embryonic VZ and can be either symmetric or asymmetric, which is defined by the fate of the two daughter cells (Gao et al., 2014; Homem et al., 2015; Lui et al., 2011; Taverna et al., 2014). The extrinsic and intracellular signaling cues that instruct the mode of cell division are not well understood. The directional segregation of cell fate determinants such as Notch, components of the planar cell polarity signaling module, or entire centrosomes (i.e., duplicated centrioles) in dividing neural stem cells indicates however that polarized secretion and/or trafficking is a key mechanism (Lui et al., 2011; Paridaen et al., 2013; Taverna et al., 2014; Wang et al., 2009a). Symmetric RGP divisions generate two RGPs to amplify the progenitor pool or two postmitotic neurons. In contrast, asymmetric divisions produce a renewing RGP and a neuron or an intermediate progenitor (IP). IPs can further divide symmetrically in the subventricular zone (SVZ) to produce neurons (Kowalczyk et al., 2009; Noctor et al., 2004). Interestingly, IPs adopt a multipolar morphology (Kowalczyk et al., 2009; Noctor et al., 2004) and it is currently not known whether the transition from bipolar (RGP) to multipolar (IP) state could correlate with, or even be instructive, for the neurogenic potential in dividing IPs. RGPs may also produce other types of transient amplifying progenitors, such as short neural precursors (SNPs; Stancik et al., 2010) and outer SVZ radial glial progenitors (oRGs aka basal RGs or bRGs; (Betizeau et al., 2013; Fietz et al., 2010; Florio et al., 2015; Hansen et al., 2010; Johnson et al., 2015; Kelava et al., 2012; Pollen et al., 2015; Shitamukai et al., 2011; Wang et al., 2011b)). Although oRGs like RGPs are bipolar, they have been shown to adopt different morphological states and thus likely exhibit distinct cellular polarity since they lack apical attachment at the ventricle. Distinct oRG morphologies may reflect distinct competence states with respect to the number and types of neurons which are generated (Betizeau et al., 2013). Although the above studies provide a framework of stem cell polarity and lineage progression at the cellular level (Figure 3), the underlying molecular and biochemical mechanisms of progenitor cell polarization are still poorly defined.

2.3.2 Polarity in Nascent Postmitotic Neurons — Implications for Neuronal Migration

The basal processes of RGPs serve as a scaffold for nascent cortical neurons, which migrate from the VZ/SVZ through the intermediate zone (IZ), in order to reach the cortical plate (CP; (Evsyukova et al., 2013; Rakic, 1972). Cortical layering occurs in an "inside-out" fashion whereby earlier born neurons populate deep layers and later born neurons occupy progressively upper layers (Angevine and Sidman, 1961; Rakic, 1974). Newly-born cortical neurons migrate, in a step-wise fashion coupled with changes in cell polarity, from the VZ/SVZ through IZ zone in order to reach the CP where they position themselves at their final location (Figure 3; Hippenmeyer, 2014; Marín et al., 2010; Nadarajah and Parnavelas, 2002; Noctor et al., 2004; Rakic, 1972; Tsai et al., 2005). Timelapse and videomicroscopy approaches (Noctor, 2011; Tabata and Nakajima, 2008; Tsai and Vallee, 2011) with the goal to trace the migration paths of individual cortical projection neurons have impressively revealed that: (1) radially migrating neurons proceed though several distinct migratory phases; (2) change their morphology and polarize along the way; and (3) adjust their mode of migration while transiting through the different zones along the radial migratory path ((Nadarajah et al., 2001; Noctor et al., 2004; Sekine et al., 2011; Tabata and Nakajima, 2003; Tsai et al., 2005); Figure 3). From these observations through live-imaging, it is evident that nascent migrating neurons undergo a series of morphological changes including the depolarization and repolarization within the SVZ/IZ. The molecular mechanisms controlling these morphological transitions are poorly defined but if they are perturbed or delayed, the development of the cortical cytoarchitecture may be compromised. This is in particular relevant in humans that suffer from e.g., Lissencephaly (a severe cortical malformation disorder) where the loss of LIS1 activity results in a defect to repolarize migrating neurons which in turn accumulate in ectopic positions instead of properly migrating into the developing CP (Tsai et al., 2005; Wynshaw-Boris et al., 2010). LIS1 is only one of many molecules which are involved in more than one cellular polarization process. As such LIS1 plays a role in neural progenitor polarization and in the establishment of polarity in postmitotic neurons. It will thus be important to precisely dissect the sequential and/or distinct functions of proteins orchestrating cellular polarity during development.

2.3.3 Establishment of Axon and Dendrite Compartments in Cortical Projection Neurons

After nascent cortical projection neurons, exhibiting bipolar (BP) morphology, have delaminated from the neuroepithelium at the ventricular surface they move radially away to the SVZ. Within the SVZ neurons “sojourn” for about 24 h or longer and most adopt a multipolar (MP) morphology, extending and retracting processes in all directions (Noctor et al., 2004; Tabata and Nakajima, 2003). While this stage is critical for the progression of the sequential migration program it is also essential for establishing the cellular compartments that later transform into axonal and dendritic processes. During this phase, multipolar (MP) neurons tend to migrate tangentially in an apparent random fashion (Jossin and Cooper, 2011; Noctor et al., 2004). At one point however, fundamental cellular polarization events take place that predetermine the future axon of the neuron (Barnes and Polleux, 2009) before the neuron again adopts a bipolar morphology (Figure 3). In the remainder of this review we synthesize a framework of neuronal polarization based upon *in vitro* biochemical, cell culture and genetic loss of function experiments in vivo. We reflect upon the relative contribution of extrinsic cues and cell-intrinsic molecular and biochemical signaling modules that dictate the break in symmetry and control polarization of cortical projection neurons.

2.4 Extracellular Cues Controlling Projection Neuron Polarity in Cortex Development

Developing cortical neurons can break symmetry in the absence of external cues suggesting that the role of the extracellular signals in the in vivo context is solely to activate/trigger an intrinsic symmetry-breaking pathway. The intrinsic signaling pathways on the other hand are dependent on the internal biochemical state of the cell (Figure 4 & Figure 5 and see below for detailed discussion). Albeit cell intrinsic mechanisms have received much more attention than extracellular regulatory cues it is clear that in the developing cortex, cell-to-cell interactions, the local microenvironment and long-range signaling constitute essential factors for the establishment of projection neuron polarity in vivo.

2.4.1 Cell-Cell Interactions

Nascent projection neurons are embedded in a heterogeneous environment and cell-cell interactions are likely to play an important role in neuronal polarization (Gärtner et al., 2015; Jossin, 2011; Namba et al., 2015). It has been suggested that the radial glial scaffold, on which neurons perform locomotion in the IZ, could be involved in the MP-to-BP transition. Experiments inhibiting the cell-adhesion molecule N-cadherin have shown that newly-born neurons expressing a dominant-negative form of N-cadherin establish abnormal leading processes (Gärtner et al., 2012, 2015). These experiments have also indicated that radial glial-neuron interactions mediated by N-cadherin play an essential role in the initial radial alignment of nascent neurons and thus possibly (albeit in an indirect manner) in the subsequent MP-to-BP transition. Interestingly, polarized N-cadherin localization has been shown to occur in a single neurite during MP-to-BP transition and thus likely represents one of the earliest consequences of the symmetry-break (Gärtner et al., 2012). In such context, it has been proposed that the interaction of multipolar cells and RGPs mediated by N-cadherin leads to the establishment of axon-dendrite polarity through polarized distribution of active RhoA in the neurite contacting the RGC and active Rac1 on the opposite side where the axon is formed (Xu et al., 2015). Physical interactions between pioneering axons from earlier generated neurons and the dynamic neurites from newly born neurons have been shown to contribute to polarization in MP neurons (Namba et al., 2014, 2015). These interactions involve the cell adhesion molecule transient axonal glycoprotein 1 (TAG-1). The highest expression of TAG-1 has been observed in the lower IZ (Namba et al., 2014), exactly where nascent neurons switch from MP-to-BP morphology. Current models propose that TAG-1 is expressed in both MP cells and pioneering axons and thus could mediate homophilic cell-cell contacts. Indeed, shRNA-mediated knockdown of TAG-1 results in the disruption of the MP-to-BP transition and axon specification. The underlying mechanism of TAG-1 action in polarization may involve: (1) an increase in physical tension in the immature neurite leading to axon induction and formation; and (2) contact-mediated activation of signaling molecules that instruct axon specification (Namba et al., 2015). Interestingly, N-cadherin is mainly expressed in the upper IZ (Xu et al., 2015) but TAG-1 in the lower IZ (Namba et al., 2014). Thus N-cadherin and TAG-1 could act as two separate polarity inducing cues which might work complementary in axon-dendrite formation as proposed by the Kaibuchi laboratory (Xu et al.,

2015). Whether the induction of cellular polarization within these two distinct zones correlates with a certain neuron type (e.g., derived from either RGCs or IPs) remains to be determined.

2.4.2 Secreted Factors

2.4.2.1 Reelin

Newly born cortical projection neurons migrate from the VZ to the CP in order to reach their final target area (Hippenmeyer, 2014; Marín et al., 2010). A key regulatory module controlling neuronal migration includes the Reelin pathway (Honda et al., 2011). The function of Reelin in neuronal migration has been studied extensively for decades and several hypotheses concerning the mechanism of Reelin action have been put forward (Honda et al., 2011). However, it has also become clear recently that Reelin fulfills an important role in the polarization of nascent projection neurons (Jossin, 2011; Jossin and Cooper, 2011). Reelin is mainly expressed by Cajal-Retzius cells in the marginal one (MZ) in the developing cortex (Ogawa et al., 1995). The Reelin protein primarily binds to its two cognate receptors, very low density lipoprotein receptor (VLDLR) and apolipoprotein E receptor 2 (ApoER2/LRP8; (D'Arcangelo et al., 1999)), which are mainly expressed in RGPs and nascent migrating neurons (Perez-Garcia et al., 2004). Binding of Reelin to its receptors triggers the activation of a Src family kinase (SFK) called Fyn which in turn phosphorylates the adaptor protein disabled-1 (DAB1; (Howell et al., 1997, 1999). Phosphorylated DAB1 functions as a hub for several downstream intracellular signals and has been shown to activate the effectors CRK, C3G and PI3K which in turn regulate the activity of Limk1, Akt and Rap1 to eventually modulate the dynamic cytoskeleton (Honda et al., 2011; Sekine et al., 2014). Thus the Reelin-DAB1 pathway translates extracellular cues into cytoskeletal changes in migrating neurons (Förster et al., 2010; Frotscher, 2010). How Reelin might regulate dynamic polarization events in nascent cortical projection neurons is less well understood. Interestingly however, it has been shown that while VLDLR is mainly localized on the leading processes of migrating neurons in the MZ, ApoER2 is primarily localized to neuronal processes and the cell membranes of multipolar neurons in the SVZ and lower IZ. In addition to strong expression of Reelin in the MZ, it was also demonstrated that Reelin is also expressed in the IZ at early developmental stages (Hirota et al., 2015). Ex vivo experiments where exogenous Reelin was

added to cultured brain slices have shown an effect on the morphology and dynamic behavior of nascent neurons in the IZ (Britto et al., 2014). Thus, based on the expression pattern of Reelin and its cognate receptors it is conceivable that Reelin could play a prominent role during the polarization process of nascent cortical projection neurons. Indeed, Jossin and Cooper propose a three step model (Jossin and Cooper, 2011) how Reelin controls the radial orientation of multipolar neurons in SVZ/IZ. First, multipolar neurons migrate tangentially in a stochastic manner in the SVZ/IZ until they encounter Reelin which leads to the activation of the small GTPase RAP1, likely via pDAB1-CRK/CRKL-C3G signaling (Ballif et al., 2004; Voss et al., 2008). Next, active RAP1 triggers an increase of the surface level of N-Cadherin in multipolar neurons. These increased cell surface levels of N-Cadherin could then allow the multipolar neurons to sample local microenvironmental cues which then could initiate the break in symmetry and induce polarization. The cortical projection neurons then progressively exit the multipolar stage and adopt a bipolar morphology (Jossin, 2011; Jossin and Cooper, 2011). Altogether, the above data and model indicates that Reelin acts as a critical cue for the directional movement of nascent migrating cortical projection neurons and could serve as a critical extracellular cue for modulating polarization of nascent migrating cortical projection neurons. It will be intriguing to decipher the precise intracellular and biochemical signaling pathways controlling RAP1-dependent N-Cadherin trafficking and how N-Cadherin-dependent signaling triggers the break in symmetry.

2.4.2.2 **Neurotrophins**

Brain derived neurotrophic factor (BDNF) and neurotrophin-3 (NT-3) are highly expressed in the developing brain and have been shown to stimulate axon specification and elongation (Morfini et al., 1994; Nakamuta et al., 2011). Both, BDNF and NT-3 as extracellular regulators of neuronal polarity are of special interest since they act in an autocrine and/or paracrine manner in cell-culture (Nakamuta et al., 2011). This feature indicates that neurons are able to produce extracellular stimuli (in form of secreted neurotrophins) that activate the intrinsic machinery for axon-dendrite specification in a cell-autonomous and non-cell-autonomous manner. BDNF and NT-3 bind to tropomyosin related kinases receptors (TRK), TRK-B and TRK-C respectively (Chao, 2003). Upon TRK receptor binding, the small GTPase Ras and PI3K are activated. This leads to the production of phosphatidylinositol (3,4,5)-trisphosphate (PIP3)

and the activation of its downstream signaling pathways (Reichardt, 2006). Neurotrophin signaling through TRK receptors also leads to increased levels of inositol triphosphate (IP3)-induced calcium release which in turn activates the calmodulin-dependent protein kinase kinase (CaMKK) and calmodulin-dependent protein kinase I (CamKI; (Nakamuta et al., 2011). The activation of CaMKK and CamKI triggers the phosphorylation of microtubule affinity regulating kinase 2 (MARK2). This leads to the phosphorylation of downstream microtubule associated proteins (MAPs) MAP2/4, Tau and DCX which reduces microtubule stability (Drewes et al., 1997; Nakamuta et al., 2011; Schaar et al., 2004). Interestingly, acute knockdown of MARK2 has been shown to stall MP-to-BP transition in the IZ in mice (Sapir et al., 2008). Thus, proper regulation of MARK2 appears to be essential for neuronal polarization in vivo.

BDNF signaling via TrkB has been demonstrated in culture experiments to lead to the activation of LKB1 (liver kinase b1 in mammals and PAR-4 in C. elegans (Figure 4 & Figure 5; (Shelly et al., 2007)). Loss of function of LKB1 either by genetic knockout or knockdown by shRNA in nascent cortical projection neurons results in striking phenotypes: axon specification is completely abolished while the dendrite appears to still be specified (Barnes et al., 2007; Shelly et al., 2007). In contrast, overexpression of LKB1 in neural progenitors and postmitotic neurons lead to formation of multiple axons. In a biochemical pathway downstream of BDNF/TrkB, LKB1 is phosphorylated by protein kinase A (PKA) or ribosomal S6 kinase (p90RSK) at Serine 431 (Collins et al., 2000; Sapkota et al., 2001). Phosphorylated LKB1 leads to downstream activation of MARK2 (Shelly et al., 2007) and the SAD kinases which in turn phosphorylate Tau-1 (Barnes et al., 2007; Kishi et al., 2005). Remarkably, SAD-A/B double knockout precisely mimic the LKB1 loss of function phenotype with complete absence of the axon (Kishi et al., 2005). In summary, the above studies established a model whereby BDNF signaling via TrkB results in the activation of LKB1 which is translated into an intracellular symmetry break in multipolar cortical projection neurons while sojourning in the SVZ/IZ. Phosphorylated LKB1 localizes into the nascent axon and is required for axon extension and development. It will be interesting to determine the extent of specificity and functional redundancy of individual downstream components along the BDNF/TrkB-LKB1-SAD-A/B signaling module while executing the break in symmetry.

2.4.2.3 **Semaphorins**

Semaphorins consist of a large family of membrane bound or secreted proteins (Nakamura et al., 2000). The secreted semaphorin, Sema3A have been shown to act as a chemotactic factor for migrating cortical projection neurons (Chen et al., 2008; Polleux et al., 2000). Sema3A expression is highest near the pial surface in the developing cortex and the Sema3A expression domain establishes a descending gradient across the emerging cortical layers (Chen et al., 2008; Polleux et al., 2000). Sema3A binds its co-receptors Plexin and Neuropilin (Negishi et al., 2005) and it has been suggested that Sema3A may actively control the process of symmetry breaking and cellular polarization. Sema3A activates a number of downstream cascades resulting in the tuning of relative levels of cGMP and cyclic adenosine 3´,5´-monophosphate (cAMP) which negatively affects axon formation by downregulation of PKA-dependent phosphorylation of LKB1 (Shelly et al., 2011). Interestingly, exposure of undifferentiated neurites to local sources of Sema3A in hippocampal neuron cell culture leads to the suppression of axon-formation but promotion of dendrite formation in culture conditions (Shelly et al., 2011). Strikingly, in vivo knockdown of the Sema3A receptor neuropilin-1 in rat embryonic cortical progenitors results in severe polarization defects. Furthermore, Sema4D inactivates Ras (Oinuma et al., 2004) while it activates RhoA (Swiercz et al., 2002) which prevents axon formation and/or outgrowth via reduced actin dynamics and actin contraction. Thus, Sema3A acting via the neuropilin-1 receptor and semaphorins in general are critically involved in the symmetry break and polarization of nascent projection neurons in the developing cortex (Shelly et al., 2011).

2.4.2.4 **TGF-β**

The transforming growth factor β (TGF-β) has been reported to play an important role in the polarization of nascent cortical projection neurons in the developing cerebral cortex (Yi et al., 2010). Upon binding of one of the three TGF-β ligands (TGF-β1-3) to the type II TGF-β receptor (TβR2), this receptor is recruited to the type I TGF-β receptor (TβR1) to form a complex which triggers the phosphorylation of the two receptors by the serine/threonine kinase domain (Shi and Massagué, 2003). The TβR2-TβR1 receptor complex has been shown to phosphorylate Par-6 which in turn regulates Cdc42/Rac1 activity by recruiting the ubiquitin ligase Smurf1 which promotes proteasomal degradation of the RhoA GTPase. This results in reduced activity

of RhoA in the nascent axon thereby stimulating its outgrowth (Gonzalez-Billault et al., 2012). Thus, RhoA activity can be precisely regulated in response to TGF-β signaling thereby controlling the dynamics of the local actin organization which is essential for axon specification and thus cellular polarization (Yi et al., 2010). Interestingly, TGF-β2-3 is highly expressed near the VZ/SVZ. Thus nascent developing neurons could be exposed to a gradient which delivers a uniform stimuli for axon specification (Yi et al., 2010). However, the majority of MP neurons extend their axons tangentially (Hatanaka and Yamauchi, 2013) rather than towards the ventricular side. It is thus conceivable that TGF-β might only act as a stimulus for axon specification rather than an axon guidance cue (Yi et al., 2010). Bone morphogenic protein (BMP), also a member of the TGF-β superfamily appears to play important functions in the MP-to-BP transition as well. BMPs are known to signal via the intracellular downstream mediator SMAD which leads to the suppression of collapsin response mediator protein 2 (CRMP2), a transcription factor known to promote microtubule assembly (Shi and Massagué, 2003; Sun et al., 2010). Strikingly, upon suppression of CRMP2 or overexpression of dominant negative forms of CRMP2 multipolar cells accumulate in the SVZ/IZ in the developing cortex. While these findings suggest that a BMP-SMAD signaling pathway, via CRMP2, regulates the polarization of cortical projection neurons the precise molecular and biochemical mechanisms remain to be determined (Sun et al., 2010). Altogether, different members of the TFG-β superfamily play important roles in multipolar cortical neurons and direct neuronal polarization through distinct signaling pathways.

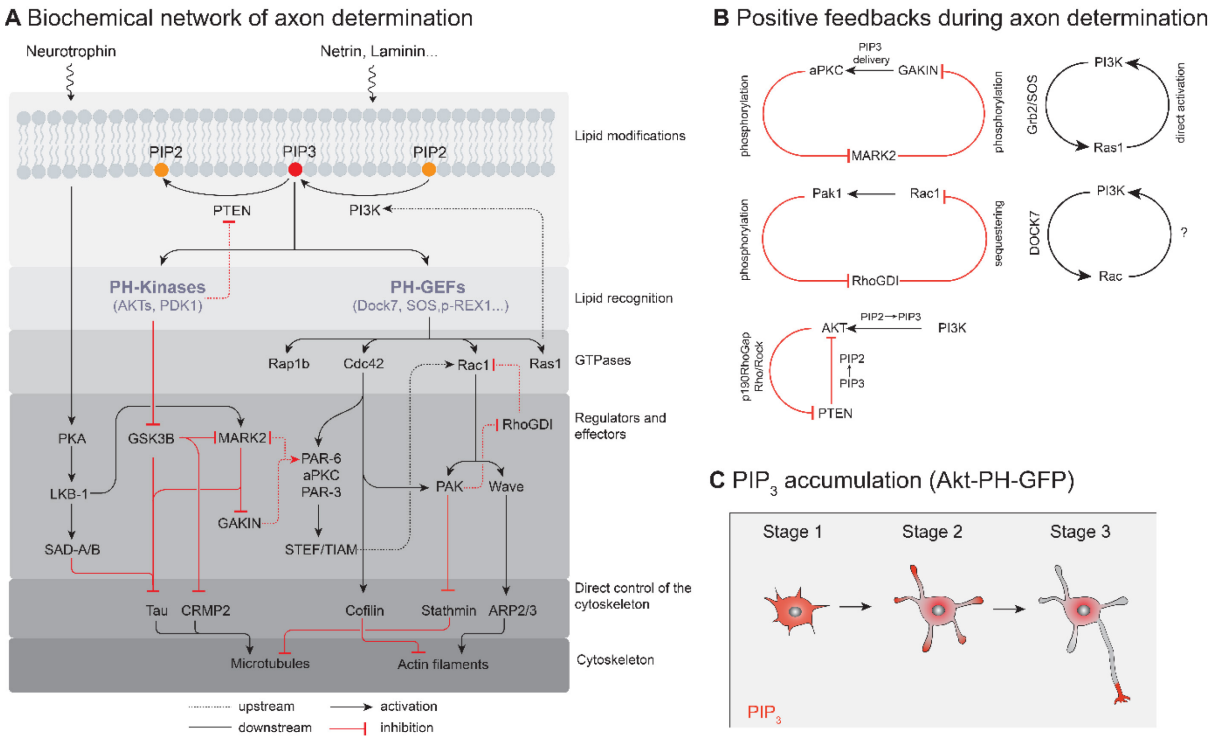

Figure 4 Molecular signaling pathways controlling neuronal polarization.

(A) A simplified illustration of the biochemical network of axon determination. Only interactions localized to the nascent axon are shown. **(B)** Positive feedback loops in the process of axon determination. **(C)** Probing PIP_3 localization and accumulation in polarizing neurons with Akt-pleckstrin-homology (PH)-GFP as a probe for PIP_3.

2.5 Intrinsic Biochemical Networks That Mediate Neuronal Polarity

While the above sections illustrated the role of extracellular cues for triggering and/or execution of neuronal polarization, the intrinsic molecular mechanisms involved in symmetry breaking will be discussed in the sections below with a focus on *in vitro* and cell culture experiments. Isolated neurons in cell culture form one axon and several dendrites. External chemical or physical cues of instructive or antagonistic nature that determine axon formation have been identified (Gomez et al., 2007; Lamoureux et al., 2002; Shelly et al., 2011). However, cultured neuronal cells are able to polarize even in the absence of any external cue (Dotti et al., 1988) suggesting that cells have intrinsic ability to break symmetry, which is solely activated externally. What are the functional cell-intrinsic networks that underlie cell polarization and determine the biochemical state of the cell? Based on Turing's idea of a reaction-diffusion mechanism to explain how spatial order during embryogenesis may arise

(Turing, 1990), Gierer and Meinhardt developed a conceptual framework for pattern formation, which is based on the local activation in the form of self-enhancing feedback, which amplifies and reinforces spatially asymmetric distributions of molecules, coupled to long-range inhibitory processes (Meinhardt and Gierer, 2000). While this concept was originally developed to explain spatial patterning during morphogenesis, it also provides a framework to understand cell polarity. Accordingly, cell polarization is seen as a self-organized process (Wennekamp et al., 2013), which involves local symmetry breaking, signal amplification and long-range inhibition (Chau et al., 2012; Wang, 2009).

Previous work was able to identify many molecular players involved in the processes that allow a neuron to choose the one neurite to become an axon (Barnes and Polleux, 2009). While cell polarization can theoretically arise from a single molecular species that features a positive feedback (Altschuler et al., 2008), symmetry breaking in neurons likely reflects interactions among multiple, partially redundant pathways with crosstalk among them (Namba et al., 2015). This network can be subdivided into several, partially overlapping modules, each of which comprises a subset of molecular players that encode for specific cellular functions. To a rough approximation, the output of one module can serve as the input for a module downstream. Here, we want to illustrate how these functional modules orchestrate neuronal polarization and how they are embedded in a more complex biochemical network giving rise to axon specification. Importantly, individual modules are often evolutionarily conserved among species and pathways that regulate cell polarization in seemingly distinct tissues and contexts are remarkably similar. Accordingly we can to some degree take advantage of known cell polarization concepts in yeast, C. elegans and migrating cells (Iden and Collard, 2008), with the goal to anticipate a better understanding of the molecular processes that underlie axon specification.

2.5.1 PIP/PI3K Module

Molecules involved in the initial symmetry breaking event are commonly localized to the plasma membrane, where not only integral membrane proteins receive extracellular signals, but where also peripherally binding membrane proteins bind reversibly to the membrane (Cho and Stahelin, 2005). This restricts the diffusion of these proteins, increases the efficiency of protein-protein interactions and/or modulates their catalytic activity (Ebner et al., 2017;

Leonard and Hurley, 2011; Vaz et al., 1984). As a result, the membrane can be interpreted as a computational platform where transient protein clusters integrate, interpret and amplify incoming biochemical signals (Groves and Kuriyan, 2010).

One component of membrane-based signaling pathways that was found to be essential for the establishment of intracellular organization include phosphoinositides (PIPs). Even though they represent only about 1% of membrane phospholipids (Di Paolo and De Camilli, 2006), the associated signaling pathways control cell growth, division, survival and differentiation, and allow to generate highly polarized neuronal morphologies such as growth cones and synapses (Sasaki et al., 2007). Cells use a precisely defined spatiotemporal distribution of PIPs to control the activity of intracellular signaling pathways. For cell polarity, it is the asymmetry of phosphatidylinositol-3,4,5-phosphate (PI(3,4,5)P3 = PIP3) at the plasma membrane that is used to establish a polarity axis in the cell. The intramembranous PIP3 concentration is controlled by activation of the phosphoinositide-3-kinase (PI3K; (Whitman et al., 1985)) as well as phosphatases such as phosphatase and tensin homolog (PTEN; (Lee et al., 1999)) that directly antagonize PI3K by dephosphorylating PIP3 to PI(4,5)P2 (PIP2) (Carracedo and Pandolfi, 2008). Overexpression of PTEN or inhibition of the PI3K were both found to abolish cell polarization and axon specification (Jiang et al., 2005; Shi et al., 2003). In contrast, reduction of PTEN expression results in neurons with multiple axons (Jiang et al., 2005). Together, these results demonstrate that the activities of these enzymes need to be tightly balanced to produce one and only one axon.

Since polarization is a dynamic spatiotemporal process, not only the total amount of phosphoinositides but also their distribution in space and time needs to be precisely regulated. In cells, the intracellular distribution of PIP3 can be visualized using a fluorescent reporter protein that specifically binds to PIP3; e.g., GFP fused to the Pleckstrin-homology (PH) domain of the serine/threonine kinase Akt (Gray et al., 1999). This probe visualized PIP3 accumulation at the tip of a neurite contributing to neuronal polarity and axon specification (Ménager et al., 2004). In contrast, EGFP-PLCd1-PH, which binds to PI(4, 5)P2 or IP3 showed a homogeneous distribution in cultured neuronal cells (Ménager et al., 2004).

The localized accumulation of PIP3 likely represents the first spatial landmark that establishes the polarity axes of the cell. In vivo, activity of PI3K and PIP3 production is most likely regulated by asymmetric distribution of extracellular factors (Namba et al., 2015), still,

neurons polarize in cell culture without obvious asymmetries in their environment (Dotti et al., 1988). This suggest that starting from a homogeneous distribution of signaling molecules, dedicated biochemical circuits are able to amplify small fluctuations of signaling lipids in the plasma membrane. These interactions eventually break the symmetry of the cell and control cell morphogenesis (Wennekamp et al., 2013). The biochemical network underlying phosphoinositide polarity was studied in detail in other model systems. For example, Dictyostelium discoideum cells (Malchow et al., 1973), leukocytes and neutrophils (Trepat et al., 2012) polarize in response to a gradient of the chemoattractant cAMP or a variety of chemokines respectively by establishing domains of different phosphoinositides: PIP3 at the leading edge of the cell and PIP2 at its tail (Petrie et al., 2009). Importantly, and similar to neurons, the ability to break symmetry is independent from directional sensing, as cells that are placed in a uniform distribution of chemoattractant are still able to polarize (Petrie et al., 2009). Again, this illustrates the intrinsic ability of biochemical networks to polarize the cell in the absence of exogenous spatial signals (Wedlich-Soldner and Li, 2003). While phosphoinositide signaling was found to spatially organize the actin cytoskeleton, the initial symmetry breaking event itself does not depend on actin filaments. Fluorescently-labeled PH_{Akt} and PTEN, which acted as probes for PIP3 and PIP2 respectively, were found to self-organize into traveling waves in Dictyostelium discoideum cells even in the presence of the actin polymerization inhibitor latrunculin A (Gerisch et al., 2012). Importantly, this finding indicates that the ability to break symmetry in the membrane is established upstream and independent of the cytoskeleton. Instead, a PIP3-dependent negative regulation of PTEN recruitment to the membrane was suggested to allow PIP3 to accumulate. In addition, PTEN localization and activity has been found to be dependent on the small GTPase RhoA, which was found to restrict PTEN to the rear of chemotaxing leukocytes (Li et al., 2005) and Dictyostelium cells. Arai et al., 2010 further suggest a Ras-dependent positive feedback of PI3K activity to stabilize the polarized state of the cell. In addition, negative regulation of PTEN activity downstream of the PIP3 activated AKT kinase has been reported, which constitutes a parallel mechanism to maintain and stabilize polarity (Papakonstanti et al., 2007).

While phosphoinositides are the most important lipid species for cellular signaling there are also other lipid species involved in neuronal polarization: plasma membrane ganglioside sialidase (PMGS), which controls the ganglioside content in the plasma membrane

of neurons was also found to show an asymmetric distribution of its activity: it is enriched in one of the stage 2 neurites and facilitates axon outgrowth by enhancing Rac and PI3K activity (Da Silva et al., 2005). Thus, the asymmetric distribution of two different kinds of lipid species appears to control the polarity of the cell.

2.5.2 GEFs and Small GTPases

Which biochemical circuits underlie signal amplification in neurons? By now, the identity of several PI3K-dependent GTPases involved in neuronal polarization is known, such as H-Ras (Yoshimura et al., 2006a), Cdc42 (Garvalov et al., 2007) or Rap1B (Nakamura et al., 2013; Schwamborn and Püschel, 2004). Similar to PI3K (Shi et al., 2003) their overexpression results in supernumerary axons (see Figure 5), while their knock down prevents axon formation (Garvalov et al., 2007; Nakamura et al., 2013; Schwamborn and Püschel, 2004; Yoshimura et al., 2006a), however, these proteins do not interact with PIP3 themselves. Instead, the phosphorylation state of phosphoinositides in the plasma membrane is recognized by soluble guanine nucleotide exchange factors (GEFs) that contain PIP3 binding domains, such as GEFs of the Dbl and DOCK180 families (Laurin and Cote, 2014; Rossman et al., 2005). These protein families in turn activate GTPases while recruiting them to the membrane (Cherfils and Zeghouf, 2013). Though a systematic characterization of GEFs that directly interact with PIP3 and control cell polarization is not complete yet, candidate proteins include SOS and RasGFR, both members of the Dbl family of GEFs that contain a canonical DH-PH domain structure (Zheng, 2001). The PH (Pleckstrin homology) domain binds to phosphoinositides and thereby controls localization and the DH (Dbl homology) domain is responsible for catalyzing nucleotide exchange (Zheng, 2001). Dock7, a Dock180 related protein that catalyzes the nucleotide exchange of Rac1 (Watabe-Uchida et al., 2006), was found to specifically bind PIP3 via its DHR-1 domain (Côté et al., 2005; Kobayashi et al., 2001). Importantly, Dock7 is enriched in one of the stage 2 neurites—potentially the designated axon—supposedly controlling polarization and morphogenesis of the neuron (Watabe-Uchida et al., 2006). Controlled by these regulators, small GTPases can show phosphoinositide dependent activity patterns and a characteristic spatial distribution in the cell. However, direct evidence that GEF enrichment is a direct consequence of elevated PIP3 levels in a stage 2 neurite is largely missing.

Accordingly, the spatial distribution of GEFs could also depend on another PIP3 binding protein which is recruited to and initiates a nascent axon.

As a result of their activation, GTP-bound GTPases engage in specific protein-protein interactions. By recruiting so-called effector proteins to the plasma membrane small GTPases determining the spatiotemporal activation pattern of other protein systems in the cell (Cherfils and Zeghouf, 2013). Effector proteins can be categorized in two classes: first, they can control cell morphology by directly acting on regulators of the actin or microtubule cytoskeleton, namely by increasing actin dynamicity and microtubule stabilization in the axon while stabilizing actin filaments in dendrites (Neukirchen and Bradke, 2011). For example, activation of Rac1 leads to a stabilization of axon microtubules via the stathmin pathway (Watabe-Uchida et al., 2006) while triggering actin remodeling (Gonzalez-Billault et al., 2012; Hall et al., 2001). In contrast, active RhoA promotes actin stabilization and contraction in dendrites as revealed by fluorescent activity sensors (Gonzalez-Billault et al., 2012). Second, effector proteins can be involved in the regulation of other small GTPases (DerMardirossian et al., 2004) or constituents of supramolecular complexes with various functions (Joberty et al., 2000; Lin et al., 2000). For example, they can act as coincidence detectors for multiple binding partners (Carlton and Cullen, 2005) or signal to additional levels of regulation. For example, a common theme for the activation of small GTPases is that they comprise positive feedback loops. These self-amplifying circuits may not only lead to a local enrichment of GTPases on the membrane, but can also lead to collective, switch-like activation of proteins (Mizuno-Yamasaki et al., 2012). Accordingly, these kind of interactions can give rise to nonlinear signaling circuits with emergent properties, which can be crucial for breaking the symmetry and spatially organizing the cell (Yoshimura et al., 2006b).

The importance of positive feedback regulation for the symmetry breaking is probably best characterized in single-cell organisms such as yeast (Johnson et al., 2011). Despite the much lower complexity of this model organism, the general architecture of the biochemical network leading to cell polarization is most probably similar. In yeast, Cdc42 is the main spatial organizer of the cell as it regulates asymmetric cell division. Active, GTP-bound Cdc42 binds to the plasma membrane via its prenylated C-terminus, while GDP-bound Cdc42 is kept soluble in the cytoplasm via its interaction with its Guanosine nucleotide dissociation inhibitor (GDI) Rdi1. Cdc42-GTP is thought to form a locally confined protein cluster on the membrane

by a local amplification of spontaneous asymmetries. The positive feedback is thought to arise from an effector-GEF complex, where the activated GTPase recruits an effector protein that in turn interacts with its activator. In yeast, a small, transient patch of Cdc42-GTP would recruit the scaffolding protein Bem-1 to the membrane, which interacts with the Cdc42 GEF Cdc24. Bem-1 not only binds to Cdc24 but also boosts its GEF activity. Thus Bem-1 efficiently catalyzes proximal Cdc42-GDP to exchange their nucleotide to Cdc42-GTP which again is able to recruit more Bem-1-Cdc24 complex (Gulli et al., 2000; Johnson et al., 2011; Nern and Arkowitz, 1998). Effector-GEF interactions have been found to be involved for the regulation of many different small GTPases (Mizuno-Yamasaki et al., 2012) and might be generally required for collective, switch-like activation of GTPases. These kind of decisive signaling reactions are of crucial importance for the cell, as they not only lead to cell polarization, but also regulate other fundamental processes such as membrane trafficking and the dynamic properties of the actin and microtubule cytoskeletons, thereby controlling the morphogenesis of the cell.

While the role of many proteins involved in neuronal polarity has been studied in neuronal cell culture, the function of Cdc42 has also been studied *in vivo* (Garvalov et al., 2007). Only about 30% of neurons derived from Cdc42 null mice were able to form a Tau-1 positive axon and the activity levels of the actin regulator cofilin were disturbed. However, when axon formation in Cdc42 null cells was initiated by cytochalasin, axons formed even if the drug was washed away. This indicates that Cdc42 is needed for the initial steps of axon specification but is dispensable for axon outgrowth (Garvalov et al., 2007).

Figure 5 Table of key polarity proteins in *C. elegans* and their neuronal homologs.

The localization of the nematode proteins is illustrated according to their anterior or posterior domain affiliation. In neurons the respective localization is classified according to the indicated patterns (A–C). A supernumerary axon phenotype is indicated by a plus sign, while 0 represents the absence of an axon upon overexpression or downregulation of the respective polarity protein. References describing neuronal protein systems are marked with an asterisk.

2.5.3 The PAR System

During cell polarization, the asymmetric distribution of phosphoinositides provides an initial signal to a number of protein systems that together control cell morphogenesis. One of those protein systems is the PAR system, which is recruited downstream of activated Cdc42 (Etienne-Manneville and Hall, 2001; Nishimura et al., 2005; Yamanaka et al., 2001). The PAR system is a set of highly conserved proteins that organize cell polarity in all metazoan cells. In neurons, it was found that the PAR system is required for axon dendrite polarity (Chen et al., 2006; Shi et al., 2003), migration (Sapir et al., 2008) and dendrite development (Terabayashi et al., 2007). However, a complete mechanistic characterization of how these proteins regulate axon formation is missing.

The PAR system is probably best studied in the nematode Caenorhabditis elegans, where it controls the first division. In a single cell embryo, the PAR proteins self-organize into two non-overlapping domains (anterior and posterior domain) to govern asymmetric spindle positioning and ultimately the generation of daughter cells with different fate (Gönczy and Rose, 2005; Kemphues et al., 1988). The PAR proteins have been categorized in anterior PARs (aPARs; PAR-3, PAR-6, PKC-3, cdc42) and posterior PARs (pPARs; PAR-2, PAR-1, LGL-1), all of which are peripheral membrane proteins. Their mutual exclusion is thought to arise from cross-phosphorylation by the two kinases PKC-3 and PAR-1, which leads to membrane detachment, controls oligomerization state and hence their diffusivity (Arata et al., 2016; Feng et al., 2007; Hoege and Hyman, 2013). PKC-3 can phosphorylate all posterior PARs (Hao et al., 2006; Hoege et al., 2010), in return, PAR-1 phosphorylates PAR-3 (Benton and Johnston, 2003; Guo and Kemphues, 1995; Motegi et al., 2011). A network of regulatory biochemical interactions between aPARs and pPARs is thought to finely tune the activity of these kinases, leading to two dynamically stable cellular domains that govern a plethora of downstream events (Goehring, 2014).

Apart from PAR-2, the PAR system is conserved among most multicellular organisms and defines polarity via mutual exclusion in different contexts such as anterior-posterior polarity in Drosophila oocytes and apical-basal polarity in epithelial tissues (Goldstein and Macara, 2007; Morton et al., 2002; Thompson, 2013). The overall importance of the PAR system for axon dendrite polarity was firmly established in dissociated hippocampal cell culture system and enrichment of anterior PARs at the tip of the outgrowing axon has been

observed (Shi et al., 2003). Subsequent knock down or overexpression studies of several PAR members showed that genetic manipulation of the PAR system either results in no or supernumerary axons (Figure 5). If mutual exclusion among aPARs and pPARs is a universal feature of the PAR system one would expect the posterior PAR-1 homolog MARK2 to be absent from the tip of the axon. Surprisingly, fluorescence sensors to measure MARK2 activity in the developing axon of cortical neurons showed highest kinase activity in the growing axon tip (Moravcevic et al., 2010; Timm et al., 2011). This indicates that both active PAR-1 kinases and aPARs are co-localizing at tip of the outgrowing axon and mutual exclusion of the "opposing" PAR complexes is not a requirement for axon dendrite polarity establishment. On a functional level, antagonism between MARK2 and the aPAR complex has been suggested (Chen et al., 2006). Analog to the C. elegans system, aPKC phosphorylates MARK2, which results in membrane detachment and most likely in reduced activity. Overexpression of MARK2 in hippocampal neurons prevented axon formation while knock down caused multiple axons (Chen et al., 2006; Wu et al., 2011). The opposite was seen for aPKC overexpression, which resulted in multiple axons (Figure 5; Parker et al., 2013). The overexpression phenotype of MARK2 was rescued by simultaneous overexpression of aPARs. No rescue was observed with a non-phosphorylatable MARK2, indicating that direct inhibition of MARK2 by aPKC is responsible for the observed rescue. In a simple view, this could mean that MARK2 is a negative regulator of axon formation which is specifically inhibited by axon enriched aPARs via aPKC phosphorylation. However, *in vivo* knock out of the other PAR-1 homologs (SAD-kinases) also inhibited axon formation (see also above), indicating that a fine balance between these activities is needed (Kishi et al., 2005). Both, MARK2 and SAD kinases have to be activated by LKB1/PAR-4 (Lizcano et al., 2004; Shelly and Poo, 2011), which itself is downstream of cAMP/PKA signaling (Shelly et al., 2007). Thus, the PAR system not only translates PIP3 dependent signaling into altered cytoskeleton dynamics but also integrates the input of heterotrimeric G protein receptor ligands. Interestingly and in contrast to C. elegans, LKB1/PAR-4 is enriched in the axon (Shelly et al., 2007) while it is homogenously distributed in the C. elegans zygote (Goehring, 2014). Knockdown of LGL-1 prevents axon formation but the precise role of LGL-1 in axon development is still poorly understood (Plant et al., 2003; Wang et al., 2011a).

Another fundamental difference between the neuronal and nematode PAR system is their dependence on a previous symmetry breaking event. In C. elegans, the sperm entry marks a single symmetry breaking event that starts actomyosin based flows and facilitates PAR domain establishment whereas no asymmetries of PIP3 have been reported. The PAR system in neurons is clearly downstream of regulators that directly control or are controlled by PIP3, such as PI3K or ATK/GSK3b, Cdc42 and Rap1B (Insolera et al., 2011), whereas initial polarity formation in C. elegans does not depend on these PIP3 controlled proteins (Insolera et al., 2011; Schlesinger et al., 1999). A possible explanation for this difference could be that neurons have to screen their environment during development (open systems) to remain a certain degree of plasticity while communication with the extracellular space is less important in the early stages of worm development. Thus, the PAR system is integrated into a more complex signaling network in neurons while it constitutes a rather autonomous polarity system in C. elegans. Since many PAR system intrinsic reactions (like phosphorylation events) seem to be conserved, it is still not clear how these reactions have to occur in space and time in neurons for faithful axon dendrite polarity establishment. Super resolution microscopy and higher temporal resolution of simultaneous activity monitoring of PARs and PIP3 may be required to solve the question of how PARs fulfil their functions during neuronal development.

2.5.4 Closing the Loop

So far, we have only considered biochemical reactions downstream of an initial asymmetry of PIP3. For robust symmetry breaking, a self-enforcing loop is required, which would give rise to a local accumulation of PIP3 despite its rapid diffusion in the plasma membrane and the proteins in the cytoplasm. One possible functional network could originate from PIP3 and at the same time further increase its local concentration on the membrane. Therefore, the described functional modules need to talk to each other and eventually feed back to the activity of PI3K.

The molecular players involved for this regulatory network could for example be GTPases or their GEFs and effector proteins, which would not only translate local PIP3 enrichment into altered cytoskeleton dynamics and transport, but themselves further enhance the activity of PI3K. For example, Ras-GTP (Sasaki et al., 2004) and Rac1-GTP

(Srinivasan et al., 2003) in combination with actin polymerization (Peyrollier et al., 2000; Wang et al., 2002) or via additional players like the Par6/Par3 aPKC complex where found to activate PI3K (Laurin and Cote, 2014; Motegi et al., 2011). Indeed, these proteins were all found to be required for axon formation (Shi et al., 2003; Tahirovic et al., 2010; Yoshimura et al., 2006a). H-Ras is a direct activator of PI3K and is also activated downstream of PI3K (Rodriguez-Viciana et al., 1994; Yang et al., 2012). Interestingly, this feedback loop results in H-Ras translocation via vesicle based transport into the future axon, which depletes H-RAS from the other neurites, presumably leading to reduced PI3K activity in other neurites and subsequently to inhibition of their outgrowth (Fivaz et al., 2008). While the idea of this amplifying circuit is at least partially based on experimentally verified protein-protein interactions, the emergent properties of this network have not been tested yet. For example, the role of PTEN localization and activity for phosphoinositide polarization in neurons is not yet clear (Kreis et al., 2014) and there might be functional networks that involve either less or a different set of molecular players. Furthermore, the connectivity of those circuits could even change with time, different extracellular inputs or in different subcellular locations.

Another layer of regulation can also be performed on the level of GDP dissociation inhibitors (GDIs), whose main function is to maintain their target, lipid-modified GTPases in an inactive, soluble state (Cherfils and Zeghouf, 2013). There is evidence that the affinity of RhoGDIs for different GTPases can be modulated by phosphorylation. For example, the kinase PAK1 is an effector protein of Rac1 that was found to phosphorylate RhoGDIs (DerMardirossian et al., 2004). Phosphorylation of these GDIs can enhance the dissociation of Rac1 from the GDI complex, thereby increasing the rate of Rac1 activation. As this leads to further stimulation of PAK1 activity such interaction may give rise to another positive feedback and symmetry breaking in neurons (Figure 4B).

Finally, and in addition to molecular processes that depend on locally confined phosphorylation and dephosphorylation of PIPs, PIP3 can also accumulate in the outgrowing axon with the help of directed microtubule-based transport. For example, the plus-end directed kinesin-like motor Gakin transports PIP3-containing vesicles through the interaction with the adaptor protein α-centaurin (Horiguchi et al., 2006). MARK2, a homolog of PAR-1, inhibits this transport by phosphorylating Gakin thereby preventing the development of axons (Yoshimura et al., 2010). MARK2 itself is deactivated by the PIP3-regulated kinase aPKC (Chen

et al., 2006; Ivey et al., 2014). Thus a high local PIP3 concentration could inhibit MARK2 in the axon shaft, further enhancing directed transport of PIP3-containing vesicles to the growth cone. Accordingly, this could result in a self-perpetuating feedback loop supporting axon outgrowth (Yoshimura et al., 2010).

Collectively, these feedback loops stabilize polarity that can arise from short-lived local concentration fluctuations of external signals, temporal fluctuations in the output signal strength of receptors (Ladbury and Arold, 2012) or subtle heterogeneities on a coverslip. These small differences then lead to high and persistent activity of modulators that favor actin dynamicity and microtubule stability in the designated axon. Studies using drugs that either stabilized microtubules (Witte et al., 2008) or destabilized actin filaments (Bradke and Dotti, 1999) are sufficient to induce the formation of multiple axons, consistent with the view that the effects of the above mentioned circuits are transmitted via selective modulation of the cytoskeleton. In particular, these are the MARK2/SAD target and microtubule stabilizing tau proteins, microtubule destabilizers such as stathmin, actin dynamics modulators cofilin and WAVE and/ or inactivation of regulators that prevent axon outgrowth such as the RhoA/Rock module. This ultimately gives rise to a permanent molecular difference between axon and dendrites that will later on be manifested in a functional/electrophysiological difference of the two compartments, axon and dendrites. How this compartmentalization is maintained is not well understood and probably also relies on long range inhibitory signals, but future research will be needed to entangle the exact communications of these compartments during neuronal development.

2.6 Conclusion and Perspectives

The phenomenon of neuronal polarization has been extensively studied in the last decades. Many of the analyses used the elegant cell culture system developed by Dotti et al. (1988). Thus the current model of neuronal polarization is to a large extent based on single hippocampal cells in an isolated system. Still, these extensive *in vitro* biochemical and cell biological analyses have provided a solid understanding of the general principles of cell polarization. A key question however remains: what are the cell-intrinsic biophysical and molecular mechanisms that induce the initial break in symmetry in cortical progenitor cells and developing cortical projection neurons *in vivo*? In order to address this question it will be

essential to establish tools that allow the visualization and/or manipulation of the precise localization of molecular markers at high resolution in an *in situ* tissue context. The CRISPR-Cas9-dependent SLENDR method promises a high-throughput platform to visualize the endogenous localization of candidate proteins at high micro- to nanometer resolution (Mikuni et al., 2016). Given that a number of "polarity signaling systems" seem quite sensitive to perturbation and not particularly resilient, the precise determination of "polarity gene" function at distinct stages in development represents a current challenge in the field. In order to probe the function of genes encoding regulators of neuronal polarity *in vivo*, the genetic mosaic analysis with double markers (MADM) technology (Hippenmeyer, 2013; Hippenmeyer et al., 2010; Zong et al., 2005) offers an experimental opportunity. By exploiting MADM, one can induce sparse genetic mosaics with wild-type and mutant cells labeled in two distinct colors at high resolution. In combination with live-imaging such an experimental MADM paradigm enables: (1) the dissection of the cell-autonomous gene function; and (2) determination of the relative contribution of non-cell-autonomous effects *in situ* at the global tissue level (Beattie et al., 2017). Altogether, the experimental platforms above promise a robust approach to determine the so far unknown functions of regulators implicated in the polarization process of progenitor cells and nascent cortical projection neurons. A key open question in a functional context is: what is the level of redundancy and specificity in extracellular cues and intracellular amplification mechanisms? Interestingly, the process of MP-to-BP transition appears to involve not only dynamic cytoskeletal-associated processes but also regulation at the transcriptional level (Hippenmeyer, 2014; Ohtaka-Maruyama and Okado, 2015). It will be important to analyze transcriptional responses at high temporal resolution and evaluate the influence on the general biochemical cell state. In future experiments it will be also important to establish biochemical and biophysical methods and assays that should allow the precise analysis of the break in symmetry at high molecular and/or structural resolution. In a broader context it will be important to address the question whether cell-type diversity may imply the necessity for adaptation in the mechanisms controlling polarization? In other words, how conserved is the process of symmetry break and polarization in distinct classes of neurons with different morphologies? The future analysis of the core signaling modules controlling cell polarity in a variety of brain areas and at high cellular and molecular resolution promises great conceptual advance.

2.7 Acknowledgments

This work was supported by IST Austria institutional funds; the European Union (FP7-CIG618444 to SH) and a program grant from the Human Frontiers Science Program (RGP0053/2014 to SH). CD was supported by a postdoctoral ISTFELLOW fellowship and CM was a postdoctoral fellow of the FWF Herta Firnberg programme.

3 Non-cell-autonomous mechanisms in radial projection neuron migration in the developing cerebral cortex

The content of this chapter was published as a review article in the Journal Frontiers in Cell and Developmental Biology

Andi H. Hansen[1] & Simon Hippenmeyer[1]

[1]Institute of Science and Technology Austria, Am Campus 1, 3400 Klosterneuburg, Austria

3.1 Author Contributions

Both authors conceived the work. A.H.H wrote the initial manuscript draft and both authors revised the manuscript and approved it for publication.

3.2 Summary

Concerted radial migration of newly born cortical projection neurons, from their birthplace to their final target lamina, is a key step in the assembly of the cerebral cortex. The cellular and molecular mechanisms regulating the specific sequential steps of radial neuronal migration *in vivo* are however still unclear, let alone the effects and interactions with the extracellular environment. In any *in vivo* context, cells will always be exposed to a complex extracellular environment consisting of (1) secreted factors acting as potential signaling cues, (2) the extracellular matrix, and (3) other cells providing cell–cell interaction through receptors and/or direct physical stimuli. Most studies so far have described and focused mainly on intrinsic cell-autonomous gene functions in neuronal migration but there is accumulating evidence that non-cell-autonomous-, local-, systemic-, and/or whole tissue-wide effects substantially contribute to the regulation of radial neuronal migration. These non-cell-autonomous effects may differentially affect cortical neuron migration in distinct cellular environments. However, the cellular and molecular natures of such non-cell-autonomous mechanisms are mostly unknown. Furthermore, physical forces due to collective migration and/or community effects (i.e., interactions with surrounding cells) may play important roles in neocortical projection neuron migration. In this concise review, we first outline distinct models of non-cell-autonomous interactions of cortical projection neurons along their radial migration trajectory during development. We then summarize experimental assays and platforms that can be utilized to visualize and potentially probe non-cell-autonomous mechanisms. Lastly, we define key questions to address in the future.

3.3 Introduction

The mammalian neocortex is built by distinct classes of neurons and glial cells which are organized into six stratified layers. Here we focus on projection neurons, the major neuronal population in the cortex. Projection neurons emerge from radial glial cells (RGCs) in the ventricular zone (VZ), intermediate progenitor cells (IPCs), and outer radial glial cells (oRGs, aka basal radial glia, bRGs) which divide in the subventricular zone (SVZ) (Ayala et al., 2007; Borrell and Götz, 2014; Hansen et al., 2010; Wang et al., 2011b). Nascent projection neurons migrate from their place of origin in the VZ/SVZ to their final target position, a process which is highly regulated (Ayala et al., 2007; Evsyukova et al., 2013; Valiente and Marín, 2010). Concerted migration of sequentially generated projections neurons results in a neocortex which is structured into six distinct layers (I-VI), each with different cellular composition and arranged in an inside-out fashion (Lodato and Arlotta, 2015; McConnell, 1995) (Figure 6A-B). In order to establish the correct cortical layering during development, projection neurons exhibit radial migration from the VZ/SVZ to the cortical plate (CP). Around embryonic day 11 (E11), post-mitotic neurons migrate mainly by pulling up the soma in the upright direction by using a basal process that is firmly attached to the pial surface. This migration mode is termed somal translocation (Nadarajah et al., 2001). The first cohort of migrating neurons form the preplate (PP), a structure which only exists transiently (Allendoerfer and Shatz, 1994; Nadarajah et al., 2001). At around E12, consecutive waves of neurons migrate toward the pial surface and establish the CP by splitting the PP into the two distinct structures: the deeper located subplate (SP) and the superficially positioned marginal zone (MZ) (Layer I) (Ayala et al., 2007) (Figure 6A). The subsequent populations of migrating neurons establish the 'first' layer of projection neurons (i.e. layer VI) in the CP which progressively expands in the vertical direction in an inside-out manner (Figure 6). In other words, earlier generated neurons settle in the deeper layers (layer VI-V) whereas later generated neurons migrate through the deep positioned neurons creating more superficial layers (IV-II) (Angevine and Sidman, 1961; McConnell, 1995; Valiente and Marín, 2010).

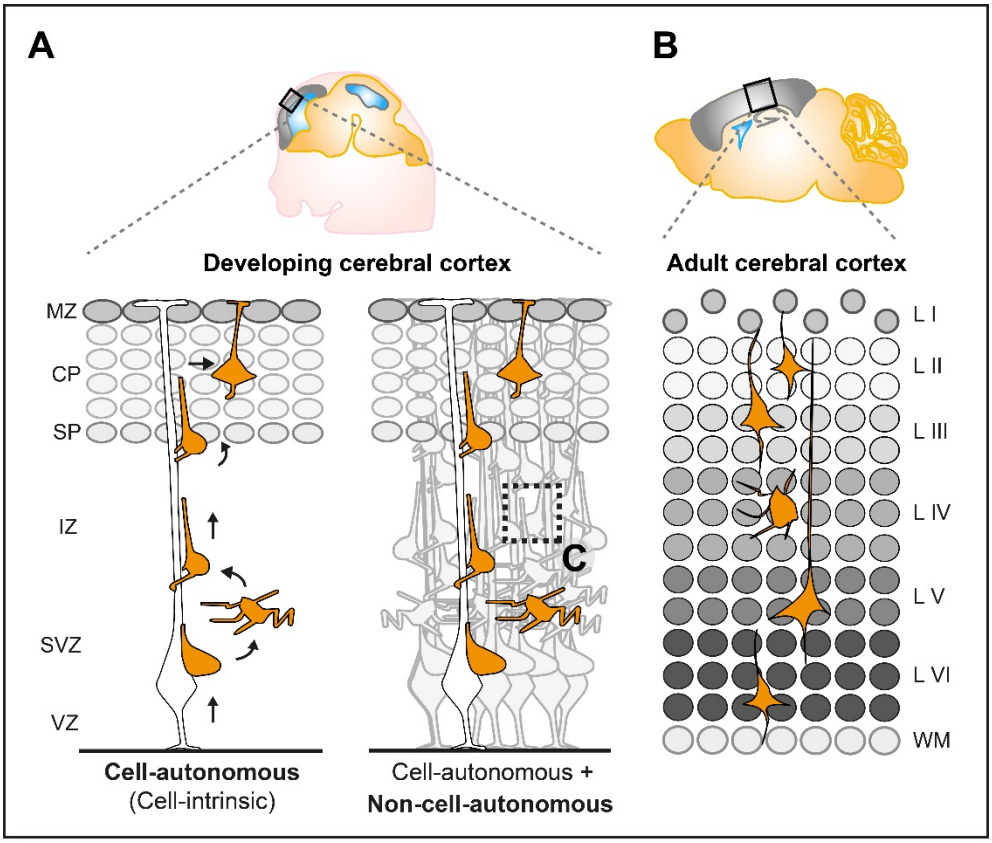

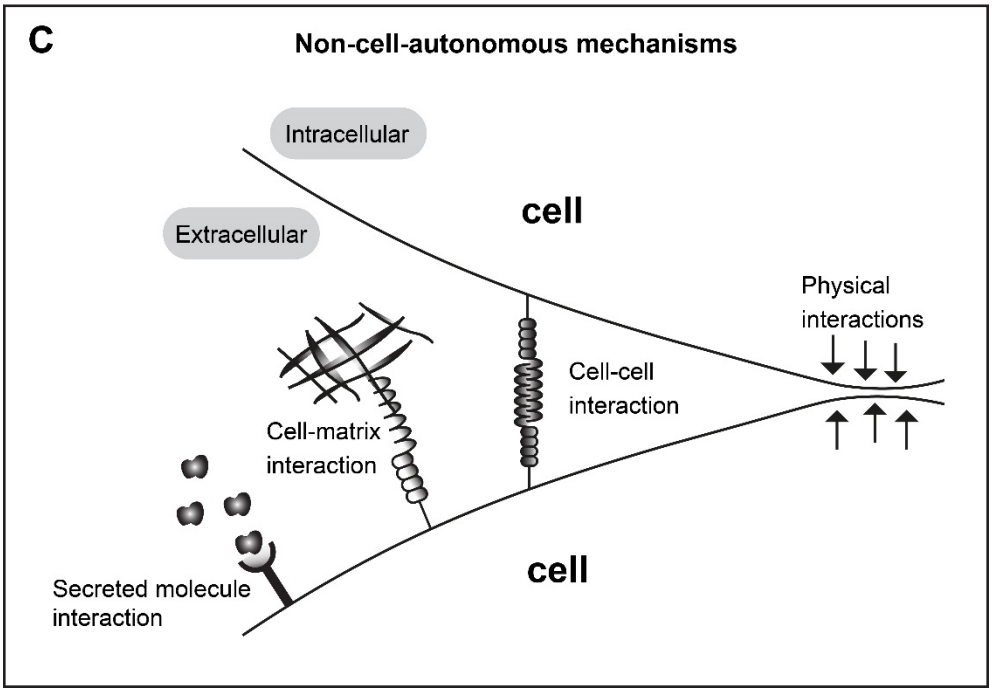

Figure 6 Non-cell-autonomous mechanisms in radial projection neuron migration.

(A) Migrating cortical projection neurons go through several steps and phases during their journey from their birthplace in the ventricular/subventricular zone (VZ/SVZ) to their final position in the CP. In the left panel, an isolated radially migrating projection neuron is shown to illustrate intrinsic cell-autonomous mechanisms controlling radial migration. The right panel illustrates that radially migrating projection neurons, which are embedded in an environment consisting of many other cells, are potentially influenced (in addition to cell

intrinsic cues) through non-cell-autonomous mechanisms (See panel C). **(B)** The six layered (L I-VI) structure of the adult mouse cerebral cortex. The layers are assembled in an inside out fashion where layer V-VI (L V-VI) are the earliest generated and layer II-IV (L II-IV) the latest generated cortical projection neurons. **(C)** Possible non-cell-autonomous cellular and molecular interactions during radial projection neuron migration. In any *in vivo* context, cells will always be exposed to a complex extracellular environment consisting of secreted factors acting as potential signaling cues, the extracellular matrix and other cells providing cell-cell interaction through receptors and/or direct physical stimuli. VZ: ventricular zone. SVZ: subventricular zone IZ: intermediate zone. SP: subplate. CP: cortical plate WM: white matter. L I-VI: layers 1-6.

Studies applying histological and time-lapse imaging techniques have shed some light on the dynamics of the radial migration process and described distinct sequential steps of projection neuron migration (Figure 6A) (Nadarajah, 2003; Noctor et al., 2004; Tabata and Nakajima, 2003). Newly-born neurons delaminate from the VZ and move towards the SVZ where they accumulate in the lower part and acquire a multipolar shape, characterized by multiple processes pointing in different directions (Tabata et al., 2009). In the SVZ, multipolar neurons move tangentially, towards the pia or towards the VZ (Noctor et al., 2004; Tabata and Nakajima, 2003). Multipolar neurons can remain up to 24 hours in the multipolar state in the SVZ. Next, within the SVZ and the lower part of the intermediate zone (IZ) multipolar neurons switch back to a bipolar state with a ventricle-oriented process that eventually develops into the axon. The pial oriented leading process is established by reorienting the Golgi and the centrosome towards the pial surface (Hatanaka et al., 2004; Yanagida et al., 2012). Upon multi-to-bipolar transition, neurons attach to the radial glial fiber in the upper part of the IZ and move along RGCs in a migration mode termed locomotion, while trailing the axon behind and rapidly extending and retracting their leading neurite before reaching the SP (Hatanaka et al., 2004; Noctor et al., 2004). Neurons then cross the SP and enter the CP still migrating along the RGCs until they reach the marginal zone (MZ). Just beneath the MZ neurons stop locomoting and detach from the radial glia fiber to perform terminal somal translocation and settle in their target position where they eventually assemble into microcircuits (Hatanaka et al., 2016; Nadarajah et al., 2001; Noctor et al., 2004; Rakic, 1972). All sequential steps of projection neuron migration are critical and disruption at any stage (e.g. due to genetic mutations in genes encoding core migration machinery) can lead to severe cortical malformations (Gleeson and Walsh, 2000; Guerrini and Parrini, 2010). Therefore each step of projection neuron migration must be tightly regulated. Many genes have been

identified as causative factors for cortical malformations (Evsyukova et al., 2013; Heng et al., 2010; Valiente and Marín, 2010) and several of the key molecules involved in neuronal migration e.g. LIS1, DCX, and REELIN have been investigated in detail by molecular genetics (Kawauchi, 2015). Recently, approaches involving *in vivo* electroporation and time-lapse imaging of brain slice cultures have shed light on crucial roles for the dynamic regulation of the cytoskeleton, extracellular cues and cell adhesion during neuronal migration (Franco et al., 2011; Jossin and Cooper, 2011; Noctor et al., 2004; Schaar and McConnell, 2005; Sekine et al., 2012; Simo et al., 2010). An emerging picture is arising with distinct molecular programs regulating neuronal migration through the different compartments VZ/SVZ, IZ and CP (Greig et al., 2013; Hansen et al., 2017; Hippenmeyer, 2014; Kwan et al., 2012; Martínez-Martínez et al., 2019). However, the precise regulatory mechanisms which coordinate each and every specific step of radial migration are still largely unknown, let alone the effects and interactions with the extracellular environment. Most studies so far have described and focused mainly on intrinsic cell-autonomous gene functions (Figure 6A) in neuronal migration (reviewed in Evsyukova et al., 2013; Heng et al., 2010; Valiente and Marín, 2010) but there is accumulating evidence that non-cell-autonomous-, local-, systemic- and/or whole tissue-wide effects (Figure 6A and C) substantially contribute to the regulation of radial neuronal migration (van den Berghe et al., 2014; Franco et al., 2011; Gorelik et al., 2017; Hammond et al., 2001; Hippenmeyer, 2014; Hippenmeyer et al., 2010; Nakagawa et al., 2019a; Sanada et al., 2004; Yang et al., 2002; Youn et al., 2009).

3.4 Nature of non-cell-autonomous mechanisms in Radial projection neuron migration

In any *in vivo* context, cells will always be exposed to a complex extracellular environment consisting of 1) secreted factors acting as potential signaling cues, 2) the extracellular matrix and 3) other cells providing cell-cell interaction through receptors and/or direct physical stimuli (Figure 6C). Therefore, most genes controlling radial neuronal migration can potentially, besides cell-autonomous functions, also act through non-cell-autonomous mechanisms. As such, non-cell-autonomous regulatory cues could involve molecular, cellular or physical components (Figure 6C). Hence, the distinction between cell-autonomous gene

function and non-cell-autonomous mechanisms is important to be able to define the different facets of a gene function *in vivo* and thus intact tissue context. Below we will describe recent studies and findings which have started to describe and characterize non-cell-autonomous effects and mechanisms in projection neuron migration.

3.5 Secreted molecules and the extracellular matrix

One of the most apparent non-cell-autonomous interactions includes secreted molecules produced in one cell and eliciting a response in another cell. In addition, interactions with the extracellular matrix are bound to happen for any cell and can occur in various ways. The extracellular matrix provides both structural organization of the cerebral cortex as well as the control of individual neurons. Neuronal migration and lamination is organized by extracellular matrix glycoproteins such as e.g. laminins, tenascins, proteoglycans and Reelin (Barros et al., 2011). The specific type of interaction of neurons with secreted molecules and the extracellular matrix and their role in radial neuronal migration have been reviewed recently in detail elsewhere (Franco and Müller, 2011; Long and Huttner, 2019; Maeda, 2015). Here we will briefly elaborate upon a few secreted molecules, mainly Reelin, which play roles in neuronal migration and brain development in general. The Reelin/Dab1 signaling cascade represents one of the best characterized signaling pathways in the developing brain. Reelin is a secreted protein mainly expressed by Cajal-Retzius cells in the MZ of the cortex (Ogawa et al., 1995) and acts via DAB1 in the control of radial projection neuron migration (Honda et al., 2011; Rice et al., 1998). The originally isolated *reeler* mouse mutant and *Dab1* KO mice show a severe disorganization of cortical projection neurons resembling a neocortex layering which is more or less inverted (Caviness and Sidman, 1973). Reelin has been hypothesized to inherit a number of distinct signaling modalities and functions in cortical neuronal migration (D'Arcangelo, 2014; Honda et al., 2011) but the precise role in the local microenvironment of migrating projection neurons is not clear (Martínez-Martínez et al., 2019). Yet, Reelin is mainly secreted from the CR-cells in the MZ and processed Reelin fragments has been shown to diffuse from the MZ into the CP and IZ of the developing cortex (D'Arcangelo, 2014; Jossin et al., 2007; Koie et al., 2014). Interestingly, when Reelin is ectopically expressed and secreted by migrating neurons in the IZ, it leads to aggregation of neurons near this ectopic Reelin-rich region resembling the structure of the MZ (Kubo et al., 2010). Furthermore, sequential

labeling of migrating neurons revealed that the late-born neurons can still pass by the early-born neurons during the formation of an ectopic Reelin rich aggregate (Kubo et al., 2010). These results indicate that Reelin may have distinct roles in long range versus local signaling. Moreover, a recent study investigating a FMCD-causing (Focal malformations of cortical development) mutation revealed that over activation of AKT3 in a fraction of migrating neurons would lead to misexpression of Reelin in these cells and thereby affect the migration of wild-type neighboring cells in a non-cell-autonomous manner (Baek et al., 2015). Moreover, RNA-seq expression profiling was employed to further investigate the non-cell-autonomous migration defect which could be due to direct physical blockade of the wild-type cells or have a more specific signaling mechanism. The gene ontology enrichment of the 835 significantly deregulated genes identified four main categories for neuronal development, migration, signaling and homeostasis and cell cycle regulation. This suggests that the non-cell-autonomous defect might underlie a more complicated mechanism than just a simple blockade of neurons (Baek et al., 2015). Clearly, the above studies show that global or local expression of a secreted molecule can cause distinct phenotypes, and demonstrating significant non-cell-autonomous impact on projection neuron migration.

Reelin signaling in the control of radial projection neuron migration acts via the intracellular adaptor protein DAB1 (Honda et al., 2011; Rice et al., 1998). Studies applying genetically engineered chimeric mice have suggested that environmental conditions play a role in proper neuronal positioning, and proposed a non-cell-autonomous effect and/or element of *Dab1* function (Hammond et al., 2001; Yang et al., 2002). By using conditional-KO (cKO) mice, in which *Dab1* is specifically deleted after preplate splitting and only in late-born neurons, it was observed that wild-type early born neurons were positioned in the outer layers instead of their usual position in the inner cortical layers. This would suggest that early-born neurons are being “passively” displaced into a deeper position by later-born neurons (Franco et al., 2011). Taken together, the pleiotropy of Reelin-Dab1 loss of function phenotypes could be significantly affected by non-cell-autonomous effects elicited by environmental factors and/or community effects in addition to the cell-autonomous function of Reelin signaling on migrating neurons.

Fibroblast Growth Factors (FGF) is a family of secreted molecules and their receptors (FGFRs) were recently shown to play an important role in radial projection neuron migration

(Ford-Perriss et al., 2001; Kon et al., 2019; Ornitz and Itoh, 2015; Szczurkowska et al., 2018). A recent study implicated FGFRs in the regulation of the migration orientation of multipolar neurons and the multipolar-to-bipolar transition. It was shown that FGFRs are activated by N-Cadherin when binding in cis on the same cell which prevents degradation and results in accumulation of FGFR which stimulate prolonged activation of extracellular signal-regulated kinase (Erk1/2) required for multipolar migration (Kon et al., 2019). In another study, NEGR1, another cell adhesion molecule, was shown to interact with FGFR2 thereby regulating neuronal migration and spine density (Szczurkowska et al., 2018). This study showed that NEGR1 physically interacts with FGFR2 and prevents it from being transported for lysosomal degradation. This accumulation of FGFR2 results in the maintenance of downstream ERK and AKT signaling. These two above studies have shown that FGFR receptors are important in neuronal migration, however the exact response mechanism of secreted FGF ligands is currently unknown. Since a large number of FGFs are expressed in the developing cortex and FGFRs are also activated by heparan sulfate proteoglycans, it is challenging to investigate which and how a specific FGF is involved in neuronal migration (Ford-Perriss et al., 2001; Ornitz and Itoh, 2015). The fact that FGFRs physically interact with different cell adhesion molecules, but act on similar downstream signaling pathways important for neuronal migration, indicates an important general role of FGFR signaling.

Recent findings suggest that alteration of individual neurons might also affect the entire cellular community. As such, a screen identified several potential non-cell autonomous regulators of radial neuronal migration and described autotaxin (ATX*)* to affect the localization and adhesion of neuronal progenitors in a cell autonomous and non-cell autonomous manner (Greenman et al., 2015). In a follow-up study, *Serping1*, a candidate gene identified in the above screen, was found to be expressed and secreted by neurons during brain development and to both affect radial neuronal migration in a cell-autonomous and non-cell-autonomous way (Gorelik et al., 2017). Besides affecting the positioning of the neurons, loss of *Serping1* gene function would also affect the cellular morphology of the neighboring neurons since knockdown neurons exhibited long leading processes which were also observed in the adjacent non-manipulated neurons (Gorelik et al., 2017).

3.6 Cell-Cell interactions among migrating cortical projection neurons

It has been observed that migrating neurons can have a positive and negative influence on each other depending on their genetic constitution and the environment. However, the nature of potential positive and/or negative non-cell-autonomous effects and how they affect the migration of mutant and wild-type cortical projection neurons is currently unclear (Hippenmeyer, 2014). Cell-cell interactions during collective cell migration, in a variety of cell types, have indeed been observed previously. Interactions mainly occur when two or more cells that retain their cell-cell contacts move together while coordinating their actin dynamics and intracellular signaling (Friedl and Gilmour, 2009; Londono et al., 2014; Tada and Heisenberg, 2012). Studies looking at collective migration e.g. in neural crest cells has provided information for the understanding of balanced interaction of cell adhesion and cell signaling between collectively migrating cells. Balancing adhesion and repulsion is one major factor mediating both individual cell and collective migratory coordination (Shellard and Mayor, 2020). Therefore, collective decision making and organization of cells is crucial for the generation of complex tissue and could also apply for the assembly of the cerebral cortex which relies on the migration of neurons. An example of such an collective effect could be physical properties where mutant (which may be less agile) neurons either “piggyback” on adjacent normally migrating neurons or get passively pushed or pulled by a migrating cellular population. Collective influences could also have a negative effect if most or all neurons are mutant and less dynamic, thereby leading to improper migration. Another effect of surrounding neurons could be through signaling, to stimulate or tune down the intrinsic migratory machinery of deficient neurons. This would suggest a mechanism whereby active signaling is utilized through transmembrane receptors and/or extracellular matrix components. Indeed such mechanisms have been described in various cell types where mutant cells negatively affect migration by direct contact inhibition (Becker et al., 2013; Huttenlocher et al., 1998). Upon ectopic expression of cell adhesion molecules, such as N-cadherin, Integrin, Focal adhesion kinase and the focal-adhesion adaptor protein Paxillin in cell culture, direct cell-cell contact inhibited migration. Interestingly, when mutant cells were surrounded by wild-type cells no such effect was seen. Nevertheless, when mutant cells were in direct contact with other mutant cells then the migratory process was inhibited (Becker et al., 2013; Huttenlocher et al., 1998). Although this effect was shown *in vitro* it could also apply

to migrating projection neurons *in vivo*. However, in the case of N-cadherin, the cause of inhibited migration could be due to intracellular trafficking and abundance of N-Cadherin rather than expression itself. A study has shown that Rab5-dependent endocytotic-, and a Rab11-dependent recycling pathway regulate N-cadherin trafficking, thereby mediating adhesion between a migrating projection neuron and the radial glial fiber (Kawauchi et al., 2010).

In vivo studies have recently shown that mutant *Ndel1* MADM (Mosaic Analysis with Double Markers)-labelled neurons, surrounded by a normal environment, exhibit different migration phenotypes when compared to mutant projection neurons in whole cortex knockout (Hippenmeyer, 2014; Hippenmeyer et al., 2010; Youn et al., 2009). *Ndel1* mutant neurons were incapable of moving in mice with a complete loss of *Ndel1* in the whole cortex, whereas *Ndel1* mutant neurons could migrate through the VZ/SVZ/IZ in a mosaic environment containing wild-type, heterozygous and mutant neurons (Hippenmeyer et al., 2010; Youn et al., 2009). Thus, the comparison of mutant *Ndel1* neurons in mutant versus normal environment clearly suggests a major influence of tissue-wide and/or community effects on radial projection neuron migration. However, the molecular and cellular mechanisms that differentially affect mutant *Ndel1* projection neurons in distinct environments remain unknown. Interestingly, differential gene expression analysis of brains from wild-type mice and full knock out mouse models for *Ndel1* (and *Lis1*, and *Ywhae* acting in the same signaling pathway) have revealed that cell adhesion, and cytoskeleton organization pathways are commonly altered in these mutants (Pramparo et al., 2011). Since cell adhesion is one of the commonly identified deregulated pathways, it would be obvious to speculate that the non-cell-autonomous response could be emerging from cell-cell or cell-matrix interactions and in the end cause the developmental phenotype observed in e.g. *Ndel1* knockout mice.

p35 (also known as Cdk5r1) is the main activator of CDK5, a serine/threonine kinase mainly expressed in the brain (Kawauchi, 2014; Su and Tsai, 2011). In a study investigating *p35,* it was found that when rescuing *p35* in a subset of neurons in an otherwise *p35*-deficient environment, rescued neurons would migrate 'normally' like wild-type neurons, indicating a prominent cell-autonomous gene function of *p35* (Gupta et al., 2003). However, in a follow-up study using *p35* chimeras (creating a mix of wild-type and *p35* deficient neurons), a partial non-cell-autonomous rescue of *p35* mutant neurons was seen. Interestingly, within the *p35*

chimeras it was observed that mutant cells were always present in a higher proportion compared to wild-type cells. These data indicate a certain degree of disadvantage of the wild-type neurons within the mutant cortical landscape, which could be due to non-cell-autonomous effects (Hammond, 2004). While p35/Cdk5 signaling may significantly influence how neurons interact with one another the nature of these interactions are currently unclear. These interactions however likely involve cell-cell adhesion and/or other community effects (Hammond, 2004; Kawauchi, 2012, 2014; Kwon et al., 2000). Interestingly, the Reelin-DAB1 pathway (see above) has also been shown to control cell-adhesion during neuronal migration (Sekine et al., 2014). Thus a common component of the underlying mechanisms inherent to non-cell-autonomous effects, and as observed in *p35* and *Dab1* mutant, may be acting through similar cell-adhesion signaling modules.

3.7 Heterogeneous cell-cell interactions of migrating cortical projection neurons

The developing brain consists of a heterogeneous mix of different cell types. Therefore, cell-cell interaction between distinct cell types, e.g. a radial glial cell and a migrating neuron, is one such example. Most radially migrating neurons are dependent on the radial glial fiber on which they locomote to move towards the pial surface and surpass earlier born neurons (Kriegstein and Noctor, 2004; Nadarajah et al., 2001; Rakic, 1972). Hence, the migrating neurons are dependent on a proper RGC fiber grid to be able to migrate properly. Indeed, disruption of the proper organization of the RGC fiber grid leads to non-cell-autonomous migration phenotypes because the main substrate of migrating neurons is perturbed (Belvindrah et al., 2007; Cappello et al., 2012; Nakagawa et al., 2019a). Such findings initially emerged in a study investigating beta1 integrins in neuronal development. In a KO mouse model which lacks beta1 integrin in the entire central nervous system, consequently in both radial glia cells and neurons, the formation of cortical layers were affected due to perturbations in the radial glial end feet contacting the marginal zone (Graus-Porta et al., 2001). Moreover, the morphology of the apical dendrites of the pyramidal neurons was also perturbed. However, when ablating beta1 integrin specifically in neurons that migrate along

radial glial fibers, and not in the radial glia cells themselves, no neurodevelopmental defect was observed (Belvindrah et al., 2007). These findings clearly showed that when one indispensable cell type (in this case the radial glial cell) was impaired, it indirectly affected the migrating neurons and resulted in disrupted layering of the cortex due to non-cell-autonomous effects (Belvindrah et al., 2007). Furthermore, investigation of the interaction of Cajal Retzius (CR) cells and migrating neurons has shown that perturbation of *Nectin1* function in CR cells alone would affect the interaction of CR cells and the leading processes of migrating neurons (Gil-Sanz et al., 2013). This altered interaction non-cell-autonomously disturbed radial glial cell-independent somal translocation of radially migrating neurons in the cortical plate (Gil-Sanz et al., 2013).

A recent study investigating *Memo1* showed that cKO in neurons and glia would cause excessive branching of the basal processes of the RGCs resulting in altered tiling of the RGC scaffolding grid and aberrant lamination of neurons (Nakagawa et al., 2019b). However, deletion of *Memo1* only in post-mitotic neurons, and not RGCs, did not affect neuronal migration. Therefore, the altered tiling of the RGCs non-cell-autonomously perturbed neuronal migration and thereby caused abnormal lamination of the cortex (Nakagawa et al., 2019b).

In *Flrt1/3* double-knockout mice, which develop macroscopic cortical sulci, it was found that the lack of *Flrt1/3* resulted in reduced intercellular adhesion which lead to a mild acceleration of radially migrating neurons and enhanced clustering of neurons along the tangential axis (del Toro et al., 2017). The clustering of neurons was hypothesized to result from repulsive interactions with neighboring neurons and radial glial cells suggesting a non-cell-autonomous effect of the *Flrt1/3* ablation on radial neuronal migration (Seiradake et al., 2014; del Toro et al., 2017). In a subsequent study it was shown that Teneurins, Latrophillins and FLRTs interact and direct radial neuronal migration by slowing down migration by possible coincidence contact repulsion between the neurons and the radial glia cells (del Toro et al., 2020).

Taken altogether, the above observations suggest that neuronal migration and proper lamination of the developing neocortex are significantly affected by non-cell-autonomous components. However, the precise underlying cellular and molecular mechanisms of non-cell-autonomous effects on radial neuronal migration have yet to be explored by rigorous qualitative and quantitative means. The lack of information on non-cell-autonomous effects

is mainly due to the limitation of experimental assays that allow for investigation of such events *in vivo* and with single cell resolution. To this end, in the below section we illustrate contemporary experimental paradigms that have the potential to systematically analyze non-cell-autonomous mechanisms in radial migration of cortical projection neurons.

3.8 Cellular Assays to Analyze and Genetically Dissect Non-Cell-Autonomous Mechanisms in Cortical Projection Neuron Migration In Vivo

In this section we will specifically elaborate on the experimental paradigms which can be utilized to dissect non-cell-autonomous mechanisms in cortical projection neuron migration.

3.8.1 Chimeras

A chimera is an animal that has two or more populations of genetically distinct cells. Therefore, chimeric animals allow for the presence of mutant cells in an otherwise wild-type background or *vice versa.* Depending on the degree of chimerism (i.e. ratio of wild-type versus mutant cells) such assay offers one way to distinguish between cell-autonomous gene function and non-cell-autonomous mechanisms *in vivo* (Figure 7A) (Gilmore and Herrup, 2001; Hammond, 2004; Hammond et al., 2001). Any phenotypic difference seen between the neurons of the same genotype, but present in distinct genotypic environments indicate non-cell-autonomous effects. However, the degree of chimerism is hard to control, especially in the embryo. Therefore comparative studies across distinct individual animals may be challenging. Yet, a few studies have very successfully applied chimeras to study radial neuronal migration in the cerebral cortex and have described the presence of non-cell-autonomous effects (Hammond, 2004; Hammond et al., 2001; Yang et al., 2002).

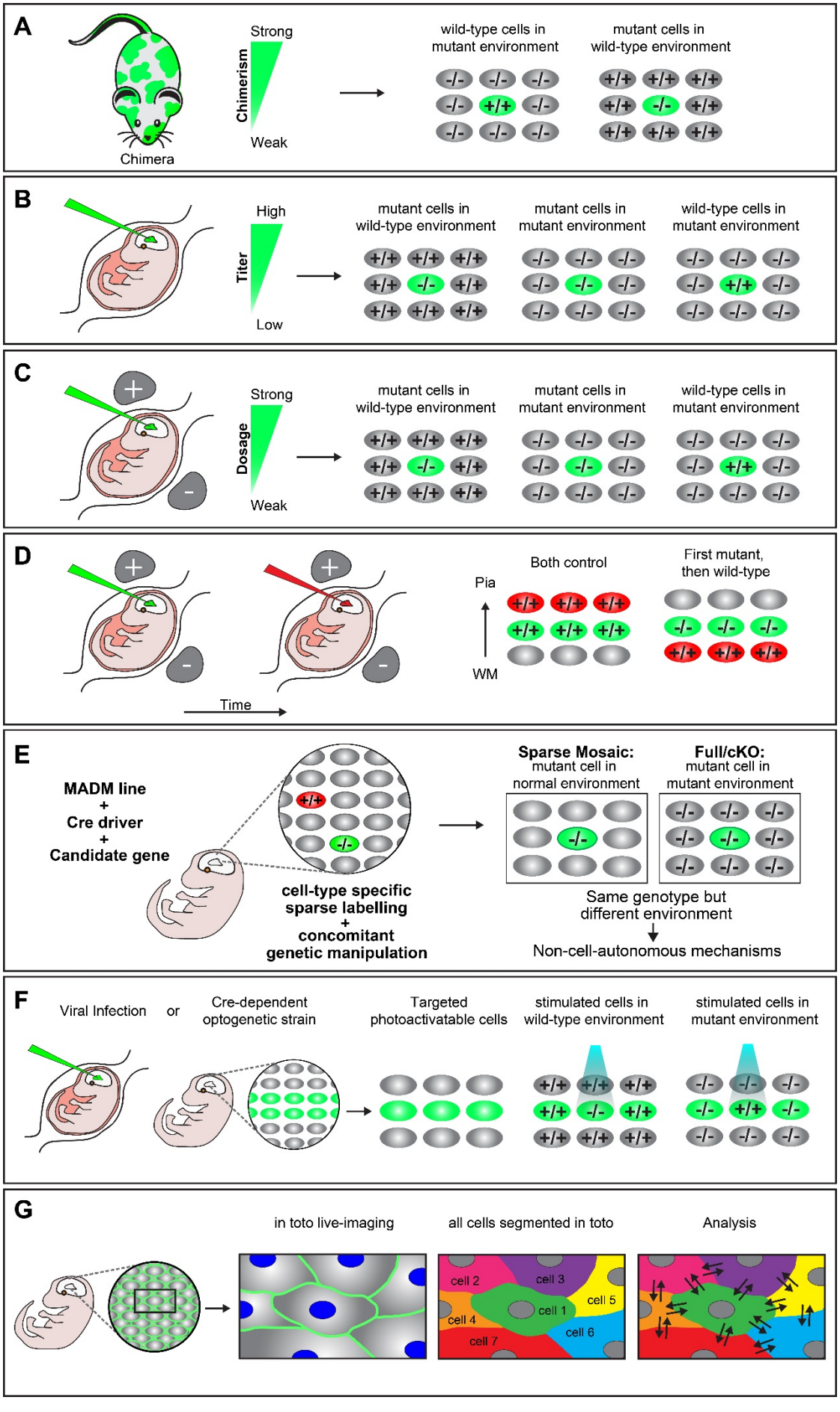
A
Chimera
Strong
Chimerism
Weak
wild-type cells in mutant environment
mutant cells in wild-type environment
B
High
Titer
Low
mutant cells in wild-type environment
mutant cells in mutant environment
wild-type cells in mutant environment
C
Strong
Dosage
Weak
mutant cells in wild-type environment
mutant cells in mutant environment
wild-type cells in mutant environment
D
Time
Pia
WM
Both control
First mutant, then wild-type
E
MADM line
+
Cre driver
+
Candidate gene
cell-type specific sparse labelling
+
concomitant genetic manipulation
Sparse Mosaic:
mutant cell in normal environment
Full/cKO:
mutant cell in mutant environment
Same genotype but different environment
Non-cell-autonomous mechanisms
F
Viral Infection
or
Cre-dependent optogenetic strain
Targeted photoactivatable cells
stimulated cells in wild-type environment
stimulated cells in mutant environment
G
in toto live-imaging
all cells segmented in toto
Analysis
cell 1
cell 2
cell 3
cell 4
cell 5
cell 6
cell 7

Figure 7 Experimental paradigms to genetically dissect non-cell-autonomous mechanisms in radial cortical neuron migration

(A) Chimeras. A chimera is an animal that has two or more populations of genetically distinct cells. Depending on the degree of chimerism (i.e., ratio of wild-type versus mutant cells), such assay offers one way to distinguish between cell-autonomous gene function and non-cell-autonomous mechanisms *in vivo*. Any phenotypic difference seen between the neurons of the same genotype, but present in distinct genotypic environments indicate non-cell-autonomous effects. **(B) Retroviral infection.** Retroviral infection allows to sparsely target developing neurons by either expression of the reporter only (e.g. in a wild-type or mutant environment) or using a viral vector that encodes a wild-type or mutant version of the gene of interest in combination with a reporter. This facilitates the inactivation or rescue of the gene of interest in either wild-type or mutant environments, allowing for the distinction of cell-autonomous gene function and non-cell-autonomous effects. Appropriately diluted retrovirus encoding the reporter and gene of interest allows for the discrimination of individual neurons and one can adjust the viral titer to generate more or less sparsely targeted neuronal populations. **(C) *In-Utero* electroporation.** Timed *in utero* electroporation for inactivation of a gene allows the sparse targeting of nascent migrating neurons in an otherwise wild-type environment. The inactivation of a specific gene can either be achieved by gene knockdown in combination with a reporter in a wild-type mouse or by electroporation of an expression vector which drives expression of CRE and a reporter into a mouse carrying a conditional floxed allele. In this paradigm one can mainly dissect the cell-autonomous gene function in the targeted neurons, although the presence of non-cell-autonomous effects provided by the wild-type environment will be present (mutant cells in wild-type environment). To investigate non-cell-autonomous effects, it is necessary to electroporate a separate set of tissue only with the fluorescent reporter in an otherwise mutant environment (mutant cells in mutant environment). Thus, neurons mutant for the same gene in two different environments allows for the distinction of non-cell-autonomous effects, provided that a different phenotype is observed between the mutant cells in each specific environment. Wild-type neurons in an otherwise mutant background by (over)expression of a rescue construct would further allow determination of non-cell-autonomous effects originating from the mutant environment (wild-type cells in mutant environment). The comparison of these three distinct paradigms will facilitate detailed description of cell-autonomous gene function and non-cell-autonomous effects. **(D) Consecutive electroporation**. Consecutive electroporation enables labeling, genetic manipulation and the monitoring of two or more distinct neuronal populations in the developing embryonic brain. The first neuronal population is electroporated for gene knockdown and the consecutive population with control fluorescent markers or vice versa (first mutant, then wild type). In such assay, the phenotype of the first cohort of electroporated cells can reflect cell-autonomous gene function whereas the phenotype of the second cohort of cells could reflect a combination of directed non-cell-autonomous effects originating from the first cohort and more global community effects. **(E) MADM.** Mosaic Analysis with Double Markers (MADM) allows for the analysis of sparse genetic mosaic (sparse mosaic) versus global/whole tissue (full-KO) ablation of a candidate gene with single cell resolution. This allows to quantitatively analyze non-cell-autonomous effects by subtracting the phenotype present in the sparse mosaic from the full-KO (cell-autonomous + non-cell-autonomous) versus cell-autonomous (sparse mosaic). It is important to note

that the background cells in a MADM sparse mosaic are heterozygous and may need adjustment of the paradigm in the case of investigation of a dosage-sensitive gene (haploinsufficiency). In that case, the MADM experiment can also provide a solution by comparing all genotypes/colors, e.g. green -/-, red +/+ and yellow +/-. For details of such application the reader is referred to Hippenmeyer et al., 2010. **(F) Optogenetics.** Optogenetics facilitates the use of genetically encoded tools to temporally control gene expression or protein function with light. Viral infection approaches and transgenic mice expressing optogenetic effector proteins in a Cre-dependent manner can be utilized to generate photoactivatable tissue. These approaches can create experimental paradigms which enable investigation of mutant neurons in an otherwise wild-type environment vs. wild-type neurons in a mutant environment in a spatiotemporal manner **(G) *In Toto* imaging.** *In Toto* live-imaging can visualize the movement of individual cells and their interactions with the surrounding cells within the whole developing tissue. This would allow for a direct assessment of non-cell-autonomous effects exerted by the neighboring cells on an individual cell or *vice versa*. *In toto* imaging mostly involves labeling of all cell membranes so each cell in the organism/microenvironment can be tracked and segmented. Here, a two-color combination of a membrane-localized fluorescent protein and a histone-fused fluorescent protein labeling chromatin which allows for tracking the cell membrane morphologies and nuclei movement has been displayed. Tracking the exact cell boundaries of the neurons spatiotemporally would enable the mapping of the physical interactions and forces which are exerted by the individual cell and that of the surrounding cells.

3.8.2 Viral infection

In utero injection of virus encoding a reporter e.g. green fluorescent protein (GFP) has widely been used to investigate neuronal migration, lineage tracing and clonal analysis *in vivo* (Gaiano et al., 1999; Gupta et al., 2003; He et al., 2015; Kaspar et al., 2002; Malatesta et al., 2000b; Sanada et al., 2004; Stott and Kirik, 2006). Retroviral encoding allows to sparsely target developing neurons by either expression of the reporter only (e.g. in a wild-type or mutant environment) or using a virus vector that encodes a wild-type or mutant gene of interest in combination with a reporter. This facilitates the inactivation or rescue of the gene of interest in either wild-type or mutant environments, allowing for the distinction of cell-autonomous gene function and non-cell-autonomous effects (Figure 7B). Appropriate dilution of the retrovirus titer and thus lowering infection rate allows for the discrimination of individual neurons and one can generate more or less sparsely targeted neuronal populations (Noctor et al., 2001; Sanada et al., 2004). In addition, delivery of an adeno-associated virus (AAV) encoding a fluorescent protein and Cre recombinase in combination with a reporter mouse carrying a conditional floxed allele of a candidate gene of interest, can be also be used to

target a specific population of neurons (Kaspar et al., 2002). Generally, any approach using a virus which can infect the cell population of interest, achieve specific stable gene expression and reporter labeling can be used to create paradigms for studying cell-autonomous gene function and non-cell-autonomous effects in radial projection neuron migration.

3.8.3 *In utero* injection and electroporation

Timed *in utero* electroporation for inactivation of a gene allows for the sparse targeting of developing neurons in an otherwise wild-type environment (Figure 7C). The inactivation of a specific gene can either be achieved by electroporation of shRNA or miRNA for gene knockdown, in combination with a reporter in a wild-type animal. Alternatively, electroporation of an expression vector which drives expression of CRE and a reporter in a mouse carrying a conditional floxed allele of a candidate gene of interest, can be used (Franco et al., 2011). These paradigms permit the dissection and analysis of cell-autonomous gene function in the targeted neurons. However, the presence of non-cell-autonomous effects originating from the wild-type environment may be present but not easily visualized (Figure 7C). Most studies so far have used this paradigm to study cell-autonomous gene function (Franco et al., 2011; Jossin and Cooper, 2011; Kon et al., 2019; Szczurkowska et al., 2018). To investigate non-cell-autonomous effects and mechanisms one would also need a separate set of tissue only electroporated with the fluorescent reporter to sparsely label the already mutant neurons in an otherwise non-labelled mutant environment (Figure 7C). Having neurons mutant for the same gene in two different environments would allow for the distinction of non-cell-autonomous mechanisms, provided that a different phenotype is observed between the mutant cells in each specific environment. In addition, having wild-type neurons in an otherwise mutant background by (over)expression of a rescue construct would further permit the determination of non-cell-autonomous effects originating from the mutant environment (Figure 7C). Only a few studies have applied this paradigm of rescuing a few cells sparsely in a mutant environment (Gupta et al., 2003; Sanada et al., 2004). Similar to chimeras (Figure 7A), it is important to consider the ratio of the mutant versus wild-type cells. For instance, sparse electroporation allows for the investigation of the direct interaction of cells of distinct genotypes. However, generating a high amount of mutant cells within the

wild-type environment might create a local mutant microenvironment where specific interactions between mutant cells could dominate. As a consequence, the presence of a local mutant microenvironment would make it difficult to distinguish cell-autonomous from non-cell-autonomous responses. Therefore, the amount of the electroporated cells should be considered carefully. While sparse single cell deletion of a candidate gene may truly report cell-autonomy of gene function, progressive local increase in the number of mutant cells may lead to a sweet spot from which onward non-cell-autonomous community effects emerge (Nakagawa et al., 2019b). Another way of generating very sparse populations of cells using this method, is to transplant micro dissected mutant cells from electroporated corticies to either another wild-type or mutant brain by intraventricular injection (Elias et al., 2007).

Consecutive electroporation enables cellular labeling, genetic manipulation and the monitoring of two or more distinct neuronal populations in the developing embryonic brain (Figure 7D). The first neuronal population could be electroporated for gene knockdown and the consecutive population with control fluorescent markers or vice versa. In such assay, the phenotype of the first cohort of electroporated cells can reflect cell-autonomous gene function whereas the phenotype of the second cohort of cells could reflect a combination of directed non-cell-autonomous cues originating from the first cohort and more global community effects (Baek et al., 2015; Gil-Sanz et al., 2013; Greenman et al., 2015; Jossin and Cooper, 2011).

In summary, sparse *in utero* electroporation for gene knockdown or CRE-dependent conditional gene inactivation in combination with fluorescent reporters facilitates the comparison of mutant phenotypes in distinct cellular environments. Such comparative studies, in principle, enable the systematic dissection of cell-autonomous gene function and/or phenotypes in response to gene inactivation and non-cell-autonomous mechanisms in radial neuronal migration.

3.8.4 Mosaic Analysis with Double Markers (MADM)

Mosaic Analysis with Double Markers (MADM) technology allows for the analysis of sparse genetic mosaic (sparse mosaic) versus global/whole tissue (full-KO) ablation of a candidate gene, and with single cell resolution (Figure 7E) (Beattie et al., 2017; Hippenmeyer et al., 2010;

Laukoter et al., 2020a; Zong et al., 2005). Therefore MADM provides a unique genetic tool to investigate cell-autonomous gene functions and the relative contribution of non-cell-autonomous effects. By using MADM one can quantitatively analyze these effects (Figure 7E) (Hippenmeyer, 2014; Hippenmeyer et al., 2010; Youn et al., 2009). In the sparse mosaic animals, mutant neurons are surrounded by 'normal' neurons and therefore mainly provide information about cell-autonomous gene function. In addition, the presence of non-cell-autonomous effects originating from the 'normal' environment may be present but not easily measured. In the full-knockout of a particular candidate gene, mutant neurons are surrounded by other mutant neurons, and it is not straightforward to distinguish between cell-autonomous gene function and non-cell-autonomous effects. However, one could quantitatively deduct non-cell-autonomous effects by subtracting the phenotype present in the sparse mosaic from the full/cKO (cell-autonomous + non-cell-autonomous versus cell-autonomous (sparse mosaic) (Figure 7E). The sparse mosaic versus full/cKO paradigm thus offers a promising experimental platform to investigate non-cell-autonomous effects because any phenotypic differences observed when the two paradigms are compared can be quantitatively assessed at single cell resolution (Beattie et al., 2017; Laukoter et al., 2020a). Nevertheless, generating a full-knockout where all cells are mutant for a particular candidate gene can be problematic since many migration genes are lethal when knocked out completely (Hirotsune et al., 1998; Sasaki et al., 2005). Conditional-knockout mice could be analyzed, provided that floxed alleles are available. In the future, systematic assay of almost any candidate gene will be in principle enabled by the whole-genome MADM library resource (Contreras et al., 2021).

3.8.5 Optogenetics

Optogenetics facilitates the use of genetically encoded tools to temporally control gene expression or protein function with light. It can facilitate localized modifications spatiotemporally within living cells and animals, targeting a wide array of proteins e.g. involved in cell-migration, cell-cell adhesion, and force transduction (Guglielmi et al., 2016; Mühlhäuser et al., 2017). Using this method one can investigate how changes in individual cells influence neighboring cells and global tissue remodeling. So far, most experiments

applying optogenetics for studying cell-migration have mainly been applied to *in-vitro* cell culture systems and small *in vivo* systems e.g. during gastrulation (Kim et al., 2014; Valon et al., 2017; Wang and Cooper, 2017; Wang et al., 2010; Weitzman and Hahn, 2014). In the mouse brain, optogenetics have mainly been used to activate, inhibit, or detect neuronal activity (Montagni et al., 2019). However, spatiotemporal control of the expression of a candidate gene or the activity of a specific signaling pathway could provide valuable insights into the dissection of non-cell-autonomous mechanisms in projection neuron migration. Currently, various viral infection approaches and transgenic mice expressing optogenetic effector proteins in a Cre-dependent manner can be utilized to generate photoactivatable cells and tissue (Guglielmi et al., 2016; Madisen et al., 2012). These approaches can create experimental paradigms similar to the ones described above (mutant neuron in an otherwise wild-type environment vs. wildtype neurons in a mutant environment) (Figure 7F), however, with spatiotemporal control of gene expression or protein function. This would allow exact targeting of specific neurons at specific sequential steps along the migratory path. In addition, one would be able to perturb cells of a specific cohort to see the exact non-autonomous effects on the surrounding non stimulated neurons (Figure 7F). An interesting aspect for which an optogenetic approach could also provide information is to what extent the ratio of mutant and wild-type cells in the same tissue is needed to see non-cell-autonomous effects. Starting from targeting only one cell and then increasing the area which is activated by light stimulation could reveal the threshold for when non-cell-autonomous mechanisms emerge dependent on the cell ratio of mutant vs. wildtype present. However, for *in vivo* and *in situ* experiments of mouse tissue, such an optogenetic approach might prove technically difficult. Activating one specific moving cell or a certain area of the tissue with a beam of light can be quite difficult *in vivo* and in three-dimensional intact tissues.

3.8.6 *In Toto* live-imaging

In Toto live-imaging can visualize the movement of individual cells and their interactions with the surrounding cells within the whole developing tissue (McDole et al., 2018; Megason and Fraser, 2007; Veeman and Reeves, 2015). This would enable a direct assessment of non-cell-autonomous effects exerted by the neighboring cells on an individual cell or *vice versa*. So far,

this method has mostly been used to visualize cell and collective migration behaviors in smaller *in vivo* systems such as e.g. drosophila (Krzic et al., 2012; Tomer et al., 2012), zebrafish (Hiscock et al., 2018; Nogare et al., 2017; Shah et al., 2019) and larger systems such as mouse gastrulation and heart tissue (McDole et al., 2018; Megason and Fraser, 2007; Stewart et al., 2009; Yue et al., 2020). *In toto* imaging mostly involves labeling of all cell membranes so each cell in the organism/microenvironment can be tracked and segmented (Nogare et al., 2017). In addition, both the cell membranes and the cell nuclei can be labelled in two individual colors for a more precise segmentation which does not rely on estimation. For *in vivo* studies of embryogenesis, a two-color combination of a membrane-localized fluorescent protein and a histone-fused fluorescent protein labeling chromatin enables the tracking of the cell membrane morphologies and nuclei movements (Megason, 2009; Stewart et al., 2009). Tracking all cells in an area of interest and their physical interactions would allow for a much more detailed analysis of the cellular dynamics which are ongoing during neuronal migration (Figure 7G). Achieving a resolution in which the exact cell boundaries of the neurons could be tracked spatiotemporally would enable the mapping of the physical interactions and forces which are exerted by the individual cell and that of the surrounding cells. Such mapping could help understand where and when certain cell dynamics are being subjected to non-cell-autonomous forces that evoke a response in the individual cell from the surrounding environment or *vice versa*. Future development of imaging approaches like e.g. light-sheet microscopy could facilitate the spatiotemporal resolution needed to visualize the migration of interacting neighboring cells in bigger tissues like the mouse cerebral cortex.

3.9 Outlook

Non-cell-autonomous mechanisms play an important role during brain development. However, little is known about the exact nature and physiological function of these non-autonomous mechanisms in radial neuronal migration. Thus, a number of open key aspects and questions require attention in future investigations. First, how can non-cell-autonomous mechanisms be distinguished from cell-autonomous cues and intrinsic gene function? Second, how can non-cell-autonomous effects be quantified and the underlying mechanisms determined? Third, what role do non-cell-autonomous mechanisms play in disease? Focal malformations of cortical development (FMCD) represent one example of a disorder where a

localized cortical lesion, i.e. mutations in a small fraction of cells, disrupts the entire cortical architecture. In the most severe cases, devastating pediatric hemimegalencephaly may emerge, which is characterized by enlargement of one entire cerebral cortex hemisphere (Lee et al., 2012; Poduri et al., 2012, 2013; Rivière et al., 2012). Hence, it is also important from a clinical perspective to precisely dissect the contribution of non-cell-autonomous, tissue-wide and systemic mechanisms in cortical development in general and neuronal migration in particular. The better understanding of the interplay of cell intrinsic gene function and non-cell-autonomous effects will enable further comprehension of the underlying etiology of neurodevelopmental disorders due to genetic mutations (Guerrini and Parrini, 2010; Guerrini et al., 2008).

3.10 Acknowledgments

We thank all members of the Hippenmeyer lab for discussion. A.H. is a recipient of a DOC Fellowship (24812) of the Austrian Academy of Sciences. This work also received support from IST Austria institutional funds; the People Programme (Marie Curie Actions) of the European Union's Seventh Framework Programme (FP7/2007-2013) under REA grant agreement No 618444 to S.H.

4 Tissue-wide Mechanisms Overrule Cell-intrinsic Gene Function in Radial Neuronal Migration

Andi H. Hansen[1], Florian M. Pauler[1], Michael Riedl[1], Christoph Sommer[1], Armel Nicholas[1], Susanne Laukoter[1], Carmen Streicher[1], Thomas Ruelicke[2], Li Huei Tsai[3], Björn Hof[1] & Simon Hippenmeyer[1, #]

[1] Institute of Science and Technology Austria, Am Campus 1, 3400 Klosterneuburg, Austria

[2] Institute of Laboratory Animal Science, University of Veterinary Medicine Vienna, Austria

[3] Picower Institute for Learning and Memory, Massachusetts Institute of Technology, Cambridge, MA 02139, USA; Department of Brain and Cognitive Sciences, Massachusetts Institute of Technology, Cambridge, MA 02139, USA; Broad Institute of Harvard and MIT, Cambridge, MA 02139, USA

[#]Corresponding author

The content of this chapter is a prepared manuscript.

4.1 Author Contributions

S.H. and A.H.H. conceived the research. A.H.H., C.St., and A.H generated all experimental MADM tissue.. A.H.H., C.St., T.R, and S.L., performed all the experiments except LCMS which was performed by A.N. A.H.H., F.M.P, and C.So. analyzed imaging data. F.M.P. performed computational and bioinformatics analysis of RNA-seq and proteomics with inputs from A.H.H. and S.H. M.R. established the computational model of migrating neurons with input from B.H., A.H.H. and S.H. A.H.H. wrote the manuscript with input from S.H., F.P. and M.R. All authors proofread the manuscript.

4.2 Summary

Concerted radial migration of newly born cortical projection neurons, from their birthplace to their final position, is a key step in the assembly of the cerebral cortex. The cellular and molecular mechanisms regulating radial neuronal migration in vivo are however still unclear. Cortical neuron migration is a complex process including cell-intrinsic components as well as the extracellular environment. The interactions of cell-intrinsic (cell-autonomous) and cell-extrinsic (non-cell-autonomous) components are largely unknown. Recent evidence suggests that distinct signaling cues act cell-autonomously but differentially at certain steps during the overall migration process. Moreover, functional analysis of genetic mosaics (mutant neurons present in wild-type/heterozygote environment) using the MADM (Mosaic Analysis with Double Markers) analyses in comparison to global knockout also indicate a significant degree of non-cell-autonomous and/or community effects in the control of cortical neuron migration. Here we established a MADM-based experimental strategy for the quantitative analysis of cell-autonomous gene function versus non-cell-autonomous and/or community effects. The direct comparison of mutant neurons from the genetic mosaic (cell-autonomous) to mutant neurons in the conditional and/or global knockout (cell-autonomous + non-cell-autonomous) allows to quantitatively analyze non-cell-autonomous effects. Such analysis enable the high-resolution analysis of projection neuron migration dynamics in distinct environments with concomitant isolation of genomic and proteomic profiles. Using these experimental paradigms and in combination with computational modeling we identified so far unknown non-cell-autonomous effects coordinating radial neuron migration.

4.3 Introduction

The six-layered structure of the mammalian cerebral cortex is formed by concerted radial migration of newly born cortical projection neurons, which migrate from their birthplace to their final target layer, and is a key step in the assembly of this structure (Ayala et al., 2007). Projection neuron migration and the laminar positioning of neurons within the mammalian neocortex have been intensely studied and a migration path containing sequential steps has been described (Hippenmeyer, 2014; Valiente and Marín, 2010). Projection neurons arise from radial glial cells (RGCs) dividing in the ventricular zone (VZ), intermediate progenitor cells (IPCs) and outer radial glial cells (oRGs, aka basal radial glia, bRGs) dividing in the subventricular zone (SVZ) (Ayala et al., 2007; Borrell and Götz, 2014; Hansen et al., 2010; Wang et al., 2011b). The newly born projection neurons display radial migration, in a bipolar fashion from the VZ/SVZ towards the pial surface, by delaminating from the VZ and moving towards the lower part of the SVZ where they accumulate and acquire a multipolar shape (Tabata et al., 2009). In time, multipolar neurons switch back to a bipolar state with a ventricle-oriented process that eventually develops into the axon, reattach to the radial glial fiber in the upper part of the intermediate zone (IZ) and move outwards along RGCs radial fiber in a migration mode termed locomotion (Hatanaka et al., 2004; Noctor et al., 2004). The early migrating neurons establish the first layer of projection neurons (layer VI) by splitting the pre-plate into a superficial layer of pioneer neurons, the marginal zone (MZ) and a deeper layer of pioneer neurons called the subplate (SP). The cortical plate (CP) expands in the vertical direction in an inside-out fashion, meaning, earlier generated neurons position in the deeper layers (layer VI-V) whereas later generated neurons migrate through the deeply positioned neurons forming the more superficial layers (IV-II) (Angevine and Sidman, 1961; McConnell, 1995; Valiente and Marín, 2010). The neurons enter the CP, still migrating along the RGCs, by crossing the SP and continue in vertical direction until they reach the MZ where they stop locomoting and detach from the radial glia fiber. Finally, neurons perform terminal somal translocation to settle in their target position and eventually assemble into microcircuits (Hatanaka et al., 2016; Nadarajah et al., 2001; Noctor et al., 2004; Rakic, 1972). The steps of projection neuron migration are tightly regulated and disruption at any stage can lead to severe cortical malformations that mostly translate into prominent neurodevelopmental diseases, which remain poorly understood and largely untreated.

(Buchsbaum and Cappello, 2019; Gleeson and Walsh, 2000; Guerrini and Parrini, 2010). In the last decades, a wide collection of genes has been implicated in neuronal migration, however, the relationship between their signaling pathways and the sequential steps of migration is still mostly unknown (Greig et al., 2013; Hansen et al., 2017; Hippenmeyer, 2014; Kwan et al., 2012; Martínez-Martínez et al., 2019). To date, studies have mainly focused on cell-intrinsic cell-autonomous gene functions of neuronal migration (Buchsbaum and Cappello, 2019; Evsyukova et al., 2013; Heng et al., 2010; Valiente and Marín, 2010). Thus, very little is known about the possible contribution of whole tissue effects (non-cell-autonomous effects) which are involved in neuronal migration and the formation of the brain. There is accumulating evidence that suggests non-cell-autonomous effects may substantially contribute to the regulation of radial neuronal migration, however, the nature of such effects remain unclear (van den Berghe et al., 2014; Franco et al., 2011; Gorelik et al., 2017; Hammond et al., 2001; Hansen and Hippenmeyer, 2020; Hippenmeyer, 2014; Hippenmeyer et al., 2010; Nakagawa et al., 2019a; Sanada et al., 2004; Yang et al., 2002; Youn et al., 2009). Any *in vivo* setting displays a complex extracellular environment where individual cells are exposed to many extrinsic elements such as secreted factors acting as potential signaling cues, the extracellular matrix, and other cells providing cell-cell interactions through receptors and/or direct physical stimuli (Hansen and Hippenmeyer, 2020). Consequently, genes regulating radial neuronal migration could act through non-cell-autonomous mechanisms besides their cell-autonomous functions (Hansen and Hippenmeyer, 2020). Perhaps surprisingly, cytoplasmic proteins have also been suggested to exert non-cell-autonomous effects on radial neuronal migration (Bai et al., 2003; Hammond, 2004; Hansen and Hippenmeyer, 2020; Hippenmeyer et al., 2010). However, the nature of such non-cell-autonomous effects is currently unknown. Recently, *in vivo* studies showed that mutant *Ndel1* projection neurons exhibit different migration phenotypes depending on the surrounding environment. While *Ndel1* mutant neurons were incapable of moving in mice with a complete loss of *Ndel1* in the whole cortex, *Ndel1* mutant neurons could migrate through the VZ/SVZ/IZ in a mosaic environment containing wild-type, heterozygous and mutant neurons (Hippenmeyer et al., 2010; Youn et al., 2009). Hence, the distinct phenotypes of mutant *Ndel1* neurons in mutant vs. normal environment suggest a major influence of tissue-wide non-cell-autonomous effects on radial projection neuron migration. Yet, the cellular and molecular mechanisms of such tissue-wide

effects remain unknown. So far, global transcriptomic analysis of entire brains from wild-type mice and whole cortex KO mouse models for *Ndel1*, *Lis1*, and *Ywhae*, all acting in the same signaling pathway, have revealed that cell adhesion and cytoskeleton organization pathways are commonly altered in these mutants (Pramparo et al., 2011). Accordingly, non-cell-autonomous effects could emerge from deregulated cell-cell or cell-matrix interactions and in the end, cause the developmental phenotype caused by e.g. in *Ndel1* knockout mice. Moreover, NDEL1 is a substrate of the serine/threonine-protein kinase CDK5 (Niethammer et al., 2000; Sasaki et al., 2000) and a study using *Cdk5r1* (gene coding for the protein p35, the main activator of CDK5) chimeras comprising a mixture of wild-type and *Cdk5r1* deficient neurons a partial non-cell-autonomous rescue of *Cdk5r1* mutant neurons was observed (Hammond, 2004). The possible non-cell-autonomous interactions are likely to involve cell adhesion and/or other community effects (Hammond, 2004; Kawauchi, 2012, 2014; Kwon et al., 2000). Remarkably, also the Reelin-DAB1 pathway has been shown to control cell-adhesion during neuronal migration (Sekine et al., 2014). Therefore, a common component of the underlying mechanisms inherent to tissue-wide effects, as observed in a handful of mutants, may be acting through similar cell-adhesion signaling modules. Yet, the precise underlying cellular and molecular mechanisms of non-cell-autonomous effects involved in radial neuronal migration have yet to be explored by rigorous qualitative and quantitative means.

Here we established a MADM-based experimental strategy for the quantitative analysis of cell-autonomous gene function versus non-autonomous and/or community effects. We pursued subtractive phenotypic analysis of genetic mosaics (mutant neurons present in wild-type/heterozygote environment) with conditional and/or global knockout (mutant environment, where all neurons are mutant), both coupled with sparse fluorescent MADM-labeling. of homozygous mutant neurons. The direct comparison of mutant neurons from the genetic mosaic (cell-autonomous) to mutant neurons in the conditional and/or global knockout (cell-autonomous + non-cell-autonomous) allows to quantitatively analyze non-cell-autonomous effects. Such assay enabled the high-resolution analysis of projection neuron migration dynamics in distinct environments with concomitant isolation of transcriptomic and proteomic profiles. In combination with computational modeling, we utilize these experimental paradigms to identify so far unknown non-cell-autonomous effects coordinating

radial neuron migration. We show that cytoplasmic proteins, besides acting cell-autonomously, exert non-cell-autonomous effects mainly through cell-adhesion molecules. In a Mosaic-MADM, which provides a normal environment, enables the mutant neurons to migrate more dynamically and to express cell-adhesion molecules like their control counterparts. However, in a KO-MADM, cell-adhesion molecules are significantly downregulated in combination with a severe migration phenotype where mutant neurons are significantly less dynamic, resulting in a complete disorganization of neuronal layering in the adult cortex. Our MADM-based analysis identified non-cell-autonomous tissue-wide effects of the environment, mainly exerted through cell-adhesion, to overrule cell-autonomous gene function i.e. the tissue wide effects are stronger than the direct function of the gene.

4.4 Results

4.4.1 MADM analysis reveals non-cell-autonomous effects on neuronal migration

To visualize and quantify the nature of non-cell-autonomous effects we employed mosaic analysis with double markers (MADM). MADM allows for the analysis of control (Control-MADM: all cells wildtype) (Figure 8A), Mosaic-MADM (GeneX-MADM: only green cells are mutant, red cells are wildtype in an otherwise heterozygous environment) (Figure 8B & Figure 15A) and KO-MADM (KO/cKO-GeneX-MADM: all cells mutant) (Figure 8C & Figure 15A) of a candidate gene with single-cell resolution (Beattie et al., 2017; Contreras et al., 2021; Hansen and Hippenmeyer, 2020). In this case case the KO-MADM refers to an environment where all cells in the whole organism are mutant, whereas in cKO-MADM the target gene is inactivated in specific cell types in a certain tissue; other cell types and tissues exhibit an unmodified, functional gene expression. Direct comparison of mutant cells from the Mosaic-MADM to mutant cells in the KO/cKO-MADM allows to quantitatively analyze non-cell-autonomous effects by comparing the phenotype present in the Mosaic-MADM (cell-autonomous) to the KO/cKO-MADM (cell-autonomous + non-cell-autonomous) (Figure 8D). To genetically investigate non-cell-autonomous effects we first generated control-MADM (*MADM-11$^{GT/TG}$; Emx1-Cre$^{+/-}$*) (Figure 16A), *Cdk5r1*-MADM (*MADM-11$^{GT/TG,Cdk5r1}$; Emx1-Cre$^{+/-}$*) (Figure 16B) and KO-*Cdk5r1*-MADM(*MADM-11$^{GT,Cdk5r1/TG,Cdk5r1}$; Emx1-Cre$^{+/-}$*) (Figure 16C) mice. We then analyzed the role of *Cdk5r1* in projection neuron migration in adult mice (P21) by quantifying

the relative distribution of labeled neurons throughout the cortical wall of the somatosensory cortex in control-MADM (*MADM-11$^{GT/TG}$; Emx1-Cre$^{+/-}$*) (Figure 8E), *Cdk5r1*-MADM (*MADM-11$^{GT/TG,Cdk5r1}$; Emx1-Cre$^{+/-}$*) (Figure 8F) and KO-*Cdk5r1*-MADM(*MADM-11$^{GT,Cdk5r1/TG,Cdk5r1}$; Emx1-Cre$^{+/-}$*) (Figure 8G). In *Cdk5r1*-MADM , where only the green neurons were mutant for *Cdk5r1* we observed a migration phenotype where most of the neurons were positioned in the lower bins, mainly the white matter (Figure 8F). However, in the KO-*Cdk5r1*-MADM, where all neurons are mutant for *Cdk5r1* we identified a more even distribution of neurons throughout the cortex (Figure 8G). When we compared the mutant green neurons from *Cdk5r1*-MADM directly to the green mutant neurons from the KO-*Cdk5r1*-MADM, we observed a significant difference in the vertical neuronal distribution which indicates the presence of non-cell-autonomous effects due to the fact that only the environment is different in the two scenarios but the quantified neurons are mutant for the same gene (Figure 8H). We also investigated Cdk5, the downstream target of p35 (encoded by *Cdk5r1),* to exclude that the phenotype we identified for *Cdk5r1* is not caused by other possible activators of Cdk5 (Su and Tsai, 2011). Thus, we analyzed control (*MADM-5$^{GT/TG}$; Emx1-Cre$^{+/-}$*) (Figure 8I), *Cdk5r1*-MADM (*MADM-5$^{GT/TG,Cdk5}$; Emx1-Cre$^{+/-}$*) (Figure 8J & Figure 15B) and KO-*Cdk5r1*-MADM (*MADM-5$^{GT,Cdk5/TG,Cdk5}$; Emx1-Cre$^{+/-}$*) (Figure 8K & Figure 15C). Correspondingly to the analysis of *Cdk5r1*, the majority of the mutant neurons were positioned in the white matter in *Cdk5*-MADM (Figure 8J) whereas the labeled projection neurons were more evenly distributed in the cKO-*Cdk5*-MADM (Figure 8K). As well as observed for *Cdk5r1*, a significant difference in the mutant neuronal distribution in the *Cdk5*-MADM versus cKO-*Cdk5*-MADM was identified, which correspondingly indicates the presence of non-cell-autonomous effects (Figure 8L). We did not identify any proliferation defect in the cerebral cortex for both *Cdk5r1* and *Cdk5* as we observed equal amounts of mutant and control neurons in the Mosaic-MADM (data not shown) which is consistent with previous studies (Delalle et al., 1997; Kwon et al., 1999; Tsai et al., 1994).

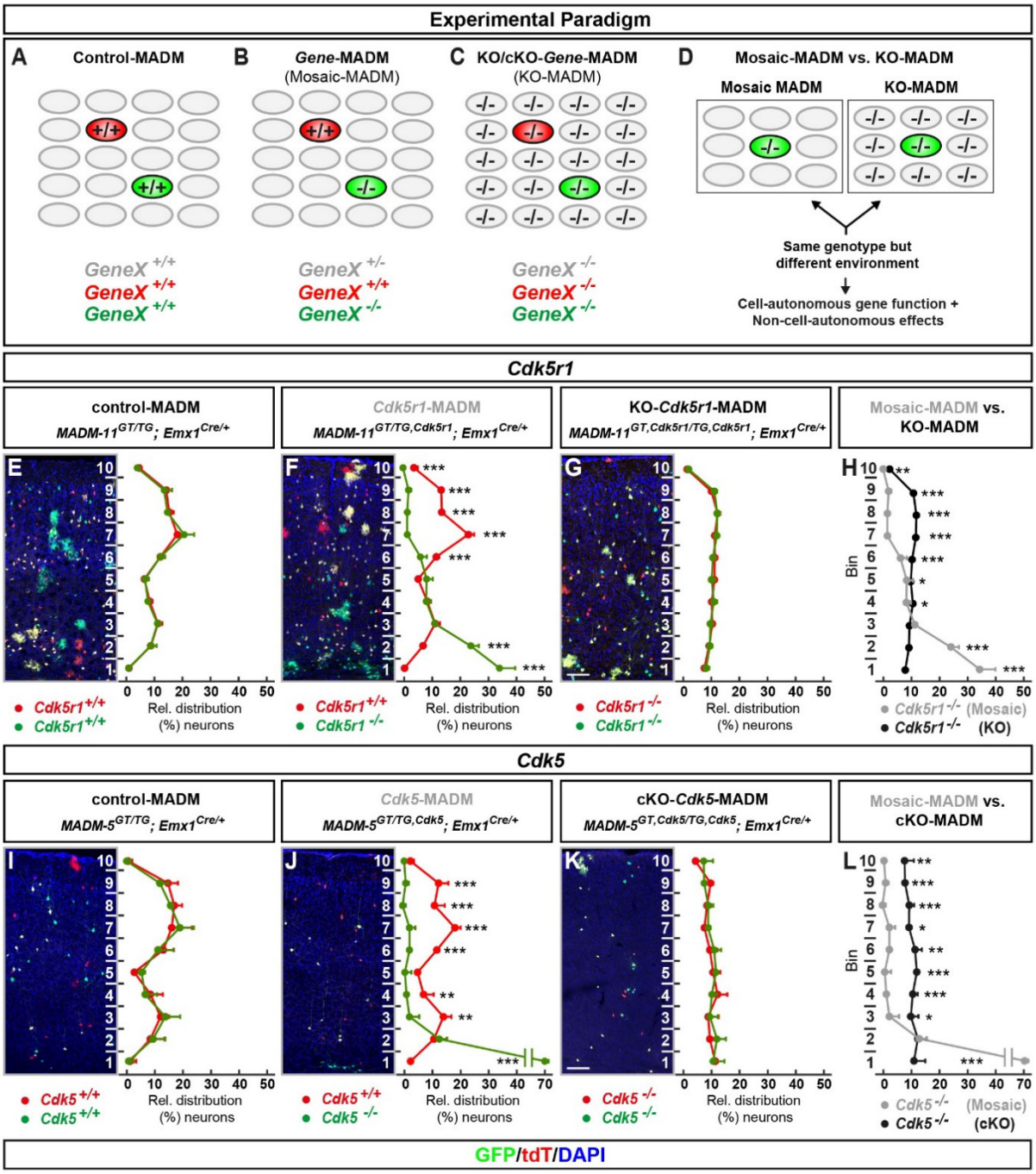

Figure 8 MADM analysis reveal cell-autonomous gene function and non-cell-autonomous effects on neuronal migration.

Mosaic analysis with double markers (MADM) allows for the analysis of **(A)** control (Control MADM: all cells wildtype), **(B)** genetic mosaic (Mosaic MADM: only green cells are mutant, red cells are wildtype in an otherwise heterozygous environment) versus **(C)** global/whole tissue (KO/cKO: all cells mutant) ablation of a candidate gene with single-cell resolution. **(D)** Direct comparison of mutant cells from the *Gene*-MADM (Mosaic MADM) to mutant cells in the KO/cKO-*Gene*-MADM (KO-MADM) allows to quantitatively analyze non-cell-autonomous effects by subtracting the phenotype present in the Mosaic-MADM from the KO-MADM (cell-autonomous + non-cell-autonomous) versus cell-autonomous (Mosaic-MADM). MADM Analysis of the somatosensory cortex of **(E)**

Control-MADM (*MADM-11$^{GT/TG}$; Emx1-Cre$^{+/-}$*), **(F)** Cdk5r1-MADM (*MADM-11$^{GT/TG,Cdk5r1}$; Emx1-Cre$^{+/-}$*) and **(G)** KO-*Cdk5r1*-MADM (*MADM-11$^{GT,Cdk5r1/TG,Cdk5r1}$; Emx1-Cre$^{+/-}$*) with quantification of the relative distribution (%) of neurons in 10 bins ranging from the ventricular surface to the pia at time point P21. **(H)** Comparison of *Cdk5r1-MADM* green mutant cell (grey) versus KO-*Cdk5r1*-MADM green mutant cell (black) distribution. Scale bar = 100µm. MADM Analysis of the somatosensory cortex of **(I)** Control-MADM (*MADM-5$^{GT/TG}$; Emx1-Cre$^{+/-}$*), **(J)** *Cdk5*-MADM (*MADM-5$^{GT/TG,Cdk5}$; Emx1-Cre$^{+/-}$*) and **(K)** cKO-*Cdk5*-MADM (*MADM-5$^{GT,Cdk5/TG,Cdk5}$; Emx1-Cre$^{+/-}$*) with quantification of the relative distribution (%) of neurons in 10 bins ranging from the ventricular surface to the pia. **(L)** Comparison of *Cdk5*-MADM green mutant neuron (grey) versus *Cdk5*-cKO green mutant neuron (black) distribution. Cortical bins are shown in numbers. Nuclei were stained using DAPI (blue). Scale bar = 100µm. n=3 for each genotype. From each animal 10 (MADM-11) or 20 (MADM-5) hemispheres were analyzed, Values represent mean SD, *p < 0.05, **p < 0.01, and ***p < 0.001.

4.4.2 Non-cell-autonomous effects commence during development

To characterize the non-cell-autonomous effects on projection neuron migration that was identified for both *Cdk5r1* and *Cdk5* in the adult stage, we analyzed the distribution of projection neurons during development (Figure 9). At time point E14, a significantly different distribution between the mutant cells in the *Cdk5r1*-MADM versus *KO-Cdk5r1-MADM* (Figure 9A-D) was observed and persisted throughout development (Figure 9E-L). In *Cdk5r1*-MADM the majority of mutant neurons accumulated below the IZ/CP border and only a fraction migrated into the cortical plate (Figure 9B-J). Hence, the cell-autonomous gene function of *Cdk5r1* appears to be important for be the ability to enter the target area, a phenotype that increased and maintained over time (Figure 9B, F, J). However, the distribution of neurons in the KO-*Cdk5r1*-MADM seemed to mimic the control at E14, yet, at time points E16 and P0 a phenotype appears which exhibit a more or less even distribution of neurons throughout the cortical wall (Figure 9G & K). Nevertheless, neuronal distribution phenotypes differ significantly between *Cdk5r1*-MADM mutant versus KO-*Cdk5r1*-MADM (Figure 9D, H, L) demonstrating that non-cell-autonomous effects were present at all three time-points. Likewise, *Cdk5*-MADM and cKO-*Cdk5*-MADM display a very similar neuronal distribution phenotypes at developing time points E14, E16 and P0, as identified for *Cdk5r1*-MADM and KO-*Cdk5r1*-MADM (Figure 9M-X).

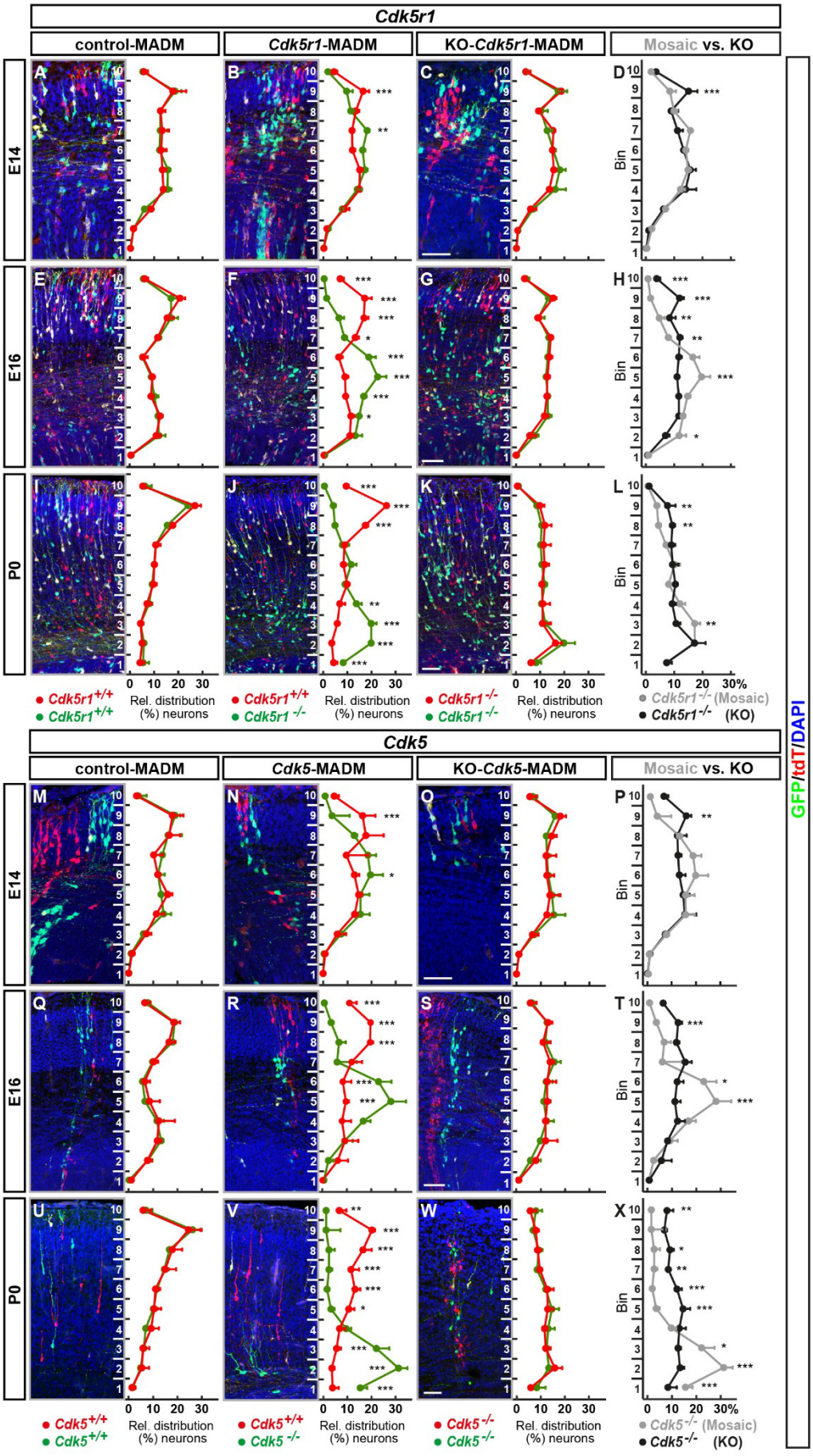
Cdk5r1
control-MADM
Cdk5r1-MADM
KO-Cdk5r1-MADM
Mosaic vs. KO
E14
E16
P0
A
B
C
D
E
F
G
H
I
J
K
L
Bin
Rel. distribution (%) neurons
Cdk5r1+/+
Cdk5r1+/+
Cdk5r1+/+
Cdk5r1 -/-
Cdk5r1-/-
Cdk5r1-/-
Cdk5r1-/- (Mosaic)
Cdk5r1-/- (KO)
Cdk5
control-MADM
Cdk5-MADM
KO-Cdk5-MADM
Mosaic vs. KO
M
N
O
P
Q
R
S
T
U
V
W
X
Cdk5+/+
Cdk5+/+
Cdk5+/+
Cdk5 -/-
Cdk5-/-
Cdk5-/-
Cdk5-/- (Mosaic)
Cdk5-/- (KO)
GFP/tdT/DAPI

Figure 9 Non-cell-autonomous effects commence during development.

MADM Analysis of developing somatosensory cortex of **(A, E I)** Control-MADM (*MADM-11$^{GT/TG}$; Emx1-Cre$^{+/-}$*), **(B, F, J)** *Cdk5r1*-MADM (*MADM-11$^{GT/TG,Cdk5r1}$; Emx1-Cre$^{+/-}$*) and **(C, G, K)** KO-*Cdk5r1*-MADM (*MADM-11$^{GT,Cdk5r1/TG,Cdk5r1}$; Emx1-Cre$^{+/-}$*) at time points E14, E16, and P0 with quantification of the relative distribution (%) of neurons in 10 bins ranging from the ventricular surface to the pia. **(D, H, L)** Comparison of *Cdk5r1*-MADM green mutant cell (grey) versus KO-*Cdk5r1*-MADM green mutant cell (black) distribution. MADM Analysis of developing somatosensory cortex of **(M, Q, U)** Control-MADM (*MADM-5$^{GT/TG}$; Emx1-Cre$^{+/-}$*), **(N, R, V)** *Cdk5*-MADM (*MADM-5$^{GT/TG,Cdk5}$; Emx1-Cre$^{+/-}$*) and **(Q, S, W)** cKO-*Cdk5*-MADM (*MADM-5$^{GT,Cdk5/TG,Cdk5}$; Emx1-Cre$^{+/-}$*) at time points E14, E16, and P0 with quantification of the relative distribution (%) of neurons in 10 bins ranging from the ventricular surface to the pia. **(P, T, X)** Comparison of *Cdk5*-MADM green mutant cell (grey) versus KO-*Cdk5*-MADM green mutant cell (black) distribution. Cortical bins are shown in numbers. n=3 for each genotype. From each animal 10 (MADM-11) or 20 (MADM-5) hemispheres were analyzed. Nuclei were stained using DAPI (blue). Scale bars 50µm. Values represent mean SD, *p < 0.05, **p < 0.01, and ***p < 0.001.

4.4.3 Transcriptomic analysis reveals cell-adhesion as a major non-cell-autonomous component

To characterize the extent of the non-cell-autonomous effects on a molecular level, we applied bulk RNA-sequencing using SMARTer technology. To isolate the labeled projection neurons we sorted the green-labeled neurons from the genotypes control-MADM (*MADM-11$^{GT/TG}$; Emx1-Cre$^{+/-}$*), *Cdk5r1*-MADM (*MADM-11$^{GT/TG,Cdk5r1}$; Emx1-Cre$^{+/-}$*) and KO-*Cdk5r1*-MADM (*MADM-11$^{GT,Cdk5r1/TG,Cdk5r1}$; Emx1-Cre$^{+/-}$*) using FACS and obtained control and mutant green cells. We then performed RNA-sequencing followed by bioinformatic analyses (Figure 10A). First, we validated efficient recombination by significant decrease of *Cdk5r1* expression in the deleted exon (Figure 17A). We then compared the mutant cells from the *Cdk5r1*-MADM and KO-*Cdk5r1*-MADM to the control-MADM (Figure 10B). In the *Cdk5r1*-MADM neurons we identified 11 significantly differentially expressed genes (DEGs, padj < 0.05, DESeq2), which is in stark contrast to the KO-*Cdk5r1*-MADM neurons where we identified 1056 DEGs (padj < 0.05, DESeq2) (Figure 10B) To directly characterize the extent of the non-cell-autonomous effects on a transcriptional level we compared KO-*Cdk5r1*-MADM neurons to *Cdk5r1*-MADM neurons directly and observed an increasing number of DEGs during development (Figure 10C, D). To apprehend the biological function of the DEGs we performed gene ontology (GO) enrichment analysis on the 670 and 927 up-, and down regulated genes at P0. Top enriched GO terms for the down regulated genes were highly significant (padj < 2.45×10^{-9},

hypergeometric test) and associated with extracellular matrix, cell membrane, and cell adhesion. GO term enrichment in the up regulated genes were not significant (padj > 0.5) and associated with synaptic terms (Figure 10E). In summary transcriptome analysis identified down regulation of cell-adhesion genes as a major non-cell-autonomous component.

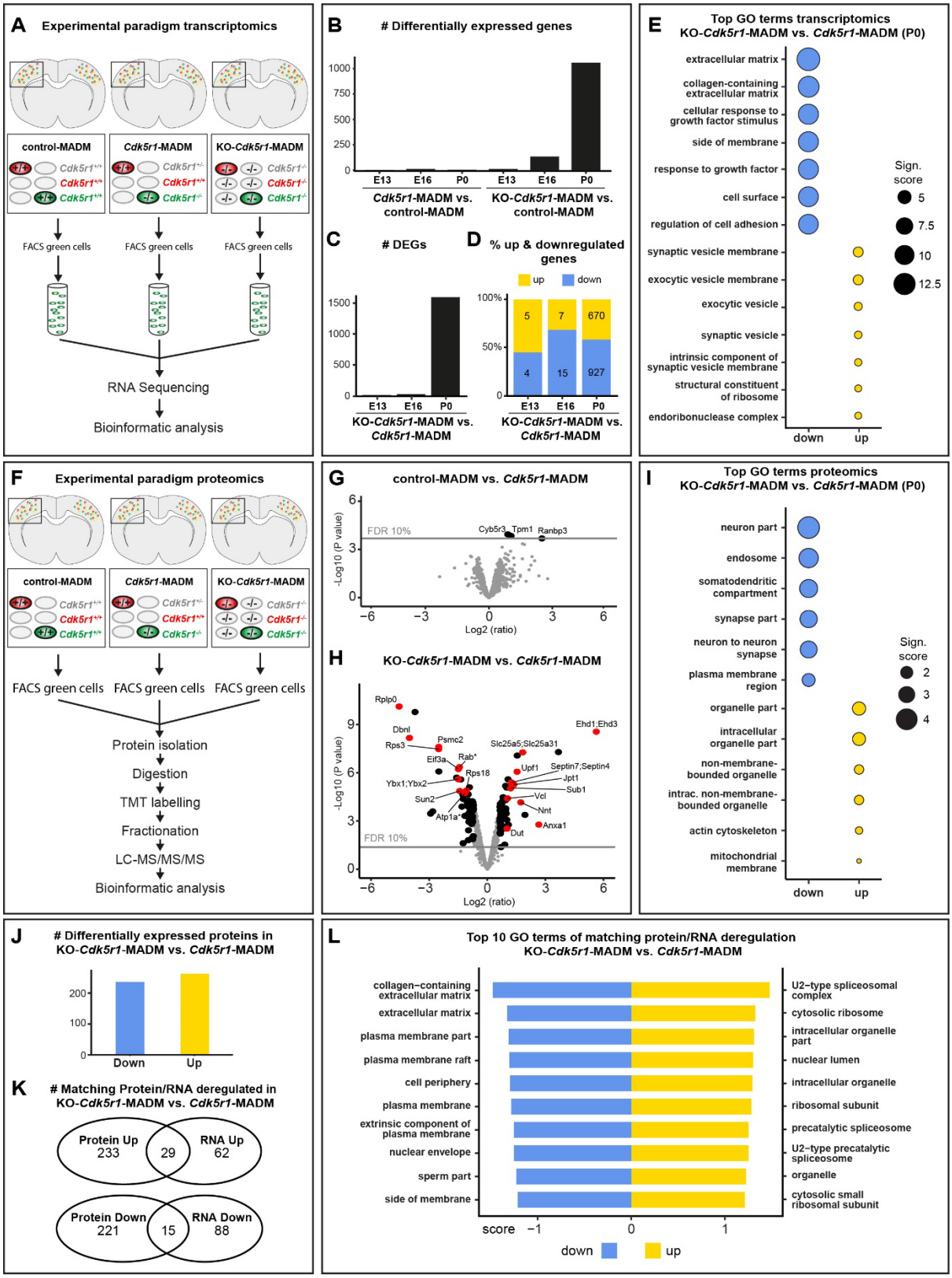

Figure 10 Transcriptomic and proteomic analyses reveal cell-adhesion as a major non-cell-autonomous component

(A) Cortical hemispheres of Control-MADM (*MADM-11$^{GT/TG}$; Emx1-Cre$^{+/-}$*), *Cdk5r1*-MADM (*MADM-11$^{GT/TG,Cdk5r1}$; Emx1-Cre$^{+/-}$*) and KO-*Cdk5r1*-MADM (*MADM-11$^{GT,Cdk5r1/TG,Cdk5r1}$; Emx1-Cre$^{+/-}$*) at time points E13, E16, and P0 were

isolated using FACS and subsequently prepared for RNA-sequencing and bioinformatics analysis. **(B)** Number of differentially expressed genes *Cdk5r1*-MADM and KO-*Cdk5r1*-MADM versus control at developmental time points E13, E16, P0. **(C)** Number of differentially expressed genes and **(D)** percentage of up- and down-regulated genes of KO-*Cdk5r1*-MADM / *Cdk5r1*-MADM at developing time points E13, E16, and P0. **(E)** Top GO terms from genes in (C, D) at time point P0. Note that GO term enrichments from up regulated genes are non-significant. **(F)** Cortical hemispheres of Control-MADM (*MADM-11$^{GT/TG}$; Emx1-Cre$^{+/-}$*), *Cdk5r1*-MADM (*MADM-11$^{GT/TG,Cdk5r1}$; Emx1-Cre$^{+/-}$*) and KO-*Cdk5r1*-MADM (*MADM-11$^{GT,Cdk5r1/TG,Cdk5r1}$; Emx1-Cre$^{+/-}$*) at time point P0 were isolated using FACS and subsequently prepared for mass spectrometry and bioinformatic analysis. **(G)** Volcano plot showing deregulated proteins for control-MADM versus *Cdk5r1*-MADM at time point P0. Note that only three 3 proteins were upregulated significantly. **(H)** Volcano plot showing deregulated proteins for KO-*Cdk5r1*-MADM / *Cdk5r1*-MADM at time point P0. **(I)** Top enriched GO terms for for genes shown in (H). **(J)** Number of genes associated with differentially expressed proteins of KO-*Cdk5r1*-MADM / *Cdk5r1*-MADM. Note that criteria for significant differential expression were relaxed compared to (H) **(K)** Venn diagrams showing the overlap of deregulated genes from the transcriptomic and proteomic datasets for KO-*Cdk5r1*-MADM / *Cdk5r1*-MADM. **(L)** Top 10 GO-terms from gene sets that are down- and up-regulated in both the transcriptomic and proteomic data sets (overlap in K).

4.4.4 Overlapping protein/mRNA deregulation substantiate cell-adhesion as a non-cell-autonomous component

To determine the nature of non-cell-autonomous effects on a proteomic level, we employed liquid chromatography–mass spectrometry (LC-MS/MS) analysis to the three genotypes control-MADM (*MADM-11$^{GT/TG}$; Emx1-Cre$^{+/-}$*), *Cdk5r1*-MADM (*MADM-11$^{GT/TG,Cdk5r1}$; Emx1-Cre$^{+/-}$*), and KO-*Cdk5r1*-MADM (*MADM-11$^{GT,Cdk5r1/TG,Cdk5r1}$; Emx1-Cre$^{+/-}$*) at time point P0 (Figure 10F). We first compared the *Cdk5r1*-MADM mutant neurons to the control which identified three significantly deregulated proteins (Figure 10G). To directly investigate non-cell-autonomously deregulated proteins we compared KO-*Cdk5r1*-MADM to *Cdk5r1*-MADM and identified 59 and 61 significantly up and down deregulated proteins respectively (Figure 10H). GO-term enrichment analysis of the genes associated with these differentially expressed proteins identified GO terms related to membrane and neuron-neuron contact in the down regulated gene group, corroborating our findings from the transcriptome analysis. Up regulated genes were mainly associated with intracellular processes such as organelles (Figure 10I). Finally we sought to directly investigate the overlap between the transcriptomic and proteomic changes. As the correlation between transcriptome and proteome is complex,

we lowered the thresholds for differential expression (see Methods) and focused on 1060 gene annotations informative in both analyses. This identified 262 (down regulated) and 236 (up regulated) DEGs from the proteomics data set (Figure 10J). Interestingly, 29 (up regulated) and 15 (down regulated) genes were common to both transcriptomic and proteomic analyses (Figure 10K). GO-term enrichment analysis of the these genes identified extracellular matrix and membrane associated GO terms in the down regulated gene group and GO terms associated with cell-intrinsic entities in the up regulated gene group (Figure 10L). In summary, this analysis revealed that deregulated mRNAs and proteins related to the membrane and the extracellular matrix, in general, is downregulated in KO-*Cdk5r1*-MADM suggesting cell adhesion as a major non-cell-autonomous component on a transcriptomic and proteomic level.

4.4.5 Non-cell-autonomous effects affect neuronal migration dynamics

Neuronal migration is a dynamic process and therefore we assessed the physical movement of migrating neurons *in-situ* by time-lapse imaging (Figure 11A) at developmental time point E16 for control-MADM (*MADM-11*$^{GT/TG}$*; Emx1-Cre*$^{+/-}$), *Cdk5r1*-MADM (*MADM-11*$^{GT/TG,Cdk5r1}$*; Emx1-Cre*$^{+/-}$) and KO-*Cdk5r1*-MADM (*MADM-11*$^{GT,Cdk5r1/TG,Cdk5r1}$*; Emx1-Cre*$^{+/-}$) to further investigate the nature of non-cell-autonomous effects on neuronal migration (Figure 11B-H). Importantly, we employed a semi-automated tracking analysis which allowed to track all labelled neurons in the areas investigated removing any experimenter bias from the analysis. To get an overview of the position of the neurons, we first analyzed the relative distribution of the neurons in all three genotypes in time frame t = 0 (Figure 11E). As previously shown (Figure 9) the neurons in the control-MADM and control neurons in *Cdk5r1*-MADM were distributed in a slight higher number in the upper bin, whereas mutant neurons in *Cdk5r1*-MADM were mainly accumulated in the lower bin (Figure 11E). In the KO-*Cdk5r1*-MADM, neurons displayed a more even distribution in the upper and lower bin (Figure 11E). Over time, the neurons did change their position in the tissue in all genotypes, however, only a fraction were observed to change from the lower bin to upper bin (~6% of all tracks changed compartment) (Figure 11E & F). Moreover, we identified a significant difference, between *Cdk5r1*-MADM and KO-*Cdk5r1*-MADM in the relative distribution of tracked neurons in both the upper and lower bins at the beginning and end of the tracking (Figure 11E & F) highlighting

that non-cell-autonomous effects are present within the analyzed time window. We then analyzed the neuronal migration dynamics of the neurons in the control (Figure 11B-B7 & Supplementary Movie 1) and observed a very dynamic movement of neurons over the time course of 725min where neurons would move outwards in direction of the pia with neurons crossing from the IZ in the CP in the time frame monitored while attaining a relatively high velocity and directionality (Figure 11B7, G-H). In the *Cdk5r1*-MADM, the tracked control neurons (red) behaved similarly to the control-MADM (Figure 11E-H & Supplementary Movie 2). Yet, the majority of mutant neurons (green) in the *Cdk5r1*-MADM moved up until the cortical plate however not entering it, and were moving significantly slower than their control counterparts in the lower and upper bins (Figure 11G), but no difference in directionality was observed in the lower bin (IZ) (Figure 11H). However, the KO-*Cdk5r1*-MADM migrating projection neurons (Figure 11D-D7 & Supplementary Movie 3) showed to be significantly slower and non-directional than the control (Figure 11G, H). Interestingly, we identified a significant dynamic difference between *Cdk5r1*-MADM mutant and KO-*Cdk5r1*-MADM in the lower bin, demonstrating a less dynamic environment in the KO-MADM (KO-*Cdk5r1*-MADM). On the other hand, the *Cdk5r1*-MADM exhibits an environment that permits mutant cells to move more dynamically than mutant cells in the KO-*Cdk5r1*-MADM. The analysis has revealed that mutant neurons in the *Cdk5r1*-MADM move faster and more directional than the mutant neurons in the KO-*Cdk5r1*-MADM in the lower bin. This result showed that the “normal” environment of the *Cdk5r1*-MADM permits the *Cdk5r1*-mutant neurons to move significantly more than the *Cdk5r1*-mutant neurons surrounded entirely by other *Cdk5r1*-mutant neurons in the KO-*Cdk5r1*-MADM. Compared to control, *Cdk5r1*-mutant neurons in both the *Cdk5r1*-MADM and KO-*Cdk5r1*-MADM do move less indicating that the *Cdk5r1*-mutation did affect migration dynamics in both scenarios, while the “normal” environment of the *Cdk5*-MADM provided for more movement when the mutant neurons were surrounded by control neurons.

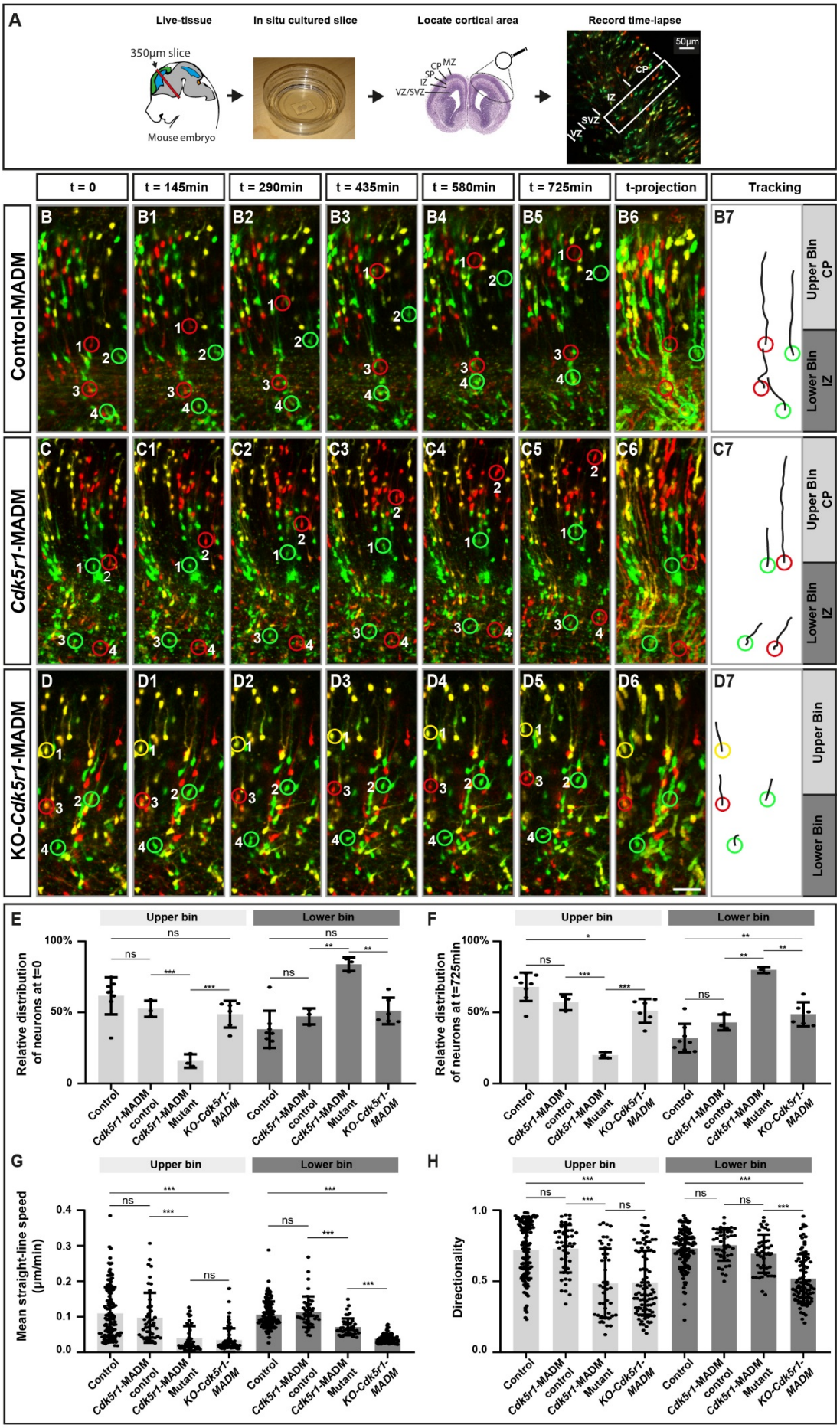
A
Live-tissue
In situ cultured slice
Locate cortical area
Record time-lapse
350µm slice
Mouse embryo
50µm
CP
MZ
SP
IZ
VZ/SVZ
SVZ
VZ
t = 0
t = 145min
t = 290min
t = 435min
t = 580min
t = 725min
t-projection
Tracking
Control-MADM
Cdk5r1-MADM
KO-Cdk5r1-MADM
Upper Bin
Lower Bin
CP
IZ
E
F
G
H
Upper bin
Lower bin
Relative distribution of neurons at t=0
Relative distribution of neurons at t=725min
Mean straight-line speed (µm/min)
Directionality
Control
Cdk5r1-MADM
control
Cdk5r1-MADM
Mutant
KO-Cdk5r1-MADM
ns

Figure 11 Non-cell-autonomous effects affect neuronal migration dynamics.

(A) Time-lapse imaging of developing somatosensory cortex of MADM-labeled tissue. Time-lapse imaging of **(B-B5)** Control-MADM (*MADM-11$^{GT/TG}$; Emx1-Cre$^{+/-}$*), **(C-C5)** *Cdk5r1*-MADM (*MADM-11$^{GT/TG,Cdk5r1}$; Emx1-Cre$^{+/-}$*) and **(D-D5)** KO-*Cdk5r1*-MADM (*MADM-11$^{GT,Cdk5r1/TG,Cdk5r1}$; Emx1-Cre$^{+/-}$*) at developmental time point E16. (**B6**, **C6, D6)** time-projection which contains 12 hours of sequential images of the intermediate zone (Lower Bin) and cortical plate (Upper bin) with a 15 min framerate. Scale bar, 40 µm. **(B7, C7, D7)** Tracking trajectories of the indicated neurons (red and green rings) for each genotype. **(E)** Relative distribution of neurons at the start of the time-lapse t = 0 for each replicate time-lapse per genotype. **(F)** Relative distribution of neurons at the end of the time-lapse t = 725min for each replicate time-lapse per genotype. **(G)** Mean straight-line speed of the top 15 tracks per replicate time-lapse per genotype. **(H)** Directionality of the top 15 tracks per replicate time-lapse per genotype. n = 3 videos from at least two independent animals. Values represent mean SD, *p < 0.05, **p < 0.01, and ***p < 0.001.

4.4.6 *In silico* modelling supports cell-adhesion as a non-cell-autonomous component altering radial neuronal migration dynamics.

The ability of cells to migrate and interact with their environment is strongly dependent on cell-adhesion molecules. In our data (Figure 10) we observed that cell-adhesion molecules are downregulated in the *KO-Cdk5r1-MADM*, but not in *Cdk5r1-MADM* mutant. To address the hypothesis that cell-adhesion molecules may represent the major non-cell-autonomous component altering projection neuron migration dynamics, we developed a minimal theoretical model inferred from experimental data (Figure 12). We had the goal to determine a minimal set of parameters sufficient to describe the dynamics of the neuronal migration on a statistical level. However, here we did not aim to describe the details of the biochemical or biomechanical steps involved in the migration process. Our modeling approach is based on tracking data which we extracted from time-lapse imaging (see Figure 11) of migrating projection neurons at developing time point E16 (Figure 12A, D and G). We analyzed the trajectories from each genotype and plotted the overall velocity distribution from the migrating neurons in the tissue, to have a reference for the dynamics of each condition (Figure 12J). Then, from the experimental data, we inferred two cell-intrinsic parameters, directionality and force generation, and one extrinsic parameter defining the environment tissue resistance (Figure 12B).

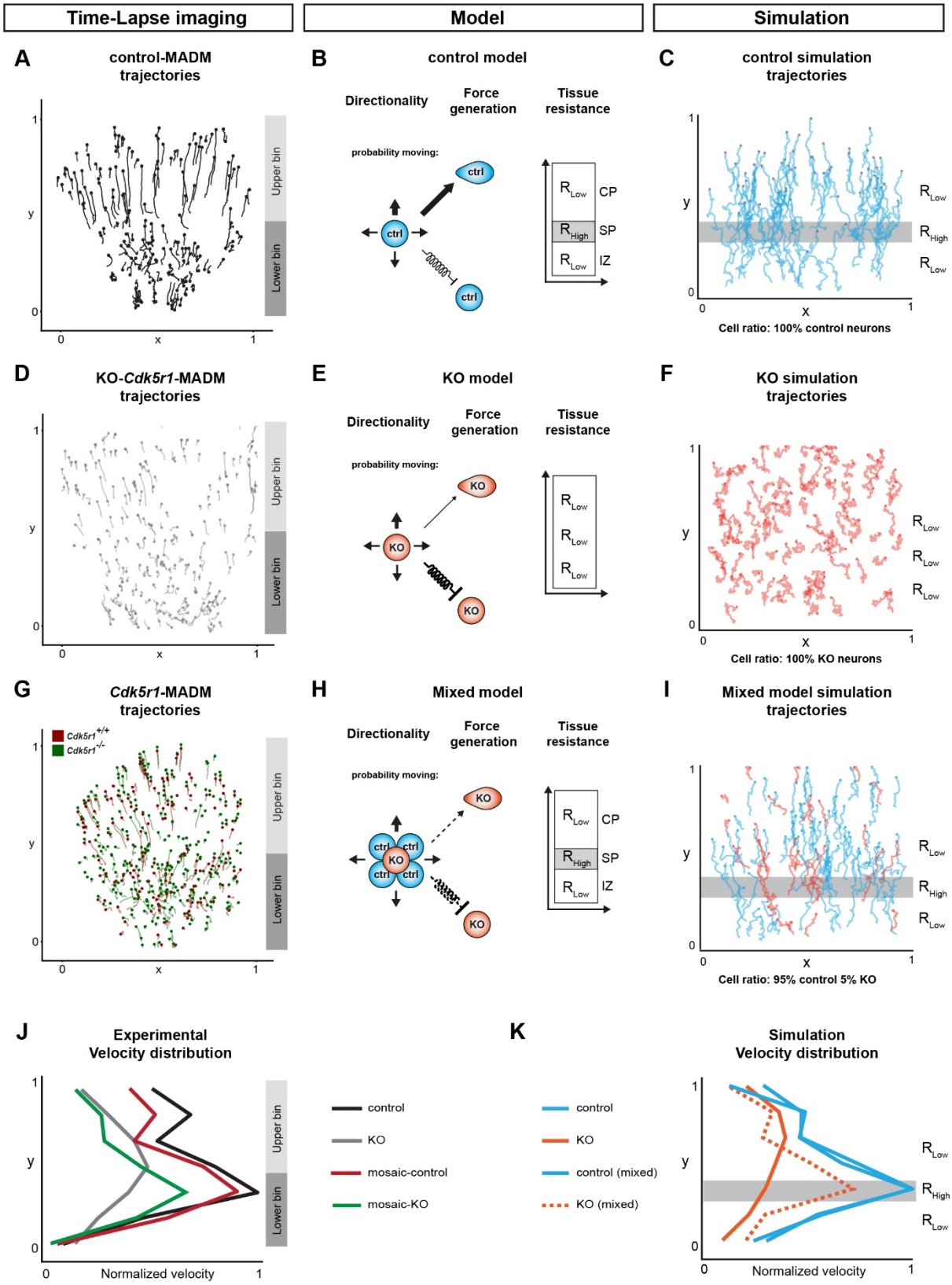

Figure 12 *In silico* modelling of cell-adhesion as a non-cell-autonomous component altering radial neuronal migration dynamics.

(A) Representative time-lapse imaging trajectories of migrating control-MADM (*MADM-11$^{GT/TG}$; Emx1-Cre$^{+/-}$*) neurons. **(B)** Model schematics of control neuron migration in control environment with corresponding

resistance zones. The thickness of the arrows indicate the probability to move in any direction, here the directionality bias is defined as 65% in pial-direction for control. **(C)** Simulated neuronal trajectories of control model. Shown resistance zones correspond to description in (B). **(D)** Representative time-lapse imaging trajectories of migrating KO-*Cdk5r1*-MADM (*MADM-11*$^{GT,Cdk5r1/TG,Cdk5r1}$*; Emx1-Cre*$^{+/-}$) neurons. **(E)** Model schematics of KO-*Cdk5r1* neuron migration in KO environment with the corresponding single resistance zone. The thickness of the arrows indicate the probability to move in any direction, here the directionality bias is defined as 51% in pial-direction. Thereby, movement is more like to be inhibited. **(F)** Simulated neuronal trajectories of mutant model with single resistant zone. **(G)** Representative time-lapse imaging trajectories of *Cdk5r1*-MADM (*MADM-11*$^{GT/TG,Cdk5r1}$*; Emx1-Cre*$^{+/-}$) neurons. **(H)** Model schematics of cross interaction, mixed model migration in control environment with corresponding resistance zones. The directionality bias is defined in pial-direction as a function of N_Ctrl/N_Mut ratio min = 51%, max = 65%. The thickness of the arrows indicate the probability to move in any direction for the mutant neuron. **(I)** Simulated neuronal trajectories of mixed model for (95% Ctrl, 5% KO). Shown resistance zones correspond to description in (H). **(J)** Averaged velocity from experimental data distributions of control-MADM (n = 4), KO-*Cdk5r1*-MADM (n = 3), *Cdk5r1*-MADM (n = 3) samples. **(K)** Corresponding velocity distributions from simulated migration tracks.

Based on the velocity distributions we introduce the environmental parameter for resistance, which results from the changes in tissue resistance along the migratory path (Figure 12B). The temporal change in position results in a distribution of velocities throughout the developing cortical wall, which ranges from the ventricle to the pia (Figure 12J). For control neurons this distribution displays a strong velocity peak within the lower half of the tissue (lower bin) followed by a sharp decrease in velocity around the border of the upper bin. However, these characteristics are non-existent in the KO-*Cdk5r1*-MADM (Figure 12J) where the velocity distribution is more or less even throughout the tissue. From the aforementioned localized changes in migration dynamics, the sharp decrease in velocity, we can infer that positional change in velocity to a change in the cortical layer-structure which corresponds to the intermediate zone-cortical plate border and suggests a difference in stiffness between the different zones. The differences in stiffness of each zone of the developing wild-type mouse brain has been measured by atomic force microscopy measurements of the Young's moduli E at different developmental stages (Iwashita et al., 2014). We include this as a zone-specific resistance inversely corresponding to the different tissue resistances. Moreover, by assuming that the layers are constructed of a homogeneous material, the differences in stiffness can be attributed to a difference in pore size distribution. While a cell is migrating through this porous environment it will have to squeeze through different pores in order to advance. The

resistance the cells are subjected to along their path decreases with increasing pore sizes. For a porous material, the resistance experienced e.g. by a fluid flow is not uniquely defined by E alone and therefore does not allow the calculation of a pore size distribution inversely. However, we infer that an increase in stiffness correspond to a decrease in pore sizes and therefore an increase in resistance. The magnitude of the resistance fields R_i is defined as a free parameter of our system. The visual identification of developing cortical zone and the allocated change in stiffness is challenging. However, cells tend to migrate with a non-uniform speed through the environment. In the wildtype environment, we can identify a strong peak in the velocity distribution preceded by a low-speed regime, which reappear at similar positions throughout our samples. This strong increase in velocity corresponds to a change in migration behavior. Cells moving through this region struggle in order to squeeze through, which is followed by a release of build-up tension that manifest as a jump-like propulsion. In the KO-*Cdk5r1*-MADM case, due to an inexistence of the physiological layer structure, the migration dynamics are independent of the location of the R_{tissue}. To integrate the two described environments in the model, we produce an environment allowing for three compartments with two different resistances R_{low}, R_{high}. In the control environment the layers are defined by $R_{control,tissue} = R_1, \mathrm{R}_2, \mathrm{R}_3$ for $\mathrm{R}_2 > R_1 \approx R_3$ (Figure 12B), while in the KO-*Cdk5r1*-MADM environment we set $R_{KO,tissue} = R_{KO}$ with magnitude on the order of R_1 , R_3 (Figure 12E). Values are given explicitly in the Supplemental Information (See table 2). Using the parameters, directionality and force generation, we modeled the cells as persistent random walkers which infers their directional bias, in addition to the tissue resistance parameter. The directional bias and the force the neurons generate are extracted from the experimental data. The force generation mechanism uses a random walk model with direction bias on a single cell level of unit mass (Caffrey et al., 2014), with the alteration from the reference, that instead of directly calculating a displacement, a 2D force F_{gen} is generated. Integrating F_{gen} over a time step dt we arrive at a displacement dx and henceforth a velocity v. The so generated assumed displacement results in a corresponding resistance dependent friction factor which together with the velocity leads to a friction force F_{drag}. If the generated force F_{gen} is larger than the resistance force produced by the tissue F_{drag} , the resulting displacement is given by the difference in forces. Neurons at the boundary between the intermediate zone and the cortical plate, tend to overcome this border

by a rapid directional "jumping" preceded by a period of nearly no displacement. We included this migration pattern by introducing a spring force F_{spring}, which stores F_{gen} in case of $F_{gen} < F_{drag}$ (Figure 18A). In the following timestep F_{spring} will be added to F_{gen}. A conceptually similar migration model has been described previously for 3D cell migration (Zaman et al., 2005). We include the cell intrinsic difference between control and KO-*Cdk5r1*-MADM in the form of a directionality parameter ρ and a force scaling parameter α (Caffrey et al., 2014). A value of $\rho = 0.5$ corresponds to a pure random walk model, which KO-*Cdk5r1*-MADM neurons tend towards, whereas control neurons are closer to $= 1$, meaning a higher directionality. The force scaling parameters α controls the magnitude in generated and henceforth higher velocities. When simulating control neuron migration based on our established model for the force generation mechanism and environment resistance (Figure 12B) we can mimic the experimentally observed migration behavior of the neurons and velocity distribution (Figure 12A, C, J, and K). The reduction of ρ and α in a uniformly low resistance environment $\mathrm{R}_{tissue,KO}$ simulates KO-*Cdk5r1*-MADM migration. The migration behavior and velocity distribution match our observations for the experimental data (Figure 12D-F & K). This result indicates that the decrease in value of the defined parameters for directionality and force generation are sufficient to generate the mutant KO-C*dk5r1*-MADM migration behavior (Figure 12J & K). Subsequently, to model the potential non-cell-autonomous effects of the control neurons identified in the *Cdk5r*-MADM scenario, we introduced mutant cells surrounded by control cells in a control tissue resistance environment (Figure 12H). The non-cell-autonomous effect is included by allowing a linear coupling of directionality and force generation coefficient with the ratio β of control cells ($N_{Control}$) to mutant cells (N_{KO}) introduced in the simulation (Figure 12I). Boundary values for α and ρ at $\beta = 0$ and $\beta = 1$ correspond to values from experimental data for KO-*Cdk5r1*-MADM and control, respectively (Supplementary Figure 18B). The simulation of the mixed model (Figure 12I), containing control and mutant neurons, mimicked the dynamics we detected in the tissue of the *Cdk5r1*-MADM where mutant neurons are more dynamic than detected in the KO-*Cdk5r1*-MADM (Figure 12J-K). Figure 18B-C shows the dynamics modelled as a gradual effect solely dependent on the ratio β, suggesting that the non-cell-autonomous effects are sensitive to the ratio of mutant cells.

In summary, our in silico model can replicate the migration dynamics measured *in situ*, thereby substantiating our hypothesis that cell-adhesion molecules represent a major non-cell-autonomous component altering projection neuron migration dynamics.

4.4.7 MADM analysis reveals similar non-autonomous effects for *Dab1* and *Cdk5r1*

Based on the data presented so far we hypothesized that disruption of cell-adhesion is a general non-autonomous feature of migration mutants. To test this hypothesis we considered *Dab1,* whose deletion causes a severe disruption of the neuronal layering of the cortex, and generated control-MADM4 (*MADM-4*$^{GT/TG}$*; Emx1-Cre*$^{+/-}$), *Dab1*-MADM4 (*MADM-4*$^{GT/TG,\ Dab1}$*; Emx1-Cre*$^{+/-}$) and KO-*Dab1*-MADM4 (*MADM-4*$^{GT,\ Dab1/TG,\ Dab1}$*; Emx1-Cre*$^{+/-}$) mice (Figure 16C). We analyzed the role of *Dab1* in radial neuronal migration at E16, P0, and P21 in the somatosensory cortex by comparing the layer distribution of control-MADM4, *Dab1*-MADM4, and KO-*Dab1*-MADM4 (Figure 13A-C). In the *Dab1*-MADM4 the majority of mutant neurons were positioned in the lower bins, whereas their control counterparts display a similar distribution as in the control-MADM4 (Figure 13A-B). Moreover, during development, the majority of *Dab1*-MADM4 mutant neurons accumulated just below the CP (Figure 19B, F). Interestingly, neurons in the KO-*Dab1*-MADM4 depicted a more even distribution throughout the cortical wall except in the lowest bin representing the white matter (Figure 13C). In addition, in the *Dab1-MADM* the mutant cells were mostly present in the lower layers showing that although the control environment provided a ”normal” environment, indicated by a normal neuronal distribution of control and the presence of MZ and WM, the neurons did not manage to migrate normally (Figure 13B, Figure 19B, F). When comparing the *Dab1* mutant neuronal distribution in the *Dab1*-MADM4 directly to the KO-*Dab1*-MADM4 (Figure 13D), we identified a significantly different distribution between the two scenarios indicating non-cell-autonomous effects of *Dab1* on neuronal migration. The difference in distribution between *Dab1*-MADM4 and KO-*Dab1*-MADM4 was also present at embryonic developmental stages (Figure 19).

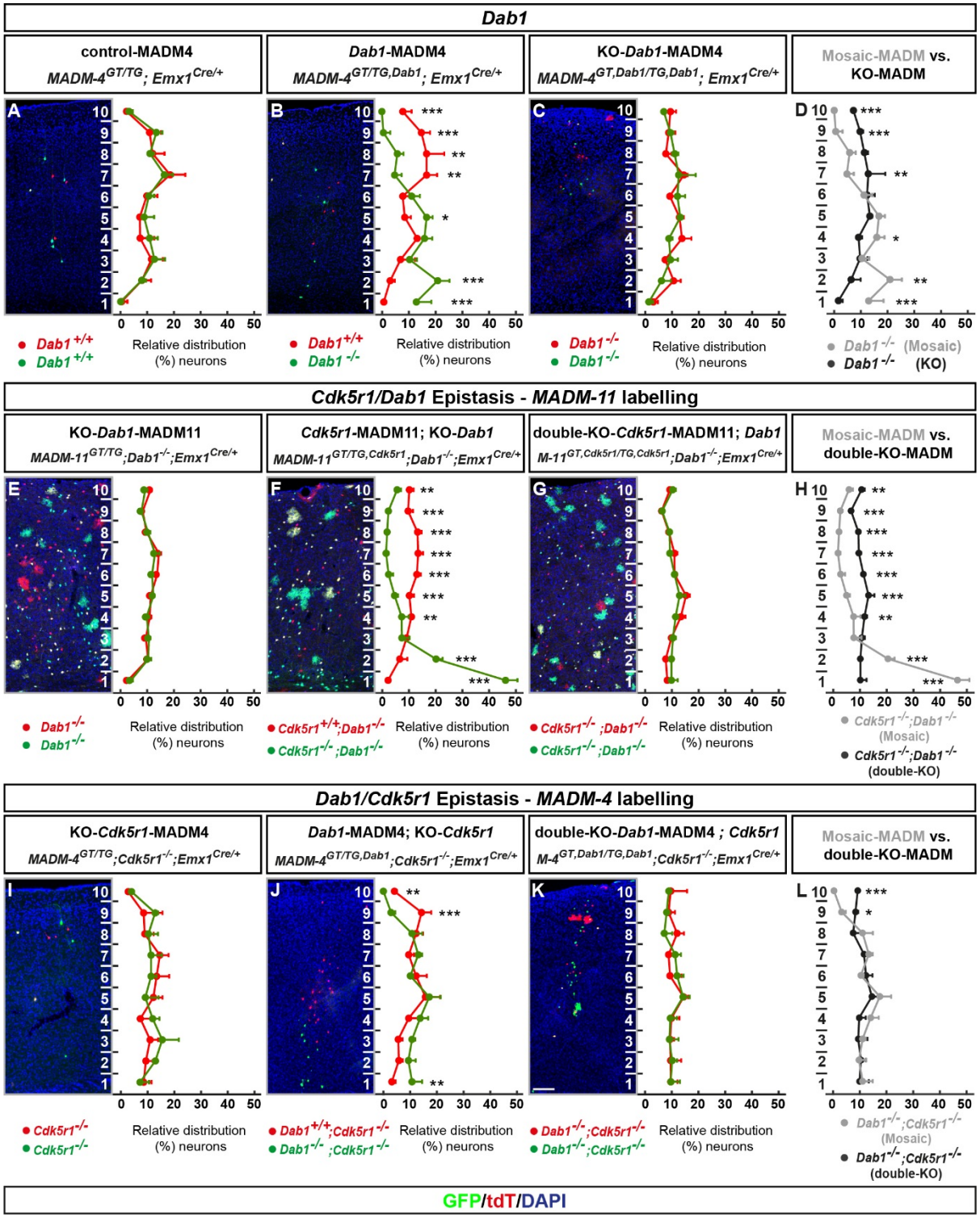

Figure 13 MADM epistasis analysis reveals similar non-cell-autonomous effects for *Dab1* and *Cdk5r1*.

MADM Analysis of developing somatosensory cortex of **(A)** Control-MADM4 (*MADM-4$^{GT/TG}$; Emx1-Cre$^{+/-}$*), **(B)** *Dab1*-MADM4 (*MADM-4$^{GT/TG,\ Dab1}$; Emx1-Cre$^{+/-}$*) and **(C)** KO-*Dab1*-MADM4 (*MADM-4$^{GT,\ Dab1/TG,\ Dab1}$; Emx1-Cre$^{+/-}$*) at time point P21 with quantification of the relative distribution (%) of neurons in 10 bins ranging from the ventricular surface to the pia. **(D)** Comparison of *Dab1*-MADM4 green mutant neuron (grey) versus KO-*Dab1*-MADM4 green mutant neuron (black) distribution. MADM Analysis of P21 somatosensory cortex of **(E)** KO-*Dab1*;

MADM11 (*MADM-11$^{GT/TG}$; Dab1$^{-/-}$; Emx1-Cre$^{+/-}$*), **(F)** *Cdk5r1*-MADM11; KO-*Dab1* (*MADM-11$^{GT/TG,\ Cdk5r1}$; Dab1$^{-/-}$; Emx1-Cre$^{+/-}$*) and **(G)** double-KO-*Cdk5r1*-MADM11; *Dab1* (*MADM-11$^{GT,\ Cdk5r1/TG,\ Cdk5r1}$; Dab1$^{-/-}$; Emx1-Cre$^{+/-}$*) at time point P21with quantification of the relative distribution (%) of neurons in 10 bins ranging from the ventricular surface to the pia. **(H)** Comparison of *Cdk5r1*-MADM11; KO-*Dab1* green mutant neurons (grey) versus double-KO-*Cdk5r1*-MADM11; *Dab1* green mutant neuron (black) distribution. **(I)** KO-*Cdk5r1*; MADM4(*MADM-4$^{GT/TG}$; Cdk5r1$^{-/-}$; Emx1-Cre$^{+/-}$*), **(J)** *Dab1*-MADM4*;* KO-*Cdk5r1* (*MADM-4$^{GT/TG,\ Dab1}$; Cdk5r1$^{-/-}$; Emx1-Cre$^{+/-}$*) and **(K)** double-KO-*Dab1*-MADM4; *Cdk5r1* (*MADM-4$^{GT,\ Dab1/TG,\ Dab1}$; Cdk5r1$^{-/-}$; Emx1-Cre$^{+/-}$*).at time point P21with quantification of the relative distribution (%) of neurons in 10 bins ranging from the ventricular surface to the pia. **(L)** Comparison of *Dab1*-MADM4*;* KO-*Cdk5r1* green mutant neuron (grey) versus double-KO-*Dab1*-MADM4; *Cdk5r1* green mutant neuron (black) distribution. Cortical bins are shown in numbers. n=3 for each genotype. From each animal 10 (MADM-11) or 20 (MADM-4) hemispheres were analyzed. Nuclei were stained using DAPI (blue). Scale bar 100µm. Values represent mean with SD, *p < 0.05, **p < 0.01, and ***p < 0.001.

To test if the non-cell-autonomous effects we identified for both *Cdk5r1* and *Dab1* are dependent on the genetic background in which they appear and could be of a general nature we conducted epistasis experiments of *Cdk5r1* and *Dab1* by generating and analyzing KO-*Dab1*; MADM11 (*MADM-11$^{GT/TG}$; Dab1$^{-/-}$; Emx1-Cre$^{+/-}$*), *Cdk5r1*-MADM11; KO-*Dab1* (*MADM-11$^{GT/TG,\ Cdk5r1}$; Dab1$^{-/-}$; Emx1-Cre$^{+/-}$*) and double-KO-*Cdk5r1*-MADM11; *Dab1* (*MADM-11$^{GT,\ Cdk5r1/TG,\ Cdk5r1}$; Dab1$^{-/-}$; Emx1-Cre$^{+/-}$*) (Figure 13E-G & Figure 20A-B). In the KO-*Dab1*; MADM11 (Figure 13E), where all neurons are mutant for *Dab1*, a similar neuronal distribution as in the KO-*Dab1*-MADM4 was identified (Figure 13C), despite the differences in MADM labeling efficiency (Contreras et al., 2021). Yet, in the *Cdk5r1*-MADM11; KO-*Dab1* the green neurons mutant for both *Cdk5r1* and *Dab1* showed a significantly different distribution compared to red neurons only mutant for *Dab1* in an otherwise *Dab1* mutant environment (Figure 13F). The majority of the green mutant neurons showed accumulation within the lower bins resembling the white matter, again indicating that the requirement of *Cdk5r1* to enter the target area of the CP in both a normal and *Dab1* mutant environment. Moreover, the difference in the mutant neuronal distributions also clearly highlighted a different cell-autonomous gene function of *Cdk5r1* and *Dab1* which supports the notion that they are not directly acting in the same pathway (Bock and May, 2016; Keshvara et al., 2002; Kwon and Tsai, 1998; Ohshima, 2015). In the double-KO-*Cdk5r1*-MADM11; *Dab1* all neurons were evenly distributed throughout the cortical wall (Figure 13G). Direct comparison of *Cdk5r1*-MADM11;KO-*Dab1* and double-KO-*Cdk5r1*-MADM11; *Dab1* identified a significantly different neuronal distribution for mutant *Cdk5r1*; *Dab1* neurons in the two different environments, again exhibiting the contribution of non-cell-autonomous effects (Figure 13H).

Next, to investigate if similar effects would be observed in the reverse scenario of what we generated in the previous experiments (Figure 13E-H), we generated KO-*Cdk5r1*; MADM4 (*MADM-4$^{GT/TG}$; Cdk5r1$^{-/-}$; Emx1-Cre$^{+/-}$*), *Dab1*-MADM4*;* KO-*Cdk5r1* (*MADM-4$^{GT/TG,\ Dab1}$; Cdk5r1$^{-/-}$; Emx1-Cre$^{+/-}$*) and double-KO-*Dab1*-MADM4; *Cdk5r1* (*MADM-4$^{GT,\ Dab1/TG,\ Dab1}$; Cdk5r1$^{-/-}$; Emx1-Cre$^{+/-}$*) (Figure 13I-K & Figure 20C-D). The KO-*Cdk5r1*; MADM4 (Figure 13I) displayed a relatively even distribution of neurons throughout the cortical wall, though with almost no neurons present in the MZ, just as observed in KO-*Cdk5r1*-MADM (Figure 8G) (which was expected as they present the same genotype but labeled using two different MADM mice, MADM4 & MADM11). The distribution in the *Dab1*-MADM4*;* KO-*Cdk5r1* of the green neurons

mutant for both *Dab1* and *Cdk5r1* significantly differed, with neurons not reaching the outer bins, compared to their red labeled counterparts which were only mutant for *Cdk5r1* (Figure 13J). Interestingly, the mutant neurons for both *Dab1* and *Cdk5r1* in the KO-*Cdk5r1* background environment (Figure 13J) displayed a different distribution as was observed in the reverse scenario involving a KO-*Dab1* environment (Figure 13F). The difference between the mutant environments displayed similar effects from the surrounding cells, however, showed two distinct distribution phenotypes for the neurons mutant for both *Cdk5r1* and *Dab1* in the *Cdk5r1* or *Dab1* mutant environments (green neurons in Figure 13F & J). Moreover the double-KO-*Dab1*-MADM4; *Cdk5r1* displayed a different neuronal distribution as observed in the *Dab1*-MADM4*;* KO-*Cdk5r1* (Figure 13J-K), and when compared directly the two distributions were significantly different in the outer two bins (Figure 13L). When comparing the *Cdk5r1* and *Dab1* epistatic mosaics to the double-KOs we observed a different neuronal distribution throughout the cortical wall, suggesting a presence of non-cell-autonomous effects from the surrounding environment, corroborating our previous findings identified in Figure 8-11.

4.4.8 Cell-adhesion is a common non-cell-autonomous component of *Cdk5r1* and *Dab1*

To identify if the overlap in the non-cell-autonomous phenotype of *Cdk5r1* and *Dab1* mutants is also present at the transcriptomic level we investigated the differential gene expression in *Cdk5r1* and *Dab1* mutants. We applied an identical approach as previously described (Figure 10) to isolate green cells from the three genotypes control-MADM11 (*MADM-11*$^{GT/TG}$*; Emx1-Cre*$^{+/-}$), KO-*Cdk5r1*-MADM11 (*MADM-11*$^{GT,Cdk5r1/TG,Cdk5r1}$*; Emx1-Cre*$^{+/-}$), and KO-*Dab1*-MADM11 (*MADM-11*$^{GT/TG}$*; Dab1*$^{-/-}$*; Emx1-Cre*$^{+/-}$) (Figure 14A & Figure 21A). Next, we analyzed the differential gene expression of KO-*Cdk5r1*-MADM11 and KO-*Dab1*-MADM11 relative to control-MADM11 and found more than 1000 deregulated genes in both mutants (Figure 14B) and observed that the majority of deregulated genes were downregulated (Figure 14C).

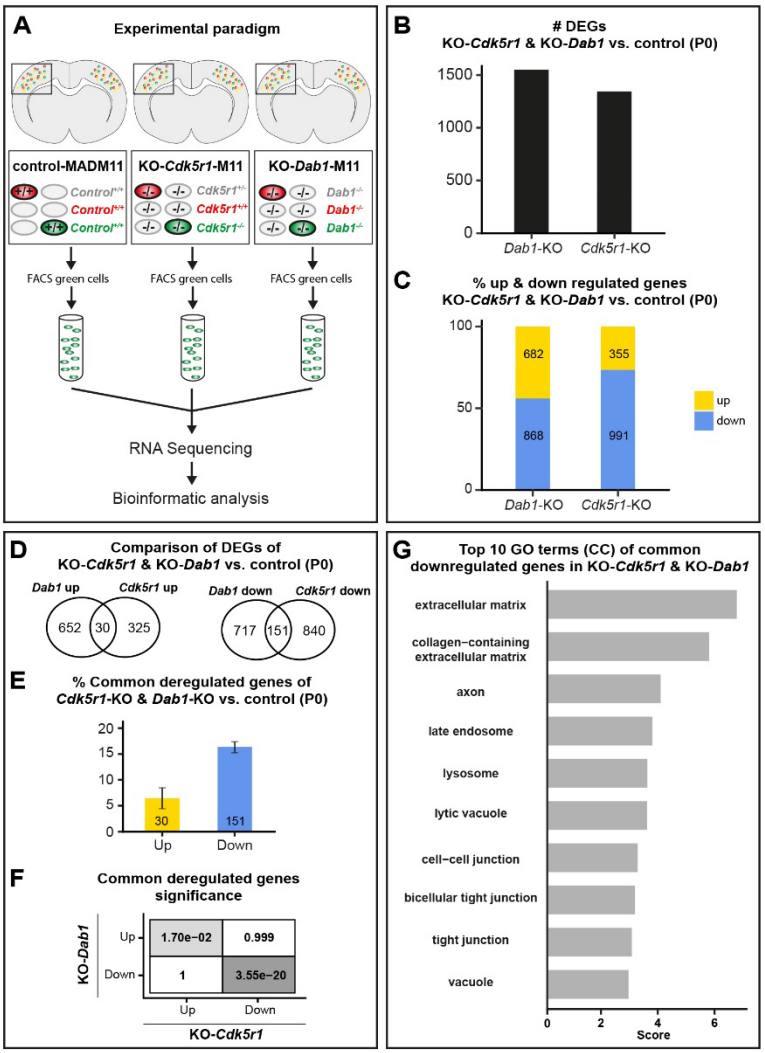

Figure 14 MADM analysis reveal non-autonomous effects for *Dab1* and *Cdk5r1*.

(A) Cortical hemispheres of Control-MADM11 (*MADM-11$^{GT/TG}$; Emx1-Cre$^{+/-}$*), KO-*Cdk5r1*-M11 (*MADM-11$^{GT,Cdk5r1/TG,Cdk5r1}$; Emx1-Cre$^{+/-}$*) and KO-*Dab1*-M11 (*MADM-11$^{GT/TG}$; Dab1$^{-/-}$; Emx1-Cre$^{+/-}$*) at P0. Green mutant neurons were isolated using FACS and subsequently prepared for RNA-sequencing and bioinformatics analysis. **(B)** Total number of differentially expressed genes and **(C)** percentage of up- and down-regulated genes for KO-*Cdk5r1* and KO-*Dab1* versus control at developmental time point P0. **(D)** Venn diagrams showing common up- and down-regulated genes for KO-*Cdk5r1* and KO-*Dab1* versus control at P0. **(E)** Percent common up- and down-regulated genes for KO-*Cdk5r1* and KO-*Dab1* versus control at P0. **(F)** Significance of all pairwise overlaps of DEGs shown in (C) **(D) (G)** Top 10 GO terms of commonly down-regulated genes of KO-*Cdkr5r1*-M11 and KO-*Dab1*-M11 (overlap of D right). Commonly up-regulated genes did not yield any significant GO term enrichment.

To compare the deregulated genes of both mutants we analyzed the overlapping differentially expressed genes and found both common and non-common deregulated genes from the two mutants (Figure 14D). The majority of the commonly deregulated genes were downregulated

(Figure 14E) and both the up- and down-regulated overlap was significant (Figure 14F). Finally, to identify what function these commonly downregulated genes are associated with, we applied gene ontology analysis (Figure 14G). From the commonly downregulated genes, we found significant GO-terms associated with cell-cell and cell-matrix interaction (Figure 14G) however for the upregulated genes we did not obtain any significantly enriched GO-terms. Moreover, the non-common deregulated genes showed overlap of many of their respective GO-terms between KO-*Dab1*-MADM11 and KO-*Cdk5r1*-MADM11 (Figure 21B). Taken together, this analysis suggests that cell-adhesion acts as a major non-cell-autonomous component in radial neuronal migration as we identify a significant overlap of deregulated mRNAs and GO term enrichment analysis for two distinct migration mutants, *Cdk5r1* and *Dab1*.

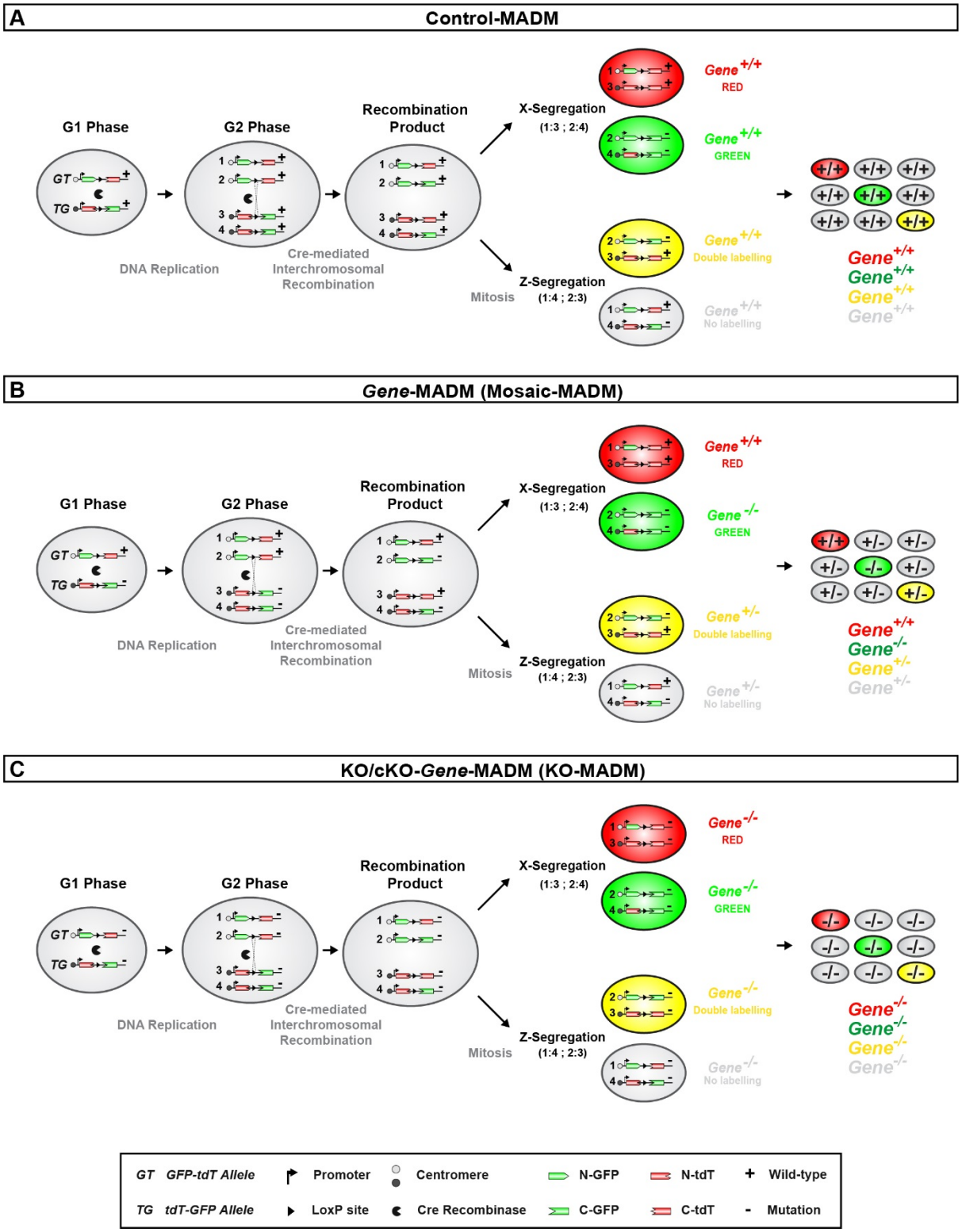

Figure 15 General MADM principle for control-MADM, Mosaic-MADM KO/cKO-MADM

(A) MADM relies on Cre/loxP-dependent interchromosomal recombination to generate sparsely and genetically defined labeled cells in mice. Thus, it is required that two reciprocal MADM cassettes, each containing the partial N-terminal of the coding sequence for one fluorescent protein (eGFP: enhanced green fluorescent protein) and the C-terminal partial coding sequence for another (tdT: tandem dimer Tomato) separated by an intron

containing the loxP-site, are introduced into identical loci on homologous chromosomes. During mitosis, a G2-X event (recombination in G2 of the cell cycle followed by X segregation (left branch)) will result in reconstituted functional green and red fluorescent proteins expressed in each of the two daughter cells, respectively, upon Cre-mediated interchromosomal recombination. If G2-Z (right branch), G1 or G0 (not shown) events occur, the two fluorescent alleles are passed on together resulting in one double-labeled yellow cell and one unlabeled cell. **(B)** Introduction of a mutation distal to one of the MADM cassettes will allow the generation of genetic mosaics where wild-type (e.g. red) and mutant (e.g. green) daughter cells are each labeled in one color in an otherwise unlabeled heterozygous environment. If G2-Z (right branch), G1 or G0 (not shown) events occur, the two fluorescent alleles are passed on together resulting in one double-labeled yellow cell and one unlabeled cell, both heterozygous. **(C)** The introduction of a mutation distal to both of the MADM cassettes allows for the generation of tissue-wide/Global KO where all cells are mutant. For more details see (Zong et al 2005 and Hippenmeyer et al 2010).

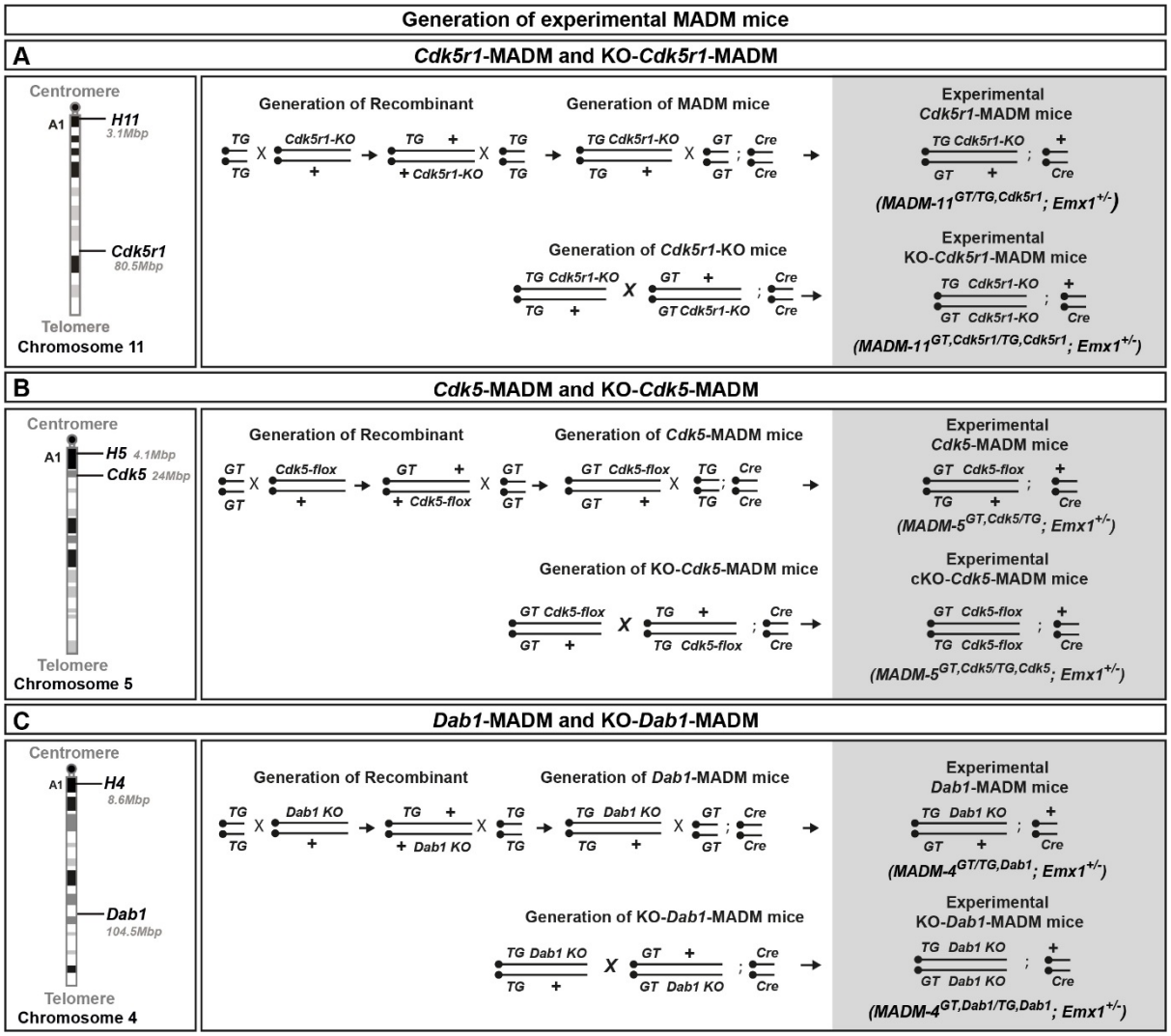

Figure 16 Chromosomal location and breeding schemes for *Cdk5r1*, *Cdk5*, and *Dab1*

(A) Location of H11 genomic locus and *Cdk5r1* on mouse chromosome 11. Breeding scheme for the generation of *Cdk5r1*-MADM and KO-*Cdk5r1*-MADM animals. **(B)** Location of H5 genomic locus and *Cdk5* on mouse chromosome 5. Breeding scheme for the generation of *Cdk5*-MADM and KO-*Cdk5*-MADM animals. **(C)** Location of H4 genomic locus and *Dab1* on mouse chromosome 4. Breeding scheme for the generation of *Dab1*-MADM4 and KO-*Dab1*-MADM4 animals.

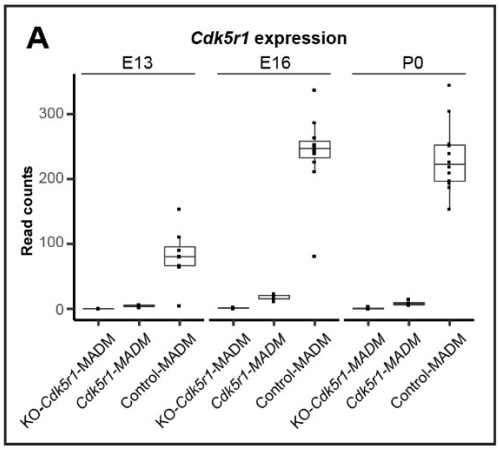

Figure 17. *Cdk5r1* expression in analyzed cells

(A) *Cdk5r1* expression (read counts) for each replicate and genotype.

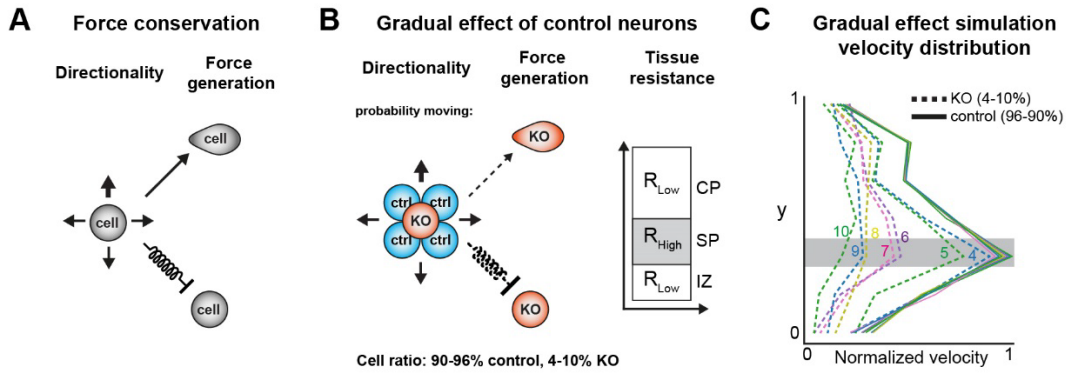

Figure 18 Model concept and gradual effects of mixed model.

(A) General concept of model: Random walk bias of cells in form of directionality and force generation when cells move and with with force conservation included as a spring constant when cells do not move. **(B)** Model setup for mixed neuron migration in control environment in order to investigate the effect if gradual increase in percentage of control neurons in mixed population. Simulated control neurons percentage is varied between 90-96% control neurons with 4-10% mutant. The thickness of the arrows indicate the probability of the mutant neuron to move in any direction. **(C)** Velocity distribution depicting the effect of a gradual increase in percentage of control cells in mixed population. Numbers indicate the percentage of mutant neurons. Note that a cell ratio

of less than 4% mutant would yield a control velocity distribution and a cell ratio of more than 10% mutant would yield a KO velocity distribution of the mutant neurons.

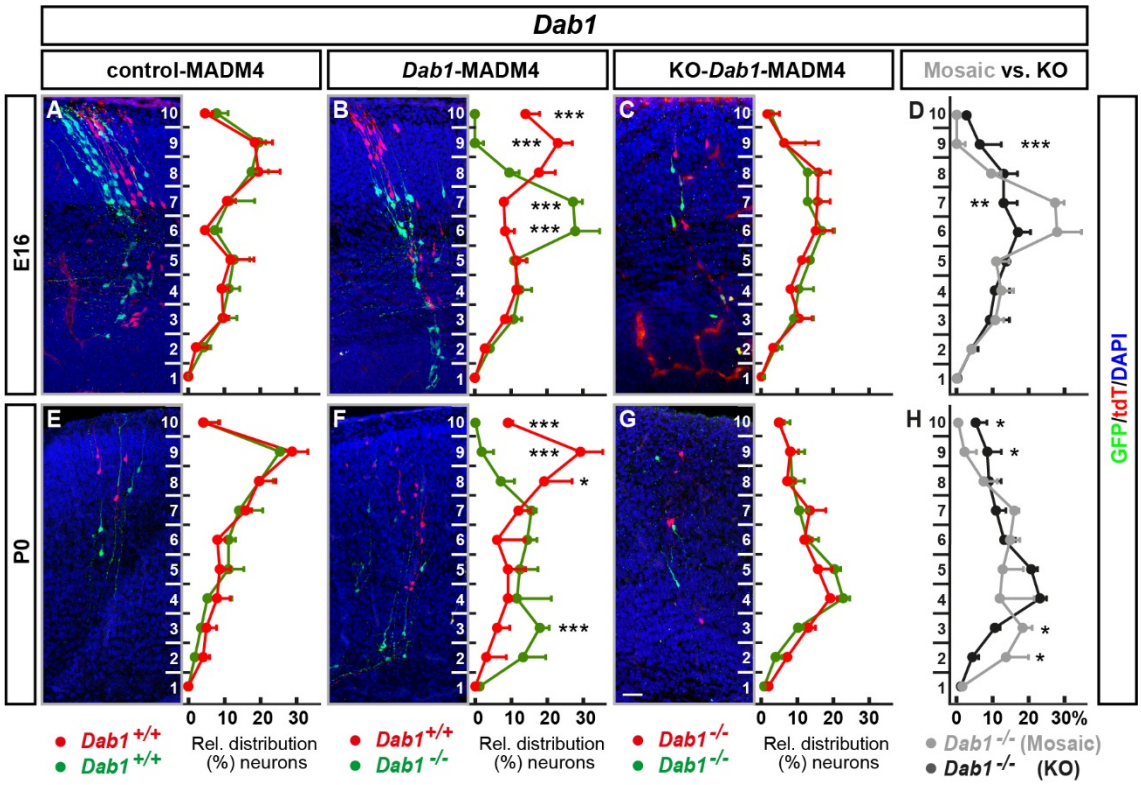

Figure 19 *Dab1* developmental time points E16 & P0 in the somatosensory cortex.

(A, E) Control-MADM4 (*MADM-4*$^{GT/TG}$*; Emx1-Cre*$^{+/-}$), **(B, F)** *Dab1*-MADM4 (*MADM-4*$^{GT/TG,\ Dab1}$*; Emx1-Cre*$^{+/-}$) and **(C, G)** KO-*Dab1*-MADM4 (*MADM-4*$^{GT,\ Dab1/TG,\ Dab1}$*; Emx1-Cre*$^{+/-}$) at time points E16 and P0 with quantification of the relative distribution (%) of neurons in 10 bins ranging from the ventricular surface to the pia. **(D & H)** Comparison of *Dab1*-MADM4 green mutant neuron (grey) versus KO-*Dab1*-MADM4 green mutant neuron (black) distribution. Cortical bins are shown in numbers. n=3 for each genotype. From each animal 20 hemispheres were analyzed. Nuclei were stained using DAPI (blue). Scale bar 50µm. Values represent mean with SD, *p < 0.05, **p < 0.01, and ***p < 0.001.

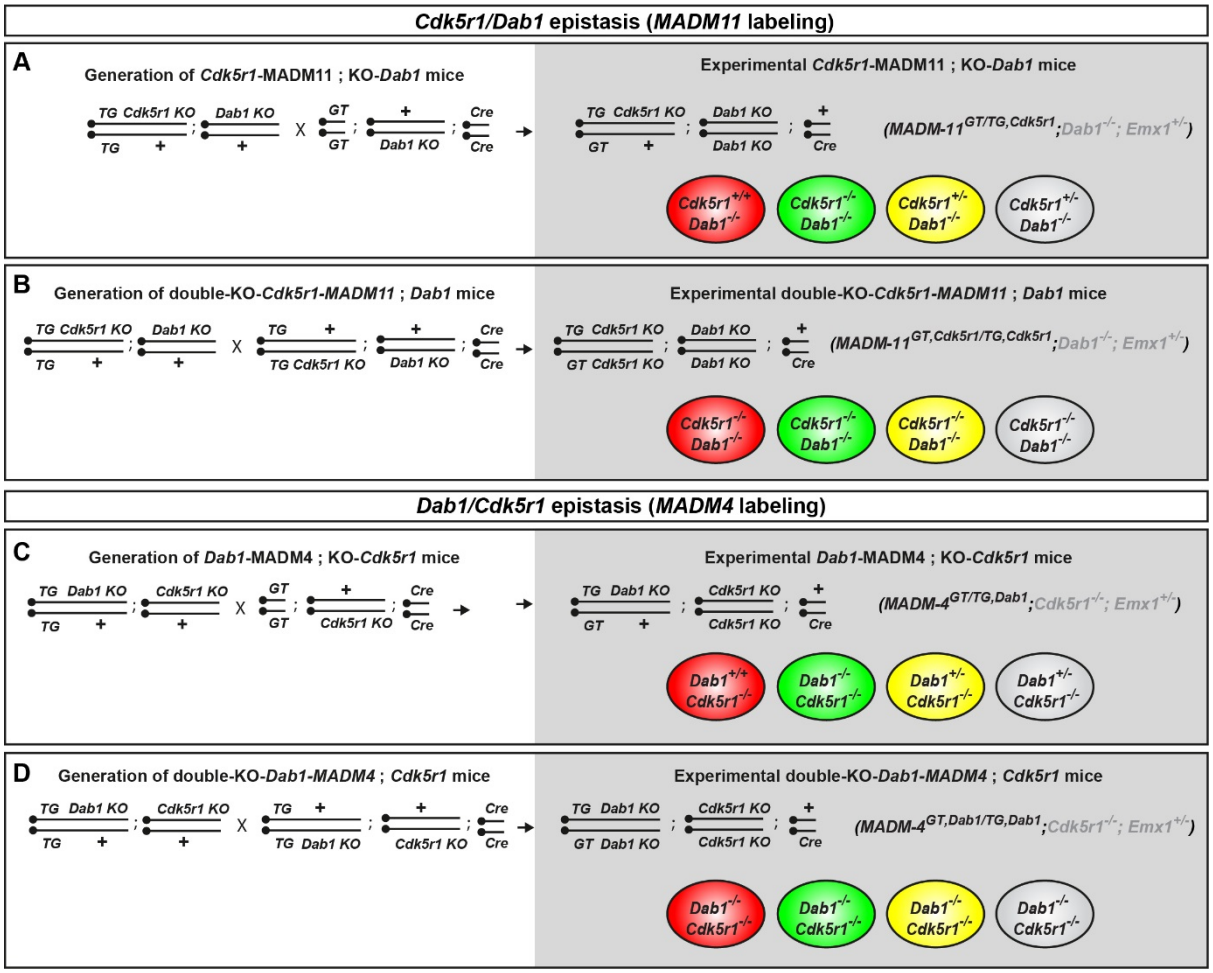

Figure 20 Breeding schemes for *Cdk5r1/Dab1* epistasis experiments.

Cdk5r1/Dab1 epistasis breeding scheme for **(A)** *Cdk5r1-MADM11*; KO-*Dab1* (*MADM-11*$^{GT/TG,\ Cdk5r1}$*; Dab1*$^{-/-}$*; Emx1-Cre*$^{+/-}$) **(B)** double-KO-*Cdk5r1*-MADM11; *Dab1* (*MADM-11*$^{GT,\ Cdk5r1/TG,\ Cdk5r1}$*; Dab1*$^{-/-}$*; Emx1-Cre*$^{+/-}$) with *MADM-11* labeling. *Dab1/Cdk5r1* epistasis breeding scheme for **(C)** *Dab1-MADM4;* KO-*Cdk5r1* (*MADM-4*$^{GT/TG,\ Dab1}$*; Cdk5r1*$^{-/-}$*; Emx1-Cre*$^{+/-}$) and **(D)** double-KO-*Dab1*-MADM4; *Cdk5r1* (*MADM-4*$^{GT,\ Dab1/TG,\ Dab1}$*; Cdk5r1*$^{-/-}$*; Emx1-Cre*$^{+/-}$) with *MADM-4* labeling. Colored cells indicate the genotype of the labeled cells in the generated animals.

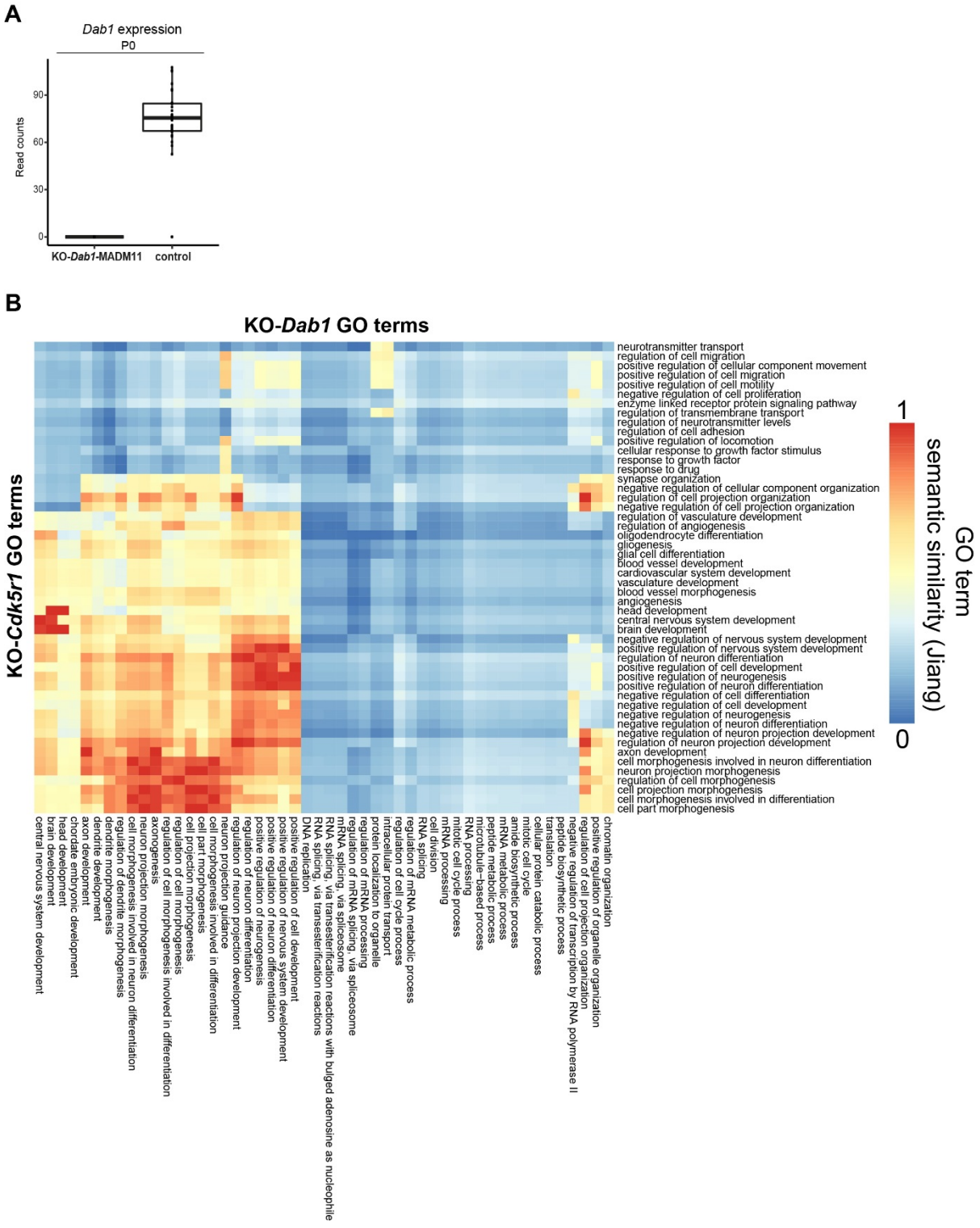

Figure 21 *Dab1* expression and GO term similarity of *Dab1* and *Cdk5r1*.

(A) *Dab1*expression (read counts) for each replicate for control-MADM11 (*MADM-11$^{GT/TG}$; Emx1-Cre$^{+/-}$*) and KO-*Dab1*; MADM11 (*MADM-11$^{GT/TG}$; Dab1$^{-/-}$; Emx1-Cre$^{+/-}$*) with *MADM-11* labeling. **(B)** GO term semantic similarity (Jiang) of non-common deregulated genes in GO terms of KO-*Dab1* and KO-*Cdk5r1*. Similarity values closer to 1 indicate a high similarity of the GO term.

4.5 Discussion

Radial neuronal migration is known to be crucial for the assembly of the layered structure of the cerebral cortex. However, the cellular and molecular mechanisms regulating radial neuronal migration *in vivo* are still not fully understood, particularly the effects and interactions with the extracellular environment. The nature of such non-cell-autonomous effects affecting the development of the brain and neuronal migration in particular still remain unclear. Here, for the first time, we quantitatively distinguish non-cell-autonomous effects from intrinsic cell-autonomous gene functions on a cellular and molecular level using a MADM based paradigm with single cell resolution. High-resolution analysis of projection neuron migration dynamics in distinct environments with concomitant isolation of transcriptomic and proteomic profiles which in combination with computational modeling identified cell-adhesion as a major tissue-wide non-cell-autonomous effects affecting projection neuron migration and thereby the development of the brain (Figure 22). In the *Cdk5r1*-MADM (Mosaic-MADM) we identified a failure of the mutant neurons to invade the cortical plate, displaying the cell-autonomous gene function. In the KO-*Cdk5r1*-MADM a tissue-wide irregular migration of neurons is observed, which is due to non-cell-autonomous effects. These non-cell-autonomous effects are likely caused by a downregulation of cell-adhesion essential proteins, as we identify it as the main downregulated in both transcriptomic and proteomic approaches. In the *Cdk5r1*-MADM, the normal environment provides a normal expression of cell-adhesion proteins in the *Cdk5r1*-MADM mutant neurons. Hence, the downregulation of cell-adhesion essential molecules identifies to be a major non-cell-autonomous component which most likely causes the irregular migration in KO-*Cdk5r1*-MADM and thereby leads to aberrant lamination in the global KO cortex. Our modelling approach could mimic KO-C*dk5r1*-MADM and *Cdk5r1*-MADM migration behavior and can therefore be correlated to the reduction of cell-adhesion molecules we measured on a transcriptomic and proteomic level to exert non-cell-autonomous effects. Inferred from the results, showing a significant overlap of a non-cell-autonomous component between the two distinct migration mutants *Cdk5r1* and *Dab1,* suggests that non-cell-autonomous/community effects involving cell-adhesion (cell-cell and cell-matrix interaction) could be a general response present in most migration mutants. Therefore, the tissue-wide non-cell-

autonomous effects might be of universal nature and could be a major source of aberrant neuronal layering observed in many migration phenotypes (Figure 22).

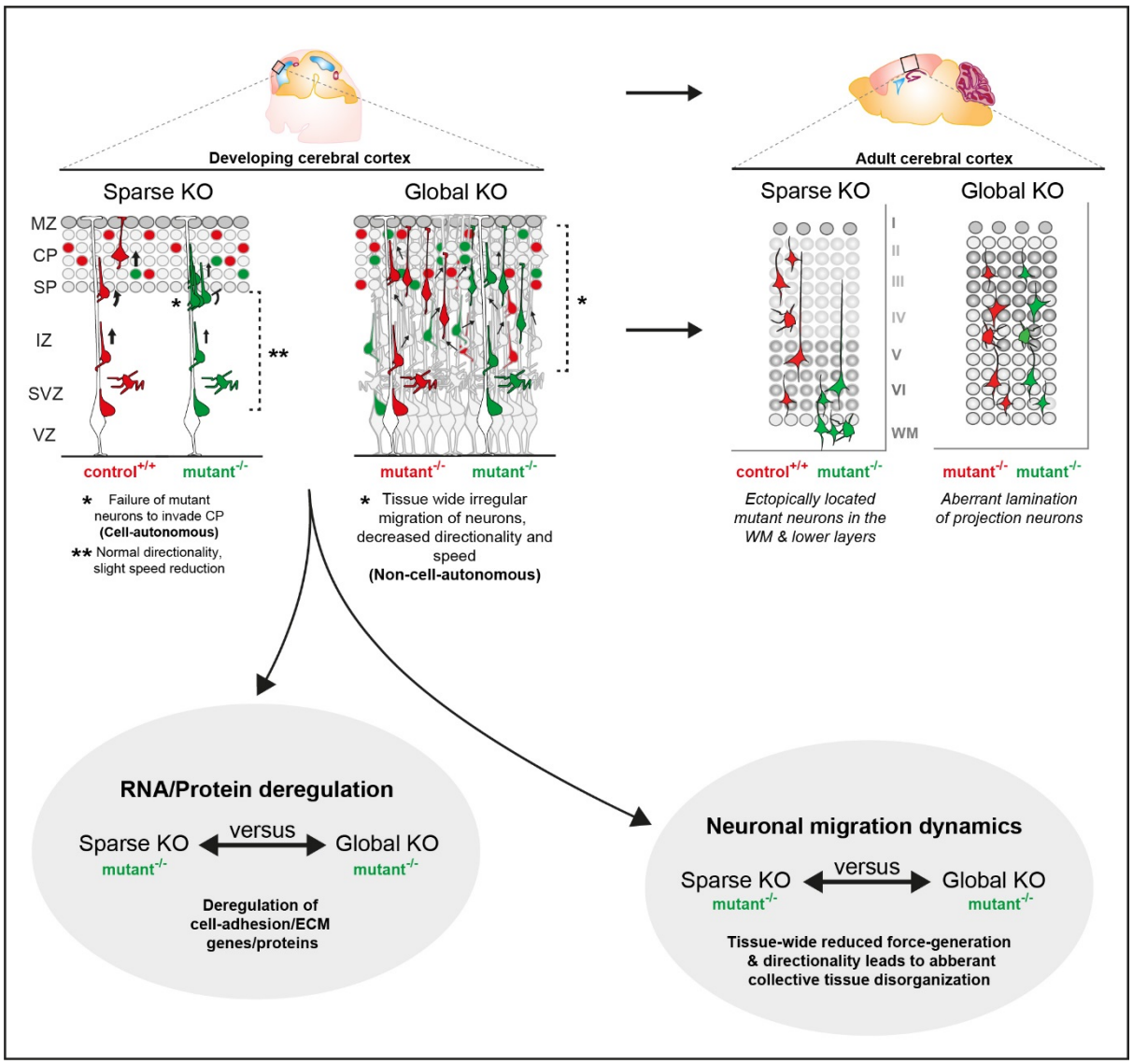

Figure 22 The Interplay of intrinsic and tissue-wide mechanisms in radial neuronal migration

To investigate the nature of non-cell-autonomous effects we pursued subtractive phenotypic analysis of genetic mosaics (Mosaic-MADM) comprising a wild-type/heterozygote environment with global knockout (KO/cKO-MADM) which has a complete environment, both coupled with sparse fluorescent MADM-labeling of homozygous mutant neurons. Such assay enabled the high-resolution analysis of projection neuron migration dynamics in distinct environments with concomitant isolation of genomic and proteomic profiles. In combination with computational modeling, we utilize these experimental paradigms to identify so far unknown non-cell-autonomous effects coordinating radial neuron migration. In a Mosaic-MADM, which provided a normal environment, enabled the mutant neurons to migrate more dynamically and to express cell-adhesion molecules like their control counterparts. However, in a KO-MADM, we observed cell-adhesion essential molecules

significantly downregulated in combination with a severe migration phenotype where mutant neurons move much less, resulting in a complete disorganization of layering in the adult cortex. Our MADM-based analysis identified non-cell-autonomous net effects of the tissue environment, exerted through cell-adhesion, to overrule cell-autonomous gene function.

Previous studies have observed that migrating neurons can have a positive and negative influence on each other depending on the environment and their genetic constitution (Hansen and Hippenmeyer, 2020). For example, cell-cell interactions during collective cell migration, in a variety of cell types, have indeed been observed previously. Studies of collective cell migration, e.g., in neural crest cells have provided evidence that balancing adhesion and repulsion is one major factor mediating both individual cell and collective migratory coordination (Shellard and Mayor, 2020). Collective decision-making and organization of cells are crucial for the generation of complex tissue and most likely apply to the assembly of the cerebral cortex to a certain degree as the assembly of this structure relies on the migration of neurons. Our results suggest that the effects of surrounding neurons could be through signaling, as the "normal" environment in the mosaic *Cdk5r1*-MADM enables *Cdk5r1* mutant neurons to express cell-adhesion essential molecules to a similar extent as the control neurons surrounding them in the same tissue. This effect of the surrounding "normal" neurons could then allow for stimulation or tuning down of the intrinsic migratory machinery of *Cdk5r1*-deficient neurons suggesting a mechanism whereby active signaling could be utilized through transmembrane receptors and/or extracellular matrix components (Cavallaro and Dejana, 2011). Such mechanisms have been described, *in vitro*, in various cell types where mutant cells negatively affect migration by direct contact inhibition upon ectopic expression of a range of cell adhesion molecules (Becker et al., 2013; Huttenlocher et al., 1998). In accordance with our results, it was observed that mutant cells surrounded by wild-type cells did not display any major negative effects. However, mutant cells in direct contact with other mutant cells showed an inhibited migratory process (Becker et al., 2013; Huttenlocher et al., 1998). Moreover, a collective, non-cell-autonomous effect/mechanism, could also be due to direct physical properties where mutant neurons (which are less dynamic and agile in terms of KO-*Cdk5r1*-MADM) could be passively pushed or pulled by a migrating "normal" cellular population or simply "piggyback" on adjacent

normally migrating neurons positively affecting the movement of the mutant neurons. Yet, the collective effects, as observed in the KO-*Cdk5r1*-MADM, can also have negative effects if most or all neurons are mutant and less dynamic, thereby leading to improper migration. On that note, an *in vivo* study investigating a FMCD-causing (focal malformations of cortical development) mutation revealed that over activation of AKT3 in a fraction of migrating neurons would lead to misexpression of Reelin in the mutant cells and thereby affect the migration of wild-type neighboring cells in a non-cell-autonomous manner (Baek et al., 2015). Moreover, they further investigated if the non-cell-autonomous migration defect observed could be due to a simple direct physical blockade of the wild-type cells or maybe have a more specific signaling mechanism. Interestingly, utilizing gene expression profiling and GO term enrichment analysis they identified significantly deregulated genes identified four main categories for neuronal development, migration, signaling and homeostasis and cell cycle regulation suggesting that the non-cell-autonomous defect underlie a more complicated mechanism than just a simple blockade of neurons (Baek et al., 2015). In accordance, we identified that gene expression can be affected by non-cell-autonomous effects causing deregulation in the KO-MADM and enabled more or less “normal” gene expression of the mutant neurons in the Mosaic-MADM environment. In the present study we observed a positive response where the wild-type control environment would rather facilitate migration of the mutant cells than inhibit them. Another recent study also suggests that mutation of a subset of neurons might affect the entire cellular community. By knockdown of the cytoplasmic proteins, *Dcx* and *Dclk* in neurons, screening for potential non-cell-autonomous regulators of radial neuronal migration identified autotaxin (ATX) to affect the localization and adhesion of neuronal progenitors in a cell-autonomous and non-cell-autonomous manner (Greenman et al., 2015). A follow-up study investigating the candidate gene Serping1, identified in the previous screening, showed to be expressed and secreted by neurons during brain development and both affect radial neuronal migration in a cell-autonomous and non-cell-autonomous way (Gorelik et al., 2017). Besides affecting the positioning of the neurons, loss of Serping1 gene function would also affect the cellular morphology of the neighboring neurons since knockdown neurons exhibited long leading processes which were also observed in the adjacent non-manipulated neurons (Gorelik et al., 2017), likewise suggesting a more complex mechanism than solely of physical nature. Studies investigating Reelin

signaling in the control of radial projection neuron migration have also suggested that environmental conditions play a role in proper neuronal positioning, and proposed a non-cell-autonomous effect and/or element of *Dab1* function (Hammond et al., 2001; Yang et al., 2002). Moreover, deletion of *Dab1* specifically in late born projection neurons and after pre-plate splitting, it was observed that wild-type early born neurons were positioned in the outer layers instead of their usual position in the inner cortical layers. This positioning of the neurons suggests that early-born neurons are being "passively" displaced into a deeper position by later-born neurons (Franco et al., 2011). We observe a non-cell-autonomous component of *Dab1*, hence, it is likely that the pleiotropy of *Reelin-Dab1* loss of function phenotypes described previously could be significantly affected by tissue-wide community effects potentially exerted through cell-adhesion essential components in addition to the cell-autonomous function of Reelin signaling on migrating neurons. Indeed, the Reelin-DAB1 pathway has been shown to control cell-adhesion during neuronal migration (Franco et al., 2011; Sekine et al., 2012, 2014).

Our findings put a new perspective on disease-causing mutations that affect radial neuronal migration and how malformations of the brain may arise, as non-cell-autonomous local or tissue-wide mechanisms might overrule cell-intrinsic gene function. For example, FMCD represents an example of a disorder where mutations in a small fraction of cells disrupt the entire cortical architecture. FMCDs can cause hemimegalencephaly, which is characterized by the enlargement of one entire cerebral cortex hemisphere (Lee et al., 2012; Poduri et al., 2012, 2013; Rivière et al., 2012). Moreover, hemimegalencephaly and other malformations of cortical development can include a large spectrum of disorders with various types of cortical dysplasias such as pachygryia, polymicrogyria, and poor formation or absence of the corpus callosum (Juric-Sekhar and Hevner, 2019). From a clinical perspective, it is therefore important to scrutinize the contribution of non-cell-autonomous, tissue-wide, and systemic mechanisms in cortical development in general, and neuronal migration in particular. Interestingly, in terms of clinical phenotype, the brain disorder characterized as lissencephaly with cerebellar hypoplasia (LCH) has been attributed to individuals identified with mutations in *CDK5* or *RELN* (Hong et al., 2000; Magen et al., 2015). The overlap of the human phenotypes could substantiate the possibility of a common non-cell-autonomous effects contributing to the phenotype as indicated by our results of a common non-cell-

autonomous cell-adhesion component of *Cdk5r1* and *Dab1*. Therefore, non-autonomous/community effects that contribute to the impaired neuronal migration could result in the disorganized layering of the cortex in the majority of migration mutants to a more or less degree, independent of the mutant gene itself. Comprehending the interaction of cell intrinsic gene function and non-cell-autonomous effects will help to further understanding the underlying etiology of neurodevelopmental disorders due to genetic mutations.

In conclusion, this study presents non-cell-autonomous effects as a major component regulating radial neuronal migration. We suggest that intrinsic cytoplasmic proteins, besides acting cell-autonomously, can exert non-cell-autonomous cell-cell interactions through cell-adhesion molecules. Our MADM-based analysis identified non-cell-autonomous net effects of the tissue environment, exerted through cell-adhesion, to overrule cell-autonomous gene function. Non-cell-autonomous effects were scarcely studied in cortical development and we hope that future studies will further elucidate the interplay of cell-autonomous gene function and non-cell-autonomous mechanisms regulating the development of the brain.

4.6 Acknowledgments

We thank J. Renno, J.Sonntag and L. Andersen for initial experiments, technical support and/or assistance; M. Sixt, J. Nimpf and all members of the Hippenmeyer lab for discussion; Ana Villalba Requena and Ximena Paniagua Contreras for comments on the manuscript. A.H. was a recipient of a DOC Fellowship (24812) of the Austrian Academy of Sciences. This work also received support from IST Austria institutional funds; the People Programme (Marie Curie Actions) of the European Union's Seventh Framework Programme (FP7/2007-2013) under REA grant agreement No 618444 to S.H.

4.7 Methods

4.7.1 Mouse Lines

All mouse colonies were maintained in accordance with protocols approved by the institutional animal care and use committee, institutional ethics committee, and the preclinical core facility (PCF) at IST Austria. Experiments were performed under a license approved by the Austrian Federal Ministry of Science and Research following the Austrian and EU animal laws (license numbers: BMWF-66.018/0007-II/3b/2012 and BMWFW-66.018/0006-WF/V/3b/2017).

Mice with specific pathogen-free status according to FELASA recommendations (Mähler (Convenor) et al., 2014) were bred and maintained in experimental rodent facilities (room temperature 21 ± 1°C [mean ± SEM]; relative humidity 40%–55%; photoperiod 12L:12D). Food (V1126, Ssniff Spezialitäten GmbH, Soest, Germany) and tap water were available ad libitum. Mouse lines with MADM cassettes inserted on Chr. 4, Chr. 5, and Chr. 11 (Contreras et al., 2021; Hippenmeyer et al., 2010) (MADM-4-GT, MADM-4-TG, MADM-5-GT, MADM-5-TG, MADM-11-GT (JAX stock # 013749), MADM-11-TG (JAX stock # 013751), *Cdk5r1* (Chae et al., 1997) (JAX stock # 004163), *Cdk*5 (Samuels et al., 2007) (JAX stock # 014156), *Dab1* (Howell et al., 1997) (JAX stock # 003581); *Emx1*-Cre (Gorski et al., 2002) (JAX stock # 005628), were previously described. We have not observed any influence of sex on the results in our study, and all experiments and analyses were thus carried out using animals of both sexes. Phenotypic time-course analysis of *Dab1*-MADM-4, *Cdk5*-MADM-5, *Cdk5r1*-MADM-11 in combination with *Emx1*-Cre was performed at E14, E16, P0, and P21. For sequencing and proteomics experiments, MADM-11 animals were used in combination with *Emx1*-Cre and were analyzed at E13, E16, and P0. Genetic epistasis experiments of *Cdk5r1* and *Dab1* on MADM-4 and MADM-11 in combination with *Emx1*-Cre were all performed at P21.

4.7.2 Isolation of fixed tissue

Tissues from adult time points (P15/P21) were collected by cardiac perfusion. Mice were deeply anesthetized through injection of a ketamine/xylazine/acepromazine solution (65 mg, 13 mg, and 2 mg/kg body weight, respectively) and unresponsiveness was confirmed through pinching the paw. The diaphragm of the mouse was opened from the abdominal side to

expose the heart. Cardiac perfusion was performed with PBS followed immediately by 4% PFA prepared in PB buffer (Sigma-Aldrich). Brains were removed and further fixed in 4% PFA for 24hours to ensure complete fixation. Brains were cryopreserved with 30% sucrose (Sigma-Aldrich) solution in PBS for approximately 48 hours. Brains were then embedded in Tissue-Tek O.C.T. (Sakura). For adult time points, 45µm coronal sections were collected in 24 multi-well dishes (Greiner Bio-one) and stored at −20°C in antifreeze solution (30% v/v ethylene glycol, 30% v/v glycerol, 10% v/v 0.244M PO4 buffer) until used. Tissue from embryonic timepoints (E14 & E16) and postnatal day zero (P0) was directly transferred into 4% PFA and kept at least 24 hours at 4°C. Cryopreservation and embedding were done as described for adult brains. Embryonic and early postnatal brains were sectioned with 25µm and directly mounted onto Superfrost glass-slides (Thermo Fisher Scientific).

4.7.3 Immunohistochemistry

Brain sections were mounted onto Superfrost glass-slides (Thermo Fisher Scientific) and let to dry, followed by 3 wash steps each of 5 minutes with PBS. Tissue sections were blocked for 30 minutes in a buffer solution containing 5% normal donkey serum (Thermo Fisher Scientific) and 0.5% Triton X-100 in PBS. Primary antibodies were mixed in the blocking buffer and incubated on the tissue for at least 12hours at 4°C. Sections were washed 3 times for 5 minutes each with PBT (0.5% Triton X-100 in PBS) and incubated with the corresponding secondary antibody diluted in PBT for 1 hour. Sections were then washed 2 times with PBT and once with PBS each for 5 minutes. Finally, nuclear staining was done using 10 minutes of incubation with PBS containing 2.5% DAPI (Thermo Fisher Scientific). Sections were embedded in mounting medium containing 1,4-diazabicyclooctane (DABCO; Roth) and Mowiol 4-88 (Roth) and stored at 4°C.

4.7.4 Imaging of fixed brain tissue

Histological brain sections were imaged using confocal microscopy (Zeiss inverted LSM800) or epifluorescence microscopy (Olympus VS120 Slide scanner). Confocal images were recorded on a Zeiss LSM 800 laser-scanning confocal microscope mounted with a plan-apochromat 10x/0.45, WD=2.1 mm objective. Excitation/emission wavelengths were 488/509 nm (EGFP), 554/581nm (tdTomato), and 353/465nm (DAPI). Z-series images were collected on a PC running ZEN 2.6 software (Zeiss). Image series were Z-projected, stitched and

contrast-enhanced using ZEN 2.6 software (Zeiss). Slidescanner images were recorded with a 10x / NA 0.4 objective. Excitation/emission wavelengths were 485/518 nm (FITCH), 560/580nm (Cy3), and 387/455nm (DAPI). Slide scanner images were processed using ImageJ software (Schindelin et al., 2012).

4.7.5 Preparation of Cell Suspension and FACS

Preparation of cell suspension for cell sorting was prepared as previously described (Laukoter et al., 2020a) for E13, E16, and P0 time points for RNA-seq and P0 for proteomics. From the MADM samples, GFP+ cells were collected for each genotype. For RNA-sequencing, cells were sorted directly into a custom-made lysis buffer (30nM TRIS pH 8, 10nM EDTA pH 8, 1% SDS and 200 µg/µL Proteinase K). For proteomics, cells were prepared as described above except no serum was added to the media and an extra wash step with DMD/F12 wash was carried out. Samples for proteomics were sorted directly into 50ul lysis buffer (LYSE-NHS, Preomics iST-NHS kit).

4.7.6 RNA Extraction of MADM Samples for RNA Sequencing

Directly after cell sorting using FACS, samples were incubated for 30min at 37°C. Total volume was filled to 250µl using RNase-free H2O (Thermo Fisher Scientific) followed by the addition of 750µl Trizol LS (Thermo Fisher Scientific). Samples were mixed by 5 times inverting. After a 5min incubation step at RT, the entire solution was transferred into a MaXtract tube (QIAGEN). 200µl chloroform (Sigma-Aldrich) was added, followed by 3 times 5sec vortexing and 2min incubation at RT. Samples were centrifuged for 2min at 12000rpm at 18°C. The supernatant was transferred to a new tube and isopropanol (Sigma-Aldrich) was added in a 1:1 ratio. For better visibility of the RNA pellet 1µl GlycoBlue (Thermo Fisher Scientific) was added and the entire solution was mixed by vortexing (3x 5sec). Samples were left for precipitation o/n at −20°C. After precipitation samples were centrifuged for 20min with 14000rpm at 4°C. The supernatant was removed and the RNA pellet was washed with 70% ethanol, followed by a 5min centrifugation step (14000rpm at 4°C). The RNA pellet was resuspended in 12,5µl RNase-free H2O. RNA quality was analyzed using RNA 6000 Pico kit (Agilent) following the manufacturer's instructions. The RNA samples were stored at −80°C until further use. RNA sequencing was performed by VBCF GmbH on Illumina platforms.

4.7.7 Sample processing for proteomics

Samples were divided into two batches, each containing 3 control samples and 5 *Cdk5r1*-MADM or KO-*Cdk5r1*-MADM samples. Batch 1, processed on day 1, contains green cells from two individual litters and corresponds to control versus KO-*Cdk5r1*-MADM comparison; batch 2, processed on day 2, contains green from 3 individual litters and was used for the control versus *Cdk5r1*-MADM comparison. Each litter contains both control and either *Cdk5r1*-MADM or KO-*Cdk5r1*-MADM. Protein extraction, tryptic digestion, and peptides cleanup were performed using a TMT-labeling compatible variant of the in-Stage Tips method (iST-NHS-12x kit, Preomics). Briefly, immediately after cell-sorting, collected cells were supplemented with 50 µL LYSE-NHS buffer, boiled for 10 min, then processed according to the manufacturer's protocol with the following minor modifications: sonication was skipped (the number of cells was low enough that DNA would not be an issue, and this would reduce the chance of proteins loss or samples contamination due to having to use a probe sonicator); and digestion was performed overnight. Prior to TMT labeling, small aliquots of each of the 16 samples were taken and mixed to generate a mixed reference sample. Individual samples were then labeled with TMT-10 plex (lot # UL291039, ThermoFisher Scientific), splitting the contents of each TMT vial to label one sample of each batch. Individual samples were combined into 2 TMT-labeled samples, each containing the 8 samples from one batch plus a mixed reference sample. Combined samples were then loaded onto the iST-NHS kit's cartridges in several steps, washed as per the manufacturer's protocol, eluted, and dried in a speedvac. Since phospho-peptides were of interest, although the amount of material as determined by a Pierce Quantitative Colorimetric Peptide Assay (Thermo Scientific) was low (~100 µg/sample), the samples were subjected to phospho-peptides enrichment (MagReSyn Ti-IMAC beads, ReSyn Biosciences) according to manufacturer's protocol but scaling down beads amount, then the flow-throughs were fractionated into 8 fractions using the Pierce High pH Reversed-Phase Peptide Fractionation Kit (ThermoFisher Scientific).

4.7.8 LCMS analysis

Samples were dried, redissolved in 0.1 % TFA and analyzed by LC-MS/MS on an Ultimate HPLC (ThermoFisher Scientific) coupled to a Q-Exactive HF (ThermoFisher Scientific). Each sample was concentrated over an Acclaim PepMap C18 pre-column (5 µm particle size, 0.3 mm ID x

5 mm length, ThermoFisher Scientific) then bound to a 50 cm EasySpray C18 analytical column (2 µm particle size, 75 µm ID x 500 mm length, ThermoFisher Scientific) and eluted over the following 90 min gradient: solvent A, water + 0.1% formic acid; solvent B, 80% acetonitrile in water + 0.08% formic acid; constant 300 nL/min flow; B percentage: start, 2%; 70 min, 31%; 90 min, 44%. Mass spectra were acquired in positive mode with a Data Dependent Acquisition method: FWHM 20s, lock mass 445.12003 m/z; MS1: profile mode, 120,000 resolution, AGC target 3e6, 50 ms maximum IT, 380 to 1,500 m/z; MS2: top 20, centroid mode, 1 microscan, 60,000 resolution, AGC target 1e5, 100 ms maximum IT, 0.7 m/z isolation window (no offset), 100 m/z fixed first mass, NCE 32, excluding charges 1 and 8 or higher, 60s dynamic exclusion.

4.7.9 Slice culture and time-lapse imaging

Embryos were collected at E16 and stored in ice-cold PBS during genotyping. Immediately after genotyping, MADM labeled embryonic brains were dissected and mounted in 4% low-melting agarose (Fisher BioReagents). 300µm coronal slices were prepared in oxygenated ice-cold artificial cerebrospinal fluid (ACSF) using a vibratome (Leica VT 1200S). Thereafter, slices were placed on Milicell culture inserts (Millipore) in 6-well glass-bottom dishes (MatTek) containing culture medium (1% 100X N2 supplement (Gibco), 1% Penicillin-Streptomycin (Gibco) in transparent F12/DMEM (Gibco)) and incubated (37°C, 5% CO2) for at least 45min prior to imaging acquisition. To reduce the evaporation of media during imaging a FoilCover lid (Pecon) was applied on top of the glass-bottom dishes during time-lapse imaging. A time-lapse of minimum 15hours with a framerate of 15± min were recorded unidirectionally at 7 Z-positions with 5µm spacing using confocal microscopy (Zeiss LSM800, Plan-Apochromat 10x/0.45, WD=2.1 mm objective, equipped with a heating chamber and stage-top incubator chamber & gas mixed (Ibidi) (37°C, 5% CO2)). Excitation/emission wavelengths were 488/509 nm (EGFP) and 554/581nm (tdTomato). Time-lapse images were collected on a PC running Zeiss ZEN Blue software. Time-lapse image series were Z-projected, time-stitched using ZEN blue software.

4.7.10 Formulation of computational migration model

The formulated 2D migration model is evaluated by a Python 3.6 script. The total force acting on a given cell at each time instance is given by:

$$\boldsymbol{F}_{tot} = \boldsymbol{F}_{gen} - \boldsymbol{F}_{drag} + \boldsymbol{F}_{spring}$$

For each timestep dt the internal molecular machinery of a cell generates a force $\boldsymbol{F}_{gen}$. If this force is insufficiently high to overcome the resulting drag force $\boldsymbol{F}_{drag}$ it is stored in form of a spring-like force $\boldsymbol{F}_{spring}$ for the next timestep. Whereas the drag force is defined as:

$$\boldsymbol{F}_{drag} = c\,\eta\boldsymbol{v}$$

Here, η denotes the dynamic viscosity and c is a parameter dependent on the cell shape, which we consider a spherical particle of unit radius. In our model both parameters are considered to be locally constant and can therefore be unified as a resistance parameter R. Similar models have been previously described for 3D cell migration in extra cellular matrices (Zaman et al., 2005). For a detailed explanation of our model and parameter see Supplemental Information (Table 1 & Figure 18).

Directionality: $\rho = \begin{cases} 0.51 & \beta < 0.1 \\ f(\beta) & 0.1 < \beta < 0.05 \\ 0.65 & \beta > 0.05 \end{cases}$	Force scaling: $\alpha = \begin{cases} 0.53\, f_{Ctrl} & \beta < 0.1 \\ f(\beta)\, f_{Ctrl} & 0.1 < \beta < 0.05 \\ 0.9\, f_{Ctrl} & \beta > 0.05 \end{cases}$
Resistance Control environment $R_{Ctrl,tissue} = \begin{cases} R_1 = 5 \cdot 10^3 & y < 0.45 \\ R_2 = 12 \cdot 10^5 & y \leq 0.65 \\ R_3 = 4 \cdot 10^3 & y > 0.65 \end{cases}$	Resistance mutant environment $R_{KO,tissue} = 7 \cdot 10^3$

Table 1 Modelling Parameters

4.7.11 Analysis of relative distribution of MADM-Labeled neurons

Images were imported into ImageJ software (Schindelin et al., 2012) and MADM-labeled neurons were manually quantified based on the respective fluorescent marker expression and their relative position, which was calculated with respect to the bottom of the ventricle and the pial surface (For details see https://github.com/sommerc/cell2layer). The analysis script used, computes the relative and absolute distances of each manually marked neuron to its layer boundaries. Layer boundaries are manually provided as segmented lines. For each neuron the shortest distance to the two layer boundaries is computed, resulting in two distances d_1 and d_2. The normalized (relative) distance is computed by:

$$\text{relative distance} = \frac{d_1}{(d_1 + d_2)}$$

Statistical analyses were done with GraphPad Prism 8.0.1, applying an arcsin conversion of relative percentages, a two-way ANOVA, and a Tukey post hoc test.

4.7.12 Statistical Analysis of RNA-Seq

Read processing, alignment and annotations are described elsewhere (Laukoter et al., 2020a). STAR alignment parameters: clip5pNbases 3, outFilterMultimapNmax 1, --outSAMtype BAM SortedByCoordinate and quantMode GeneCounts. Downstream analyses were performed in R (v3.6.1). Read coverages of the deleted *Cdk5r1* region (chr11:80477417-80478722, mm10) and the deleted Dab1 region (chr4:104605298-104605437, mm10) were calculated using bedtools intersect with the -split option on the aligned bam file produced by STAR. These read counts were added to the count tables produced by STAR with the gene name *Cdk5r1*_del and *Dab1*_del respectively.

For Figure 10 we analyzed 81 samples and removed 9 samples with a low percentage of uniquely aligned reads (<50%) or due to their position on the PCA plot. Statistics on differential expression between all pairs of genotypes were calculated with DESeq2 using contrasts for each developmental time point separately. To reduce noise only genes with an average read coverage of >10 were used in the analyses. We used an adjusted p-value (padj) cutoff of 0.05 for differential expressed genes (DEG) for all analyses in Figure 10. Up- and down-regulated genes were determined by a $\log_2$ fold-change of >0 or <0 respectively. For Gene Ontology term enrichment we used the enrichGO function from the clusterProfiler package (v3.14.0) with parameters: universe = [all informative genes in the respective

comparison], ont = "ALL", pool = T, readable = T, OrgDb = org.Mm.eg.db, minGSSize = 20, maxGSSize = 500, pvalueCutoff = 0.1, qvalueCutoff = 0.2. For the GO term plot in Figure 10 we focused on P0 timepoint and first removed GO terms that are not related to neuronal development by removing GO terms with blood, vascu, or angio in their description. Then we calculated the negative log10 of the uncorrected p-value for the remaining GO terms (score). Finally, we ranked GO terms by the score and plotted the score of the top 10 GO terms focusing on the ontology BP.

For Figure 14 we analyzed 38 samples consisting of 22 samples already used for Figure 10 (control, *KO-Cdk5r1-MADM*, P0 time point) and 16 new samples (control, *Dab1*-KO). We removed 3 samples due to their position on a PCA plot. Statistics on differential expression were calculated as for Figure 10 using genes with an average read coverage over all samples > 20. For all analyses in Figure 14 we used an adjusted p-value (padj) cutoff of 0.05 and an absolute $\log_2$ fold-change < 0.35 to define DEGs. Figure 14E: We calculated the % common up-, down-regulated genes relative to all DEG in KO-*Dab1*/control and *KO-Cdk5r1-MADM*/control respectively and plotted the mean of these 2 values. Figure 14F: Significance of the overlap between DEG groups was calculated using newGOM from package GeneOverlap using the number of informative genes in this comparison as genome.size. We used different gene groups for further analysis: Common_up defines genes that are common up-regulated DEGs (intersection Figure 14D left), Common_down defines genes that are common down-regulated DEGs (intersection Figure 14D right), Dab1_spec defines genes that are DEG in *Dab1*-KO/control but not in *KO-Cdk5r1-MADM*/control (*Cdk5r1* up, *Cdk5r1* down in Figure 14D) and *Cdk5r1*_spec defines genes that are DEG in *KO-Cdk5r1-MADM*/control but do not overlap (*Cdk5r1* up, *Cdk5r1* down Figure 14D). GO term enrichment for the respective gene group was performed using enrichGO with parameters: enrichGO(OrgDb = org.Mm.eg.db, readable=T, pool=T, maxGSSize = 900, minGSSize = 100, pvalueCutoff = 0.05, qvalueCutoff = 0.1, separately for different GO ontologies. For Figure 14G we calculated a score as in Figure 14E and plotted the top 10 GO terms from cellular components (CC) ontology without prior filtering. For Figure 21 we used the used top 50 GO terms (ranked by adjusted p-value) from *Dab1*_spec and *Cdk5r1*_spec analysis and calculated all pairwise semantic similarity goSim from GOSemSim package with parameters: measure="Jiang". We plotted the resulting similarity matrix using the pheatmap package.

4.7.13 Statistical Analysis of Proteomics

Raw files were searched in MaxQuant 1.6.14.0 against the Mus musculus reference proteome from UniProtKB. Fixed cysteine modification was set to H11OC6N. Variable modifications were Oxidation (M), Acetyl (Protein N-term), Deamidation (NQ), Gln->pyro-Glu and Phospho (STY). Match between runs, dependent peptides and second peptides were active. All FDRs were set to 1%. MaxQuant results were further processed in R using in-house scripts, starting from evidence (PSM) tables. Briefly, potential contaminants, reverse database hits, or evidences with null intensity values were excluded. Evidence reporter intensities were scaled to integrated feature intensity, normalised using the Levenberg-Marquardt procedure row-wise, then assembled into peptidoforms (post-translationally modified peptides), summing up intensities per sample. Peptidoform reporter intensities were corrected for TMT lot label impurity values, median normalized, log-transformed, subjected to Variance Stabilizing Normalisation, re-normalised using the Levenberg-Marquardt procedure row-wise, then corrected for TMT batch effect using the Internal Reference Standardisation method. Ratios to the average of all either control or Cdk5r1-MADM samples (two parallel analyses) were calculated, then protein groups were inferred from peptidoforms. Because the focus was on discovering and quantifying as many protein groups as possible from limiting sample amounts, all groups including those with just one peptide were retained. Protein groups were quantified by averaging the intensity profile of matching peptidoforms (excluding phospho-peptides and counterparts), weighted by the inverse of individual Posterior Error Probabilities, then these values were averaged per sample and P values calculated using a moderated t-test and an F-test (limma package). Significance thresholds were calculated using the Benjamini Hochberg procedure for 10, 20 and 30 % FDR. In addition, protein groups with an absolute log2 ratio smaller than 95% of individual to average reference log2 ratios were excluded. Figure 10G & H: We plotted the Moderated.t-test:.-log10(Pvalue) against the Ratio:.log2.-.Mean for the respective comparison. All genes that were marked “up, FDR = 10%', 'down, FDR = 10%” were labeled in the volcano plot. For Figure 10I: We used all gene names linked to peptide groups for subsequent analyses. We defined significant DEGs as genes marked “up, FDR = 10%', 'down, FDR = 10%” and calculated GO term enrichments using clusterProfiler (v3.14.3) with parameters: Universe = [all genes in “Genes”], OrgDb = org.Mm.eg.db (v3.10.0), ont = 'CC', pvalueCutoff = 0.1, minGSSize = 50, maxGSSize = 2000,

pool=F, readable = T. We plotted selected terms of the top 15 GO terms, ranked by p-value. Figure 10J & K: Comparison to RNA-Seq: We defined RNA-Seq DEGs by using statistics calculated in Figure 10B and extracting genes with and adjusted p-value of < 0.1 and a log2 fold-change >0 (RNA Up) or <0 (RNA Down). DEGs based on proteomics were defined as having a "+" in the "Significant:.FDR=10%.-.full-KO" column and "Ratio:.log2.-.Mean.-.full-KO" < 0 (Protein Down) or >0 (Protein Up). Note that we only used genes that were informative on both RNA-Seq and Proteomics for this analysis. Figure 10L: For GO term analysis we used gene sets commonly up-, and down-regulated in both RNA-Seq and proteomics (intersection Figure 10K). GO term enrichment was calculated using enrichGO with parameters: universe = [all genes informative in RNA-Seq and proteomics], OrgDb = org.Mm.eg.db, ont = 'CC', pvalueCutoff = 0.9, minGSSize = 10, maxGSSize = 2000, pool=F, readable = T. We plotted the top 10 GO terms, ranked by p-value.

4.7.14 Correction of non-linear local drift in time-lapse images

To correct any local tissue drift in the original 3D multi-channel movies, we developed the Python package undrift. First, dense optical flow from successive image pairs is estimated with the Farnebäck method (Farnebäck, 2003) using the OpenCV library (version 3.3.1). For movies with more than one input channel, we used the averaged channel intensities before estimating the optical flow for each pixel. Input parameters for the Farneback method were set as follows: the number of image pyramid levels to 3, the averaging window size to 512x512 (px), the size of the pixel neighborhood used to find polynomial expansions to 5 px, the standard deviation of the Gaussian that is used to smooth derivatives to 0.4 px and the number of iterations per pyramid level to 3. Parameters were optimized to capture the movement of single cells and the locally coherent drift of tissue regions (if present). Then, the pairwise optical flow fields were smoothed (locally weighted averaged) with a spatio-temporal Gaussian (σ_t=1 px and σ_{xy}=25.6 px) using the scikit-image library (0.16.2). The strong spatial smoothing effectively removes movement on a small scale (single cells), whereas spatially coherent optical flow on a bigger scale (tissue drift) is maintained in the output. The smoothed pairwise optical flow fields are integrated over time to obtain an optical flow field relative to the reference frame (first time-point) using cubic spline interpolation and the Python scipy library (version 1.4.1). New movies are rendered by

artificially unwarping this integrated flow field on the original movie channels starting from the reference frame. For more information see http://github.com/sommerc/undrift.

4.7.15 Analysis of Neuronal Trajectories

Neurons were tracked semi-automatically with the ImageJ plugin TrackMate (Tinevez et al., 2017) using the LoG detector (estimated blob diameter: 10.0micron, threshold: 2.0, Median filter: enabled, sub-pixel localization: enabled) and the linear motion LAP tracker (initial search radius: 15, max search radius: 15, max frame gap: 2) for each channel. Tracks were manually curated to ensure correct tracking of neurons. Only red and green neuronal tracks were included in the analysis, all yellow neurons were excluded in the analysis. Tissue compartments (upper/lower bin) were drawn manually. All parameters were extracted in a .csv file for analysis. For each neuron, we first determined if it was located in the located in the upper / lower bin in the first frame or last frame. Figure 11E-F: Each cell-track was grouped into Upper Bin if in any frame the cell was positioned in the Upper Bin area. The cell-track was grouped into Lower Bin if the cell was in no frame placed in the Upper Bin area. An arcsin conversion were performed of relative percentages for statistical calculations. Figure 11G-H: We extracted the x/y coordinates of cells based on their position (Upper Bin, Lower Bin). The resulting cells were re-grouped into cell-tracks and for each track, we calculated mean straight-line speed and directionality:
Distance of one cell between two frames as:

$$d(x_i, x_j) \sqrt{\sum_{d=1}^{2} (x_{i,d} - x_{j,d})^2}$$

Sum of all distances (total distance traveled) with N being the number of frames a cell was tracked in:

$$d_{tot} = \sum_{i=1}^{N-1} d\,(x_i, x_{i+1})$$

Net distance traveled:

$$d_{net} = d(x_{1,} x_N)$$

Net time traveled:

$$t_{net} = t_n - t_1$$

Mean straight line speed:

$$d_{net}/t_{net}$$

Directionality (meandering) index:

$$d_{net}/d_{tot}$$

Note that the time between frames can differ for each cell (for example if a cell was not identified in one frame) and that the total time a cell was tracked can also differ between cells. Therefore, to assure the same framerate for the analysis, we calculated the velocities in micrometer per minute. Note that a single track can be divided into sub-tracks if crossing the middle line. These tracks are “crossing” and make up on average ~6% of all tracks. For Figure 11F-H we ranked each cell-track from each video based on d_{net} and plotted the indicated values for the top 15 cells for each video. Statistical analyses were done with GraphPad Prism 8.0.1, applying a two-way ANOVA and a Tukey post hoc test.

5 Future Perspective

The fascinating field of neuronal migration is in simple terms all about how neurons get to their correct position. Radial neuronal migration has been studied for many years, however, we are still uncovering new features of the migratory process and the assembly of cerebral cortex. So far, the field of neuronal migration has mainly been focused on the cell-autonomous function of disease causing genes. However, considering non-cell-autonomous effects might benchmark a new standard of characterizing disease causing genes, as the function of a gene on a cell-intrinsic level could be different from what is caused on a tissue wide level resulting in a morphological phenotype. Being able to quantify and distinguish non-cell-autonomous effects from the cell-autonomous gene functions opens new horizons for understanding the underlying mechanisms of neurodevelopmental disease and development of the brain. In general, cells in multicellular organisms are never alone, hence there will always exist an interaction of many intrinsic and extrinsic cellular and molecular factors in any tissue environment. In biology, a tissue is an ensemble of cells and their extracellular matrix that together carry out a specific function. Therefore, it would be naïve to disregard cell-extrinsic tissue wide effects when describing a cellular phenomenon. In the past, mostly due to the lack of model systems which do allow for the dissection of cell-intrinsic gene function and cell-extrinsic effects, we may need to revise previous findings to understand the true function of the genes investigated on a whole tissue level. So far, previous studies have mainly used model systems where mutated cells are present in an otherwise normal wildtype environment, when investigating the function of candidate genes. However, the phenotypes that are observed by the use of a somewhat artificial experimental system composed of a tissue environment which rarely is present in the disease environment where it was identified, might mask the effect which is caused by the genetic mutation. In other words, the cellular and molecular mechanisms identified in such an artificial system most likely does not reflect the phenotype present in the patient. As described in chapter 3, there are currently methods which do allow for the dissection of cell-intrinsic gene function versus non-cell-autonomous effects (Hansen and Hippenmeyer, 2020). However, the amount of studies employing the methods to distinguish cell-autonomous gene function versus non-cell-autonomous effects is currently very sparse and therefore non-cell-autonomous effects still remains a scarcely studied phenomenon in cortical development.

Furthermore, to achieve a deeper understanding of the interplay of cell-intrinsic and cell-extrinsic factors we also rely on technological approaches which can visualize and/or directly measure the non-cell-autonomous effects. Besides genetic paradigms e.g. MADM (see also Chapter 3, Figure 7) which allows to distinguish cell-autonomous gene function from non-cell-autonomous effects, we also rely on a combination of tools like microscopy, omics (including transcriptomics & proteomics), biophysical (experimental and theoretical) and data analysis approaches to quantify and analyze such effects. Below I will elaborate on concrete examples which could be used in future experiments to dissect non-cell-autonomous effects *in vivo* or *in situ* (See also chapter 3).

5.1 Microscopy

Cell migration and the formation of tissues is a dynamic process involving the coordinated movements of many individual cells bodies and their environment, not to speak of the signaling happening during this process. Hence, it is important to image and record the cellular processes in the tissue directly to mimic the physiological condition as closely as possible. So far *in vitro* studies have described a vast array of cell intrinsic and extrinsic mechanisms happening during development, however, on the whole tissue level we are still just at the beginning at comprehending the nature of complex tissue systems like e.g. the brain.

5.1.1 Imaging live tissue

Imaging living brain tissue has been instrumental to describe the migration process of neurons (Hatten, 2005; Kriegstein and Noctor, 2004; Nadarajah, 2003). Recent developments in super resolution microscopy have enabled to resolve the extracellular space of the brain. The extracellular space is filled with extracellular fluid and molecules of the extracellular matrix. Emerging techniques based on super resolution e.g. super-resolution shadow imaging (SUSHI) now allow for visualization of the extracellular space in live brain tissue (Tønnesen et al., 2018). Applying SUSHI to mouse organotypic slices have allowed unparalleled optical access to the structure and dynamics of the extracellular space. The SUSHI method can achieve super resolved images of all cells in the imaged tissue revealing the entirety of the micro environment organization. Moreover, the method allows to monitor migrating cells and at

the same time visualize their surrounding environment. The ability to both track the cells and their surrounding environment *in situ* opens new horizons for directly observing cell-cell and cell-ECM interactions at high resolution. The reality of being able to visualize all cells and their surroundings and directly track their morphology and dynamics allows for a deeper understanding of the interaction of the various components that build up tissue structures. Hence, for future studies with focus on non-cell-autonomous effects the SUSHI technology offers a very powerful tool.

5.1.2 Image analysis

Future developments in advanced microscopy approaches require advanced image analysis. Currently, most image analysis is still done completely or partially manually. Hence, with the naked eye of a human expert analyzing the image dynamics might not see what could be detected by an image analysis algorithm. Moreover, computational image analysis could enable new types of analysis to reanalyze already existing image data and thereby help discover biological phenomena which could not be identified with the naked eye of the experimenter previously and remove any potential bias (Meijering, 2020; Sullivan and Lundberg, 2018). Furthermore, automated computational image analysis also promises a high throughput approach which could generate extensive datasets while saving time in place of laborious manual analysis (Sommer and Gerlich, 2013). Over the recent years approaches based on deep learning algorithms are slowly replacing traditional data analysis approaches in bio image analysis (LeCun et al., 2015; Meijering, 2020). Generally deep learning, a subfield of machine learning, refers to the use of artificial neural networks, which consist of many layers of computational “neurons” to extract complex data representations at high levels of abstraction of given input data in order to perform data analysis tasks on future unseen data. However, it is important to note that the quality of the input data has a huge impact on how good the machine “learns”. In other words, poor data representation mostly result in low performance of a complex machine learning algorithm, whereas good quality data allow for high performance (Najafabadi et al., 2015). Taking advantage of deep learning approaches for image analysis can help enhance image quality e.g. denoising, correcting for sample drift and other aberrations. This is particularly important in e.g. time-lapse images which mostly show a certain degree of drift due to the nature of culturing the live tissue. A central challenge of

most image analysis tasks is to determine and identify if the objects of interest are present in the biological sample imaged. Only recently, deep learning approaches for the task of object recognition have been explored (Christiansen et al., 2018; Oktay and Gurses, 2019). Moreover, image segmentation has benefitted vastly from deep learning to change the representation of an image into something that is meaningful and which can be analyzed (Meijering, 2020). Object tracking, e.g. tracking moving cells over time, is a common task of image analysis. However, object tracking is a challenging problem manually and is also considered a very challenging computer vision problem. Emerging methodology using deep learning will allow for future end-to-end deep-learning based cell and particle tracking methods which could allow for full automation of cell tracking (Meijering, 2020). Investigation of radial neuronal migration mostly involves time-lapse imaging and therefore deep learning could provide a powerful tool to track the migrating cells. So far, most studies investigating migrating cells still track and analyze manually due to the lack of sufficient tracking methods. However with the arrival of new methodologies based on deep learning future analysis would allow for a much deeper analysis including many parameters such e.g. cell dynamics, morphology on a high throughput scale. The high throughput automatic analysis and classification of e.g. different migration modes and neuronal morphology will allows for a complete picture of the neuronal migration process. Tracking of neuronal migration mostly includes speed and direction, however, deep learning approaches could allow for cell and tissue segmentation which could give detailed information of the cell dynamics, in place of just the tracking of the center of the neuronal soma which is common practice currently. Particularly, investigating cell-cell or cell-extracellular interactions could benefit from a deeper understanding of e.g. membrane interactions which could be analyzed using deep learning image analysis approaches. Advanced image analysis methods like deep learning offers a tool of high potential to expand our understanding of neuronal migration and non-cell-autonomous effects in particular.

5.2 Omics

The vast complexity of the brain has held back its systemic exploration for many years but emerging powerful “omic” approaches are now enabling to push the boundaries of neuroscience research at an ever increasing speed (Hosp and Mann, 2017; Lee et al., 2020).

5.2.1 Transcriptomics

To further explore the molecular changes due to non-cell-autonomous effects involved in the radial migration process the dissection of the gene expression profiles of projection neurons during different steps of migration can be explored. In order to understand any mutant phenotype it will be important to first have a baseline of the gene expression profile in the wildtype through RNA-seq approaches. For example, dissociating neurons present in the intermediate zone and cortical plate at different developmental stages allows for a transcriptomic profile on a compartment based level. Moreover, the spatial distribution of neurons based on the identified expressed genes can be examined and validated by examining brain tissue with immunohistochemistry, if antibodies are available, or in situ hybridization to identify in which cortical layer/zone these genes are expressed. A bulk RNA-seq approach has been applied previously in combination with MADM, however not on a compartment specific level (see Chapter 4, Figure 10; Laukoter et al., 2020b, 2020a).

The bulk approach, even when extracting the specific compartment, is limited in spatial resolution and only provides information about differences between a broad ranges of cell types present in the specific compartment extracted. Applying single-cell RNA sequencing using e.g. Drop-seq which allow for sequencing of thousands of single cells (Macosko et al., 2015) will allows to increase spatial and cell type specific resolution. Subsequent bioinformatical analysis of the sequencing data could identify markers that will define subgroups of migrating neurons, which then can be correlated with their spatial position. Previous studies have applied similar approaches but mainly with focus on cell-type specificity in each zone and not specifically analyzing genes involved in neuronal migration and not with any focus on non-cell-autonomous effects (Miyoshi and Fishell, 2012; Satija et al., 2015; Shekhar et al., 2016; Zhang et al., 2016).

The single-cell RNA-seq approach with cells obtained from a whole tissue and does not directly provide information about gene expression changes at each particular stage during radial migration and lacks genuine spatial resolution. Hence, a micro pipetting assay e.g. PATCH-seq (Cadwell et al., 2016) can allow to directly pick the neurons to be sequenced directly in the tissue. This approach provides a high spatial resolution because one can select single cells within each migration zone and compare gene expression profiles of neurons at all stages of radial neuronal migration. The micropipette approach goes well in hand with

MADM-labelled tissue as it allows for sparse labelling of single cells and generation of genetic mosaics and tissue-wide knockouts. Ultimately, comparison of gene expression profiles from all three approaches can help establish a ranked list of most significant candidate genes and enable to narrow down the molecules specifically attributed to non-cell-autonomous effects in radial neuronal migration.

5.2.2 Proteomics

Neuronal processes like e.g. neuronal migration underlie complex and tightly regulated protein-protein interactions. In contrast to transcriptomic approaches, proteomics have had less impact on neuroscience research the recent years and is largely due to the lack of powerful tools to study proteins in an unbiased, quantitative and sensitive manner (Hosp and Mann, 2017). However, all functions of the brain is ultimately mediated by proteins and therefore it is essential to understand their function. Modern proteomic techniques slowly allow to achieve a comparable proteome coverage to that which is achieved in RNA-seq approaches and can even allow for investigating e.g. post translational modifications. As well as providing information in differential protein expression, mass spectrometry-based proteomics can be combined with enrichment of cellular organelles e.g. membrane proteins or of other cell compartments. Applying an enrichment step for peptides bearing specific post-translational modifications also enable investigation at a phospho-proteomic level (Hosp and Mann, 2017). On a bulk level, meaning taking a tissue and isolating the proteins from mix of a large number of different cell populations present in the brain has been feasible recent years (Fingleton et al., 2021). Yet, a proteomic approach has yet to be applied for investigation of non-cell-autonomous effects in brain development. Analyzing proteins from many different cell types at the same time most likely will mask the results obtained, especially when interested in one specific cell population like e.g. projection neurons. Cell type specific proteomics would provide the resolution needed to investigate the proteomic profile of a specific type of neurons. Cell type-specific isolation can be performed by e.g. fluorescence-activated sorting (FACS) or by laser capture microdissection (LCM) (Datta et al., 2015). However, many analytical techniques used for protein detection and quantitation remain insensitive to the low amounts of protein extracted from low numbers of specific cell populations. Yet, methods to improve proteomic yield and increase resolution are emerging

(Wilson and Nairn, 2018). Moreover, the cellular heterogeneity of the brain demands analytical methods that enable analysis at the single cell level. Single cell proteomic technology has advanced rapidly recent years, however, the technology has not yet matured to the level of single cell RNA-seq (Hosp and Mann, 2017). Recent advances of methods in liquid chromatography mass spectrometry (LC–MS)-based proteomics have improved some of the limitations in the detection sensitivity and throughput which is required for single cell proteomics (Schoof et al., 2021) . Future methods for single cell protein detection and analysis will provide insights into collections of proteins with great relevance to cell and disease biology. Having an extensive map of the protein-protein interactions of neurons during a dynamic process like migration will provide a deeper understanding of the underlying mechanisms of disease causing genes and the possible tissue wide non-cell-autonomous effects. Applying proteomic approaches in combination with genetic paradigms which can distinguish between cell-autonomous gene/protein function and non-cell-autonomous effects in the future will further elucidate such effects on the molecular machinery of cells directly mediated by proteins.

5.3 Biophysics

The molecular mechanics underlying neuronal migration is beginning to be elucidated through emerging mechanobiological approaches. Cellular and tissue environment mechanophenotyping promises an exciting research direction for a deeper understanding of the biophysics taking place during neuronal migration and tissue development in general (Kozminsky and Sohn, 2020).

5.3.1 Atomic force microscopy

Atomic force microscopy (AFM) based methods are capable of directly scanning the surface of a biological sample. Thereby, AFM can measure e.g. detachment force between individual cells and a substrate and/or the elasticity of the tissue substrate itself (Beaussart and El-Kirat-Chatel, 2019; Iwashita et al., 2014; Jembrek et al., 2015). To elucidate tissue wide non-cell-autonomous effects of a disease causing gene on a biophysical level, it would be important to systematically profile tissue and cellular stiffness. By comparison of the stiffness profiles from wildtype and mutant tissues could provide important insights into the biophysical properties of a disease phenotype. As neuronal migration involves many sequential steps where a

neuron travels through different compartments before reaching its final position, it is exposed to different environments having different physical properties e.g. stiffness. In a wildtype environment one would assume that optimal conditions are present for the neurons to move, however, if the elasticity or stiffness of the tissue environment would change in a mutant condition, it most likely would affect migration of the mutant cells. Being able to directly measure the properties of the environment in where neurons are moving we would be able to further dissect the non-cell-autonomous contributions to the mutant phenotype. In an experimental paradigm using e.g. MADM one could benefit from a wide range of measurable parameters using an AFM approach with fluorescent imaging. It would be possible to monitor not only the structural and mechanical properties of the neuronal membranes but also properties of the cytoplasm, cell nucleus, and particularly cytoskeletal components of single cells. AFM is particularly useful for investigating the mechanical properties of cell adhesion and for the quantification of the involved forces. It allows for the characterization of mechanical contact between cells in a resolution which can be down to the level of a single molecule (Benoit and Gaub, 2002). AFM can be used to correlate elastic behavior and cell migration. E.g. the organization of the cytoskeleton affects cell adhesion because intracellular cytoskeletal components are connected to the surface by integrin adhesion receptors. Hence, the comparison of neuronal elasticity could serve as an indicator of cytoskeletal reorganization and the state of neuron adhesion during migration (Jembrek et al., 2015). AFM offers a powerful tool facilitating the measurement of material properties at tissue wide, cellular and subcellular level (Jembrek et al., 2015). Future studies will benefit from applying this technology to provide a deeper understanding of non-cell-autonomous effects in the context of brain development.

5.3.2 Modeling

Although biology is complex and often seen as a very stochastic entity (Wilkinson, 2009), the biological phenomena could be reduced to simple physics to help reduce complexity which could generate hypotheses and suggests future experiments to further explain the biological mechanism investigated (Motta and Pappalardo, 2013). The more functions of genes and proteins are explored the more mechanisms and effects we will have described and thus would be able to define the biological system in physical terms to reduce

the complexity. At this point in time research has already attempted to describe findings with models based on mathematics and physical laws because testing and measuring the phenomena which is identified cannot always be easily tested (Caffrey et al., 2014; Gunawardena, 2014; Setty et al., 2011; Takeo et al., 2021). As an example, a neuron migrating in a complex environment involves a lot of processes which currently cannot always be measured directly *in situ*. Therefore, being able to reduce the complexity of such a system one could extract the minimal necessary parameters to replicate the cellular phenotype and mathematically test if these parameters are sufficient to generate the observed phenotype. If the phenotype can be replicated with the minimal parameters, it can support the findings and help generate a working model and hypothesis. However, if the parameters do not replicate the phenotype, it also helpful as it can help point in a direction where future research should or should not focus. However, applying modelling to experimentally derived parameters is in most cases pure correlation and only predicts how the system might work. Importantly, if the system can be reduced to the minimal amount of parameters which correlate to a biological value we are already at a level where we have reduced the biological system to physical properties. Hence, in the future, instead of visualizing a concept in a simple imagined drawing consisting of arrows and question marks, one could establish an *in silico* model which could be tested and simulated computationally. This could help us predict how likely is it that the entity that we measured actually is physically possible and would work as hypothesized. To find out how it works in reality one would need to carry out an experiment, however, if that is not feasible at that specific moment in time, turning to mathematical modelling and simulation does allow to predict the possible outcome and therefore can help pointing to a solution (Gunawardena, 2014; Motta and Pappalardo, 2013).

5.4 Advanced cell culture systems

Recent developments in advanced cell culture systems like organoids (Klaus et al., 2019) will enable to investigate the interactions of cells in their microenvironment at a simpler scale and could allow for experiments which are currently not possible *in vivo* or *in situ* in other model systems like the e.g. mouse. Moreover, the research can be done in organoids derived from human stem cells giving access to perform experiments investigating the behavior of human cells and human genetic mutations (Dyer, 2016). Mouse models carrying genetic mutations

of genes identified in human cannot fully recapitulate the phenotypes seen in the patients and are therefore only suited for a limited understanding molecular and cellular mechanisms responsible for the disease conditions (Dyer, 2016; Klaus et al., 2019). However, due to the artificial organoid system, the research will need to be complemented by applying mammalian *in vivo* models to fairly achieve the actual complexity existent in a living system like the human brain.

5.5 Collective cell migration – lessons from other cellular systems

Collective cell migration is defined as the coordinated and synchronized movement of more cells by contacting and affecting one another while migrating thereby contributing to their overall directionality (Rørth, 2009; Scarpa and Mayor, 2016). Collective migration has been observed *in vitro* and *in vivo* and features the movement of clusters of cells displaying different sizes, shapes and adhesive properties (Norden and Lecaudey, 2019). The cell-cell interactions necessary for collective migration range from a direct physical linking of cells in a group (e.g. epithelial cells) to temporary interactions between cell neighbors (e.g. neural crest cells) (Rørth, 2009; Shellard and Mayor, 2020). As collective migration is dependent on cell-cell contacts it is quite clear that cell adhesion play a major role in this process. Collective migration where cells remain physically connected throughout their migration has been observed in various systems including invasive carcinomas, germ layer morphogenesis during gastrulation, lateral line migration in zebrafish and during wound healing involving epithelial sheet migration (Rørth, 2009; Shellard and Mayor, 2020). This kind of collective migration involving a maintained cell-cell connection involves leader and follower cells, where the leading cells guide and physically pull the follower cells as the cell group migrates (De Pascalis and Etienne-Manneville, 2017). E.g. Cadherin-2 is essential in mediating neuron-to-neuron interactions that drive the collective migration of facial branchiomotor neurons in zebrafish (Rebman et al., 2016). Likewise, E-cadherin is important for proper migration of epithelial sheets in wound healing (Li et al., 2012). Distinct from a constant physical connection between collectively migrating cells, cells can also display collective migration with brief transient contacts throughout the migratory process (Scarpa and Mayor, 2016). E.g. neural crest cells migrate as a stream of cells where individual cells make brief direct contacts with other neighboring neural crest cell (De Pascalis and Etienne-Manneville, 2017; Scarpa and Mayor,

2016). An interesting example displayed that neural crest cells only could migrate directionally when a large enough density of other neural crest cells was present when placed in a chemo attractive gradient (Theveneau et al., 2010). Without the presence of other neural crest cells the cells would mostly wander randomly indicating that cell-cell contact is required for neural crest cells to migrate and respond to extrinsic cues in the environment. Moreover, by impairing Cadherin-2 in neural crest cells, the cells would migrate randomly and display diffused cell-cell contacts indicating that cell cluster polarity and collective migration is mainly determined by cell contacts rather than by a chemoattractant (Theveneau et al., 2010). Moreover, Shootin1, a cytoplasmic protein involved in neuronal polarization and axon guidance, has been shown to mediate collective cell migration in zebrafish (Kubo et al., 2015; Minegishi et al., 2018; Urasaki et al., 2019).

The nature and function of cell-cell interactions that lead to potential collective migration of neurons remains unclear. As mentioned above, a recent study of facial branchio motor neurons showed that the cell adhesion molecules, cadherin-2, play an important role in collective migration (Rebman et al., 2016). Extrapolating from the fact that Cadherin-2 is also widely involved with neuronal migration in the cerebral cortex it is possible that similar collective effects could be present in neuronal migration. However, it is unclear to what extent cell-cell contacts & cell-adhesion molecules affect neuronal migration non-cell-autonomously in the mammalian brain. To date, collective migration of neurons in the cerebral cortex has not been observed or described. That might be due to the fact that excitatory projection neurons mainly migrate along radial glial fibers and therefore have a physical guide and therefore probably do not depend on the assistance of other neurons to migrate. The reason for the potential absence of collective migration could also be due to the nature of the projection neuron morphology. While projection neurons migrate they already extent their developing axon before they arrive at their final position. As the neurons extent their individual axons, collective migration might rather compromise this process as each in a potential cell cluster would consist of highly bipolar neurons with extended axons and leading neurites. Moreover, during multipolar migration neurons display a highly polarized morphology with numerous very dynamic neurites which rather doubtfully would allow collective migration in the classical sense, as described for cells outside the central nervous system. However, the mechanisms of which collective migration is driven in other cellular

systems could potentially exist in the cerebral cortex and be of a similar nature during projection neuron migration. As most of the genes described to direct collective migration in e.g. zebrafish are also involved in migration of projection neurons e.g. Cadherin-2, a potential collective effect of these genes could exist. Moreover, the rostral migratory stream presents a site for collective cell migration in the adult rodent brain (Gupta and Giangrande, 2014; Kaneko et al., 2017). Originating in the subventricular zone, neuroblasts migrate towards the olfactory bulb in the rostral migratory stream, without the use of radial glia or axonal fibers (Gupta and Giangrande, 2014). The neuroblasts migrate and navigate using their neighboring cells as a migration scaffold in a manner called “chain migration (Gupta and Giangrande, 2014). Clusters of neuroblasts form a chain of moving cells through their homophilic interactions of adhesion molecules, while being flanked by astrocytes (Gupta and Giangrande, 2014; Kaneko et al., 2017). However, to what degree collective migration is present in the developing cerebral cortex and in radial neuronal migration remains to be observed and elucidated.

5.6 Closing remarks

Future developments in microscopy, omics and biophysics will enable new types of analysis and could discover biological phenomena which so far remained enigmatic and out of reach. With the arrival of high-throughput single-cell omics, live cell and tissue environment tracing *in situ* in combination with advanced analysis to associate experimental the various experimental measurements, we have tools for elucidating the mechanism of the development of the cerebral cortex. Currently, non-cell-autonomous tissue wide effects are not well studied but we are currently in an era of biological research where we have tools and knowledge to achieve a deeper understanding of these phenomena by applying more holistic approaches. Pairing the multiple approaches mentioned above, based on bulk and single cell data, enables to decipher the molecular signatures of radially migrating neurons and could identify non-cell-autonomous effects at e.g. specific migration mode and cell type level. Moreover, lessons in collective migration from other cellular systems could provide insight and further understanding of non-cell-autonomous effects in the brain. In the future, through a collective effort applying a combination of tools and knowledge we will be able to further describe and understand the complex enigmatic marvels of biology, and neuroscience in particular.

6 Conclusion

Radial neuronal migration has been studied for many decades and research has continued to unravel the underlying cellular and molecular mechanisms involved in the migration process. This thesis has described and discussed some of the main processes during radial neuronal migration and the current state at which is the research field has progressed so far. Although neuronal migration widely investigated field of study the underlying function and mechanism of genes involved in this migratory process are still unknown and the neurodevelopmental diseases caused by mutations remain largely untreated. One of the reasons for the lack of understanding the underlying mechanisms neurodevelopmental disease lies in the fact that most genes so far have only been studied on the cell-intrinsic (cell-autonomous) level. Nevertheless, in addition to cell-intrinsic functions of genes, cell-extrinsic (non-cell-autonomous) effects have been presented to affect the migratory process of neurons. However, the nature of such non-cell-autonomous effects are still largely unknown. Thus, we have established a quantitative genetic strategy to distinguish the cell-autonomous gene function from non-cell-autonomous effects. Using a MADM-based paradigm in combination with tissue histology, transcriptomic and proteomic profiling, slice culture time-lapse imaging in combination with *in silico* modelling, this work identified cell-adhesion as a central component of non-cell-autonomous effects caused by mutation of genes involved in radial neuronal migration. The research highlights the importance of studying non-cell-autonomous effects present in diseased tissue caused by genetic mutations. It revealed that non-cell-autonomous effects, exerted through cell-adhesion, can overrule the cell-intrinsic gene function and likely is a major component contributing to the severe phenotypes seen in individuals carrying mutations in genes important for neuronal migration.

Finally, I have discussed and put a perspective on the possible future research on understanding the interplay of cell-intrinsic versus cell-extrinsic mechanisms in brain development and neuronal migration.

References

Allendoerfer, K.L., and Shatz, C.J. (1994). The subplate, a transient neocortical structure: its role in the development of connections between thalamus and cortex. Annu. Rev. Neurosci. *17*, 185–218.

Altschuler, S.J., Angenent, S.B., Wang, Y., and Wu, L.F. (2008). On the spontaneous emergence of cell polarity. Nature *454*, 886–889.

Angevine, J.B., and Sidman, R.L. (1961). Autoradiographic study of cell migration during histogenesis of cerebral cortex in the mouse. Nature *192*, 766–768.

Anthony, T.E., Klein, C., Fishell, G., and Heintz, N. (2004). Radial Glia Serve as Neuronal Progenitors in All Regions of the Central Nervous System. Neuron *41*, 881–890.

Arai, Y., Shibata, T., Matsuoka, S., Sato, M.J., Yanagida, T., and Ueda, M. (2010). Self-organization of the phosphatidylinositol lipids signaling system for random cell migration. Proc. Natl. Acad. Sci. *107*, 12399–12404.

Arata, Y., Hiroshima, M., Pack, C.-G., Ramanujam, R., Motegi, F., Nakazato, K., Shindo, Y., Wiseman, P.W., Sawa, H., Kobayashi, T.J., et al. (2016). Cortical Polarity of the RING Protein PAR-2 Is Maintained by Exchange Rate Kinetics at the Cortical-Cytoplasmic Boundary. Cell Rep. *16*, 2156–2168.

Ayala, R., Shu, T., and Tsai, L.H. (2007). Trekking across the Brain: The Journey of Neuronal Migration. Cell *128*, 29–43.

Ayoub, A.E., Oh, S., Xie, Y., Leng, J., Cotney, J., Dominguez, M.H., Noonan, J.P., and Rakic, P. (2011). Transcriptional programs in transient embryonic zones of the cerebral cortex defined by high-resolution mRNA sequencing. Proc. Natl. Acad. Sci. U. S. A. *108*, 14950–14955.

Baek, S.T., Copeland, B., Yun, E.-J., Kwon, S.-K., Guemez-Gamboa, A., Schaffer, A.E., Kim, S., Kang, H.-C., Song, S., Mathern, G.W., et al. (2015). An AKT3-FOXG1-reelin network underlies defective migration in human focal malformations of cortical development. Nat. Med. *21*, 1445–1454.

Bai, J., Ramos, R.L., Ackman, J.B., Thomas, A.M., Lee, R. V, and LoTurco, J.J. (2003). RNAi reveals doublecortin is required for radial migration in rat neocortex. Nat. Neurosci. *6*, 1277–1283.

Ballif, B.A., Arnaud, L., Arthur, W.T., Guris, D., Imamoto, A., and Cooper, J.A. (2004). Activation of a Dab1/CrkL/C3G/Rap1 Pathway in Reelin-Stimulated Neurons. Curr. Biol. *14*, 606–610.

Barkovich, A.J., Hevner, R., and Guerrini, R. (1999). Syndromes of bilateral symmetrical polymicrogyria. AJNR. Am. J. Neuroradiol. *20*, 1814–1821.

Barnes, A.P., and Polleux, F. (2009). Establishment of Axon-Dendrite Polarity in Developing Neurons. Annu. Rev. Neurosci. *32*, 347–381.

Barnes, A.P., Lilley, B.N., Pan, Y.A., Plummer, L.J., Powell, A.W., Raines, A.N., Sanes, J.R., and Polleux, F. (2007). LKB1 and SAD kinases define a pathway required for the polarization of cortical neurons. Cell *129*, 549–563.

Barros, C.S., Franco, S.J., and Muller, U. (2011). Extracellular Matrix: Functions in the Nervous System. Cold Spring Harb. Perspect. Biol. *3*, a005108–a005108.

Beattie, R., Postiglione, M.P., Burnett, L.E., Laukoter, S., Streicher, C., Pauler, F.M., Xiao, G., Klezovitch, O., Vasioukhin, V., Ghashghaei, T.H., et al. (2017). Mosaic Analysis with Double Markers Reveals Distinct Sequential Functions of Lgl1 in Neural Stem Cells. Neuron *94*, 517-533.e3.

Beaussart, A., and El-Kirat-Chatel, S. (2019). Microbial adhesion and ultrastructure from the single-molecule to the single-cell levels by Atomic Force Microscopy. Cell Surf. *5*, 100031.

Becker, S.F.S., Mayor, R., and Kashef, J. (2013). Cadherin-11 mediates contact inhibition of locomotion during Xenopus neural crest cell migration. PLoS One *8*, e85717.

Belvindrah, R., Graus-Porta, D., Goebbels, S., Nave, K.-A., and Muller, U. (2007). 1 Integrins in Radial Glia But Not in Migrating Neurons Are Essential for the Formation of Cell Layers in the Cerebral Cortex. J. Neurosci. *27*, 13854–13865.

Benoit, M., and Gaub, H.E. (2002). Measuring Cell Adhesion Forces with the Atomic Force Microscope at the Molecular Level. Cells Tissues Organs *172*, 174–189.

Benton, R., and Johnston, D.S. (2003). Drosophila PAR-1 and 14-3-3 Inhibit Bazooka/PAR-3 to Establish Complementary Cortical Domains in Polarized Cells. Cell *115*, 691–704.

van den Berghe, V., Stappers, E., and Seuntjens, E. (2014). How Cell-Autonomous Is Neuronal Migration in the Forebrain? Molecular Cross-Talk at the Cell Membrane. Neurosci. *20*, 571–575.

Betizeau, M., Cortay, V., Patti, D., Pfister, S., Gautier, E., Bellemin-Ménard, A., Afanassieff, M., Huissoud, C., Douglas, R.J., Kennedy, H., et al. (2013). Precursor Diversity and Complexity of Lineage Relationships in the Outer Subventricular Zone of the Primate. Neuron *80*, 442–457.

Bock, H.H., and May, P. (2016). Canonical and non-canonical Reelin signaling. Front. Cell.

Neurosci. *10*, 1–20.

Borrell, V., and Götz, M. (2014). Role of radial glial cells in cerebral cortex folding. Curr. Opin. Neurobiol. *27*, 39–46.

Borrell, V., and Reillo, I. (2012). Emerging roles of neural stem cells in cerebral cortex development and evolution. Dev. Neurobiol. *72*, 955–971.

Bradke, F., and Dotti, C.G. (1999). The role of local actin instability in axon formation. Science *283*, 1931–1934.

Britto, J.M., Tait, K.J., Lee, E.P., Gamble, R.S., Hattori, M., and Tan, S.-S. (2014). Exogenous Reelin Modifies the Migratory Behavior of Neurons Depending on Cortical Location. Cereb. Cortex *24*, 2835–2847.

Buchsbaum, I.Y., and Cappello, S. (2019). Neuronal migration in the CNS during development and disease: insights from in vivo and in vitro models. Development *146*.

Cadwell, C.R., Palasantza, A., Jiang, X., Berens, P., Deng, Q., Yilmaz, M., Reimer, J., Shen, S., Bethge, M., Tolias, K.F., et al. (2016). Electrophysiological, transcriptomic and morphologic profiling of single neurons using Patch-seq. Nat. Biotechnol. *34*, 199–203.

Caffrey, J.R., Hughes, B.D., Britto, J.M., and Landman, K.A. (2014). An In Silico Agent-Based Model Demonstrates Reelin Function in Directing Lamination of Neurons during Cortical Development. *9*, 1–11.

Cappello, S., Böhringer, C.R.J., Bergami, M., Conzelmann, K.K., Ghanem, A., Tomassy, G.S., Arlotta, P., Mainardi, M., Allegra, M., Caleo, M., et al. (2012). A Radial Glia-Specific Role of RhoA in Double Cortex Formation. Neuron *73*, 911–924.

Carlton, J.G., and Cullen, P.J. (2005). Coincidence detection in phosphoinositide signaling. Trends Cell Biol. *15*, 540–547.

Carracedo, A., and Pandolfi, P.P. (2008). The PTEN–PI3K pathway: of feedbacks and cross-talks. Oncogene *27*, 5527–5541.

Cavallaro, U., and Dejana, E. (2011). Adhesion molecule signalling: Not always a sticky business. Nat. Rev. Mol. Cell Biol. *12*, 189–197.

Caviness, V.S., and Sidman, R.L. (1973). Time of origin or corresponding cell classes in the cerebral cortex of normal and reeler mutant mice: an autoradiographic analysis. J. Comp. Neurol. *148*, 141–151.

Chae, T., Kwon, Y.T., Bronson, R., Dikkes, P., En, L., and Tsai, L.H. (1997). Mice lacking p35, a

neuronal specific activator of Cdk5, display cortical lamination defects, seizures, and adult lethality. Neuron *18*, 29–42.

Chao, M. V (2003). Neurotrophins and their receptors: A convergence point for many signalling pathways. Nat. Rev. Neurosci. *4*, 299–309.

Chau, A.H., Walter, J.M., Gerardin, J., Tang, C., and Lim, W.A. (2012). Designing Synthetic Regulatory Networks Capable of Self-Organizing Cell Polarization. Cell *151*, 320–332.

Chen, G., Sima, J., Jin, M., Wang, K.-Y., Xue, X.-J., Zheng, W., Ding, Y.-Q., and Yuan, X.-B. (2008). Semaphorin-3A guides radial migration of cortical neurons during development. Nat. Neurosci. *11*, 36–44.

Chen, Y.M., Wang, Q.J., Hu, H.S., Yu, P.C., Zhu, J., Drewes, G., Piwnica-Worms, H., and Luo, Z.G. (2006). Microtubule affinity-regulating kinase 2 functions downstream of the PAR-3/PAR-6/atypical PKC complex in regulating hippocampal neuronal polarity. Proc. Natl. Acad. Sci. U. S. A. *103*, 8534–8539.

Cherfils, J., and Zeghouf, M. (2013). Regulation of Small GTPases by GEFs, GAPs, and GDIs. Physiol. Rev. *93*, 269–309.

Cho, W., and Stahelin, R. V. (2005). Membrane-Protein Interactions in Cell Signaling and Membrane Trafficking. Annu. Rev. Biophys. Biomol. Struct. *34*, 119–151.

Christiansen, E.M., Yang, S.J., Ando, D.M., Javaherian, A., Skibinski, G., Lipnick, S., Mount, E., O'Neil, A., Shah, K., Lee, A.K., et al. (2018). In Silico Labeling: Predicting Fluorescent Labels in Unlabeled Images. Cell *173*, 792-803.e19.

Collins, S.P., Reoma, J.L., Gamm, D.M., and Uhler, M.D. (2000). LKB1, a novel serine/threonine protein kinase and potential tumour suppressor, is phosphorylated by cAMP-dependent protein kinase (PKA) and prenylated in vivo. Biochem. J. *345 Pt 3*, 673–680.

Contreras, X., Amberg, N., Davaatseren, A., Hansen, A.H., Sonntag, J., Andersen, L., Bernthaler, T., Streicher, C., Heger, A., Johnson, R.L., et al. (2021). A genome-wide library of MADM mice for single-cell genetic mosaic analysis. Cell Rep. *35*.

Cooper, J. a (2013). Mechanisms of cell migration in the nervous system. J. Cell Biol. *202*, 725–734.

Côté, J.-F., Motoyama, A.B., Bush, J.A., and Vuori, K. (2005). A novel and evolutionarily conserved PtdIns(3,4,5)P3-binding domain is necessary for DOCK180 signalling. Nat. Cell Biol. *7*, 797–807.

D'Agostino, M.D., Bernasconi, A., Das, S., Bastos, A., Valerio, R.M., Palmini, A., Costa da Costa, J., Scheffer, I.E., Berkovic, S., Guerrini, R., et al. (2002). Subcortical band heterotopia (SBH) in males: clinical, imaging and genetic findings in comparison with females. Brain *125*, 2507–2522.

D'Arcangelo, G. (2014). Reelin in the Years: Controlling Neuronal Migration and Maturation in the Mammalian Brain. Adv. Neurosci. *2014*, 1–19.

D'Arcangelo, G., Homayouni, R., Keshvara, L., Rice, D.S., Sheldon, M., and Curran, T. (1999). Reelin Is a Ligand for Lipoprotein Receptors. Neuron *24*, 471–479.

Datta, S., Malhotra, L., Dickerson, R., Chaffee, S., Sen, C.K., and Roy, S. (2015). Laser capture microdissection: Big data from small samples. Histol. Histopathol. *30*, 1255–1269.

Delalle, I., Bhide, P.G., Caviness Jr., V.S., and Tsai, L.H. (1997). Temporal and spatial patterns of expression of p35, a regulatory subunit of cyclin-dependent kinase 5, in the nervous system of the mouse. J. Neurocytol. *26*, 283–296.

DerMardirossian, C., Schnelzer, A., and Bokoch, G.M. (2004). Phosphorylation of RhoGDI by Pak1 Mediates Dissociation of Rac GTPase. Mol. Cell *15*, 117–127.

Dobyns, W.B. (1993). Lissencephaly. A human brain malformation associated with deletion of the LIS1 gene located at chromosome 17p13. JAMA J. Am. Med. Assoc. *270*, 2838–2842.

Di Donato, N., Timms, A.E., Aldinger, K.A., Mirzaa, G.M., Bennett, J.T., Collins, S., Olds, C., Mei, D., Chiari, S., Carvill, G., et al. (2018). Analysis of 17 genes detects mutations in 81% of 811 patients with lissencephaly. Genet. Med. *20*, 1354–1364.

Dotti, C.G., Sullivan, C.A., and Banker, G. a (1988). The establishment of polarity by hippocampal neurons in culture. J. Neurosci. *8*, 1454–1468.

Drewes, G., Ebneth, A., Preuss, U., Mandelkow, E.-M., and Mandelkow, E. (1997). MARK, a Novel Family of Protein Kinases That Phosphorylate Microtubule-Associated Proteins and Trigger Microtubule Disruption. Cell *89*, 297–308.

Dyer, M.A. (2016). Stem Cells Expand Insights into Human Brain Evolution. Cell Stem Cell *18*, 425–426.

Ebner, M., Lučić, I., Leonard, T.A., and Yudushkin, I. (2017). PI(3,4,5)P 3 Engagement Restricts Akt Activity to Cellular Membranes. Mol. Cell *65*, 416-431.e6.

Elias, L.A., Wang, D.D., and Kriegstein, A.R. (2007). Gap junction adhesion is necessary for radial migration in the neocortex. Nature *448*, 901–907.

Etienne-Manneville, S., and Hall, A. (2001). Integrin-Mediated Activation of Cdc42 Controls Cell Polarity in Migrating Astrocytes through PKCζ. Cell *106*, 489–498.

Evsyukova, I., Plestant, C., and Anton, E.S. (2013). Integrative Mechanisms of Oriented Neuronal Migration in the Developing Brain. Annu. Rev. Cell Dev. Biol. *29*, 299–353.

Farnebäck, G. (2003). Two-frame motion estimation based on polynomial expansion. Lect. Notes Comput. Sci. (Including Subser. Lect. Notes Artif. Intell. Lect. Notes Bioinformatics) *2749*, 363–370.

Feng, Y., and Walsh, C.A. (2001). Protein–Protein interactions, cytoskeletal regulation and neuronal migration. Nat. Rev. Neurosci. *2*, 408–416.

Feng, W., Wu, H., Chan, L.-N., and Zhang, M. (2007). The Par-3 NTD adopts a PB1-like structure required for Par-3 oligomerization and membrane localization. EMBO J. *26*, 2786–2796.

Fietz, S.A., Kelava, I., Vogt, J., Wilsch-Bräuninger, M., Stenzel, D., Fish, J.L., Corbeil, D., Riehn, A., Distler, W., Nitsch, R., et al. (2010). OSVZ progenitors of human and ferret neocortex are epithelial-like and expand by integrin signaling. Nat. Neurosci. *13*, 690–699.

Fingleton, E., Li, Y., and Roche, K.W. (2021). Advances in Proteomics Allow Insights Into Neuronal Proteomes. Front. Mol. Neurosci. *14*, 1–12.

Fivaz, M., Bandara, S., Inoue, T., and Meyer, T. (2008). Robust Neuronal Symmetry Breaking by Ras-Triggered Local Positive Feedback. Curr. Biol. *18*, 44–50.

Florio, M., Albert, M., Taverna, E., Namba, T., Brandl, H., Lewitus, E., Haffner, C., Sykes, A., Wong, F.K., Peters, J., et al. (2015). Human-specific gene ARHGAP11B promotes basal progenitor amplification and neocortex expansion. Science (80-.). *347*, 1465–1470.

Ford-Perriss, M., Abud, H., and Murphy, M. (2001). Fibroblast Growth Factors In The Developing Central Nervous System. Clin. Exp. Pharmacol. Physiol. *28*, 493–503.

Förster, E., Bock, H.H., Herz, J., Chai, X., Frotscher, M., and Zhao, S. (2010). Emerging topics in Reelin function. Eur. J. Neurosci. *31*, no-no.

Fox, J.W., Lamperti, E.D., Ekşioğlu, Y.Z., Hong, S.E., Feng, Y., Graham, D.A., Scheffer, I.E., Dobyns, W.B., Hirsch, B.A., Radtke, R.A., et al. (1998). Mutations in filamin 1 Prevent Migration of Cerebral Cortical Neurons in Human Periventricular Heterotopia. Neuron *21*, 1315–1325.

Franco, S.J., and Müller, U. (2011). Extracellular matrix functions during neuronal migration and lamination in the mammalian central nervous system. Dev. Neurobiol. *71*, 889–900.

Franco, S.J., and Müller, U. (2013). Shaping Our Minds: Stem and Progenitor Cell Diversity in

the Mammalian Neocortex. Neuron *77*, 19–34.

Franco, S.J., Martinez-Garay, I., Gil-Sanz, C., Harkins-Perry, S.R., and Müller, U. (2011). Reelin Regulates Cadherin Function via Dab1/Rap1 to Control Neuronal Migration and Lamination in the Neocortex. Neuron *69*, 482–497.

Friedl, P., and Gilmour, D. (2009). Collective cell migration in morphogenesis, regeneration and cancer. Nat. Rev. Mol. Cell Biol. *10*, 445–457.

Frotscher, M. (2010). Role for Reelin in stabilizing cortical architecture. Trends Neurosci. *33*, 407–414.

Gaiano, N., Kohtz, J.D., Turnbull, D.H., and Fishell, G. (1999). A method for rapid gain-of-function studies in the mouse embryonic nervous system. Nat. Neurosci. *2*, 812–819.

Galaburda, A.M. (2005). Dyslexia—A molecular disorder of neuronal migration. Ann. Dyslexia *55*, 151–165.

Gao, P., Postiglione, M.P., Krieger, T.G., Hernandez, L., Wang, C., Han, Z., Streicher, C., Papusheva, E., Insolera, R., Chugh, K., et al. (2014). Deterministic Progenitor Behavior and Unitary Production of Neurons in the Neocortex. Cell *159*, 775–788.

Gärtner, A., Fornasiero, E.F., Munck, S., Seuntjens, E., Huttner, W.B., Valtorta, F., and Dotti, C.G. (2012). N-cadherin specifies first asymmetry in developing neurons. EMBO J. *31*, 1893–1903.

Gärtner, A., Fornasiero, E.F., and Dotti, C.G. (2015). Cadherins as regulators of neuronal polarity. Cell Adhes. Migr. *9*, 175–182.

Garvalov, B.K., Flynn, K.C., Neukirchen, D., Meyn, L., Teusch, N., Wu, X., Brakebusch, C., Bamburg, J.R., and Bradke, F. (2007). Cdc42 Regulates Cofilin during the Establishment of Neuronal Polarity. J. Neurosci. *27*, 13117–13129.

Gerisch, G., Schroth-Diez, B., Müller-Taubenberger, A., and Ecke, M. (2012). PIP3 Waves and PTEN Dynamics in the Emergence of Cell Polarity. Biophys. J. *103*, 1170–1178.

Gil-Sanz, C., Franco, S.J., Martinez-Garay, I., Espinosa, A., Harkins-Perry, S., and Müller, U. (2013). Cajal-Retzius Cells Instruct Neuronal Migration by Coincidence Signaling between Secreted and Contact-Dependent Guidance Cues. Neuron *79*, 461–477.

Gilmore, E.C., and Herrup, K. (2001). Neocortical cell migration: GABAergic neurons and cells in layers I and VI move in a cyclin-dependent kinase 5-independent manner. J. Neurosci. *21*, 9690–9700.

Gleeson, J.G., and Walsh, C.A. (2000). Neuronal migration disorders: From genetic diseases to developmental mechanisms. Trends Neurosci. *23*, 352–359.

Gleeson, J.G., Allen, K.M., Fox, J.W., Lamperti, E.D., Berkovic, S., Scheffer, I., Cooper, E.C., Dobyns, W.B., Minnerath, S.R., Ross, M.E., et al. (1998). doublecortin, a Brain-Specific Gene Mutated in Human X-Linked Lissencephaly and Double Cortex Syndrome, Encodes a Putative Signaling Protein. Cell *92*, 63–72.

Goehring, N.W. (2014). PAR polarity: From complexity to design principles. Exp. Cell Res. *328*, 258–266.

Golan, M.H., Mane, R., Molczadzki, G., Zuckerman, M., Kaplan-Louson, V., Huleihel, M., and Perez-Polo, J.R. (2009). Impaired migration signaling in the hippocampus following prenatal hypoxia. Neuropharmacology *57*, 511–522.

Goldstein, B., and Macara, I.G. (2007). The PAR Proteins: Fundamental Players in Animal Cell Polarization. Dev. Cell *13*, 609–622.

Gomez, N., Chen, S., and Schmidt, C.E. (2007). Polarization of hippocampal neurons with competitive surface stimuli: contact guidance cues are preferred over chemical ligands. J. R. Soc. Interface *4*, 223–233.

Gönczy, P., and Rose, L.S. (2005). Asymmetric cell division and axis formation in the embryo. WormBook 1–20.

Gonzalez-Billault, C., Muñoz-Llancao, P., Henriquez, D.R., Wojnacki, J., Conde, C., and Caceres, A. (2012). The role of small GTPases in neuronal morphogenesis and polarity. Cytoskeleton (Hoboken). *69*, 464–485.

Gorelik, A., Sapir, T., Woodruff, T.M., and Reiner, O. (2017). Serping1/C1 Inhibitor Affects Cortical Development in a Cell Autonomous and Non-cell Autonomous Manner. Front. Cell. Neurosci. *11*, 1–14.

Graus-Porta, D., Blaess, S., Senften, M., Littlewood-Evans, A., Damsky, C., Huang, Z., Orban, P., Klein, R., Schittny, J.C., and Müller, U. (2001). β1-Class integrins regulate the development of laminae and folia in the cerebral and cerebellar cortex. Neuron *31*, 367–379.

Gray, A., Van Der Kaay, J., and Downes, C.P. (1999). The pleckstrin homology domains of protein kinase B and GRP1 (general receptor for phosphoinositides-1) are sensitive and selective probes for the cellular detection of phosphatidylinositol 3,4-bisphosphate and/or phosphatidylinositol 3,4,5-trisphosphate . Biochem. J. *344 Pt 3*, 929–936.

Greenman, R., Gorelik, A., Sapir, T., Baumgart, J., Zamor, V., Segal-Salto, M., Levin-Zaidman, S., Aidinis, V., Aoki, J., Nitsch, R., et al. (2015). Non-cell autonomous and non-catalytic activities of ATX in the developing brain. Front. Neurosci. *9*, 1–17.

Greig, L.C., Woodworth, M.B., Galazo, M.J., Padmanabhan, H., and Macklis, J.D. (2013). Molecular logic of neocortical projection neuron specification, development and diversity. Nat. Rev. Neurosci. *14*, 755–769.

Gressens, P., Kosofsky, B.E., and Evrard, P. (1992). Cocaine-induced disturbances of corticogenesis in the developing murine brain. Neurosci. Lett. *140*, 113–116.

Groves, J.T., and Kuriyan, J. (2010). Molecular mechanisms in signal transduction at the membrane. Nat. Struct. Mol. Biol. *17*, 659–665.

Guerrini, R., and Parrini, E. (2010). Neuronal migration disorders. Neurobiol. Dis. *38*, 154–166.

Guerrini, R., Dobyns, W.B., and Barkovich, A.J. (2008). Abnormal development of the human cerebral cortex: genetics, functional consequences and treatment options. Trends Neurosci. *31*, 154–162.

Guglielmi, G., Falk, H.J., and De Renzis, S. (2016). Optogenetic Control of Protein Function: From Intracellular Processes to Tissue Morphogenesis. Trends Cell Biol. *26*, 864–874.

Guidi, L.G., Velayos-Baeza, A., Martinez-Garay, I., Monaco, A.P., Paracchini, S., Bishop, D.V.M., and Molnár, Z. (2018). The neuronal migration hypothesis of dyslexia: A critical evaluation 30 years on. Eur. J. Neurosci. *48*, 3212–3233.

Gulli, M.-P., Jaquenoud, M., Shimada, Y., Niederhäuser, G., Wiget, P., and Peter, M. (2000). Phosphorylation of the Cdc42 Exchange Factor Cdc24 by the PAK-like Kinase Cla4 May Regulate Polarized Growth in Yeast. Mol. Cell *6*, 1155–1167.

Gunawardena, J. (2014). Models in biology: 'accurate descriptions of our pathetic thinking.' BMC Biol. *12*, 29.

Guo, S., and Kemphues, K.J. (1995). par-1, a gene required for establishing polarity in C. elegans embryos, encodes a putative Ser/Thr kinase that is asymmetrically distributed. Cell *81*, 611–620.

Gupta, T., and Giangrande, A. (2014). Collective Cell Migration: "All for One and One for All." J. Neurogenet. *28*, 190–198.

Gupta, A., Sanada, K., Miyamoto, D.T., Rovelstad, S., Nadarajah, B., Pearlman, A.L., Brunstrom, J., and Tsai, L.-H. (2003). Layering defect in p35 deficiency is linked to improper neuronal-glial

interaction in radial migration. Nat. Neurosci. *6*, 1284–1291.

Hall, C., Brown, M., Jacobs, T., Ferrari, G., Cann, N., Teo, M., Monfries, C., and Lim, L. (2001). Collapsin Response Mediator Protein Switches RhoA and Rac1 Morphology in N1E-115 Neuroblastoma Cells and Is Regulated by Rho Kinase. J. Biol. Chem. *276*, 43482–43486.

Hammond, V. (2004). Control of Cortical Neuron Migration and Layering: Cell and Non Cell-Autonomous Effects of p35. J. Neurosci. *24*, 576–587.

Hammond, V., Howell, B., Godinho, L., and Tan, S.S. (2001). Disabled-1 Functions Cell Autonomously During Radial Migration and Cortical Layering of Pyramidal Neurons. J. Neurosci. *21*, 8798–8808.

Hansen, A.H., and Hippenmeyer, S. (2020). Non-Cell-Autonomous Mechanisms in Radial Projection Neuron Migration in the Developing Cerebral Cortex. Front. Cell Dev. Biol. *8*.

Hansen, A.H., Duellberg, C., Mieck, C., Loose, M., and Hippenmeyer, S. (2017). Cell Polarity in Cerebral Cortex Development—Cellular Architecture Shaped by Biochemical Networks. Front. Cell. Neurosci. *11*, 176.

Hansen, D. V., Lui, J.H., Parker, P.R.L., and Kriegstein, A.R. (2010). Neurogenic radial glia in the outer subventricular zone of human neocortex. Nature *464*, 554–561.

Hao, Y., Boyd, L., and Seydoux, G. (2006). Stabilization of Cell Polarity by the C. elegans RING Protein PAR-2. Dev. Cell *10*, 199–208.

Hatanaka, Y., and Yamauchi, K. (2013). Excitatory Cortical Neurons with Multipolar Shape Establish Neuronal Polarity by Forming a Tangentially Oriented Axon in the Intermediate Zone. Cereb. Cortex *23*, 105–113.

Hatanaka, Y., Hisanaga, S.I., Heizmann, C.W., and Murakami, F. (2004). Distinct migratory behavior of early- and late-born neurons derived from the cortical ventricular zone. J. Comp. Neurol. *479*, 1–14.

Hatanaka, Y., Zhu, Y., Torigoe, M., Kita, Y., and Murakami, F. (2016). From migration to settlement: the pathways, migration modes and dynamics of neurons in the developing brain. Proc. Jpn. Acad. Ser. B. Phys. Biol. Sci. *92*, 1–19.

Hatten, M.E. (2005). LIS-less neurons don't even make it to the starting gate. J. Cell Biol. *170*, 867–871.

He, S., Li, Z., Ge, S., Yu, Y.-C., and Shi, S.-H. (2015). Inside-Out Radial Migration Facilitates Lineage-Dependent Neocortical Microcircuit Assembly. Neuron *86*, 1159–1166.

Heng, J.I.T., Chariot, A., and Nguyen, L. (2010). Molecular layers underlying cytoskeletal remodelling during cortical development. Trends Neurosci. *33*, 38–47.

Hippenmeyer, S. (2013). Dissection of gene function at clonal level using mosaic analysis with double markers. Front. Biol. (Beijing). *8*, 557–568.

Hippenmeyer, S. (2014). Cellular and Molecular Control of Neuronal Migration. Adv. Exp. Med. Biol. *800*, 1–24.

Hippenmeyer, S., Youn, Y.H., Moon, H.M., Miyamichi, K., Zong, H., Wynshaw-Boris, A., and Luo, L. (2010). Genetic mosaic dissection of Lis1 and Ndel1 in neuronal migration. Neuron *68*, 695–709.

Hirota, Y., Kubo, K., Katayama, K., Honda, T., Fujino, T., Yamamoto, T.T., and Nakajima, K. (2015). Reelin receptors ApoER2 and VLDLR are expressed in distinct spatiotemporal patterns in developing mouse cerebral cortex. J. Comp. Neurol. *523*, 463–478.

Hirotsune, S., Fleck, M.W., Gambello, M.J., Bix, G.J., Chen, A., Clark, G.D., Ledbetter, D.H., McBain, C.J., and Wynshaw-Boris, A. (1998). Graded reduction of Pafah1b1 (Lis1) activity results in neuronal migration defects and early embryonic lethality. Nat. Genet. *19*, 333–339.

Hiscock, T.W., Miesfeld, J.B., Mosaliganti, K.R., Link, B.A., and Megason, S.G. (2018). Feedback between tissue packing and neurogenesis in the zebrafish neural tube. Development *145*, dev157040.

Hoege, C., and Hyman, A.A. (2013). Principles of PAR polarity in Caenorhabditis elegans embryos. Nat. Rev. Mol. Cell Biol. *14*, 315–322.

Hoege, C., Constantinescu, A.-T., Schwager, A., Goehring, N.W., Kumar, P., and Hyman, A.A. (2010). LGL Can Partition the Cortex of One-Cell Caenorhabditis elegans Embryos into Two Domains. Curr. Biol. *20*, 1296–1303.

Homem, C.C.F., Repic, M., and Knoblich, J.A. (2015). Proliferation control in neural stem and progenitor cells. Nat. Rev. Neurosci. *16*, 647–659.

Honda, T., Kobayashi, K., Mikoshiba, K., and Nakajima, K. (2011). Regulation of Cortical Neuron Migration by the Reelin Signaling Pathway. Neurochem. Res. *36*, 1270–1279.

Hong, S.E., Shugart, Y.Y., Huang, D.T., Shahwan, S. a, Grant, P.E., Hourihane, J.O., Martin, N.D., and Walsh, C. a (2000). Autosomal recessive lissencephaly with cerebellar hypoplasia is associated with human RELN mutations. Nat. Genet. *26*, 93–96.

Horiguchi, K., Hanada, T., Fukui, Y., and Chishti, A.H. (2006). Transport of PIP3 by GAKIN, a

kinesin-3 family protein, regulates neuronal cell polarity. J. Cell Biol. *174*, 425–436.

Hosp, F., and Mann, M. (2017). A Primer on Concepts and Applications of Proteomics in Neuroscience. Neuron *96*, 558–571.

Howell, B.W., Hawkes, R., Soriano, P., and Cooper, J. a (1997). Neuronal position in the developing brain is regulated by mouse disabled-1. Nature *389*, 733–737.

Howell, B.W., Herrick, T.M., and Cooper, J. a. (1999). Reelin-induced tryosine phosphorylation of Disabled 1 during neuronal positioning. Genes Dev. *13*, 643–648.

Huttenlocher, A., Lakonishok, M., Kinder, M., Wu, S., Truong, T., Knudsen, K.A., and Horwitz, A.F. (1998). Integrin and cadherin synergy regulates contact inhibition of migration and motile activity. J. Cell Biol. *141*, 515–526.

Iden, S., and Collard, J.G. (2008). Crosstalk between small GTPases and polarity proteins in cell polarization. Nat. Rev. Mol. Cell Biol. *9*, 846–859.

Insolera, R., Chen, S., and Shi, S.-H. (2011). Par proteins and neuronal polarity. Dev. Neurobiol. *71*, 483–494.

Ivey, R.A., Sajan, M.P., and Farese, R. V. (2014). Requirements for Pseudosubstrate Arginine Residues during Autoinhibition and Phosphatidylinositol 3,4,5-(PO4)3-dependent Activation of Atypical PKC. J. Biol. Chem. *289*, 25021–25030.

Iwashita, M., Kataoka, N., Toida, K., and Kosodo, Y. (2014). Systematic profiling of spatiotemporal tissue and cellular stiffness in the developing brain. Development *141*, 3793–3798.

Jaglin, X.H., Poirier, K., Saillour, Y., Buhler, E., Tian, G., Bahi-Buisson, N., Fallet-Bianco, C., Phan-Dinh-Tuy, F., Kong, X.P., Bomont, P., et al. (2009). Mutations in the β-tubulin gene TUBB2B result in asymmetrical polymicrogyria. Nat. Genet. *41*, 746–752.

Jembrek, M.J., Šimić, G., Hof, P.R., and Šegota, S. (2015). Atomic force microscopy as an advanced tool in neuroscience. Transl. Neurosci. *6*, 117–130.

Jiang, H., Guo, W., Liang, X., and Rao, Y. (2005). Both the Establishment and the Maintenance of Neuronal Polarity Require Active Mechanisms. Cell *120*, 123–135.

Joberty, G., Petersen, C., Gao, L., and Macara, I.G. (2000). The cell-polarity protein Par6 links Par3 and atypical protein kinase C to Cdc42. Nat. Cell Biol. *2*, 531–539.

Johnson, J.M., Jin, M., and Lew, D.J. (2011). Symmetry breaking and the establishment of cell polarity in budding yeast. Curr. Opin. Genet. Dev. *21*, 740–746.

Johnson, M.B., Wang, P.P., Atabay, K.D., Murphy, E.A., Doan, R.N., Hecht, J.L., and Walsh, C.A. (2015). Single-cell analysis reveals transcriptional heterogeneity of neural progenitors in human cortex. Nat. Neurosci. *18*, 637–646.

Jossin, Y. (2011). Polarization of migrating cortical neurons by Rap1 and N-cadherin: Revisiting the model for the Reelin signaling pathway. Small GTPases *2*, 322–328.

Jossin, Y., and Cooper, J.A. (2011). Reelin, Rap1 and N-cadherin orient the migration of multipolar neurons in the developing neocortex. Nat. Neurosci. *14*, 697–703.

Jossin, Y., Gui, L., and Goffinet, A.M. (2007). Processing of Reelin by embryonic neurons is important for function in tissue but not in dissociated cultured neurons. J. Neurosci. *27*, 4243–4252.

Judkins, A.R., Martinez, D., Ferreira, P., Dobyns, W.B., and Golden, J.A. (2011). Polymicrogyria Includes Fusion of the Molecular Layer and Decreased Neuronal Populations But Normal Cortical Laminar Organization. J. Neuropathol. Exp. Neurol. *70*, 438–443.

Juric-Sekhar, G., and Hevner, R.F. (2019). Malformations of Cerebral Cortex Development: Molecules and Mechanisms. Annu. Rev. Pathol. *14*, 293–318.

Kakita, A., Wakabayashi, K., Su, M., Piao, Y.-S., and Takahashi, H. (2001). Experimentally Induced Leptomeningeal Glioneuronal Heterotopia and Underlying Cortical Dysplasia of the Lateral Limbic Area in Rats Treated Transplacentally with Methylmercury. J. Neuropathol. Exp. Neurol. *60*, 768–777.

Kaneko, N., Sawada, M., and Sawamoto, K. (2017). Mechanisms of neuronal migration in the adult brain. J. Neurochem. *141*, 835–847.

Kaspar, B.K., Vissel, B., Bengoechea, T., Crone, S., Randolph-Moore, L., Muller, R., Brandon, E.P., Schaffer, D., Verma, I.M., Lee, K.-F., et al. (2002). Adeno-associated virus effectively mediates conditional gene modification in the brain. Proc. Natl. Acad. Sci. *99*, 2320–2325.

Kawauchi, T. (2012). Cell adhesion and its endocytic regulation in cell migration during neural development and cancer metastasis. Int. J. Mol. Sci. *13*, 4564–4590.

Kawauchi, T. (2014). Cdk5 regulates multiple cellular events in neural development, function and disease. Dev. Growth Differ. *56*, 335–348.

Kawauchi, T. (2015). Cellullar insights into cerebral cortical development: focusing on the locomotion mode of neuronal migration. Front. Cell. Neurosci. *9*, 1–9.

Kawauchi, T., Sekine, K., Shikanai, M., Chihama, K., Tomita, K., Kubo, K.I., Nakajima, K.,

Nabeshima, Y.I., and Hoshino, M. (2010). Rab GTPases-dependent endocytic pathways regulate neuronal migration and maturation through N-cadherin trafficking. Neuron *67*, 588–602.

Keays, D.A., Tian, G., Poirier, K., Huang, G.-J., Siebold, C., Cleak, J., Oliver, P.L., Fray, M., Harvey, R.J., Molnár, Z., et al. (2007). Mutations in α-Tubulin Cause Abnormal Neuronal Migration in Mice and Lissencephaly in Humans. Cell *128*, 45–57.

Kelava, I., Reillo, I., Murayama, A.Y., Kalinka, A.T., Stenzel, D., Tomancak, P., Matsuzaki, F., Lebrand, C., Sasaki, E., Schwamborn, J.C., et al. (2012). Abundant Occurrence of Basal Radial Glia in the Subventricular Zone of Embryonic Neocortex of a Lissencephalic Primate, the Common Marmoset Callithrix jacchus. Cereb. Cortex *22*, 469–481.

Kemphues, K.J., Priess, J., Cheng, N.S., and Morton, D. (1988). Identification of Genes Required for Cytoplasmic Localization in C-Elegans. J. Cell. Biochem. *52*, 20.

Keshvara, L., Magdaleno, S., Benhayon, D., Curran, T., Suetsugu, S., Tezuka, T., Morimura, T., Hattori, M., Mikoshiba, K., Yamamoto, T., et al. (2002). Cyclin-dependent kinase 5 phosphorylates disabled 1 independently of Reelin signaling. J. Neurosci. *22*, 4869–4877.

Kim, N., Kim, J.M., Lee, M., Kim, C.Y., Chang, K.Y., and Heo, W. Do (2014). Spatiotemporal control of fibroblast growth factor receptor signals by blue light. Chem. Biol. *21*, 903–912.

Kishi, M., Pan, Y.A., Crump, J.G., and Sanes, J.R. (2005). Mammalian SAD kinases are required for neuronal polarization. Science *307*, 929–932.

Klaus, J., Kanton, S., Kyrousi, C., Ayo-Martin, A.C., Di Giaimo, R., Riesenberg, S., O'Neill, A.C., Camp, J.G., Tocco, C., Santel, M., et al. (2019). Altered neuronal migratory trajectories in human cerebral organoids derived from individuals with neuronal heterotopia. Nat. Med. *25*, 561–568.

Knoblich, J.A. (2008). Mechanisms of Asymmetric Stem Cell Division. Cell *132*, 583–597.

Kobayashi, S., Shirai, T., Kiyokawa, E., Mochizuki, N., Matsuda, M., and Fukui, Y. (2001). Membrane recruitment of DOCK180 by binding to PtdIns(3,4,5)P3. Biochem. J. *354*, 73–78.

Koie, M., Okumura, K., Hisanaga, A., Kamei, T., Sasaki, K., Deng, M., Baba, A., Kohno, T., and Hattori, M. (2014). Cleavage within reelin repeat 3 regulates the duration and range of the signaling activity of reelin protein. J. Biol. Chem. *289*, 12922–12930.

Kon, E., Calvo-Jiménez, E., Cossard, A., Na, Y., Cooper, J.A., and Jossin, Y. (2019). N-cadherin-regulated FGFR ubiquitination and degradation control mammalian neocortical projection

neuron migration. Elife *8*, 1–28.

Kowalczyk, T., Pontious, A., Englund, C., Daza, R.A.M., Bedogni, F., Hodge, R., Attardo, A., Bell, C., Huttner, W.B., and Hevner, R.F. (2009). Intermediate Neuronal Progenitors (Basal Progenitors) Produce Pyramidal–Projection Neurons for All Layers of Cerebral Cortex. Cereb. Cortex *19*, 2439–2450.

Kozminsky, M., and Sohn, L.L. (2020). The promise of single-cell mechanophenotyping for clinical applications. Biomicrofluidics *14*, 031301.

Kreis, P., Leondaritis, G., Lieberam, I., and Eickholt, B.J. (2014). Subcellular targeting and dynamic regulation of PTEN: implications for neuronal cells and neurological disorders. Front. Mol. Neurosci. *7*, 1–19.

Kriegstein, A.R., and Noctor, S.C. (2004). Patterns of neuronal migration in the embryonic cortex. Trends Neurosci. *27*, 392–399.

Krzic, U., Gunther, S., Saunders, T.E., Streichan, S.J., and Hufnagel, L. (2012). Multiview light-sheet microscope for rapid in toto imaging. Nat. Methods *9*, 730–733.

Kubo, K. -i., Honda, T., Tomita, K., Sekine, K., Ishii, K., Uto, A., Kobayashi, K., Tabata, H., and Nakajima, K. (2010). Ectopic Reelin Induces Neuronal Aggregation with a Normal Birthdate-Dependent “Inside-Out” Alignment in the Developing Neocortex. J. Neurosci. *30*, 10953–10966.

Kubo, Y., Baba, K., Toriyama, M., Minegishi, T., Sugiura, T., Kozawa, S., Ikeda, K., and Inagaki, N. (2015). Shootin1-cortactin interaction mediates signal-force transduction for axon outgrowth. J. Cell Biol. *210*, 663–676.

Kwan, K.Y., Sestan, N., and Anton, E.S. (2012). Transcriptional co-regulation of neuronal migration and laminar identity in the neocortex. Development *139*, 1535–1546.

Kwon, Y.T., and Tsai, L.H. (1998). A novel disruption of cortical development in p35(-/-) mice distinct from reeler. J. Comp. Neurol. *395*, 510–522.

Kwon, Y.T., Tsai, L.-H., and Crandall, J.E. (1999). Callosal axon guidance defects in p35?/? mice. J. Comp. Neurol. *415*, 218–229.

Kwon, Y.T., Gupta, A., Zhou, Y., Nikolic, M., and Tsai, L.H. (2000). Regulation of N-cadherin-mediated adhesion by the p35-Cdk5 kinase. Curr. Biol. *10*, 363–372.

Ladbury, J.E., and Arold, S.T. (2012). Noise in cellular signaling pathways: causes and effects. Trends Biochem. Sci. *37*, 173–178.

Lamoureux, P., Ruthel, G., Buxbaum, R.E., and Heidemann, S.R. (2002). Mechanical tension can specify axonal fate in hippocampal neurons. J. Cell Biol. *159*, 499–508.

Laukoter, S., Beattie, R., Pauler, F.M., Amberg, N., Nakayama, K.I., and Hippenmeyer, S. (2020a). Imprinted Cdkn1c genomic locus cell-autonomously promotes cell survival in cerebral cortex development. Nat. Commun. *11*, 1–14.

Laukoter, S., Pauler, F.M., Beattie, R., Amberg, N., Hansen, A.H., Streicher, C., Penz, T., Bock, C., and Hippenmeyer, S. (2020b). Cell-Type Specificity of Genomic Imprinting in Cerebral Cortex. Neuron *107*, 1160-1179.e9.

Laurin, M., and Cote, J.-F. (2014). Insights into the biological functions of Dock family guanine nucleotide exchange factors. Genes Dev. *28*, 533–547.

LeCun, Y., Bengio, Y., and Hinton, G. (2015). Deep learning. Nature *521*, 436–444.

Lee, H.O., and Norden, C. (2013). Mechanisms controlling arrangements and movements of nuclei in pseudostratified epithelia. Trends Cell Biol. *23*, 141–150.

Lee, J., Hyeon, D.Y., and Hwang, D. (2020). Single-cell multiomics: technologies and data analysis methods. Exp. Mol. Med. *52*, 1428–1442.

Lee, J.H., Huynh, M., Silhavy, J.L., Kim, S., Dixon-Salazar, T., Heiberg, A., Scott, E., Bafna, V., Hill, K.J., Collazo, A., et al. (2012). De novo somatic mutations in components of the PI3K-AKT3-mTOR pathway cause hemimegalencephaly. Nat. Genet. *44*, 941–945.

Lee, J.O., Yang, H., Georgescu, M.M., Di Cristofano, A., Maehama, T., Shi, Y., Dixon, J.E., Pandolfi, P., and Pavletich, N.P. (1999). Crystal structure of the PTEN tumor suppressor: implications for its phosphoinositide phosphatase activity and membrane association. Cell *99*, 323–334.

Leonard, T.A., and Hurley, J.H. (2011). Regulation of protein kinases by lipids. Curr. Opin. Struct. Biol. *21*, 785–791.

Leventer, R.J., Guerrini, R., and Dobyns, W.B. (2008). Malformations of cortical development and epilepsy. Dialogues Clin. Neurosci. *10*, 47–62.

Li, L., Hartley, R., Reiss, B., Sun, Y., Pu, J., Wu, D., Lin, F., Hoang, T., Yamada, S., Jiang, J., et al. (2012). E-cadherin plays an essential role in collective directional migration of large epithelial sheets. Cell. Mol. Life Sci. *69*, 2779–2789.

Li, Z., Dong, X., Wang, Z., Liu, W., Deng, N., Ding, Y., Tang, L., Hla, T., Zeng, R., Li, L., et al. (2005). Regulation of PTEN by Rho small GTPases. Nat. Cell Biol. *7*, 399–404.

Lin, D., Edwards, A.S., Fawcett, J.P., Mbamalu, G., Scott, J.D., and Pawson, T. (2000). A mammalian PAR-3–PAR-6 complex implicated in Cdc42/Rac1 and aPKC signalling and cell polarity. Nat. Cell Biol. *2*, 540–547.

Lizcano, J.M., Göransson, O., Toth, R., Deak, M., Morrice, N.A., Boudeau, J., Hawley, S.A., Udd, L., Mäkelä, T.P., Hardie, D.G., et al. (2004). LKB1 is a master kinase that activates 13 kinases of the AMPK subfamily, including MARK/PAR-1. EMBO J. *23*, 833–843.

Lodato, S., and Arlotta, P. (2015). Generating Neuronal Diversity in the Mammalian Cerebral Cortex. Annu. Rev. Cell Dev. Biol. *31*, 699–720.

Londono, C., Loureiro, M.J., Slater, B., Lücker, P.B., Soleas, J., Sathananthan, S., Aitchison, J.S., Kabla, A.J., and McGuigan, A.P. (2014). Nonautonomous contact guidance signaling during collective cell migration. Proc. Natl. Acad. Sci. *111*, 1807–1812.

Long, K.R., and Huttner, W.B. (2019). How the extracellular matrix shapes neural development. Open Biol. *9*.

Lui, J.H., Hansen, D. V., and Kriegstein, A.R. (2011). Development and Evolution of the Human Neocortex. Cell *146*, 18–36.

Macosko, E.Z., Basu, A., Satija, R., Nemesh, J., Shekhar, K., Goldman, M., Tirosh, I., Bialas, A.R., Kamitaki, N., Martersteck, E.M., et al. (2015). Highly Parallel Genome-wide Expression Profiling of Individual Cells Using Nanoliter Droplets. Cell *161*, 1202–1214.

Madisen, L., Mao, T., Koch, H., Zhuo, J., Berenyi, A., Fujisawa, S., Hsu, Y.-W.A., Garcia, A.J., Gu, X., Zanella, S., et al. (2012). A toolbox of Cre-dependent optogenetic transgenic mice for light-induced activation and silencing. Nat. Neurosci. *15*, 793–802.

Maeda, N. (2015). Proteoglycans and neuronal migration in the cerebral cortex during development and disease. Front. Neurosci. *9*, 1–15.

Magen, D., Ofir, A., Berger, L., Goldsher, D., Eran, A., Katib, N., Nijem, Y., Vlodavsky, E., Zur, S., Behar, D.M., et al. (2015). Autosomal recessive lissencephaly with cerebellar hypoplasia is associated with a loss-of-function mutation in CDK5. Hum. Genet. *134*, 305–314.

Mähler (Convenor), M., Berard, M., Feinstein, R., Gallagher, A., Illgen-Wilcke, B., Pritchett-Corning, K., and Raspa, M. (2014). FELASA recommendations for the health monitoring of mouse, rat, hamster, guinea pig and rabbit colonies in breeding and experimental units. Lab. Anim. *48*, 178–192.

Malatesta, P., Hartfuss, E., and Götz, M. (2000a). Isolation of radial glial cells by fluorescent-

activated cell sorting reveals a neural lineage. Development *127*, 5253–5263.

Malatesta, P., Hartfuss, E., and Götz, M. (2000b). Isolation of radial glial cells by fluorescent-activated cell sorting reveals a neuronal lineage. Development *127*, 5253–5263.

Malchow, D., Fuchila, J., and Jastorff, B. (1973). Correlation of substrate specificity of cAMP-phosphodiesterase in Dictyostelium discoideum with chemotactic activity of cAMP-analogues. FEBS Lett. *34*, 5–9.

Marín, O., Valiente, M., Ge, X., and Tsai, L.H. (2010). Guiding neuronal cell migrations. Cold Spring Harb. Perspect. Biol. *2*, 1–21.

Martínez-Martínez, M.Á., Ciceri, G., Espinós, A., Fernández, V., Marín, O., and Borrell, V. (2019). Extensive branching of radially-migrating neurons in the mammalian cerebral cortex. J. Comp. Neurol. *527*, 1558–1576.

Mattson, S.N., and Riley, E.P. (1998). A Review of the Neurobehavioral Deficits in Children with Fetal Alcohol Syndrome or Prenatal Exposure to Alcohol. Alcohol. Clin. Exp. Res. *22*, 279–294.

McConnell, S.K. (1995). Constructing the cerebral cortex: neurogenesis and fate determination. Neuron *15*, 761–768.

McDole, K., Guignard, L., Amat, F., Berger, A., Malandain, G., Royer, L.A., Turaga, S.C., Branson, K., and Keller, P.J. (2018). In Toto Imaging and Reconstruction of Post-Implantation Mouse Development at the Single-Cell Level. Cell *175*, 859-876.e33.

Megason, S.G. (2009). In Toto Imaging of Embryogenesis with Confocal Time-Lapse Microscopy. In Zebrafish : Methods and Protocols, G.J. Lieschke, A.C. Oates, and K. Kawakami, eds. (Totowa, NJ: Humana Press), pp. 317–332.

Megason, S.G., and Fraser, S.E. (2007). Imaging in Systems Biology. Cell *130*, 784–795.

Meijering, E. (2020). A bird's-eye view of deep learning in bioimage analysis. Comput. Struct. Biotechnol. J. *18*, 2312–2325.

Meinhardt, H., and Gierer, A. (2000). Pattern formation by local self-activation and lateral inhibition. BioEssays *22*, 753–760.

Ménager, C., Arimura, N., Fukata, Y., and Kaibuchi, K. (2004). PIP3 is involved in neuronal polarization and axon formation. J. Neurochem. *89*, 109–118.

Mikuni, T., Nishiyama, J., Sun, Y., Kamasawa, N., and Yasuda, R. (2016). High-Throughput, High-Resolution Mapping of Protein Localization in Mammalian Brain by In Vivo Genome

Editing. Cell *165*, 1803–1817.

Minegishi, T., Uesugi, Y., Kaneko, N., Yoshida, W., Sawamoto, K., and Inagaki, N. (2018). Shootin1b Mediates a Mechanical Clutch to Produce Force for Neuronal Migration. Cell Rep. *25*, 624-639.e6.

Miyoshi, G., and Fishell, G. (2012). Dynamic FoxG1 Expression Coordinates the Integration of Multipolar Pyramidal Neuron Precursors into the Cortical Plate. Neuron *74*, 1045–1058.

Mizuno-Yamasaki, E., Rivera-Molina, F., and Novick, P. (2012). GTPase Networks in Membrane Traffic. Annu. Rev. Biochem. *81*, 637–659.

Moffat, J.J., Ka, M., Jung, E.-M., and Kim, W.-Y. (2015). Genes and brain malformations associated with abnormal neuron positioning. Mol. Brain *8*, 72.

Montagni, E., Resta, F., Mascaro, A.L.A., and Pavone, F.S. (2019). Optogenetics in Brain Research: From a Strategy to Investigate Physiological Function to a Therapeutic Tool. Photonics *6*, 92.

Moravcevic, K., Mendrola, J.M., Schmitz, K.R., Wang, Y.-H., Slochower, D., Janmey, P.A., and Lemmon, M.A. (2010). Kinase Associated-1 Domains Drive MARK/PAR1 Kinases to Membrane Targets by Binding Acidic Phospholipids. Cell *143*, 966–977.

Morfini, G., Ditella, M.C., Feiguin, F., Carri, N., and Cáceres, A. (1994). Neurotrophin-3 enhances neurite outgrowth in cultured hippocampal pyramidal neurons. J. Neurosci. Res. *39*, 219–232.

Morton, D.G., Shakes, D.C., Nugent, S., Dichoso, D., Wang, W., Golden, A., and Kemphues, K.J. (2002). The Caenorhabditis elegans par-5 Gene Encodes a 14-3-3 Protein Required for Cellular Asymmetry in the Early Embryo. Dev. Biol. *241*, 47–58.

Motegi, F., Zonies, S., Hao, Y., Cuenca, A.A., Griffin, E., and Seydoux, G. (2011). Microtubules induce self-organization of polarized PAR domains in Caenorhabditis elegans zygotes. Nat. Cell Biol. *13*, 1361–1367.

Motta, S., and Pappalardo, F. (2013). Mathematical modeling of biological systems. Brief. Bioinform. *14*, 411–422.

Mühlhäuser, W.W.D., Fischer, A., Weber, W., and Radziwill, G. (2017). Optogenetics - Bringing light into the darkness of mammalian signal transduction. Biochim. Biophys. Acta - Mol. Cell Res. *1864*, 280–292.

Muraki, K., and Tanigaki, K. (2015). Neuronal migration abnormalities and its possible

implications for schizophrenia. Front. Neurosci. *9*, 1–10.

Nadarajah, B. (2003). Neuronal Migration in the Developing Cerebral Cortex: Observations Based on Real-time Imaging. Cereb. Cortex *13*, 607–611.

Nadarajah, B., and Parnavelas, J.G. (2002). Modes of neuronal migration in the developing cerebral cortex. Nat. Rev. Neurosci. *3*, 423–432.

Nadarajah, B., Brunstrom, J.E., Grutzendler, J., Wong, R.O., and Pearlman, a L. (2001). Two modes of radial migration in early development of the cerebral cortex. Nat. Neurosci. *4*, 143–150.

Najafabadi, M.M., Villanustre, F., Khoshgoftaar, T.M., Seliya, N., Wald, R., and Muharemagic, E. (2015). Deep learning applications and challenges in big data analytics. J. Big Data *2*, 1.

Nakagawa, N., Plestant, C., Yabuno-Nakagawa, K., Li, J., Lee, J., Huang, C.-W., Lee, A., Krupa, O., Adhikari, A., Thompson, S., et al. (2019a). Memo1-Mediated Tiling of Radial Glial Cells Facilitates Cerebral Cortical Development. Neuron *103*, 836-852.e5.

Nakagawa, N., Plestant, C., Yabuno-Nakagawa, K., Li, J., Lee, J., Huang, C.W., Lee, A., Krupa, O., Adhikari, A., Thompson, S., et al. (2019b). Memo1-Mediated Tiling of Radial Glial Cells Facilitates Cerebral Cortical Development. Neuron *103*, 836-852.e5.

Nakamura, F., Kalb, R.G., and Strittmatter, S.M. (2000). Molecular basis of semaphorin-mediated axon guidance. J. Neurobiol. *44*, 219–229.

Nakamura, T., Yasuda, S., Nagai, H., Koinuma, S., Morishita, S., Goto, A., Kinashi, T., and Wada, N. (2013). Longest neurite-specific activation of Rap1B in hippocampal neurons contributes to polarity formation through RalA and Nore1A in addition to PI3-kinase. Genes to Cells *18*, 1020–1031.

Nakamuta, S., Funahashi, Y., Namba, T., Arimura, N., Picciotto, M.R., Tokumitsu, H., Soderling, T.R., Sakakibara, A., Miyata, T., Kamiguchi, H., et al. (2011). Local Application of Neurotrophins Specifies Axons Through Inositol 1,4,5-Trisphosphate, Calcium, and Ca2+/Calmodulin-Dependent Protein Kinases. Sci. Signal. *4*, ra76–ra76.

Namba, T., Kibe, Y., Funahashi, Y., Nakamuta, S., Takano, T., Ueno, T., Shimada, A., Kozawa, S., Okamoto, M., Shimoda, Y., et al. (2014). Pioneering axons regulate neuronal polarization in the developing cerebral cortex. Neuron *81*, 814–829.

Namba, T., Funahashi, Y., Nakamuta, S., Xu, C., Takano, T., and Kaibuchi, K. (2015). Extracellular and Intracellular Signaling for Neuronal Polarity. Physiol. Rev. *95*, 995–1024.

Negishi, M., Oinuma, I., and Katoh, H. (2005). Plexins: axon guidance and signal transduction. Cell. Mol. Life Sci. *62*, 1363–1371.

Nern, A., and Arkowitz, R.A. (1998). A GTP-exchange factor required for cell orientation. Nature *391*, 195–198.

Neukirchen, D., and Bradke, F. (2011). Neuronal polarization and the cytoskeleton. Semin. Cell Dev. Biol. *22*, 825–833.

Nguyen, L., and Hippenmeyer, S. (2014). Cellular and Molecular Control of Neuronal Migration.

Niethammer, M., Smith, D.S., Ayala, R., Peng, J., Ko, J., Lee, M.-S., Morabito, M., and Tsai, L.-H. (2000). NUDEL Is a Novel Cdk5 Substrate that Associates with LIS1 and Cytoplasmic Dynein. Neuron *28*, 697–711.

Nishimura, T., Yamaguchi, T., Kato, K., Yoshizawa, M., Nabeshima, Y., Ohno, S., Hoshino, M., and Kaibuchi, K. (2005). PAR-6–PAR-3 mediates Cdc42-induced Rac activation through the Rac GEFs STEF/Tiam1. Nat. Cell Biol. *7*, 270–277.

Noctor, S.C. (2011). Time-lapse imaging of fluorescently labeled live cells in the embryonic mammalian forebrain. Cold Spring Harb. Protoc. *2011*, 1350–1361.

Noctor, S.C., Flint, A.C., Weissman, T.A., Dammerman, R.S., and Kriegstein, A.R. (2001). Neurons derived from radial glial cells establish radial units in neocortex. Nature *409*, 714–720.

Noctor, S.C., Martínez-Cerdeño, V., Ivic, L., and Kriegstein, A.R. (2004). Cortical neurons arise in symmetric and asymmetric division zones and migrate through specific phases. Nat. Neurosci. *7*, 136–144.

Nogare, D.D., Nikaido, M., Somers, K., Head, J., Piotrowski, T., and Chitnis, A.B. (2017). In toto imaging of the migrating Zebrafish lateral line primordium at single cell resolution. Dev. Biol. *422*, 14–23.

Norden, C., and Lecaudey, V. (2019). Collective cell migration: general themes and new paradigms. Curr. Opin. Genet. Dev. *57*, 54–60.

Ogawa, M., Miyata, T., Nakajimat, K., Yagyu, K., Seike, M., Ikenaka, K., Yamamoto, H., and Mikoshibat, K. (1995). The reeler gene-associated antigen on cajal-retzius neurons is a crucial molecule for laminar organization of cortical neurons. Neuron *14*, 899–912.

Ohshima, T. (2015). Neuronal migration and protein kinases. Front. Neurosci. *9*, 1–7.

Ohtaka-Maruyama, C., and Okado, H. (2015). Molecular Pathways Underlying Projection Neuron Production and Migration during Cerebral Cortical Development. Front. Neurosci. *9*, 1–24.

Oinuma, I., Ishikawa, Y., Katoh, H., and Negishi, M. (2004). The Semaphorin 4D receptor Plexin-B1 is a GTPase activating protein for R-Ras. Science *305*, 862–865.

Oktay, A.B., and Gurses, A. (2019). Automatic detection, localization and segmentation of nano-particles with deep learning in microscopy images. Micron *120*, 113–119.

Oliveira Melo, A.S., Malinger, G., Ximenes, R., Szejnfeld, P.O., Alves Sampaio, S., and Bispo de Filippis, A.M. (2016). Zika virus intrauterine infection causes fetal brain abnormality and microcephaly: tip of the iceberg? Ultrasound Obstet. Gynecol. *47*, 6–7.

Ornitz, D.M., and Itoh, N. (2015). The Fibroblast Growth Factor signaling pathway. Wiley Interdiscip. Rev. Dev. Biol. *4*, 215–266.

Pan, Y.-H., Wu, N., and Yuan, X.-B. (2019). Toward a Better Understanding of Neuronal Migration Deficits in Autism Spectrum Disorders. Front. Cell Dev. Biol. *7*, 1–8.

Di Paolo, G., and De Camilli, P. (2006). Phosphoinositides in cell regulation and membrane dynamics. Nature *443*, 651–657.

Papakonstanti, E.A., Ridley, A.J., and Vanhaesebroeck, B. (2007). The p110δ isoform of PI 3-kinase negatively controls RhoA and PTEN. EMBO J. *26*, 3050–3061.

Paridaen, J.T.M.L., Wilsch-Bräuninger, M., and Huttner, W.B. (2013). Asymmetric Inheritance of Centrosome-Associated Primary Cilium Membrane Directs Ciliogenesis after Cell Division. Cell *155*, 333–344.

Parker, S.S., Mandell, E.K., Hapak, S.M., Maskaykina, I.Y., Kusne, Y., Kim, J.-Y., Moy, J.K., St. John, P.A., Wilson, J.M., Gothard, K.M., et al. (2013). Competing molecular interactions of aPKC isoforms regulate neuronal polarity. Proc. Natl. Acad. Sci. *110*, 14450–14455.

De Pascalis, C., and Etienne-Manneville, S. (2017). Single and collective cell migration: the mechanics of adhesions. Mol. Biol. Cell *28*, 1833–1846.

Perez-Garcia, C.G., Tissir, F., Goffinet, A.M., and Meyer, G. (2004). Reelin receptors in developing laminated brain structures of mouse and human. Eur. J. Neurosci. *20*, 2827–2832.

Petrie, R.J., Doyle, A.D., and Yamada, K.M. (2009). Random versus directionally persistent cell migration. Nat. Rev. Mol. Cell Biol. *10*, 538–549.

Peyrollier, K., Hajduch, E., Gray, A., Litherland, G.J., Prescott, A.R., Leslie, N.R., and Hundal,

H.S. (2000). A role for the actin cytoskeleton in the hormonal and growth-factor-mediated activation of protein kinase B. Biochem. J. *352 Pt 3*, 617–622.

Piao, X. (2004). G Protein-Coupled Receptor-Dependent Development of Human Frontal Cortex. Science (80-.). *303*, 2033–2036.

Plant, P.J., Fawcett, J.P., Lin, D.C.C., Holdorf, A.D., Binns, K., Kulkarni, S., and Pawson, T. (2003). A polarity complex of mPar-6 and atypical PKC binds, phosphorylates and regulates mammalian Lgl. Nat. Cell Biol. *5*, 301–308.

Poduri, A., Evrony, G.D., Cai, X., Elhosary, P.C., Beroukhim, R., Lehtinen, M.K., Hills, B.L., Heinzen, E.L., Hill, A., Hill, S.R., et al. (2012). Somatic Activation of AKT3 Causes Hemispheric Developmental Brain Malformations. Neuron *74*, 41–48.

Poduri, A., Evrony, G.D., Cai, X., and Walsh, C.A. (2013). Somatic mutation, genomic variation, and neurological disease. Science *341*, 1237758.

Poirier, K., Saillour, Y., Bahi-Buisson, N., Jaglin, X.H., Fallet-Bianco, C., Nabbout, R., Castelnau-Ptakhine, L., Roubertie, A., Attie-Bitach, T., Desguerre, I., et al. (2010). Mutations in the neuronal β-tubulin subunit TUBB3 result in malformation of cortical development and neuronal migration defects. Hum. Mol. Genet. *19*, 4462–4473.

Pollen, A.A., Nowakowski, T.J., Chen, J., Retallack, H., Sandoval-Espinosa, C., Nicholas, C.R., Shuga, J., Liu, S.J., Oldham, M.C., Diaz, A., et al. (2015). Molecular Identity of Human Outer Radial Glia during Cortical Development. Cell *163*, 55–67.

Polleux, F., Morrow, T., and Ghosh, A. (2000). Semaphorin 3A is a chemoattractant for cortical apical dendrites. Nature *404*, 567–573.

Postiglione, M.P., and Hippenmeyer, S. (2014). Monitoring neurogenesis in the cerebral cortex: an update. Future Neurol. *9*, 323–340.

Pramparo, T., Libiger, O., Jain, S., Li, H., Youn, Y.H., Hirotsune, S., Schork, N.J., and Wynshaw-Boris, A. (2011). Global developmental gene expression and pathway analysis of normal brain development and mouse models of human neuronal migration defects. PLoS Genet. *7*, e1001331.

Price, D.J., Aslam, S., Tasker, L., and Gillies, K. (1997). Fates of the earliest generated cells in the developing murine neocortex. J. Comp. Neurol. *377*, 414–422.

Rakic, P. (1972). Mode of cell migration to the superficial layers of fetal monkey neocortex. J. Comp. Neurol. *145*, 61–83.

Rakic, P. (1974). Neurons in Rhesus Monkey Visual Cortex: Systematic Relation between Time of Origin and Eventual Disposition. Science (80-.). *183*, 425–427.

Rebman, J.K., Kirchoff, K.E., and Walsh, G.S. (2016). Cadherin-2 Is Required Cell Autonomously for Collective Migration of Facial Branchiomotor Neurons. PLoS One *11*, e0164433.

Reichardt, L.F. (2006). Neurotrophin-regulated signalling pathways. Philos. Trans. R. Soc. Lond. B. Biol. Sci. *361*, 1545–1564.

Reiner, O., Carrozzo, R., Shen, Y., Wehnert, M., Faustinella, F., Dobyns, W.B., Caskey, C.T., and Ledbetter, D.H. (1993). Isolation of a Miller–Dicker lissencephaly gene containing G protein β-subunit-like repeats. Nature *364*, 717–721.

Rice, D.S., Sheldon, M., D'Arcangelo, G., Nakajima, K., Goldowitz, D., and Curran, T. (1998). Disabled-1 acts downstream of Reelin in a signaling pathway that controls laminar organization in the mammalian brain. Development *125*, 3719–3729.

Rivière, J.B., Mirzaa, G.M., O'Roak, B.J., Beddaoui, M., Alcantara, D., Conway, R.L., St-Onge, J., Schwartzentruber, J.A., Gripp, K.W., Nikkel, S.M., et al. (2012). De novo germline and postzygotic mutations in AKT3, PIK3R2 and PIK3CA cause a spectrum of related megalencephaly syndromes. Nat. Genet. *44*, 934–940.

Rodriguez-Viciana, P., Warne, P.H., Dhand, R., Vanhaesebroeck, B., Gout, I., Fry, M.J., Waterfield, M.D., and Downward, J. (1994). Phosphatidylinositol-3-OH kinase direct target of Ras. Nature *370*, 527–532.

Rørth, P. (2009). Collective Cell Migration. Annu. Rev. Cell Dev. Biol. *25*, 407–429.

Rossman, K.L., Der, C.J., and Sondek, J. (2005). GEF means go: turning on RHO GTPases with guanine nucleotide-exchange factors. Nat. Rev. Mol. Cell Biol. *6*, 167–180.

Samuels, B.A., Hsueh, Y.-P., Shu, T., Liang, H., Tseng, H.-C., Hong, C.-J., Su, S.C., Volker, J., Neve, R.L., Yue, D.T., et al. (2007). Cdk5 Promotes Synaptogenesis by Regulating the Subcellular Distribution of the MAGUK Family Member CASK. Neuron *56*, 823–837.

Sanada, K., Gupta, A., and Tsai, L.H. (2004). Disabled-1-regulated adhesion of migrating neurons to radial glial fiber contributes to neuronal positioning during early corticogenesis. Neuron *42*, 197–211.

Sapir, T., Sapoznik, S., Levy, T., Finkelshtein, D., Shmueli, A., Timm, T., Mandelkow, E.-M., and Reiner, O. (2008). Accurate Balance of the Polarity Kinase MARK2/Par-1 Is Required for Proper Cortical Neuronal Migration. J. Neurosci. *28*, 5710–5720.

Sapkota, G.P., Kieloch, A., Lizcano, J.M., Lain, S., Arthur, J.S., Williams, M.R., Morrice, N., Deak, M., and Alessi, D.R. (2001). Phosphorylation of the protein kinase mutated in Peutz-Jeghers cancer syndrome, LKB1/STK11, at Ser431 by p90(RSK) and cAMP-dependent protein kinase, but not its farnesylation at Cys(433), is essential for LKB1 to suppress cell vrowth. J. Biol. Chem. *276*, 19469–19482.

Sasaki, A.T., Chun, C., Takeda, K., and Firtel, R.A. (2004). Localized Ras signaling at the leading edge regulates PI3K, cell polarity, and directional cell movement. J. Cell Biol. *167*, 505–518.

Sasaki, S., Shionoya, A., Ishida, M., Gambello, M.J., Yingling, J., Wynshaw-Boris, A., and Hirotsune, S. (2000). A LIS1/NUDEL/Cytoplasmic Dynein Heavy Chain Complex in the Developing and Adult Nervous System. Neuron *28*, 681–696.

Sasaki, S., Mori, D., Toyo-oka, K., Chen, A., Garrett-beal, L., Muramatsu, M., Miyagawa, S., Hiraiwa, N., Yoshiki, A., Wynshaw-boris, A., et al. (2005). Complete Loss of Ndel1 Results in Neuronal Migration Defects and Early Embryonic Lethality. Mol. Cell. Biol. *25*, 7812–7827.

Sasaki, T., Sasaki, J., Sakai, T., Takasuga, S., and Suzuki, A. (2007). The Physiology of Phosphoinositides. Biol. Pharm. Bull. *30*, 1599–1604.

Satija, R., Farrell, J.A., Gennert, D., Schier, A.F., and Regev, A. (2015). Spatial reconstruction of single-cell gene expression data. Nat. Biotechnol. *33*, 495–502.

Scarpa, E., and Mayor, R. (2016). Collective cell migration in development. J. Cell Biol. *212*, 143–155.

Schaar, B.T., and McConnell, S.K. (2005). Cytoskeletal coordination during neuronal migration. Proc. Natl. Acad. Sci. *102*, 13652–13657.

Schaar, B.T., Kinoshita, K., and McConnell, S.K. (2004). Doublecortin Microtubule Affinity Is Regulated by a Balance of Kinase and Phosphatase Activity at the Leading Edge of Migrating Neurons. Neuron *41*, 203–213.

Schindelin, J., Arganda-Carreras, I., Frise, E., Kaynig, V., Longair, M., Pietzsch, T., Preibisch, S., Rueden, C., Saalfeld, S., Schmid, B., et al. (2012). Fiji: an open-source platform for biological-image analysis. Nat. Methods *9*, 676–682.

Schlesinger, A., Shelton, C.A., Maloof, J.N., Meneghini, M., and Bowerman, B. (1999). Wnt pathway components orient a mitotic spindle in the early Caenorhabditis elegans embryo without requiring gene transcription in the responding cell. Genes Dev. *13*, 2028–2038.

Schoof, E.M., Furtwängler, B., Üresin, N., Rapin, N., Savickas, S., Gentil, C., Lechman, E., Keller,

U. auf dem, Dick, J.E., and Porse, B.T. (2021). Quantitative single-cell proteomics as a tool to characterize cellular hierarchies. Nat. Commun. *12*, 3341.

Schwamborn, J.C., and Püschel, A.W. (2004). The sequential activity of the GTPases Rap1B and Cdc42 determines neuronal polarity. Nat. Neurosci. *7*, 923–929.

Seiradake, E., delToro, D., Nagel, D., Cop, F., Härtl, R., Ruff, T., Seyit-Bremer, G., Harlos, K., Border, E.C., Acker-Palmer, A., et al. (2014). FLRT Structure: Balancing Repulsion and Cell Adhesion in Cortical and Vascular Development. Neuron *84*, 370–385.

Sekine, K., Honda, T., Kawauchi, T., Kubo, K. -i., and Nakajima, K. (2011). The Outermost Region of the Developing Cortical Plate Is Crucial for Both the Switch of the Radial Migration Mode and the Dab1-Dependent “Inside-Out” Lamination in the Neocortex. J. Neurosci. *31*, 9426–9439.

Sekine, K., Kawauchi, T., Kubo, K., Honda, T., Herz, J., Hattori, M., Kinashi, T., and Nakajima, K. (2012). Reelin Controls Neuronal Positioning by Promoting Cell-Matrix Adhesion via Inside-Out Activation of Integrin α5β1. Neuron *76*, 353–369.

Sekine, K., Kubo, K., and Nakajima, K. (2014). How does Reelin control neuronal migration and layer formation in the developing mammalian neocortex? Neurosci. Res. *86*, 50–58.

Setty, Y., Chen, C.-C., Secrier, M., Skoblov, N., Kalamatianos, D., and Emmott, S. (2011). How neurons migrate: a dynamic in-silico model of neuronal migration in the developing cortex. BMC Syst. Biol. *5*, 154.

Shah, G., Thierbach, K., Schmid, B., Waschke, J., Reade, A., Hlawitschka, M., Roeder, I., Scherf, N., and Huisken, J. (2019). Multi-scale imaging and analysis identify pan-embryo cell dynamics of germlayer formation in zebrafish. Nat. Commun. *10*, 5753.

Sheen, V.L., Ganesh, V.S., Topcu, M., Sebire, G., Bodell, A., Hill, R.S., Grant, P.E., Shugart, Y.Y., Imitola, J., Khoury, S.J., et al. (2004). Mutations in ARFGEF2 implicate vesicle trafficking in neural progenitor proliferation and migration in the human cerebral cortex. Nat. Genet. *36*, 69–76.

Shekhar, K., Lapan, S.W., Whitney, I.E., Tran, N.M., Macosko, E.Z., Kowalczyk, M., Adiconis, X., Levin, J.Z., Nemesh, J., Goldman, M., et al. (2016). Comprehensive Classification of Retinal Bipolar Neurons by Single-Cell Transcriptomics. Cell *166*, 1308-1323.e30.

Shellard, A., and Mayor, R. (2020). Rules of collective migration: from the wildebeest to the neural crest. Philos. Trans. R. Soc. B Biol. Sci. *375*, 20190387.

Shelly, M., and Poo, M.-M. (2011). Role of LKB1-SAD/MARK pathway in neuronal polarization. Dev. Neurobiol. *71*, 508–527.

Shelly, M., Cancedda, L., Heilshorn, S., Sumbre, G., and Poo, M. (2007). LKB1/STRAD Promotes Axon Initiation During Neuronal Polarization. Cell *129*, 565–577.

Shelly, M., Cancedda, L., Lim, B.K., Popescu, A.T., Cheng, P., Gao, H., and Poo, M. (2011). Semaphorin3A regulates neuronal polarization by suppressing axon formation and promoting dendrite growth. Neuron *71*, 433–446.

Shi, Y., and Massagué, J. (2003). Mechanisms of TGF-beta signaling from cell membrane to the nucleus. Cell *113*, 685–700.

Shi, S.-H., Jan, L.Y., and Jan, Y.-N. (2003). Hippocampal Neuronal Polarity Specified by Spatially Localized mPar3/mPar6 and PI 3-Kinase Activity. Cell *112*, 63–75.

Shitamukai, A., and Matsuzaki, F. (2012). Control of asymmetric cell division of mammalian neural progenitors. Dev. Growth Differ. *54*, 277–286.

Shitamukai, A., Konno, D., and Matsuzaki, F. (2011). Oblique Radial Glial Divisions in the Developing Mouse Neocortex Induce Self-Renewing Progenitors outside the Germinal Zone That Resemble Primate Outer Subventricular Zone Progenitors. J. Neurosci. *31*, 3683–3695.

Siedlecka, M., Grajkowska, W., Galus, R., Dembowska-Bagińska, B., and Jóźwiak, J. (2016). Focal cortical dysplasia: Molecular disturbances and clinicopathological classification (Review). Int. J. Mol. Med. *38*, 1327–1337.

Da Silva, J.S., Hasegawa, T., Miyagi, T., Dotti, C.G., and Abad-Rodriguez, J. (2005). Asymmetric membrane ganglioside sialidase activity specifies axonal fate. Nat. Neurosci. *8*, 606–615.

Simo, S., Jossin, Y., and Cooper, J.A. (2010). Cullin 5 Regulates Cortical Layering by Modulating the Speed and Duration of Dab1-Dependent Neuronal Migration. J. Neurosci. *30*, 5668–5676.

Sommer, C., and Gerlich, D.W. (2013). Machine learning in cell biology – teaching computers to recognize phenotypes. J. Cell Sci. *126*, 5529–5539.

Srinivasan, S., Wang, F., Glavas, S., Ott, A., Hofmann, F., Aktories, K., Kalman, D., and Bourne, H.R. (2003). Rac and Cdc42 play distinct roles in regulating PI(3,4,5)P3 and polarity during neutrophil chemotaxis. J. Cell Biol. *160*, 375–385.

Stancik, E.K., Navarro-Quiroga, I., Sellke, R., and Haydar, T.F. (2010). Heterogeneity in Ventricular Zone Neural Precursors Contributes to Neuronal Fate Diversity in the Postnatal Neocortex. J. Neurosci. *30*, 7028–7036.

Stanwood, G.D. (2001). Identification of a Sensitive Period of Prenatal Cocaine Exposure that Alters the Development of the Anterior Cingulate Cortex. Cereb. Cortex *11*, 430–440.

Stewart, M.D., Jang, C.-W., Hong, N.W., Austin, A.P., and Behringer, R.R. (2009). Dual fluorescent protein reporters for studying cell behaviors in vivo. Genesis *47*, spcone-spcone.

Stott, S.R.W., and Kirik, D. (2006). Targeted in utero delivery of a retroviral vector for gene transfer in the rodent brain. Eur. J. Neurosci. *24*, 1897–1906.

Su, S.C., and Tsai, L.-H. (2011). Cyclin-Dependent Kinases in Brain Development and Disease. Annu. Rev. Cell Dev. Biol. *27*, 465–491.

Sullivan, D.P., and Lundberg, E. (2018). Seeing More: A Future of Augmented Microscopy. Cell *173*, 546–548.

Sun, Y., Fei, T., Yang, T., Zhang, F., Chen, Y.G., Li, H., and Xu, Z. (2010). The suppression of CRMP2 expression by Bone Morphogenetic Protein (BMP)-SMAD gradient signaling controls multiple stages of neuronal development. J. Biol. Chem. *285*, 39039–39050.

Swiercz, J.M., Kuner, R., Behrens, J., and Offermanns, S. (2002). Plexin-B1 directly interacts with PDZ-RhoGEF/LARG to regulate RhoA and growth cone morphology. Neuron *35*, 51–63.

Szczurkowska, J., Pischedda, F., Pinto, B., Managò, F., Haas, C.A., Summa, M., Bertorelli, R., Papaleo, F., Schäfer, M.K., Piccoli, G., et al. (2018). NEGR1 and FGFR2 cooperatively regulate cortical development and core behaviours related to autism disorders in mice. Brain *141*, 2772–2794.

Tabata, H., and Nakajima, K. (2003). Multipolar migration: the third mode of radial neuronal migration in the developing cerebral cortex. J. Neurosci. *23*, 9996–10001.

Tabata, H., and Nakajima, K. (2008). Labeling embryonic mouse central nervous system cells by in utero electroporation. Dev. Growth Differ. *50*, 507–511.

Tabata, H., Kanatani, S., and Nakajima, K. (2009). Differences of migratory behavior between direct progeny of apical progenitors and basal progenitors in the developing cerebral cortex. Cereb. Cortex *19*, 2092–2105.

Tada, M., and Heisenberg, C.-P. (2012). Convergent extension: using collective cell migration and cell intercalation to shape embryos. Development *139*, 3897–3904.

Tahirovic, S., Hellal, F., Neukirchen, D., Hindges, R., Garvalov, B.K., Flynn, K.C., Stradal, T.E., Chrostek-Grashoff, A., Brakebusch, C., and Bradke, F. (2010). Rac1 Regulates Neuronal Polarization through the WAVE Complex. J. Neurosci. *30*, 6930–6943.

Takeo, Y.H., Shuster, S.A., Jiang, L., Hu, M.C., Luginbuhl, D.J., Rülicke, T., Contreras, X., Hippenmeyer, S., Wagner, M.J., Ganguli, S., et al. (2021). GluD2- and Cbln1-mediated competitive interactions shape the dendritic arbors of cerebellar Purkinje cells. Neuron *109*, 629-644.e8.

Taverna, E., Götz, M., and Huttner, W.B. (2014). The cell biology of neurogenesis: toward an understanding of the development and evolution of the neocortex.

Terabayashi, T., Itoh, T.J., Yamaguchi, H., Yoshimura, Y., Funato, Y., Ohno, S., and Miki, H. (2007). Polarity-Regulating Kinase Partitioning-Defective 1/Microtubule Affinity-Regulating Kinase 2 Negatively Regulates Development of Dendrites on Hippocampal Neurons. J. Neurosci. *27*, 13098–13107.

Theveneau, E., Marchant, L., Kuriyama, S., Gull, M., Moepps, B., Parsons, M., and Mayor, R. (2010). Collective Chemotaxis Requires Contact-Dependent Cell Polarity. Dev. Cell *19*, 39–53.

Thompson, B.J. (2013). Cell polarity: models and mechanisms from yeast, worms and flies. Development *140*, 13–21.

Thompson, B.L., Levitt, P., and Stanwood, G.D. (2009). Prenatal exposure to drugs: effects on brain development and implications for policy and education. Nat. Rev. Neurosci. *10*, 303–312.

Timm, T., von Kries, J.P., Li, X., Zempel, H., Mandelkow, E., and Mandelkow, E.-M. (2011). Microtubule Affinity Regulating Kinase Activity in Living Neurons Was Examined by a Genetically Encoded Fluorescence Resonance Energy Transfer/Fluorescence Lifetime Imaging-based Biosensor. J. Biol. Chem. *286*, 41711–41722.

Tinevez, J.-Y., Perry, N., Schindelin, J., Hoopes, G.M., Reynolds, G.D., Laplantine, E., Bednarek, S.Y., Shorte, S.L., and Eliceiri, K.W. (2017). TrackMate: An open and extensible platform for single-particle tracking. Methods *115*, 80–90.

Tomer, R., Khairy, K., Amat, F., and Keller, P.J. (2012). Quantitative high-speed imaging of entire developing embryos with simultaneous multiview light-sheet microscopy. Nat. Methods *9*, 755–763.

Tønnesen, J., Inavalli, V.V.G.K., and Nägerl, U.V. (2018). Super-Resolution Imaging of the Extracellular Space in Living Brain Tissue. Cell *172*, 1108-1121.e15.

del Toro, D., Ruff, T., Cederfjäll, E., Villalba, A., Seyit-Bremer, G., Borrell, V., and Klein, R. (2017). Regulation of Cerebral Cortex Folding by Controlling Neuronal Migration via FLRT

Adhesion Molecules. Cell *169*, 621-635.e16.

del Toro, D., Carrasquero-Ordaz, M.A., Chu, A., Ruff, T., Shahin, M., Jackson, V.A., Chavent, M., Berbeira-Santana, M., Seyit-Bremer, G., Brignani, S., et al. (2020). Structural Basis of Teneurin-Latrophilin Interaction in Repulsive Guidance of Migrating Neurons. Cell *180*, 323-339.e19.

Trepat, X., Chen, Z., and Jacobson, K. (2012). Cell Migration. In Comprehensive Physiology, (Hoboken, NJ, USA: John Wiley & Sons, Inc.), pp. 2369–2392.

Tsai, J., and Vallee, R.B. (2011). Stem Cell Migration (Totowa, NJ: Humana Press).

Tsai, J.W., Chen, Y., Kriegstein, A.R., and Vallee, R.B. (2005). LIS1 RNA interference blocks neural stem cell division, morphogenesis, and motility at multiple stages. J. Cell Biol. *170*, 935–945.

Tsai, L.H., Delalle, I., Caviness, V.S., Chae, T., and Harlow, E. (1994). P35 Is a Neural-Specific Regulatory Subunit of Cyclin-Dependent Kinase 5. Nature *371*, 419–423.

Turing, A.M. (1990). The chemical basis of morphogenesis. Bull. Math. Biol. *52*, 153–197.

Urasaki, A., Morishita, S., Naka, K., Uozumi, M., Abe, K., Huang, L., Watase, E., Nakagawa, O., Kawakami, K., Matsui, T., et al. (2019). Shootins mediate collective cell migration and organogenesis of the zebrafish posterior lateral line system. Sci. Rep. *9*, 12156.

Valiente, M., and Marín, O. (2010). Neuronal migration mechanisms in development and disease. Curr. Opin. Neurobiol. *20*, 68–78.

Valon, L., Marín-Llauradó, A., Wyatt, T., Charras, G., and Trepat, X. (2017). Optogenetic control of cellular forces and mechanotransduction. Nat. Commun. *8*.

Vaz, W.L.C., Goodsaid-Zalduondo, F., and Jacobson, K. (1984). Lateral diffusion of lipids and proteins in bilayer membranes. FEBS Lett. *174*, 199–207.

Veeman, M., and Reeves, W. (2015). Quantitative and in toto imaging in ascidians: Working toward an image-centric systems biology of chordate morphogenesis. Genesis *53*, 143–159.

Verrotti, A., Spalice, A., Ursitti, F., Papetti, L., Mariani, R., Castronovo, A., Mastrangelo, M., and Iannetti, P. (2010). New trends in neuronal migration disorders. Eur. J. Paediatr. Neurol. *14*, 1–12.

Voss, A.K., Britto, J.M., Dixon, M.P., Sheikh, B.N., Collin, C., Tan, S.-S., and Thomas, T. (2008). C3G regulates cortical neuron migration, preplate splitting and radial glial cell attachment. Development *135*, 2139–2149.

Wang, F. (2009). The Signaling Mechanisms Underlying Cell Polarity and Chemotaxis. Cold Spring Harb. Perspect. Biol. *1*, a002980–a002980.

Wang, L., and Cooper, J.A. (2017). Optogenetic control of the Dab1 signaling pathway. Sci. Rep. *7*, 43760.

Wang, F., Herzmark, P., Weiner, O.D., Srinivasan, S., Servant, G., and Bourne, H.R. (2002). Lipid products of PI(3)Ks maintain persistent cell polarity and directed motility in neutrophils. Nat. Cell Biol. *4*, 513–518.

Wang, T., Liu, Y., Xu, X.-H., Deng, C.-Y., Wu, K.-Y., Zhu, J., Fu, X.-Q., He, M., and Luo, Z.-G. (2011a). Lgl1 Activation of Rab10 Promotes Axonal Membrane Trafficking Underlying Neuronal Polarization. Dev. Cell *21*, 431–444.

Wang, X., Tsai, J.W., Imai, J.H., Lian, W.N., Vallee, R.B., and Shi, S.H. (2009a). Asymmetric centrosome inheritance maintains neural progenitors in the neocortex. Nature *461*, 947–955.

Wang, X., He, L., Wu, Y.I., Hahn, K.M., and Montell, D.J. (2010). Light-mediated activation reveals a key role for Rac in collective guidance of cell movement in vivo. Nat. Cell Biol. *12*, 591–597.

Wang, X., Tsai, J.W., Lamonica, B., and Kriegstein, A.R. (2011b). A new subtype of progenitor cell in the mouse embryonic neocortex. Nat. Neurosci. *14*, 555–562.

Wang, Z., Gerstein, M., and Snyder, M. (2009b). RNA-Seq: a revolutionary tool for transcriptomics. Nat. Rev. Genet. *10*, 57–63.

Watabe-Uchida, M., John, K.A., Janas, J.A., Newey, S.E., and Van Aelst, L. (2006). The Rac Activator DOCK7 Regulates Neuronal Polarity through Local Phosphorylation of Stathmin/Op18. Neuron *51*, 727–739.

Wedlich-Soldner, R., and Li, R. (2003). Spontaneous cell polarization: undermining determinism. Nat. Cell Biol. *5*, 267–270.

Weitzman, M., and Hahn, K.M. (2014). Optogenetic approaches to cell migration and beyond. Curr. Opin. Cell Biol. *30*, 112–120.

Wennekamp, S., Mesecke, S., Nédélec, F., and Hiiragi, T. (2013). A self-organization framework for symmetry breaking in the mammalian embryo. Nat. Rev. Mol. Cell Biol. *14*, 452–459.

Whitman, M., Kaplan, D.R., Schaffhausen, B., Cantley, L., and Roberts, T.M. (1985). Association of phosphatidylinositol kinase activity with polyoma middle-T competent for

transformation. Nature *315*, 239–242.

Wilkinson, D.J. (2009). Stochastic modelling for quantitative description of heterogeneous biological systems. Nat. Rev. Genet. *10*, 122–133.

Wilson, R.S., and Nairn, A.C. (2018). Cell-Type-Specific Proteomics: A Neuroscience Perspective. Proteomes *6*, 51.

Witte, H., Neukirchen, D., and Bradke, F. (2008). Microtubule stabilization specifies initial neuronal polarization. J. Cell Biol. *180*, 619–632.

Wu, P.-R., Tsai, P.-I., Chen, G.-C., Chou, H.-J., Huang, Y.-P., Chen, Y.-H., Lin, M.-Y., Kimchi, A., Chien, C.-T., and Chen, R.-H. (2011). DAPK activates MARK1/2 to regulate microtubule assembly, neuronal differentiation, and tau toxicity. Cell Death Differ. *18*, 1507–1520.

Wynshaw-Boris, A., Pramparo, T., Youn, Y.H., and Hirotsune, S. (2010). Lissencephaly: Mechanistic insights from animal models and potential therapeutic strategies. Semin. Cell Dev. Biol. *21*, 823–830.

Xu, C., Funahashi, Y., Watanabe, T., Takano, T., Nakamuta, S., Namba, T., and Kaibuchi, K. (2015). Radial Glial Cell-Neuron Interaction Directs Axon Formation at the Opposite Side of the Neuron from the Contact Site. J. Neurosci. *35*, 14517–14532.

Yamanaka, T., Horikoshi, Y., Suzuki, A., Sugiyama, Y., Kitamura, K., Maniwa, R., Nagai, Y., Yamashita, A., Hirose, T., Ishikawa, H., et al. (2001). PAR-6 regulates aPKC activity in a novel way and mediates cell-cell contact-induced formation of the epithelial junctional complex. Genes to Cells *6*, 721–731.

Yanagida, M., Miyoshi, R., Toyokuni, R., Zhu, Y., and Murakami, F. (2012). Dynamics of the leading process, nucleus, and Golgi apparatus of migrating cortical interneurons in living mouse embryos. Proc. Natl. Acad. Sci. *109*, 16737–16742.

Yang, H., Jensen, P., and Goldowitz, D. (2002). The community effect and Purkinje cell migration in the cerebellar cortex: analysis of scrambler chimeric mice. J. Neurosci. *22*, 464–470.

Yang, H.W., Shin, M.-G., Lee, S., Kim, J.-R., Park, W.S., Cho, K.-H., Meyer, T., and Do Heo, W. (2012). Cooperative Activation of PI3K by Ras and Rho Family Small GTPases. Mol. Cell *47*, 281–290.

Yi, J.J., Barnes, A.P., Hand, R., Polleux, F., and Ehlers, M.D. (2010). TGF-beta signaling specifies axons during brain development. Cell *142*, 144–157.

Yingling, J., Youn, Y.H., Darling, D., Toyo-oka, K., Pramparo, T., Hirotsune, S., and Wynshaw-Boris, A. (2008). Neuroepithelial Stem Cell Proliferation Requires LIS1 for Precise Spindle Orientation and Symmetric Division. Cell *132*, 474–486.

Yoshimura, T., Arimura, N., Kawano, Y., Kawabata, S., Wang, S., and Kaibuchi, K. (2006a). Ras regulates neuronal polarity via the PI3-kinase/Akt/GSK-3β/CRMP-2 pathway. Biochem. Biophys. Res. Commun. *340*, 62–68.

Yoshimura, T., Arimura, N., and Kaibuchi, K. (2006b). Signaling Networks in Neuronal Polarization. J. Neurosci. *26*, 10626–10630.

Yoshimura, Y., Terabayashi, T., and Miki, H. (2010). Par1b/MARK2 Phosphorylates Kinesin-Like Motor Protein GAKIN/KIF13B To Regulate Axon Formation. Mol. Cell. Biol. *30*, 2206–2219.

Youn, Y.H., Pramparo, T., Hirotsune, S., and Wynshaw-Boris, A. (2009). Distinct Dose-Dependent Cortical Neuronal Migration and Neurite Extension Defects in Lis1 and Ndel1 Mutant Mice. J. Neurosci. *29*, 15520–15530.

Yue, Y., Zong, W., Li, X., Li, J., Zhang, Y., Wu, R., Liu, Y., Cui, J., Wang, Q., Bian, Y., et al. (2020). Long-term, in toto live imaging of cardiomyocyte behaviour during mouse ventricle chamber formation at single-cell resolution. Nat. Cell Biol. *22*, 332–340.

Zaman, M.H., Kamm, R.D., Matsudaira, P., and Lauffenburger, D.A. (2005). Computational Model for Cell Migration in Three-Dimensional Matrices. Biophys. J. *89*, 1389–1397.

Zhang, X., Chen, M.H., Wu, X., Kharchenko, P. V, Sharp, P.A., Walsh, C.A., Zhang, X., Chen, M.H., Wu, X., Kodani, A., et al. (2016). Cell-Type-Specific Alternative Splicing Governs Cell Fate in the Developing Cerebral Cortex Article Cell-Type-Specific Alternative Splicing Governs Cell Fate in the Developing Cerebral Cortex. Cell *166*, 1147-1162.e15.

Zheng, Y. (2001). Dbl family guanine nucleotide exchange factors. Trends Biochem. Sci. *26*, 724–732.

Zong, H., Espinosa, J.S., Su, H.H., Muzumdar, M.D., and Luo, L. (2005). Mosaic analysis with double markers in mice. Cell *121*, 479–492.

A. Appendix 1

REAGENT or RESOURCE	SOURCE	IDENTIFIER
Antibodies		
GFP - Chick	Aves Labs Inc.	Cat#GFP-1020; RRID:AB_10000240
RFP - Rabbit	MBL	Cat#PM005; RRID:AB_591279
Alexa Fluor 488 Anti-Chicken IgG	Jackson ImmunoResearch Labs	Cat#703-545-155; RRID:AB_2340375
Cy3 Anti-Rabbit IgG	Jackson ImmunoResearch Labs	Cat#711-165-152; RRID:AB_2307443
Chemicals, Peptides, and Recombinant Proteins		
Papain Vial Source	Worthington	Cat#PAP2
DNase Vial Source	Worthington	Cat#D2
Inhibitor Vial Source	Worthington	Cat#OI-BSA
Penicillin-Streptomycin (5,000 U/mL) (PenStrep)	Gibco	Cat#15070063
DMEM/F12, no phenol red	Gibco	Cat#21041025
N-2 Supplement (100X)	Gibco	Cat#17502001
Critical Commercial Assays		
SMARTer Stranded Total RNA Sample Prep Kit – Low Input Mammalian	Clonetech	Cat#634861
iST-NHS Kit 12x	PreOmics	Cat#P.O.00026
TMT10plex™ Isobaric Label Reagent Set	Thermo Scientific	Cat#90110
Deposited Data		
RNA-Seq of	To be done	N/A
RNA-Seq of	To de done	N/A

Proteomics	To be done	N/A
Experimental Models: Organisms/Strains		
Mouse: *MADM-11-GT*	The Jackson Laboratory	RRID:IMSR_JAX:013749
Mouse: *MADM-11-TG*	The Jackson Laboratory	RRID:IMSR_JAX:013751
Mouse: *MADM-5-GT*	Hippenmeyer Lab	
Mouse: *MADM-5-TG*	Hippenmeyer Lab	
Mouse: *MADM-4-GT*	Hippenmeyer Lab	
Mouse: *MADM-4-TG*	Hippenmeyer Lab	
Mouse: *Cdk5r1*	The Jackson Laboratory	RRID:IMSR_JAX:004163
Mouse: *Cdk5*	The Jackson Laboratory	RRID:IMSR_JAX:014156
Mouse: *Dab1*	The Jackson Laboratory	RRID:IMSR_JAX:003581
Mouse: *Emx1-Cre*	The Jackson Laboratory	RRID:IMSR_JAX:005628
Software and Algorithms		
ZEN 2.6 (blue edition) Digital Imaging for Light Microscopy	Zeiss	http://www.zeiss.com/microscopy/en_us/products/microscope-software/zen.html#introduction
FACS Diva	BD Biosciences	
ImageJ 1.52n	N/A	https://imagej.net/
TrackMate v3.8.0	N/A	https://imagej.net/TrackMate

Graphpad Prism 8.0.1	Graphpad	https://www.graphpad.com/scientific-software/prism/
R v3.4.4	NA	https://www.r-project.org/
DESeq2 v1.16.1	Love et al., Genome Biology 2014	http://www.bioconductor.org/
Other		
FACS Aria III	BD Biosciences	N/A
LSM 800 inverted confocal	Zeiss	N/A
Gas Incubation System for CO2 and O2	Ibidi	Cat#11922
FoilCover-Set for Multiplates	Pecon	Cat#0430.100
Glass-bottom dishes	MatTek	Cat#P06G-1.5-10-F
Milicell culture inserts	Millipore	Cat#PICM03050
Olympus VS120 Slidescanner (OLYMPUS VS-ASW 2.9 (Build 13753))	Olympus	N/A
Vibratome VT 1200S	Leica	N/A
Cryostat Cryostar NX70	Thermo Fisher Scientific	N/A
Bioanalyzer	Agilent	N/A
Qubit Fluorometer	Thermo Fisher Scientific	N/A
HiSeq 2500	Illumina	N/A

Table 2 Key Resources Table